


APPENDIX

F

TIDAL HYDRODYNAMICS, FLOODING AND WATER QUALITY (PATTERSON BRITTON)




GHD



**POTENTIAL IMPACTS OF PROPOSED
DREDGING OF SOUTH ARM ON TIDAL
HYDRODYNAMICS, FLOODING AND
WATER QUALITY**

**Issue No. 3
OCTOBER 2003**



**Patterson Britton
& Partners Pty Ltd**
consulting engineers

GHD

POTENTIAL IMPACTS OF PROPOSED DREDGING OF SOUTH ARM ON TIDAL HYDRODYNAMICS, FLOODING AND WATER QUALITY

Issue No. 3
OCTOBER 2003

Document Amendment and Approval Record

Issue	Description of Amendment	Prepared by [date]	Verified by [date]	Approved by [date]
1	Final Draft	PRH [25/3/03]	GWB	GWB
2	Final	PRH [8/8/03]	GWB	GWB
3	Revised Final	PRH [21/10/03] <i>Peter Hobart</i>	GWB	GWB <i>WJH 21/10/03</i>

Note: This document is preliminary unless it is approved by a principal of Patterson Britton & Partners.

Document Reference: rp3878prh031020-main report.doc

Time and Date Printed: 9:05 AM 21 October, 2003

© Copyright The concepts and information in this document are the property of Patterson Britton & Partners Pty Ltd. Use of this document or passing onto others or copying, in part or in full, without the written permission of Patterson Britton & Partners Pty Ltd is an infringement of copyright.



level 2
104 Mount Street
North Sydney 2060

PO Box 515
North Sydney 2059
Australia

telephone: (02) 9957 1619
facsimile: (02) 9957 1291
reception@patbrit.com.au
ABN 89 003 220 228

Newcastle Office
8 Telford Street
Newcastle East 2300

PO Box 668
Newcastle 2300
Australia

telephone: (02) 4928 7777
facsimile: (02) 4926 2111
mail@newcastle.patbrit.com.au

**Patterson Britton
& Partners Pty Ltd**

consulting engineers

TABLE OF CONTENTS

Page No.

1	INTRODUCTION	1
2	EXISTING ENVIRONMENT	2
2.1	GENERAL	2
2.2	TIDAL HYDRODYNAMICS	3
2.3	FLOODING	6
2.4	SALINITY STRUCTURE	10
2.5	WATER QUALITY	12
2.6	SEDIMENT TRANSPORT	14
2.6.1	Sediment Properties	14
2.6.2	Sediment Budget	14
2.6.3	Suspended Sediment Concentrations	15
2.6.4	Effect of Sedimentation on Mangroves	16
2.7	FISH, PRAWNS AND OYSTERS	17
2.8	HISTORICAL IMPACTS	18
2.8.1	Summary of Impacts	18
2.8.2	Entrance Breakwaters and Dredging	19
2.8.3	Flood Mitigation Works	20
2.8.4	Reclamation	21
2.8.5	Riparian Vegetation	21
3	IMPACT ASSESSMENT	22
3.1	GENERAL	22
3.2	TIDAL HYDRODYNAMICS	22
3.2.1	Water Levels	22
3.2.2	Tidal Planes	25
3.2.3	Velocities	26
3.2.4	Flows	28
3.2.5	Effect of Temporary Sheet Pile Wall	29
3.3	FLOODING	34
3.3.1	Effect of Temporary Sheet Pile Wall	34
3.3.2	Discharge Pipeline	37
3.3.3	Post Dredging Conditions	41
3.3.4	Groundwater Characteristics	49
3.4	SALINITY STRUCTURE	50
3.4.1	Simulations of Salinity Intrusion	50
3.4.2	Effect of Altered Salinities on Biota	55
3.4.3	Impact on Proposed Opening of Ironbark Creek Floodgates	56

TABLE OF CONTENTS

Page No.

3.5	WATER QUALITY	56
3.5.1	Simulation of Pollutant Flushing	56
3.5.2	Simulation of Pollutant Dispersion	60
3.5.3	Effect of Deepening on Water Quality Processes	62
3.5.4	Local Water Quality Impacts at Dredging Site due to Contamination	64
3.6	SEDIMENT TRANSPORT	66
3.6.1	Deposition of Suspended Sediment Generated During Dredging	66
3.6.2	Pollutant Transport (with Sediment) During Dredging	69
3.6.3	Effects on Sediment Transport after Completion of Dredging	70
3.6.4	Bed Stability Upstream of Tourle St Bridge	70
3.7	FISH, PRAWNS AND OYSTERS	71
4	RECOMMENDED MITIGATION MEASURES	73
4.1.1	Summary of Impacts	73
4.1.2	Mitigation Measures	74
5	CONCLUSIONS	76
6	REFERENCES	78

APPENDIX A: THE RMA MODEL SUITE

APPENDIX B: DEVELOPMENT, CALIBRATION AND VERIFICATION OF TIDAL HYDRODYNAMIC MODEL

APPENDIX C: DEVELOPMENT OF FLOOD MODEL

APPENDIX D: WATER QUALITY SIMULATIONS (SALINITY AND SEDIMENT TRANSPORT)

LIST OF FIGURES

Page No.

FIGURE 1:	WATER LEVEL AT HUNTER RIVER ENTRANCE DURING TYPICAL TIDAL CONDITIONS, INDICATING SEMI-DIURNAL, DIURNAL INEQUALITY AND SPRING-NEAP FEATURES	4
FIGURE 2:	EXTENT OF THE 1% AEP FLOOD (FROM PATTERSON BRITTON & PARTNERS, 2001B)	7
FIGURE 3:	CONCEPTUAL REPRESENTATION OF FLOW DISTRIBUTION AT HEXHAM AT PEAK OF THE 1% AEP FLOOD (FROM PATTERSON BRITTON & PARTNERS, 2001B)	8
FIGURE 4:	FLOW DISTRIBUTION AROUND KOORAGANG ISLAND AT PEAK OF 1% AEP EVENT (FROM PATTERSON BRITTON & PARTNERS, 2001A)	9
FIGURE 5:	HUNTER ESTUARY SALINITY DISTRIBUTION AS A FUNCTION OF FLOW AS DERIVED BY SANDERSON ET AL (2002)	11
FIGURE 6:	AVERAGE SALINITY DISTRIBUTION ALONG HUNTER ESTUARY FROM 1975-2000, BASED ON SIMPLE ADVECTION-DIFFUSION RELATIONSHIP, FROM SANDERSON ET AL (2002)	12
FIGURE 7:	SIMULATED EXISTING AND POST-DREDGING WATER LEVELS AT TOURLE ST BRIDGE UNDER TIDAL CONDITIONS – DAY 1 TO 7	23
FIGURE 8:	SIMULATED EXISTING AND POST-DREDGING WATER LEVELS AT TOURLE ST BRIDGE UNDER TIDAL CONDITIONS – DAY 7 TO 15	24
FIGURE 9:	SIMULATED EXISTING AND POST-DREDGING WATER LEVELS AT TOURLE ST BRIDGE UNDER TIDAL CONDITIONS – DAY 15 TO 22	24
FIGURE 10:	SIMULATED EXISTING AND POST-DREDGING WATER LEVELS AT TOURLE ST BRIDGE UNDER TIDAL CONDITIONS – DAY 22 TO 29	25
FIGURE 11:	SIMULATED EXISTING AND POST-DREDGING TIDAL VELOCITIES AT THE RAILWAY BRIDGE – DAY 15 TO 22	27
FIGURE 12:	SIMULATED EXISTING AND POST-DREDGING TIDAL VELOCITIES IN THE EAST DIRECTION AT THE RAILWAY BRIDGE – DAY 15 TO 22	27
FIGURE 13:	PEAK EBB TIDE VELOCITY CONTOURS (M/S) BETWEEN TOURLE ST BRIDGE AND KOORAGANG BERTHS FOR EXISTING CONDITIONS	30
FIGURE 14:	PEAK EBB TIDE VELOCITY CONTOURS (M/S) BETWEEN TOURLE ST BRIDGE AND KOORAGANG BERTHS WITH TEMPORARY SHEET PILE WALL IN PLACE	30
FIGURE 15:	PEAK EBB TIDE VELOCITY CONTOURS (M/S) IN PORT AREA FOR EXISTING CONDITIONS	32
FIGURE 16:	PEAK EBB TIDE VELOCITY CONTOURS (M/S) IN PORT AREA WITH TEMPORARY SHEET PILE WALL IN PLACE	32
FIGURE 17:	VELOCITY VECTORS (M/S) FOR PEAK EBB TIDE IN VICINITY OF WALSH POINT (EXISTING CONDITIONS)	33
FIGURE 18:	VELOCITY VECTORS (M/S) FOR PEAK EBB TIDE IN VICINITY OF WALSH POINT (TEMPORARY SHEET PILE WALL IN PLACE)	33
FIGURE 19:	PEAK WATER LEVELS FOR VARIOUS AEP FLOODS UNDER EXISTING CONDITIONS AND WITH TEMPORARY SHEET PILE WALL IN PLACE (ENTRANCE AND NORTH ARM)	34

LIST OF FIGURES

Page No.

FIGURE 20:	PEAK WATER LEVELS FOR VARIOUS AEP FLOODS UNDER EXISTING CONDITIONS AND WITH TEMPORARY SHEET PILE WALL IN PLACE (SOUTH ARM)	35
FIGURE 21:	PEAK VELOCITY CONTOURS (M/S) BETWEEN TOURLE ST BRIDGE AND KOORAGANG BERTHS FOR EXISTING CONDITIONS (5% AEP FLOOD)	36
FIGURE 22:	PEAK VELOCITY CONTOURS (M/S) BETWEEN TOURLE ST BRIDGE AND KOORAGANG BERTHS WITH TEMPORARY SHEET PILE WALL IN PLACE (5% AEP FLOOD)	37
FIGURE 23:	VARIATION IN PEAK WATER LEVEL (M) DUE TO 700MM PIPELINE (1% AEP FLOOD)	39
FIGURE 24:	VARIATION IN PEAK WATER LEVEL (M) DUE TO 700MM PIPELINE (2% AEP FLOOD)	39
FIGURE 25:	VARIATION IN PEAK WATER LEVEL (M) DUE TO 700MM PIPELINE (5% AEP FLOOD)	40
FIGURE 26:	VARIATION IN PEAK WATER LEVEL (M) DUE TO 700MM PIPELINE (10% AEP FLOOD)	40
FIGURE 27:	PEAK WATER LEVELS FOR VARIOUS AEP FLOODS UNDER EXISTING AND POST DREDGING CONDITIONS (ENTRANCE AND NORTH ARM)	42
FIGURE 28:	PEAK WATER LEVELS FOR VARIOUS AEP FLOODS UNDER EXISTING AND POST DREDGING CONDITIONS (SOUTH ARM)	42
FIGURE 29:	APPROXIMATE LOCATIONS OF CROSS SECTIONS FOR FLOW HYDROGRAPH DETERMINATION	44
FIGURE 30:	FLOW HYDROGRAPHS FOR LOCATION A, 1% AEP EVENT	46
FIGURE 31:	FLOW HYDROGRAPHS FOR LOCATION B, 1% AEP EVENT	46
FIGURE 32:	FLOW HYDROGRAPHS FOR LOCATION C, 1% AEP EVENT	47
FIGURE 33:	FLOW HYDROGRAPHS FOR LOCATION A, 10% AEP EVENT	47
FIGURE 34:	FLOW HYDROGRAPHS FOR LOCATION B, 10% AEP EVENT	48
FIGURE 35:	FLOW HYDROGRAPHS FOR LOCATION C, 10% AEP EVENT	48
FIGURE 36:	SALINITY CONTOURS (PPT) AFTER 29 DAY TIDAL SIMULATION, ASSUMING INITIALLY FRESH ESTUARY, FOR EXISTING CONDITIONS	51
FIGURE 37:	SALINITY CONTOURS AFTER 29 DAY TIDAL SIMULATION, ASSUMING INITIALLY FRESH ESTUARY, FOR POST-DREDGING CONDITIONS	51
FIGURE 38:	PRE AND POST DREDGING VARIATION IN SALINITY AT WALSH POINT OVER 29 DAY SIMULATION	52
FIGURE 39:	PRE AND POST DREDGING VARIATION IN SALINITY AT TOURLE ST BRIDGE OVER 29 DAY SIMULATION	53
FIGURE 40:	PRE AND POST DREDGING VARIATION IN SALINITY AT IRONBARK CREEK OVER 29 DAY SIMULATION	53
FIGURE 41:	PRE AND POST DREDGING VARIATION IN SALINITY AT MOSCHETO CREEK OVER 29 DAY SIMULATION	54
FIGURE 42:	PRE AND POST DREDGING VARIATION IN SALINITY AT HEXHAM BRIDGE OVER 29 DAY SIMULATION	54

LIST OF FIGURES

Page No.

FIGURE 43:	HYPOTHETICAL POLLUTANT CONCENTRATIONS (%) RELATIVE TO INITIAL CONCENTRATION, AFTER 29 DAY TIDAL SIMULATION, FOR EXISTING CONDITIONS (POLLUTANT INITIALLY EVERYWHERE)	57
FIGURE 44:	HYPOTHETICAL POLLUTANT CONCENTRATIONS (%) RELATIVE TO INITIAL CONCENTRATION, AFTER 29 DAY TIDAL SIMULATION, FOR POST-DREDGING CONDITIONS (POLLUTANT INITIALLY EVERYWHERE)	57
FIGURE 45:	PRE AND POST DREDGING VARIATION IN HYPOTHETICAL POLLUTANT CONCENTRATION AT WALSH POINT OVER 29 DAY SIMULATION	58
FIGURE 46:	PRE AND POST DREDGING VARIATION IN HYPOTHETICAL POLLUTANT CONCENTRATION AT TOURLE ST BRIDGE OVER 29 DAY SIMULATION	59
FIGURE 47:	PRE AND POST DREDGING VARIATION IN HYPOTHETICAL POLLUTANT CONCENTRATION AT IRONBARK CREEK OVER 29 DAY SIMULATION	59
FIGURE 48:	PRE AND POST DREDGING VARIATION IN HYPOTHETICAL POLLUTANT CONCENTRATION AT MOSCHETO CREEK OVER 29 DAY SIMULATION	60
FIGURE 49:	HYPOTHETICAL POLLUTANT CONCENTRATIONS (MG/L) AFTER 29 DAY TIDAL SIMULATION, FOR EXISTING CONDITIONS (100G/S POLLUTANT SOURCE IN SOUTH ARM)	61
FIGURE 50:	HYPOTHETICAL POLLUTANT CONCENTRATIONS (MG/L), AFTER 29 DAY TIDAL SIMULATION, FOR POST-DREDGING CONDITIONS (100G/S POLLUTANT SOURCE IN SOUTH ARM)	61
FIGURE 51:	POST-FLOOD DISSOLVED OXYGEN MEASUREMENTS OF SANDERSON ET AL (2002), FOR TWO DAYS IN MARCH 2001	63
FIGURE 52:	PREDICTED DEPTHS OF DEPOSITED SEDIMENT (MM) AT END OF DREDGING OPERATION	68
FIGURE 53:	PREDICTED DEPTHS OF DEPOSITED SEDIMENT (MM) AT END OF DREDGING OPERATION, IN SOUTH ARM	68
FIGURE 54:	SUSPENDED SEDIMENT CONCENTRATIONS (MG/L) AT END OF 29 DAY TIDAL SIMULATION	72

LIST OF TABLES

Page No.

	Page No.
TABLE 1: TIDAL PLANES FOR THE HUNTER ESTUARY DERIVED BY MHL (2002) AND MHL (1995)	4
TABLE 2: TIDAL VELOCITIES, DISCHARGES AND PRISMS RECORDED IN OCTOBER 1995 GAUGING EXERCISE DURING FLOOD TIDE (MHL, 1995)	5
TABLE 3: TIDAL VELOCITIES, DISCHARGES AND PRISMS RECORDED IN OCTOBER 1995 GAUGING EXERCISE DURING EBB TIDE (MHL, 1995)	5
TABLE 4: DESIGN PEAK FLOOD LEVELS FROM PWD (1994) FLOOD STUDY	9
TABLE 5: DESIGN PEAK FLOOD DISCHARGES FROM PWD (1994) FLOOD STUDY	10
TABLE 6: MAJOR POINT SOURCES OF NITROGEN AND PHOSPHORUS IN THE HUNTER ESTUARY (FROM MHL, 2002)	13
TABLE 7: PREDICTED SUSPENDED SEDIMENT CONCENTRATIONS AT HEXHAM FOR VARYING FLOWS	16
TABLE 8: PREDICTED CHANGES IN WATER LEVEL DUE TO DREDGING OF SOUTH ARM UNDER TIDAL CONDITIONS	23
TABLE 9: PREDICTED CHANGES (IN METRES) IN TIDAL PLANES DUE TO DREDGING OF SOUTH ARM	26
TABLE 10: PREDICTED CHANGES IN TIDAL VELOCITIES DUE TO DREDGING OF SOUTH ARM	26
TABLE 11: PREDICTED PRE AND POST DREDGING AVERAGE TIDAL FLOW RATES IN THE HUNTER ESTUARY	28
TABLE 12: PREDICTED PRE AND POST DREDGING MAXIMUM TIDAL FLOW RATES IN THE HUNTER ESTUARY	28
TABLE 13: AVERAGE AND PEAK MEAN TIDAL VELOCITIES ALONG TEMPORARY SHEET PILE WALL LOCATION AND AT TOURLE ST BRIDGE FOR EXISTING CONDITIONS AND WITH WALL IN PLACE	29
TABLE 14: PEAK MEAN VELOCITIES ALONG TEMPORARY SHEET PILE WALL LOCATION AND AT TOURLE ST BRIDGE FOR EXISTING CONDITIONS AND WITH WALL IN PLACE (5% AEP FLOOD)	36
TABLE 15: MAXIMUM INCREASES IN PEAK WATER LEVEL DUE TO DISCHARGE PIPELINE CONSTRUCTION	38
TABLE 16: PEAK FLOWS AND FLOOD HYDROGRAPH VOLUMES FOR THE 1% AEP FLOOD, FOR EXISTING AND POST DREDGING CONDITIONS (% OF TOTAL FOR EACH SECTION IN BRACKETS)	45
TABLE 17: PEAK FLOWS AND FLOOD HYDROGRAPH VOLUMES FOR THE 10% AEP FLOOD, FOR EXISTING AND POST DREDGING CONDITIONS (% OF EACH SECTION IN BRACKETS)	45
TABLE 18: PEAK MEAN VELOCITIES ALONG DREDGED PROFILE AND NEARBY UPSTREAM SITES FOR EXISTING AND POST-DREDGING CONDITIONS (1% AEP FLOOD)	49
TABLE 19: SALINITY VALUES AFTER 29 DAY SIMULATION AT VARIOUS LOCATIONS IN ESTUARY FOR EXISTING AND POST-DREDGING CONDITIONS	50

LIST OF TABLES

Page No.

TABLE 20:	HYPOTHETICAL POLLUTANT CONCENTRATIONS AFTER 29 DAY SIMULATION AT VARIOUS LOCATIONS IN ESTUARY FOR EXISTING AND POST-DREDGING CONDITIONS	58
-----------	---	----

1 INTRODUCTION

GHD engaged Patterson Britton & Partners to undertake various components of work as part of an Environmental Impact Statement (EIS) being prepared for proposed dredging of the South Arm of the Hunter River in NSW.

In this report, the potential impacts of the proposed dredging on tidal hydrodynamics, flooding and water quality are described. It is understood that this report will form an Appendix to the EIS document. Further details on the proposal can be found in the main EIS report and other supporting Appendices.

This report is structured as follows:

In Section 2, the existing environment of the Hunter estuary is described, with particular discussion on tidal hydrodynamics, flooding, salinity structure, water quality, sediment transport, and fish, prawns and oysters. The anthropogenic historical impacts to these aspects of the estuary are also outlined.

In Section 3, the impacts of the proposed dredging on tidal hydrodynamics, flooding, salinity structure, water quality, sediment transport, and fish, prawns and oysters are outlined. The effects on fish, prawns and oysters are related to the physical and water quality impacts, but are also identified separately given the commercial and ecological importance of these species.

Recommended mitigation measures are provided in Section 4.

The report conclusions are given in Section 5, with references provided in Section 6.

Further information is also provided in four Appendices. In **Appendix A**, a description of the RMA model suite is given. This numerical model was used as a tool to assist in interpretation of the tidal hydrodynamic, flooding and water quality impacts of the proposed dredging.

In **Appendix B**, the development, calibration and verification of the tidal hydrodynamic model is outlined. A flood model was also developed separately, as described in **Appendix C**.

Water quality simulations were also undertaken with the RMA model. Background information on this work is provided in **Appendix D**, in particular investigation of potentially altered salinity intrusion after dredging, and sediment transport associated with the dredging operation.

Note that impacts of stormwater (including leachate from contaminated sediments placed on land) on water quality are considered separately, and are not discussed in this particular report.

2 EXISTING ENVIRONMENT

2.1 GENERAL

Water levels, flows and water velocities vary within the Hunter River estuary due to a number of processes, including:

- astronomical tides, ocean storm surges¹, coastal trapped waves² and potential sea level rise transferring from the ocean up the estuary;
- freshwater flow, generally from rainfall-runoff; and,
- local wind setup³ within the estuary.

In general, in non-rainfall periods, astronomical tides are the major factor affecting the hydrodynamics of the main channel (Port Hunter, North Arm and South Arm) and fringing mangrove and saltmarsh areas of the Hunter River. In events of sufficient magnitude, rainfall-runoff generated freshwater flow is the dominant process governing the movement of water within the estuary. Wetland areas, which are rarely or never inundated by tides, rely on flood flows to be submerged.

Manly Hydraulics Laboratory [MHL] (2002) estimated that the annual water balance (change in volume) of the Hunter estuary was dominated by tidal inflow and outflow⁴ (85% of inflows and 99.9% of outflows). Other contributions to estuary inflow comprised catchment runoff (8%), groundwater flow (7%) and direct rainfall (0.1%). Evaporation made up the other very small proportion of outflow (0.1%). Note that the relative importance of tidal inflow and outflow diminishes moving upstream in the estuary.

Sanderson et al (2002) calculated the arithmetic mean of river flows from 1975-2000 to be 3120 ML/d, with a median of 720 ML/d. The latter value indicates that for most of the time the freshwater flow is much less than its mean value.

The existing environment of the Hunter estuary is described in more detail in subsequent sections. Specifics on the tidal hydrodynamics of the estuary are given in Section 2.2, while the flooding regime is described in Section 2.3. The salinity distribution of the Hunter estuary is affected by tidal and flooding processes as outlined in Section 2.4.

The general water quality of the estuary is described in Section 2.5, including discussion of nutrients and turbidity, which are two of the major water quality issues in the Hunter. The

¹ Storm surge comprises barometric setup and wind setup as measured at the open coast.

² Coastal trapped waves are low frequency sea level oscillations with periods exceeding about 4 days, causing ocean water level changes of between 0.1 and 0.4m.

³ Wind setup is the increase in mean water level caused by the “piling up” of water on a shoreline by wind action acting on the water surface.

⁴ Note that inflows are defined here as fluxes of water that flow into the estuary and increase its volume, such as flood tides and freshwater flows. Outflows are defined as fluxes of water that flow out of the estuary and decrease its volume, such as ebb tides and evaporation.

turbidity problem is discussed further in relation to sediment transport in the estuary in Section 2.6, including consideration of the effect of sedimentation on mangroves.

Particular details on fish, prawns and oysters are provided in Section 2.7, given the ecological and commercial importance of these species, and sensitivity to water quality.

Finally, in Section 2.8, a summary of the historical modifications to the estuary is given, which may have impacted on the tidal hydrodynamics, flooding and water quality of the estuary.

2.2 TIDAL HYDRODYNAMICS

The existing tidal behaviour of the Hunter River estuary has been described by MHL (2002). As applies to the NSW coast in general, the tides acting at the entrance to the estuary are semi-diurnal⁵ (with significant diurnal inequality⁶), with a strong spring-neap⁷ cycle. An example of the water level record near the entrance to the Hunter River over a 28 day period (with low freshwater flows) is shown in **Figure 1**. The location of the measurements was at the Pilot Station.

Tides in the Hunter estuary vary from the ocean entrance to the tidal limits, generally with a gradual reduction in the mean tidal range proceeding upstream (excluding slight amplification within the Williams and Paterson Rivers). The tidal limit in the Hunter River is approximately at Oakhampton (64km upstream from the ocean), with tides also intruding into major tributaries including the Paterson River (as far as Gostwyck, about 73km from the ocean) and Williams River (as far as the weir at Seaham, about 46km from the ocean).

The general reduction in tidal range moving upstream can be understood in terms of tidal excursion, the distance a water particle travels over a tidal cycle. In the lower estuary, the tidal excursion is about 10km, while at Morpeth it reduces to around 3km (MHL, 2002).

Numerous tributary creeks are also tidal, including Wallis Creek, Fishery Creek, Ironbark Creek, Throsby Creek, Styx Creek and Cottage Creek. However, floodgates at the entrance to the Wallis and Fishery Creek system, and also Ironbark Creek, significantly attenuate tidal intrusion upstream of the gates.

There is also a lag in the times of high and low water moving upstream (that is, the peaks and troughs occur later compared to the entrance), with the relative delay greater for low tides.

⁵ Semi-diurnal tides have high and low water approximately equally spaced in time and occurring twice daily (that is, on average, there are two high tides and two low tides in any 24 hour period).

⁶ Diurnal inequality is the difference in height of the two high waters or the two low waters of each tidal day.

⁷ Spring tides occur twice per month (during new or full moons) and result in higher high tides and lower low tides (that is, a larger tidal range, compared to the average). Neap tides also occur twice per month (during quarter moons) and result in lower high tides and higher low tides (that is, a smaller tidal range, compared to the average).

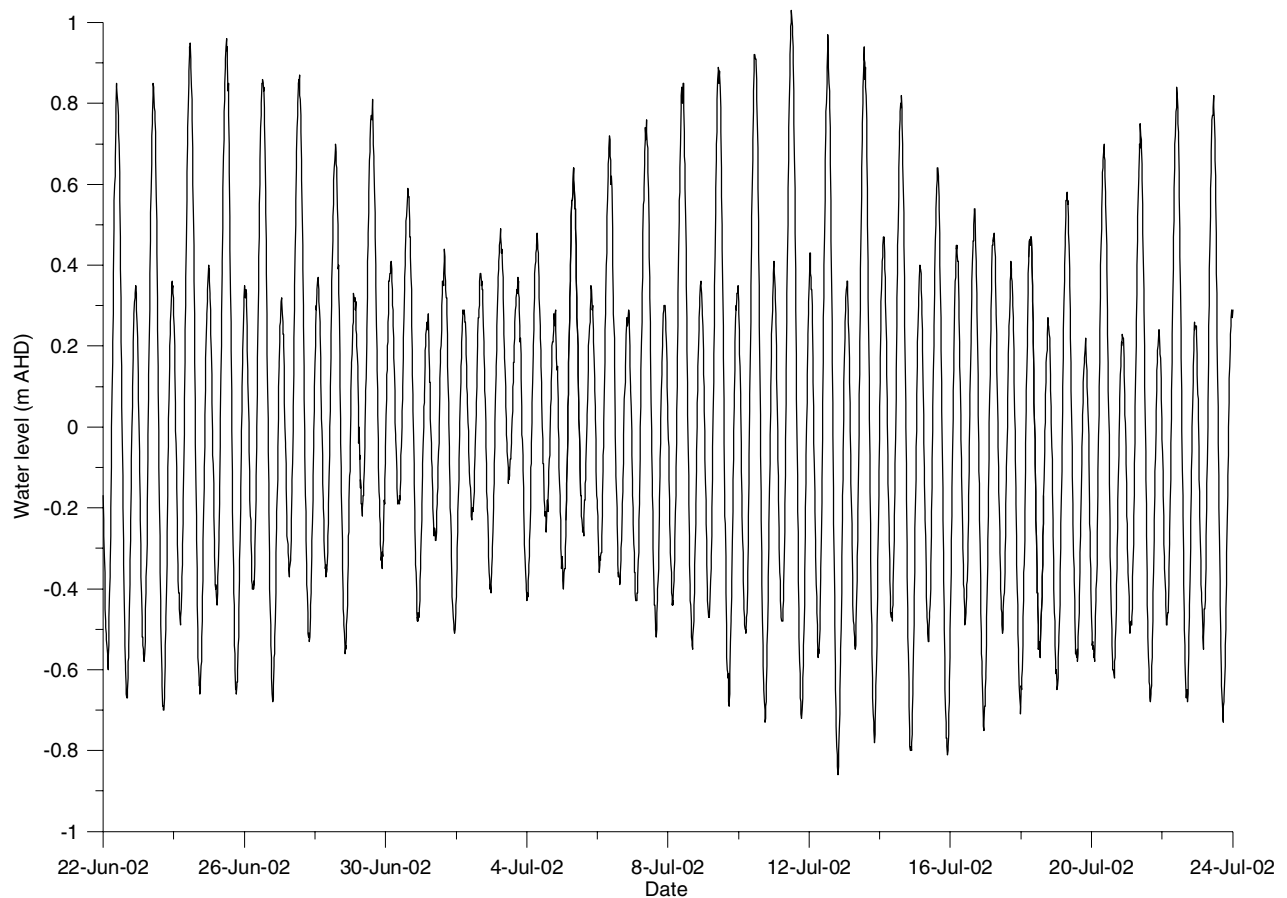


Figure 1: Water level at Hunter River entrance during typical tidal conditions, indicating semi-diurnal, diurnal inequality and spring-neap features

A summary of the tidal planes derived by MHL (2002) for the Hunter River estuary are shown in **Table 1**. Note that MHW is Mean High Water and MLW is Mean Low Water, and the Mean Range is given by MHW-MLW⁸. Lags given are relative to the ocean entrance.

Table 1: Tidal planes for the Hunter estuary derived by MHL (2002) and MHL (1995)

River or Creek	Location	Distance from ocean (km)	MHW (m AHD)	MLW (m AHD)	Mean Range (m)	High Tide Lag (hours)	Low Tide Lag (hours)
Hunter River	Stockton Bridge	6	0.54	-0.51	1.05	0.08	0.54
Hunter River	Hexham Bridge	20	0.61	-0.39	1.00	0.58	1.4
Williams River	Raymond Terrace	29	0.63	-0.28	0.91	1.3	2.5
Hunter River	Green Rocks	40	0.56	-0.28	0.84	-	-
Williams River	Seaham	45	0.62	-0.34	0.96	1.8	2.9
Hunter River	Morpeth	48	0.54	-0.15	0.70	3.5	4.2
Paterson River	Hinton Bridge	48	0.52	-0.17	0.69	3.0	4.2
Wallis Creek	Downstream of Floodgates	55	0.52	0.11	0.41	3.6	6.3
Hunter River	Belmore Bridge	60	0.57	0.18	0.39	3.8	6.7
Paterson River	Railway Bridge	63	0.61	-0.03	0.64	4.3	5.7

⁸ Note that AHD is Australian Height Datum, with 0m AHD approximately equal to mean sea level.

The lags given in **Table 1** are based on a gauging exercise carried out on 9 October 1995 as reported by MHL (1995), representing only one recorded high tide and the average of two recorded low tides. Other statistics given in **Table 1** were derived from MHL (2002), based on a harmonic analysis of hourly observations over at least a 30 day period.

Based on the tidal gauging carried out in October 1995 (MHL, 1995), tidal velocities, discharges and tidal prisms⁹ were recorded at various locations in the estuary as shown in **Table 2**.

Table 2: Tidal velocities, discharges and prisms recorded in October 1995 gauging exercise during flood tide (MHL, 1995)

River	Location	Distance from ocean (km)	Tidal Range (m)	Maximum Velocity (m/s)	Maximum Discharge (m ³ /s)	Tidal Prism (m ³ × 10 ⁶)	% of Entrance Prism
Hunter	Walsh Point (North Arm)	5		0.94	1680	23.7	66
Hunter	Walsh Point (South Arm)	5		0.43	360	5.4	15
Williams	Raymond Terrace	29	1.33	0.61	190	2.4	7
Hunter	Raymond Terrace	29		0.61	210	2.9	8
Hunter	Morpeth	48	0.95	0.58	60	0.7	2
Paterson	Hinton Bridge	48	0.93	0.65	100	1.4	4
Paterson	Paterson	55		0.29	30	0.3	1
Hunter	Bolwarra	60	0.22	0.05	0.5	0.0	0.0

Table 3: Tidal velocities, discharges and prisms recorded in October 1995 gauging exercise during ebb tide (MHL, 1995)

River	Location	Distance from ocean (km)	Tidal Range (m)	Maximum Velocity (m/s)	Maximum Discharge (m ³ /s)	Tidal Prism (m ³ × 10 ⁶)	% of Entrance Prism
Hunter	Walsh Point (North Arm)	5		0.99	1550	25.8	68
Hunter	Walsh Point (South Arm)	5		0.26	490	7.9	21
Williams	Raymond Terrace	29	1.33	0.51	180	2.4	6
Hunter	Raymond Terrace	29		0.56	200	3.2	8
Hunter	Morpeth	48	0.94	0.54	50	0.7	2
Paterson	Hinton Bridge	48	0.92	0.56	70	1.2	3
Paterson	Paterson	55		0.26	20	0.4	1
Hunter	Bolwarra	60	0.22	0.29	3	0.1	0.3

It can be seen that, during this exercise, maximum tidal velocities were around 1 m/s (near the ocean entrance). The North Arm was found to dominate the tidal prism, carrying about 80% of the tidal flow at Walsh Point, with the South Arm conveying about 20%. The upstream tributaries had relatively small contributions to the tidal prism, namely about 7% in the Williams, 4% in the Paterson and 2% in the Hunter upstream of Morpeth (relative to the entrance).

Maximum tidal velocities reduced to about half of the entrance values by Raymond Terrace, with the tidal prism having reduced to only about 15% of the entrance prism at this location (including the contributions of both the Hunter and Williams Rivers).

⁹ The tidal prism is the total volume of water exchanged at a particular cross section during a complete tidal cycle.

2.3 FLOODING

Flooding behaviour in the Hunter estuary has been modified substantially since European settlement, due to construction of levees, spillways, canals, floodgates, and diversion banks. Much of these works were undertaken as part of the Lower Hunter Valley Flood Mitigation Scheme, in almost immediate response to the largest flood that has occurred since European settlement, which occurred in 1955. In total, 160km of levees and spillways, 111km of flood canals, 175 floodgates, 14km of bank protection works and 40km of control and diversion banks were built as part of this scheme (MHL, 2002).

Most of the works were constructed between Morpeth and Hexham. There was also a levee created from Tomago to the eastern side of Fullerton Cove.

In higher annual exceedance probability (AEP) flood events, the flood flow is contained within the main channel of the river and surrounding levees. As the flood severity increases (AEP reduces), floodwaters begin to overtop the natural and constructed levees and flow across the floodplain. For the 20% AEP and rarer events, the majority of flow is across the floodplain. The flood extents in the 1% AEP event are shown in **Figure 2**.

As described by MHL (2002) and Patterson Britton & Partners (1996), in high magnitude events (1% AEP), only about 30% of the flood flow is carried in the main channel upstream of Purgatory Creek (near Hexham), with 70% carried by the Millers Forest and Woodberry Swamp floodplains. However, floodwaters are constricted at Purgatory Creek by the New England Highway and North Coast Railway, as well as high ground at Tarro. Some flow is able to pass through culverts under the Highway and Railway (in particular at the Tarro control on the Highway), or pass over these in floods larger than the 10% AEP, with up to about 30% of the flow entering Hexham Swamp in the 1% AEP event¹⁰. The flow distribution in the vicinity of Hexham is shown in **Figure 3**.

Therefore, much of the overbank flow is forced back into the main channel just upstream of Hexham. This flow tends to spill over Kooragang Island and Tomago Swamp, which are both completely inundated (excluding the southern part of the Island) during moderate to major floods (exceeding 10% AEP). About 65% of the flood flow is overbank across Kooragang Island at the peak of the 1% AEP event, emphasising its importance in flood conveyance. The flow distribution around Kooragang Island at the peak of the 1% AEP event is shown in **Figure 4**.

The southern part of Kooragang Island is protected from floodwaters by a large railway embankment, forcing far more floodwaters into the North Arm compared to the South Arm. At Walsh Point, about 75-80% of the flood flow is carried in the North Arm, with 20-25% conveyed by the South Arm. Only about 6% of the flow goes overbank at Hexham and travels through Tomago Swamp to Fullerton Cove.

¹⁰ The Ironbark Creek floodgates and levees along the south bank of the South Arm prevent floods up to about the 2% AEP from entering Hexham Swamp via this flow path (PWD, 1994).

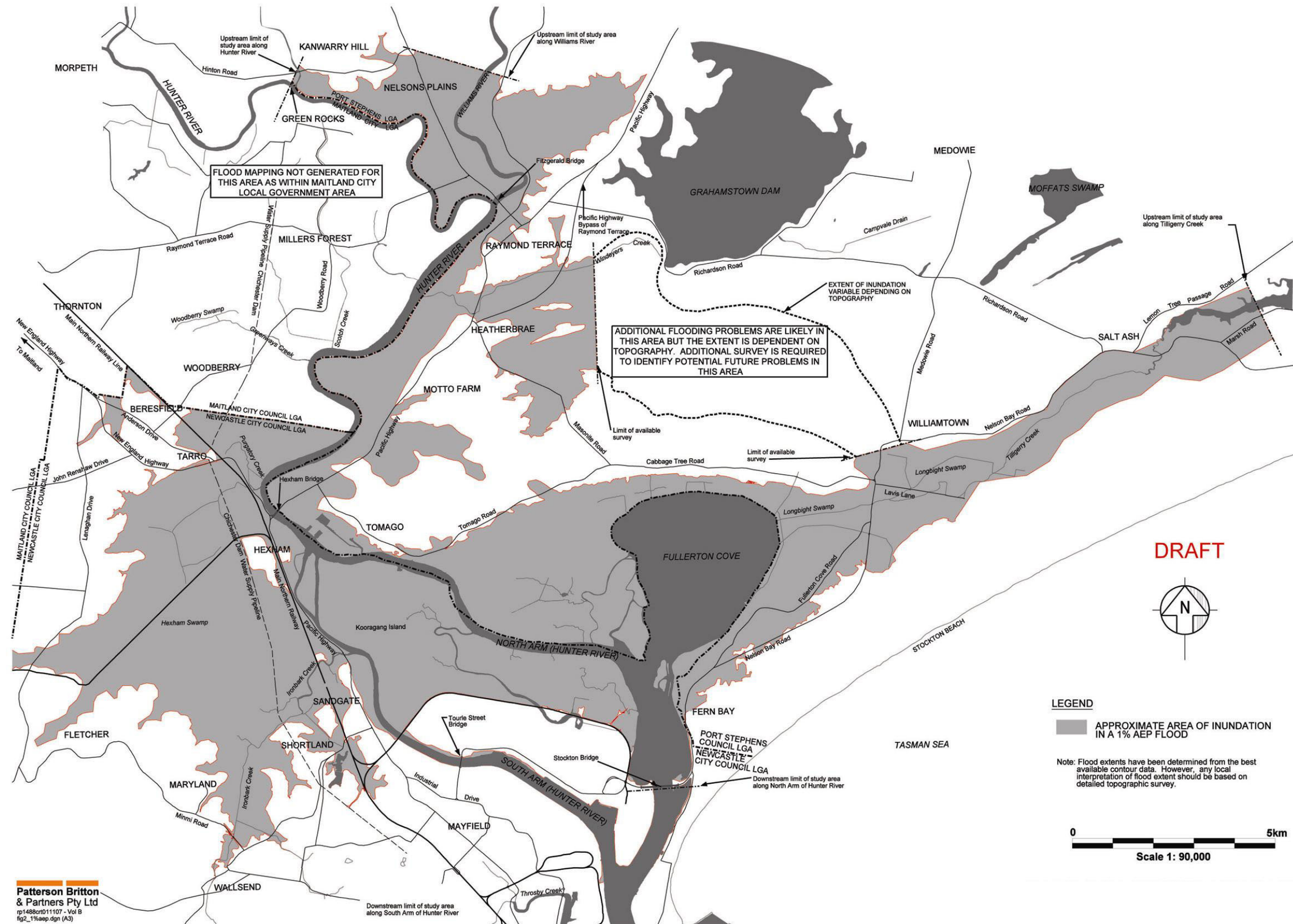


Figure 2: Extent of the 1% AEP Flood (from Patterson Britton & Partners, 2001b)

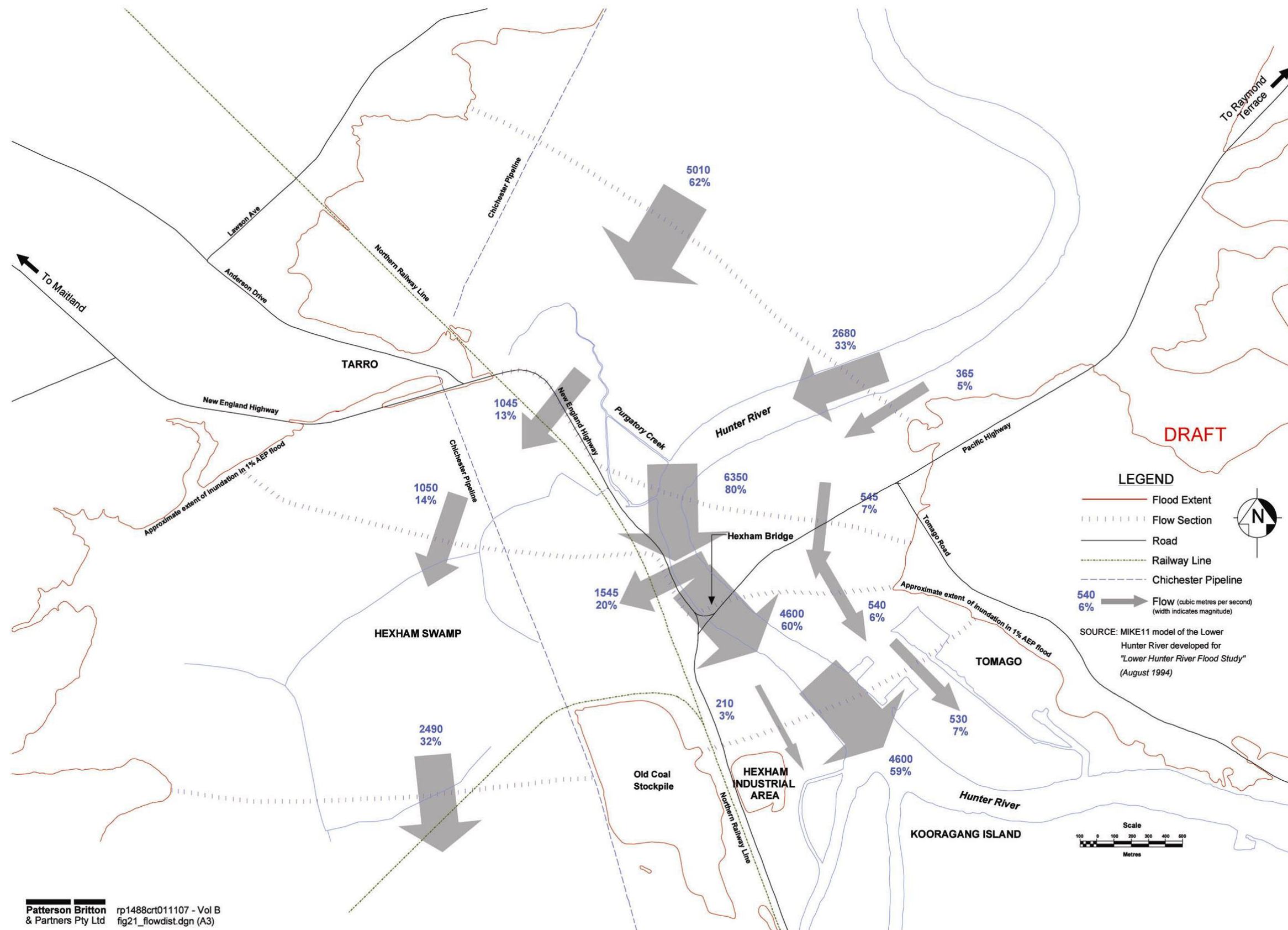


Figure 3: Conceptual representation of flow distribution at Hexham at peak of the 1% AEP flood (from Patterson Britton & Partners, 2001b)

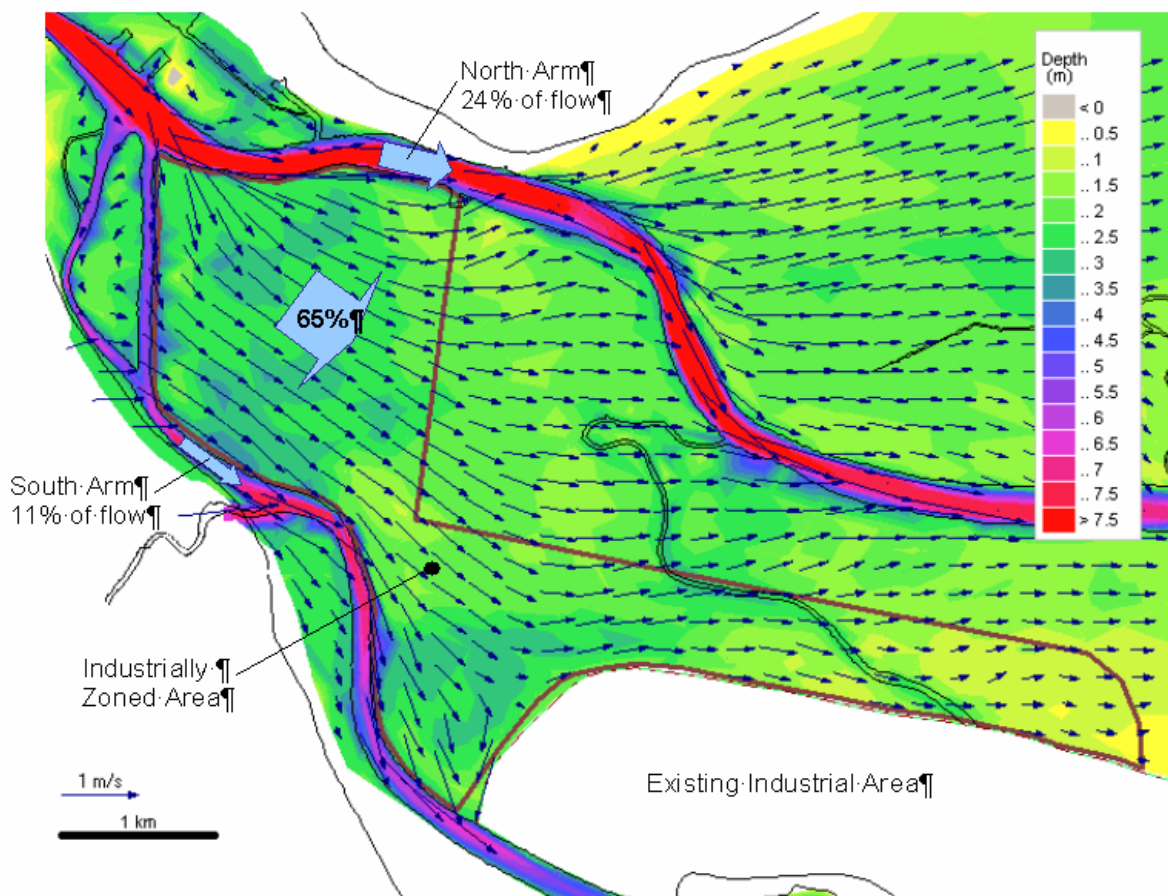


Figure 4: Flow distribution around Kooragang Island at peak of 1% AEP event (from Patterson Britton & Partners, 2001a)

The most recent flood study of the estuary was undertaken by the Public Works Department [PWD] (1994), covering the area from Green Rocks to the ocean entrance. Green Rocks is 40km upstream from the entrance, upstream of the Williams River junction. The design peak flood levels determined in this study for various AEP events are shown in **Table 4**, while the design peak discharges are shown in **Table 5**.

Table 4: Design peak flood levels from PWD (1994) flood study

Location	Peak Flood Level (m AHD) for Design Event AEP				
	20%	10%	5%	2%	1%
Green Rocks	3.49	4.12	4.57	4.91	5.55
Raymond Terrace	2.12	2.71	3.12	3.70	4.76
Hexham Bridge	1.44	1.99	2.45	2.81	3.73
Stockton Bridge	1.21	1.24	1.27	1.31	1.61
Port Newcastle	1.21	1.24	1.27	1.31	1.34

Table 5: Design peak flood discharges from PWD (1994) flood study

Location	Peak Discharge (m ³ /s) for Design Event AEP				
	20%	10%	5%	2%	1%
Hunter River upstream of Green Rocks	1100	2000	3300	4600	6200
Williams River upstream of Raymond Terrace	400	1000	1200	1200	1100

Note that the highest astronomical tide at Port Newcastle is 1.0m AHD, which would occur once every 18.6 years if there were no non-astronomical water level influences. Storm surge (barometric and wind setup), wave setup, coastal trapped waves and freshwater flow may all increase water levels above the predicted astronomical tide levels, with the maximum combination of items expected to be less than 0.4m¹¹. The peak water levels derived in **Table 4** for Port Newcastle were based on an analysis of recorded water levels over a 24 year period (MHL, 2002).

Following on from the PWD (1994) Flood Study, Patterson Britton & Partners (1996) completed a Floodplain Management Study. One of the most hydraulically effective management options assessed for reducing flood levels was dredging the North Arm to -11m AHD, which was estimated to reduce flood levels downstream of Hexham by 0.4-0.6m over the full range of floods.

2.4 SALINITY STRUCTURE

Sanderson et al (2002) measured vertical profiles of salinity (and temperature, turbidity and dissolved oxygen) at various locations in the Hunter estuary on 23 days in 2001, from January to April. Measurements were taken at a total of 42 locations, from the entrance as far upstream as Duckenfield (about 41km upstream from the entrance).

The measurements were generally made at high tide, covering a spring-neap tidal cycle coinciding with low riverine freshwater inputs, and immediately prior to, during and following a minor flood (peak flow about 200,000 ML/d, approximately a 10-20% AEP event) on 9 March 2001.

The spring-neap tidal cycle was observed to only play a minor role in modifying estuarine salinities, compared to river freshwater flows. Flows of sufficient magnitude (floods) were found to discharge most of the salt out of the estuary, excluding the salt in deep dredged areas.

After floods, the salt was found to slowly intrude upstream. Turbulent mixing through the water column, as well as wind generated mixing, was found to generally mix the salt in the vertical. That is, the estuary was described as well mixed, with very little stratification during low freshwater flows.

Sanderson et al (2002) derived empirical relationships to determine the position along the estuary of the 10, 15, 20 and 30 ppt salinity isohalines as a function of river flow on the previous day. These were derived for flows exceeding 200,000 ML/d (2 GL/d). The relationships are shown graphically in **Figure 5**.

¹¹ This figure was dominated by storm surge. At the downstream end of the estuary, freshwater flow was considered to have little influence. The highest recorded water level at Port Newcastle was 1.37m AHD, measured in May 1974, during a non-flood period. The peak water level at Port Newcastle in the highest recorded flood of February 1955 was 1.34m AHD.

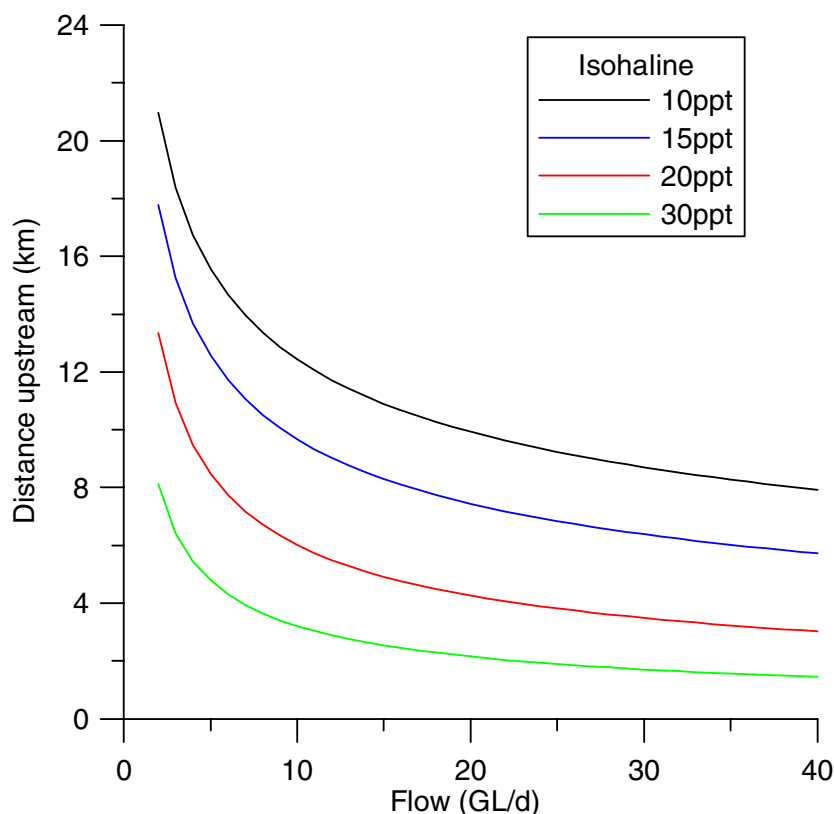


Figure 5: Hunter estuary salinity distribution as a function of flow as derived by Sanderson et al (2002)

Sanderson et al (2002) applied these relationships to the 1975-2000 flow record, and found that the 10ppt isohaline was most frequently around 24km upstream. However, given that the freshwater flow is less than 200,000 ML/d for most of the time, Sanderson et al (2002) considered that salinity intrusion is likely to be overestimated during the most prevalent low flow conditions using these equations.

To provide a potentially improved estimate of historical salinity intrusion, Sanderson et al (2002) applied a simple advection-diffusion relationship based on an idealised channel bathymetry to the 1975-2000 flow record. The average salinity distribution (with \pm one standard deviation) determined in this manner is shown in **Figure 6**. According to MHL (2002), salinities upstream of Raymond Terrace in the Hunter River are typically about 0.2 to 0.5 ppt.

Note also that saline discharges from coal mines and electricity generators in the Hunter River are managed through the Hunter River Salinity Trading Scheme. In this Scheme, saline discharges are scheduled to occur during relatively high freshwater flows to minimise the salinity increases in the river, and therefore reduce impacts on irrigators and other water users, as well as aquatic ecosystems.

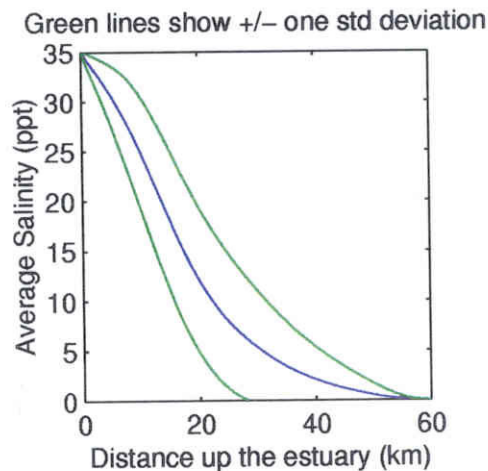


Figure 6: Average salinity distribution along Hunter estuary from 1975-2000, based on simple advection-diffusion relationship, from Sanderson et al (2002)

2.5 WATER QUALITY

The processes controlling exchange and mixing within the Hunter estuary comprise (MHL, 2002):

- freshwater flows displacing the volume of the estuary, especially evident during floods;
- salt intrusion, density driven flow and tidal pumping propagating against the freshwater flow, evident after floods; and,
- upstream transport of salt by tidal diffusion during sustained periods of low flow.

At the mean freshwater flow rate, the estimated estuary flushing time was about 32 days.

The measurements of Sanderson et al (2002), as discussed in Section 2.4, indicated that:

- temperature distributions in the Hunter estuary were usually inversely related to those of salinity (with temperature generally increasing moving upstream), except for heat fluxes associated with warm or cold weather;
- turbidity was often high in upstream areas and during increased freshwater flows; and,
- dissolved oxygen levels were often low in the upper estuary following increased freshwater flows, as material deposited in sediments was oxidised.

Sanderson et al (2002) considered that salinity had a much greater effect on density than temperature in the Hunter estuary. Given that temperatures generally increase (except in Winter) and salinities decrease moving upstream, densities usually decrease moving upstream.

Vertical stratification may limit mixing and has implications for water quality including depletion of dissolved oxygen in deep water, algal blooms in surface waters and sediment deposition at the freshwater/saltwater interface¹² (MHL, 2002). As reported in Section 2.4, the vertical salinity stratification of the Hunter estuary is generally weak; it only typically occurs for a few days after

¹² The location of the fresh/salt interface dictates where maximum sediment deposition occurs in the estuary.

flood events. However, in backwater areas where turbulent mixing is weaker, the likelihood of vertical stratification persisting for longer is far greater.

As a contribution to the MHL (2002) report, Sanderson and Redden (2001) compiled 28 years of water quality measurements made by Hunter Water Corporation, the NSW Environment Protection Authority, and Maitland City Council into a database, and analysed the measurements. The data set included 25 water quality variables, collected at irregular locations and times.

In summary, the major water quality issues in the estuary were found to be:

- excessive levels of nutrients¹³;
- high turbidity levels; and,
- high concentrations of chlorophyll-a¹⁴.

For these variables, ANZECC and ARMCANZ (2000) water quality guidelines (aquatic ecosystem trigger levels or recreational guidelines) were exceeded.

It was considered that greater control and management of the diffuse and point source production of nutrients was required to protect the aquatic ecosystem, recreational and aquaculture values of the estuary. MHL (2002) estimated that point sources of nutrients were far more significant than diffuse catchment runoff sources, with about 98% of total nitrogen mass and 97% of total phosphorus mass entering the estuary predicted to be coming from point sources. The point sources were dominated by the industries listed in **Table 6**. Note that the point loading of total nitrogen into the estuary is about 7 times larger than the total phosphorus load.

Table 6: Major point sources of nitrogen and phosphorus in the Hunter estuary (from MHL, 2002)

Industry	Percentage of total point source load	
	Total Nitrogen	Total Phosphorus
Incitec Ltd fertiliser manufacturing, Kooragang Island	63%	-
Steggles poultry processing, Beresfield	22%	33%
Morpeth Wastewater Treatment Works	11%	35%
Raymond Terrace Wastewater Treatment Works	4%	11%
Shortland Wastewater Treatment Works	-	13%
Stockton Wastewater Treatment Works	-	8%

Other observations of MHL (2002) on the work of Sanderson and Redden (2001) included that:

- as per Sanderson et al (2002), dissolved oxygen levels reduced with large freshwater flows, with concentrations also low in late summer in the upper estuary due to higher temperatures;
- mean dissolved oxygen concentrations over the river were 6.4mg/L with increasing concentrations moving downstream;

¹³ Specifically, total nitrogen, soluble reactive phosphorus, total phosphorus, ammonia and oxidised nitrogen exceeded the ANZECC and ARMCANZ (2000) guidelines.

¹⁴ Chlorophyll-a generally peaked in February-March.

- high turbidity values were common, with turbidity values highest during large freshwater flows; and,
- the mean turbidity value was 15 NTU, with increasing values moving upstream;

Turbidity was considered to be visually unappealing, symptomatic of land degradation and probably impacting many benthic processes. However, high turbidity was also predicted to limit light penetration into the water and therefore limit phytoplankton blooms and growth of undesirable plants and algae. Given the high nutrient loads into the Hunter estuary, high turbidity levels were therefore considered to have some desirable side effects as far as phytoplankton control was concerned.

The negative impacts of high turbidity could include effects on seagrass, although there is little seagrass present in the Hunter estuary, generally being restricted to Fullerton Cove. It has also been suggested that high turbidity is the reason for the small numbers of oysters present in the Hunter. Increases in turbidity may also affect the foraging behaviour of fish, and suspended sediments may abrade the protective mucus coats on fish, thereby increasing their susceptibility to disease, clogging gill filaments, or suffocating the fish (MHL, 2002).

2.6 SEDIMENT TRANSPORT

2.6.1 Sediment Properties

Patterson Britton & Partners (1989) found that between 30-70% of surface sediments in the port area of the Hunter River were clays and fine silts, with a grain size less than 0.005mm. For 21 samples collected, the median grain size, including all material (that is the sand fraction as well), was between 0.001 and 0.05mm.

Settling tests were also carried out on two of these samples (or at least the silt fractions) as reported in Patterson Britton & Partners (1989). The settling rates in seawater were about 0.01 and 0.05 mm/s at 9% and 2% solids concentrations (by volume) respectively. Note that for cohesive sediment in saline water there is no means of analytically predicting fall velocities based on grain size, since settling rates depend on the degree of flocculation achieved, which in turn depends on the electrochemical nature of the cohesive sediment.

The Department of Public Works (1967) also determined fall velocities for Hunter estuary sediments, in both fresh water and water with varying salinities, and compared these to results obtained for the Thames estuary and San Francisco Bay. However, only limited details are provided in the report. A fall velocity of 0.7 mm/s was reported for silt particles in quiescent seawater, although it is not certain how the material was graded before this was derived.

2.6.2 Sediment Budget

Land clearing and flood mitigation works have altered the sediment transport processes in the Hunter catchment. In general, channel infilling has been accelerated due to the resulting catchment erosion and impedance of sediment transport, and this represents a significant threat to continued bank erosion. Bank erosion has also been exacerbated by clearing of riparian vegetation and widespread cattle access to banks.

Thomas and Druery (1996) estimated that most sediment had been deposited between Singleton and Maitland during large floods. However, they noted evidence that this sediment was moving downstream towards Raymond Terrace, with the movement manifest as erosion between Maitland and Morpeth and accretion between Morpeth and Hexham.

MHL (2002), by comparing 1857 and 1990 hydrosurveys, estimated that the South Arm of the Hunter had become shallower between 10km (near Tourle St Bridge) and 20km (near Hexham) upstream from the entrance, the latter being the limit of the comparison.

MHL (2002) also estimated that:

- the typical suspended sediment influx to downstream of Hexham was about 1 million tonnes per year, with a minimum bedload sediment flux of 25,000 tonnes per year;
- the average amount of sediment accumulating in the Hunter estuary downstream of Hexham (excluding the port area) was about 100,000 tonnes per year, based on measured bed elevation increases of 2.3 mm/year at Fullerton Cove;
- maintenance dredging indicated that about 400,000 tonnes of sediment accumulated in the port each year; and,
- about 500,000 tonnes of sediment discharged from the Hunter estuary and accumulated in a large mud deposit offshore each year.

Patterson Britton & Partners (1989) noted that the deepened areas of the port had a high sediment trapping efficiency. This would mainly be due to the reduced velocities with the increased cross-sectional areas, as well as the longitudinal salinity density gradient.

2.6.3 Suspended Sediment Concentrations

The effects of turbidity (related to suspended sediment concentration) on water quality, and its distribution in the Hunter estuary, were discussed in Section 2.5.

Patterson Britton & Partners (1989) described the suspended sediment concentrations in the Hunter estuary for various freshwater flow magnitudes, namely:

- Low freshwater flows, during which negligible quantities of sediment were estimated to be carried downstream. Suspended sediment concentrations were estimated to be about 4 to 30 mg/L in the port area during these periods. The highest concentrations were predicted to be in the vicinity of Hexham, near the limit of saline intrusion.
- Wet weather flows (not extreme floods), during which there is concentrated deposition of sediment in the port area. In this case, the saline limit would be in the vicinity of the port. As flows increase, a greater amount of sediment would be carried out to sea, typically in a fresh surface layer a few metres thick. For example, measurements in June 1989 indicated the suspended sediment concentration at the Hunter mouth was about 210 mg/L in the top 4m of the water column, with the lower layer at about 60 mg/L.
- Extreme floods, during which the estuary could be purged of all saline water, and virtually no deposition would occur within it. That is, medium floods are likely to cause greater sedimentation in the port compared to large floods.

Patterson Britton & Partners (1989) devised a suspended sediment rating curve at Hexham Bridge, adopting the relationship:

$$C = 3.39 \times 10^{-6} Q^{1.17}$$

where C is the section averaged concentration of suspended sediment (g/L), and Q is the freshwater flow at Hexham Bridge (ML/d).

Suspended sediment concentrations at Hexham predicted using this relationship are shown in **Table 7** for a variety of flows ranging from the median flow to the peak of a large flood. Note that flow magnitudes were derived from MHL (2002).

Table 7: Predicted suspended sediment concentrations at Hexham for varying flows

Flow Type	Flow Value (ML/d)	Predicted Suspended Sediment Concentration at Hexham (mg/L)
Median	720	7
Mean	3120	40
95 th percentile	11,920	200
Peak of small flood	20,000	365
Peak of large flood	200,000	5400

2.6.4 Effect of Sedimentation on Mangroves

In some areas of NSW, mangrove areas have declined due to clearing or reclamation and changes in water flow attributable to adjacent developments. In other areas, mangroves are increasing due to colonisation on the build up of sediment (NSW Fisheries, 1999).

For example, in the Parramatta River, mangroves have increased since European settlement, associated with sedimentation caused by urbanisation and catchment clearing. That is, the mangroves have tended to regenerate by colonising the mud flats created by increased sedimentation. There was no evidence of mangroves in the upper river from Subiaco Creek to Parramatta until the 1870's (McLoughlin, 2000). Furthermore, landward mangrove growth has occurred in conjunction with a loss of saltmarsh communities, an established trend in south-east Australia (Saintilan and Williams, 1999; Harty and Cheng, 2002).

In the Hunter, mangrove areas within the estuary have increased since the 1950's, outside areas that have had mangroves removed for industrial and port facilities. This is likely to be due to this same phenomenon of colonisation of sediment flats as described, and has also occurred along with the loss of saltmarsh communities. The main areas of mangrove expansion have been along the North Arm near Tomago, Fullerton Cove and Stockton, and also on parts of Kooragang Island (MHL, 2002).

However, it should be noted that sedimentation does not always benefit mangroves. For example, West et al (1983) noted mangrove death in the Hawkesbury River due to rapid sedimentation covering pneumatophores.

Ellison (1999) also found that excess input of sediment to mangroves could cause reduced vigour or death of trees owing to root smothering. She described 26 cases from the literature where

mangroves had been adversely affected by sediment burial of roots. The impacts depended on the amount and type of sedimentation, and the species involved. However, there was insufficient data to establish specific tolerances.

Ellison (1999) summarised numerous measurements of sedimentation rates in thriving mangrove forests, and found that at most sites the accretion rate was less than 5mm/year, with a maximum of 10mm/year. She also noted 15 studies in which measurements of sedimentation depths had been made where mangroves had died or were stressed as a result of the accretion. The total depth of deposition at sites where mangroves had died was between 5cm and 200cm, with an average depth of about 40cm. Two-thirds of these measurements were for *Avicennia* species. *Avicennia marina* is the dominant mangrove species in the Hunter estuary (MHL, 2002).

2.7 FISH, PRAWNS AND OYSTERS

Over 100 species of fresh and saltwater fish have been recorded in the Hunter estuary since 1975, of which 32 species are economically important. Mangrove areas are generally known to provide excellent fish habitat (Lynch and Burchmore, 2002), and have been specifically identified along with saltmarsh, *Phragmites australis* reed beds and freshwater wetlands as being important habitat and nursery areas for fish and prawns in the Hunter (MHL, 2002).

The most commercially important fishery in the Hunter is the estuarine finfish¹⁵ industry, being the tenth largest in NSW. The catch is dominated by sea mullet. Fish trawling is not permitted anywhere in the estuary, with a variety of alternative methods used (MHL, 2002).

Prawns are an important commercial operation in the Hunter, being only one of five estuaries in NSW where prawn trawling is permitted. Prawns move around the estuary depending on the stage in their life cycle. Breeding takes place in the ocean, with post-larval prawns migrating up the estuary to less saline areas. The extent of migration is typically to around the 20 ppt isohaline, but some prawns travel upstream of Maitland where salinities are less than 1 ppt (MHL, 2002).

In the Hunter, the school prawn (*Metapenaeus macleayi*) enters the estuary between December and April. They grow rapidly in September, typically moving out to the ocean to breed in response to flood events from October onwards through summer. It is during this downstream movement that the largest catches are made, both in the Hunter and offshore at Stockton Bight (MHL, 2002).

Oyster leases include Fern Bay in the North Arm (just north of Stockton). Oysters also colonise a variety of artificial rock walls such as much of the southern shoreline of the South Arm, and numerous bridge and wharf piles. However, the high turbidity of the Hunter has been suggested as a factor in the relatively small numbers of oysters found in the estuary. The South Arm is closed to the taking of oysters and mussels (MHL, 2002).

The discharge of contaminants into the Hunter River has been occurring for many decades. The oyster industry was devastated around 1965 when oysters were contaminated by industrial

¹⁵ Finfish is a term that refers to sharks, some rays and bony fishes that have gills and live in water, and are commercially harvestable.

pollution, and prawning has also been affected by apparent pollution from industry. Prawns caught in the South Arm are known to have a “gassy” taste, affecting their value (MHL, 2002).

2.8 HISTORICAL IMPACTS

2.8.1 Summary of Impacts

The Hunter estuary has been modified by a number of human impacts in the past. The most significant of these impacts in terms of tidal hydrodynamics, flooding and water quality are:

- entrance breakwaters/groynes constructed for navigation;
- dredging of the lower estuary for port infrastructure (this and above point discussed further in Section 2.8.2);
- levees constructed for flood mitigation;
- construction of floodgates and drainage channels to convert low lying waterlogged lands to agricultural use (this and above point discussed further in Section 2.8.3);
- reclamation to amalgamate up to 10 islands into the single Kooragang Island (see Section 2.8.4); and,
- destruction of riparian vegetation (see Section 2.8.5).

As noted above, further details on these impacts are provided in subsequent Sections.

MHL (2002) attempted a harmonic analysis of water level records from Stockton Bridge to the Paterson River junction, based on the 1955 and 2000 data sets. This was undertaken to investigate the effect of estuary changes in this 45 year period (such as dredging, levee bank construction and floodgate construction) on tidal hydrodynamics.

They found that the mean spring tide range had increased by up to 0.2m between 1955 and 2000, with the mean neap range unchanged. The difference between the HHWSS (High High Water Solstices Springs) and ISLW (Indian Springs Low Water) had also increased by up to 0.4m between 1955 and 2000. The effect on the mean spring range was most pronounced at a distance between 20km and 40km upstream from the ocean (between Hexham Bridge and Green Rocks).

MHL (2002) postulated that the alteration to the mean spring range was probably most likely mainly due to construction of floodgates, particularly noting those in the Hexham Swamp area. However, MHL (2002) also referred to Umwelt (2002), who suggested harbour dredging had the dominant impact on tides at Hexham between 1950 and 1990.

Umwelt (2002) also reviewed historical tidal plane information, and found that at Stockton Bridge and Hexham Bridge, the range of mean tides and neap tides had not altered between the 1950's and the 1990's. They found that the spring range had increased by 0.05m at Stockton and 0.13m at Hexham. The solstice range (HHWSS-ISLW) was also found to have increased by 0.1m at Stockton and 0.25m at Hexham. It was estimated that the tidal exchange through the entrance had increased by about 5% between the 1950's and 1990's.

The Department of Public Works (1967) reported on a tidal limit survey of January 1958. They found the tidal limit in the Hunter River was about 53km upstream from the entrance, near

Maitland. The tidal limit in the Paterson River was at Gostwyck, while in the Williams River the limit was at Mill Rocks (the weir at Seaham had not been constructed).

Given that MHL (2002) found the tidal limit in the Hunter was about 64km upstream from the entrance at Oakhampton, this is further potential evidence of the increase in tidal range since the 1950's. Note however that MHL (2002) also found the tidal limit in the Paterson River was at Gostwyck.

2.8.2 Entrance Breakwaters and Dredging

The Hunter River entrance has breakwaters constructed on both the southern and northern sides. The southern breakwater was completed in 1891, with the northern breakwater completed in 1912 (Umwelt, 2002).

About 133 million m³ (in situ) of material was dredged from the port of Newcastle between 1859 and 1989. In 1961, the port was about 8m deep. From 1962 to 1967, the depth was increased to 11m. Between 1977 and 1983 it was further deepened to its present depth, that is 15.2m within the harbour extending to 18m deep at the eastern end of the northern breakwater (Umwelt, 2002).

Prior to the deepening and breakwater construction, the harbour had a central channel about 6m deep, with large areas of shallow sand shoals. There was an active alluvial bedload that was added to by flood flows.

Umwelt (2002) proposed that there were a number of factors that may have modified sediment behaviour around the Hunter mouth (particularly in relation to erosion of Stockton Beach), namely:

- construction of the entrance breakwaters;
- deepening of the harbour and entrance to accommodate ships;
- maintenance dredging of these areas;
- increased tidal volumes entering and leaving the harbour;
- changes to sediment supply to the entrance channel; and,
- offshore dumping of dredge spoil.

Umwelt (2002) postulated that the harbour deepening would have the strongest link to the altered tidal behaviour and sediment movement. However, as noted in Section 2.8.1, MHL (2002) considered that tidal behaviour was more likely to have been altered by the installation of floodgates.

The Department of Public Works NSW [DPW] (1967) undertook an investigation with the purpose of devising techniques to reduce the maintenance dredging requirements of Newcastle harbour as much as economically possible. At the time, between 1956 and 1960, the average rate of dredging was 2.8 million barge tons (about 1.6 million m³ of in situ sediment) per annum (15% of this quantity was estimated to be developmental dredging)¹⁶.

¹⁶ Newcastle Ports Corporation currently has a permit for the removal and offshore disposal of up to 500,000m³ of in situ dredged sediments per annum. In recent years the actual quantities dredged have been below the maximum allowance, reflecting the general absence of flooding (which leads to sedimentation) during this time.

The recommended scheme involved the closure of the Fullerton Cove entrance with an earth dam and controlled gate structure (the gate being about 70m wide), which would be shut during higher river flows (exceeding 280m³/s) and very windy weather (wind speeds exceeding 37km/h). This was designed to reduce the sedimentation of Fullerton Cove in floods (estimated to be accreting at a rate of 8.5mm/year), so more sediment would be discharged to the ocean, and to reduce future wind-driven resuspension and supply of sediment to downstream areas. The scheme was never implemented.

2.8.3 Flood Mitigation Works

Flood mitigation works have placed considerable pressure on the river and floodplain environment, by isolating the floodplain from the river with the use of levees and floodgates, and by decreasing riparian, wetland and floodplain habitat through drainage, agriculture and development. Culverts and causeways also restrict tidal inundation to some areas (MHL, 2002).

Floodgates are designed to prevent the inflow of floodwaters but also prevent saline waters from entering wetlands and saltmarsh areas (eventually converting them from estuarine to freshwater systems), limit tidal flows and flushing, and affect the movement of aquatic fauna such as fish. Drainage works may also lead to exposure of potential acid sulfate soils. Notable floodgates include those on Wallis Creek and Ironbark Creek, the latter constructed in 1972¹⁷. Seaham Weir on the Williams River also prevents access for fish to formerly tidal areas upstream. Gross pollutant traps on Throsby and Styx Creeks also limit fish passage.

At the entrance to Wallis Creek, the substantial floodgate structure consists of 8 culverts, each of 3m² cross sectional area, of which 7 are closed under tidal conditions (non-flood periods). At Ironbark Creek, a narrow gap of only 0.1m width allows a minimal amount of tidal intrusion upstream (Evans, 2003).

There are plans for the complete opening of the Ironbark Creek floodgates in non-flood periods to allow natural tidal exchange to return to the system, with the expectation that this will be achieved by the end of 2003. Ironbark Creek links up with Hexham Swamp. Hexham Swamp is a noted former prawn nursery area.

Drains occur throughout the Hunter estuary catchment, particularly north of Hexham and around Fullerton Cove. These drains lead to saline wetlands becoming fresh or brackish, reducing faunal diversity, or may eliminate or reduce their permanence.

Levees occur extensively in the upper estuary upstream of Hexham, and also around Fullerton Cove. The construction of levees has resulted in the elimination or reduction in permanence of floodplain wetlands, and an increase in river sedimentation (MHL, 2002).

¹⁷ Floodgates are also located on Purgatory Creek and Greenways Creek. In total, there are 176 floodgates in the Hunter estuary, mainly in grazing areas upstream of Hexham and around Fullerton Cove. There are also about 59 culverts in the estuary, especially on Kooragang Island, around Fullerton Cove and in Newcastle. Like floodgates, culverts restrict tidal flushing and convert upstream areas from estuarine to freshwater systems (MHL, 2002).

2.8.4 Reclamation

The prawn trawling industry has recommended that swamp and saltmarsh areas on the north-west of Kooragang Island, and Moschetto Creek, are rehabilitated to improve their value as habitat areas for the species. Moschetto Creek is disconnected from the South Arm due to past reclamation.

The reclamation that formed the single Kooragang Island commenced in the late 1800's, with completion in 1953, destroying up to 10km² of estuarine wetlands. It has also been estimated that 37% of the open waters of the Hunter estuary were lost between 1801 and 1994, mainly due to the Kooragang Island reclamation, and also sedimentation of Fullerton Cove and the North Arm in general (MHL, 2002).

2.8.5 Riparian Vegetation

Riparian vegetation coverage is generally sparse and degraded within Newcastle Port; upstream of Hexham in the Hunter River; in the north-west of Kooragang Island; and in upstream areas of Ironbark Creek, Williams River, Paterson River, Wallis Creek and Fishery Creek (MHL, 2002).

3 IMPACT ASSESSMENT

3.1 GENERAL

As a convenient tool to assess the potential alteration to the Hunter estuary as part of the proposed dredging of the South Arm, a numerical model was developed. The RMA model suite was used, for which further details are provided in **Appendix A**. The model suite was able to simulate tidal hydrodynamics, flooding and water quality. Specifically, variables simulated under tidal conditions comprised:

- *hydrodynamics*, enabling assessment of any alteration to tidal ranges and phasing throughout the estuary as a result of the proposed dredging works (see Section 3.2);
- *salinity*, in order to assess the potential alteration to the salinity structure of the estuary as a result of the proposed dredging (Section 3.4);
- an *arbitrary conservative constituent*, to provide a picture of any likely alteration to flushing and pollutant dispersion characteristics in the estuary due to the dredging (Section 3.5); and,
- *cohesive (muddy) and non-cohesive (sandy) sediment*, to assist in prediction of the transport of suspended sediment generated during dredging and likely deposition zones (Section 3.6), and hence any potential impacts on fish, prawns and oysters and their habitats (Section 3.7).

A flood model was also developed. This was used as tool to estimate the likely changes to flood levels and flood behaviour during the dredging activities (in particular construction of a temporary sheet pile wall restricting channel flows in the South Arm, and also installation of a temporary pipeline crossing Kooragang Island), and after completion of the dredging, as described in Section 3.3. Note that the pipeline impacts were assessed based on an assumed potential westerly corridor route to Tomago, and are thus only preliminary results.

3.2 TIDAL HYDRODYNAMICS

3.2.1 Water Levels

A tidal hydrodynamic model was developed, calibrated and verified as described in **Appendix B**.

Based on a 29 day tidal simulation covering the range of spring and neap tide cycles, the alteration to water levels throughout the Hunter estuary due to the proposed dredging of South Arm is given in **Table 8**. The tidal boundary condition was based on recorded tides measured from 16 October to 14 November 2002 at Newcastle Pilot Station. The statistics given in Table 8 are based on comparison of model outputs at 15 minute intervals over the entire 29 day simulation.

Table 8: Predicted changes in water level due to dredging of South Arm under tidal conditions

Site	Average change (m)	Maximum positive change (m)	Maximum negative change (m)
Pilot Station (near entrance)	0.000	0.007	-0.008
Stockton Bridge (North Arm)	0.000	0.009	-0.009
Fullerton Cove (North Arm)	0.000	0.005	-0.006
Moscheto Creek (North Arm)	0.000	0.009	-0.007
Tourle St Bridge (South Arm)	-0.006	0.077	-0.127
Railway Bridge (South Arm)	-0.004	0.064	-0.077
Ironbark Creek (South Arm)	-0.002	0.054	-0.050
Hexham	0.000	0.006	-0.007
Green Rocks	0.000	0.005	-0.005

It can be seen that there would be very little alteration to water levels in the estuary under tidal conditions as a result of the proposed dredging. The average change in simulated water levels at most sites was essentially zero. Changes to average water levels were localised to upstream of the dredged area in the South Arm, where the average changes in water levels at Tourle St Bridge, the Railway Bridge and the entrance to Ironbark Creek were only 6mm, 4mm and 2mm respectively.

The existing and post-dredging water level record at Tourle St Bridge is shown in 7.25 day increments in **Figure 7** to **Figure 10**. This was the site noted with the greatest average deviation between existing and post dredging water levels under tidal conditions in Table 8.

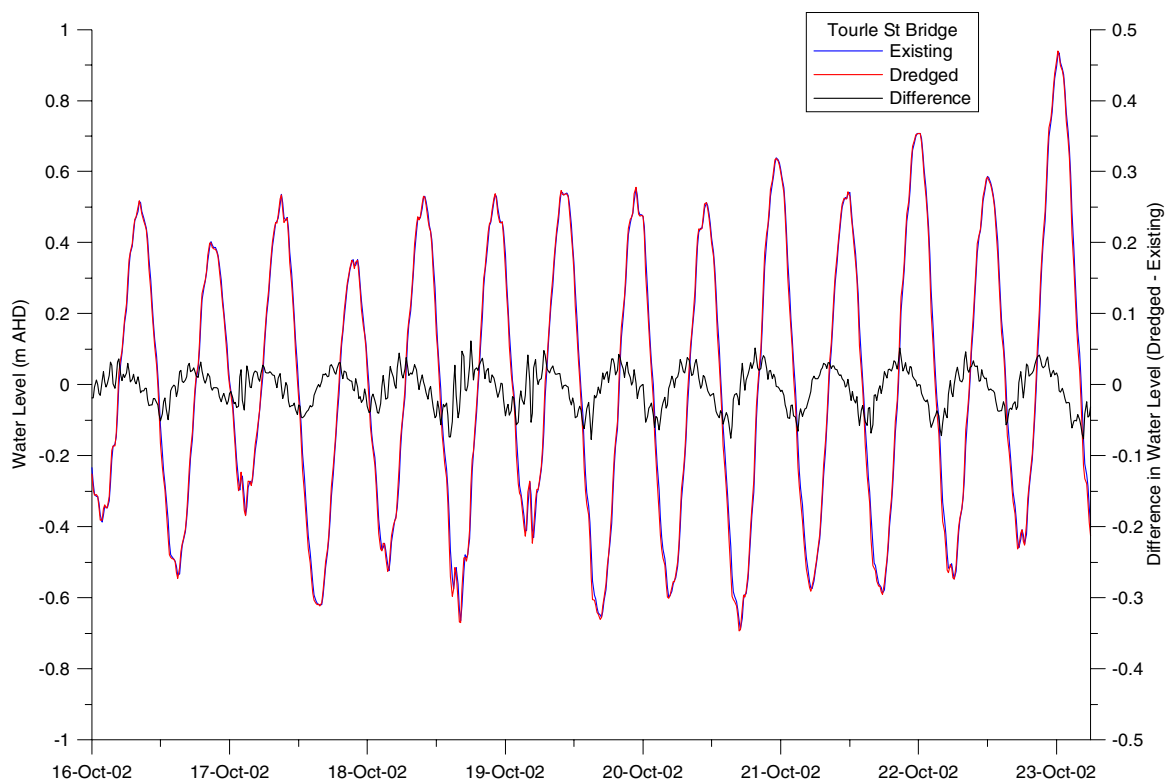


Figure 7: Simulated existing and post-dredging water levels at Tourle St Bridge under tidal conditions – Day 1 to 7

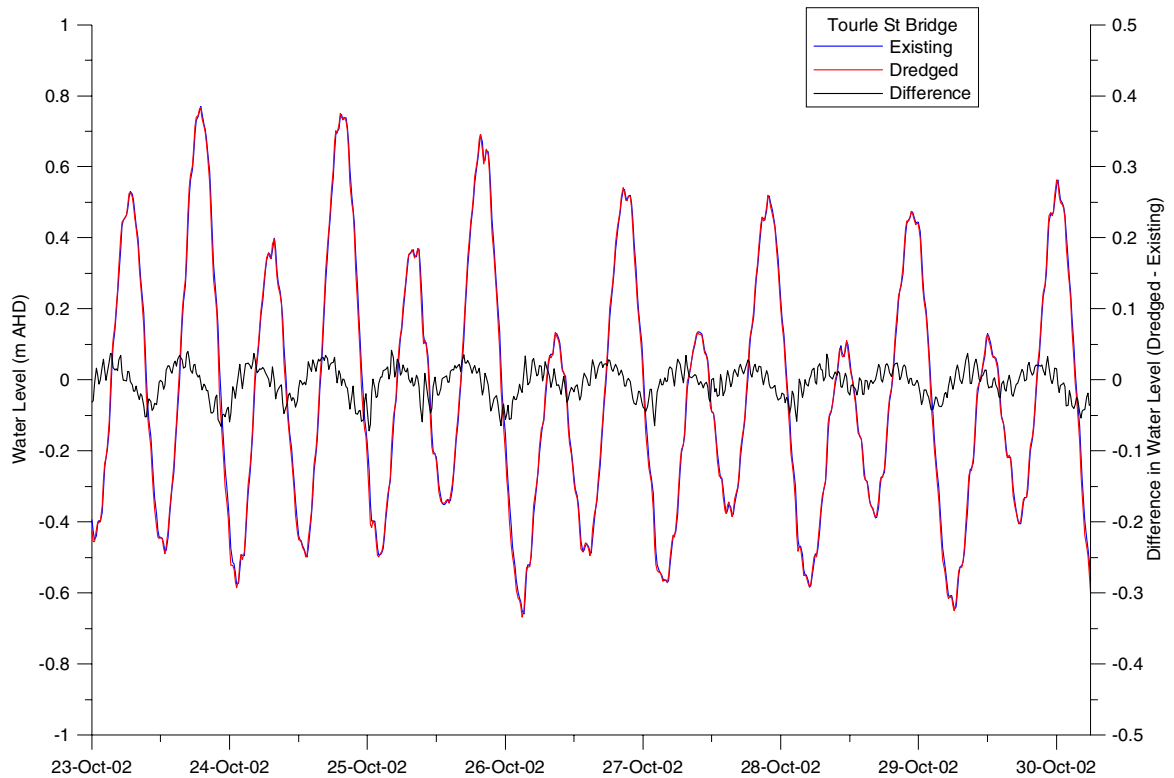


Figure 8: Simulated existing and post-dredging water levels at Tourle St Bridge under tidal conditions – Day 7 to 15

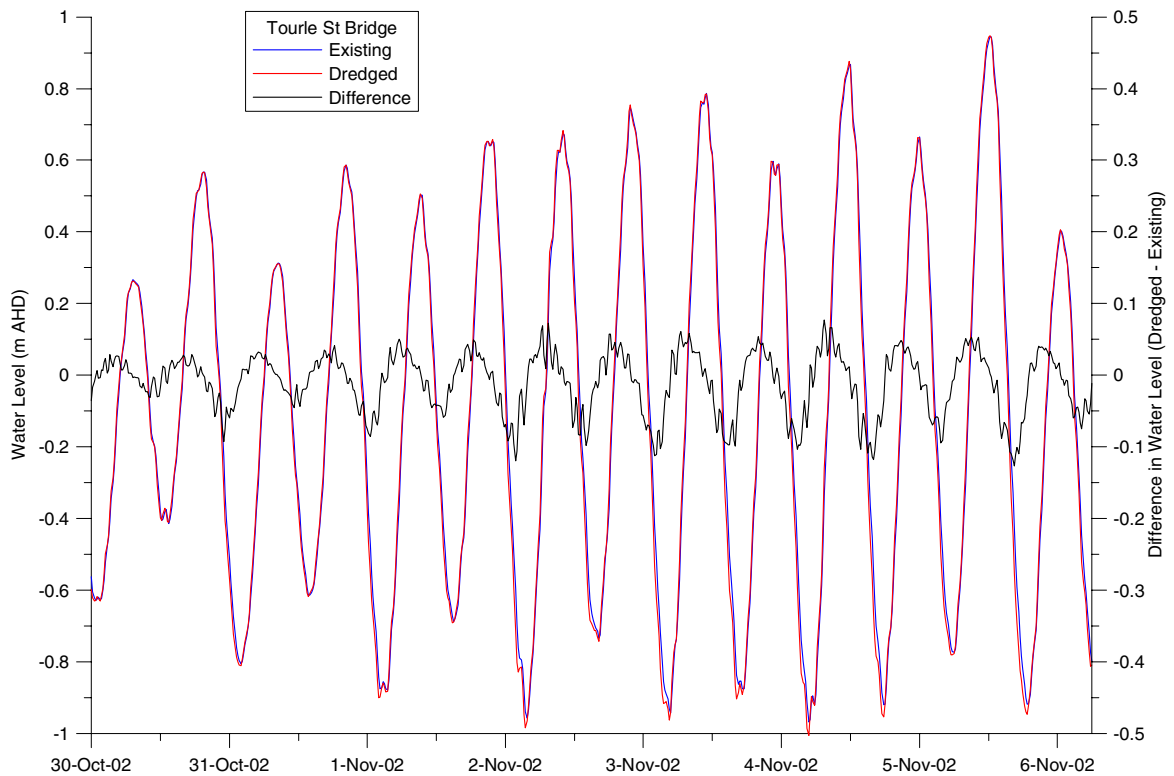


Figure 9: Simulated existing and post-dredging water levels at Tourle St Bridge under tidal conditions – Day 15 to 22

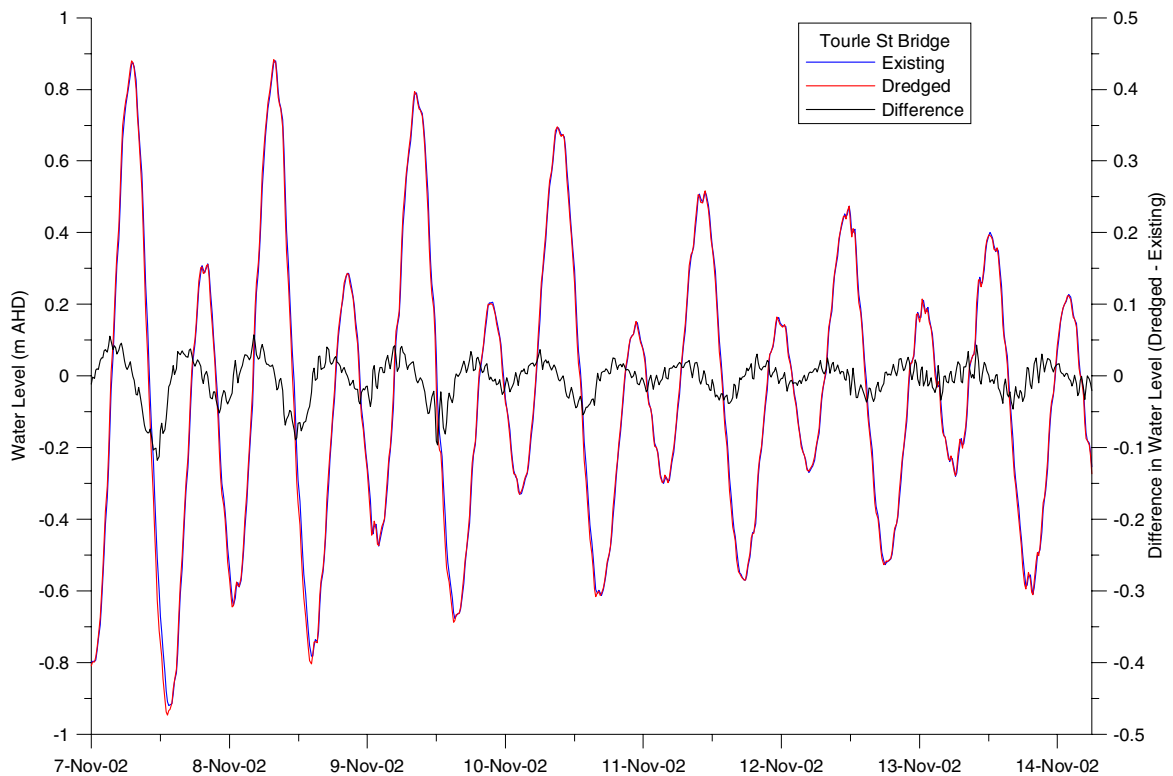


Figure 10: Simulated existing and post-dredging water levels at Tourle St Bridge under tidal conditions – Day 22 to 29

It can be seen that, in these simulations, the maximum instantaneous alterations to water level at Tourle St Bridge occurred midway along the rising and falling limbs of the tide. That is, the maximum deviations coincided with the maximum flood and ebb velocities. The post dredging levels were lower during the ebb tide and higher during the flood at this point in time.

3.2.2 Tidal Planes

Based on a least squares harmonic analysis of the water level records at various sites pre and post dredging, changes in tidal planes were determined as shown in **Table 9**.

It can be seen that, in these simulations, there was virtually no effect on tidal planes in the estuary due to the proposed dredging. The only small effects on tidal planes were localised to the dredged area itself, with the tidal range increasing at Tourle St Bridge by 6, 10, 14 and 18mm respectively for neap, mean, spring and absolute (full range) tides. The increase in tidal range was mainly manifested as a slight reduction in low water levels after dredging, with high tide levels virtually unaltered.

Table 9: Predicted changes (in metres) in tidal planes due to dredging of South Arm

Tidal Plane	Site				
	Pilot Station	Stockton Bridge	Tourle St Bridge	Ironbark Creek	Hexham
High High Water Solstices Springs (HHWSS)	0.001	0.001	0.003	-0.003	-0.001
Mean High Water Springs (MHWS)	0.000	0.000	0.002	-0.002	0.000
Mean High Water (MHW)	0.000	0.000	-0.001	-0.002	0.000
Mean High Water Neaps (MHWN)	0.000	0.000	-0.002	-0.001	-0.001
Mean Sea Level (MSL)	0.000	0.000	-0.006	-0.002	0.000
Mean Low Water Neaps (MLWN)	0.000	0.000	-0.009	-0.002	0.000
Mean Low Water (MLW)	0.000	0.000	-0.011	-0.002	0.000
Mean Low Water Springs (MLWS)	0.000	0.000	-0.013	-0.002	0.000
Indian Spring Low Water (ISLW)	0.000	-0.001	-0.014	-0.001	0.000
Mean Spring Range (MHWS-MLWS)	0.000	0.000	0.014	0.000	0.000
Mean Neap Range (MHWN-MLWN)	0.000	0.000	0.006	0.000	-0.002
Mean Range (MHW-MLW)	0.000	0.000	0.010	0.000	0.000
Range (HHWSS-ISLW)	0.001	0.002	0.018	-0.002	0.000

3.2.3 Velocities

Based on the 29 day tidal simulation undertaken, the alteration to water velocities¹⁸ throughout the Hunter estuary due to the proposed dredging of South Arm is given in **Table 10**.

Table 10: Predicted changes in tidal velocities due to dredging of South Arm

Site	Average change (m/s)	Maximum positive change (m/s)	Maximum negative change (m/s)
Pilot Station (near entrance)	0.001	0.016	-0.013
Stockton Bridge (North Arm)	-0.001	0.020	-0.018
Fullerton Cove (North Arm)	0.000	0.049	-0.031
Moscheto Creek (North Arm)	-0.001	0.004	-0.005
Tourle St Bridge (South Arm)	-0.001	0.116	-0.095
Railway Bridge (South Arm)	0.010	0.081	-0.086
Ironbark Creek (South Arm)	0.000	0.016	-0.010
Hexham	0.000	0.006	-0.010
Green Rocks	0.000	0.007	-0.008

It can be seen that there is likely to be very little alteration to water velocities in the estuary under tidal conditions as a result of the proposed dredging. The average change in simulated velocities at most sites was essentially zero. Maximum changes in velocities were generally much less than 0.1 m/s (0.2 knots).

Day 15-22 of the existing and post-dredging velocity record at the Railway Bridge is shown in **Figure 11**. This was the site noted with the greatest average deviation between existing and post dredging tidal velocities in Table 10. The easterly velocity component during this same period is

¹⁸ Note that all velocities reported are total velocities, that is the vector sum of the east and north components of velocity.

shown in **Figure 12**, where positive velocities occur during ebb tides, and negative velocities occur during flood tides.

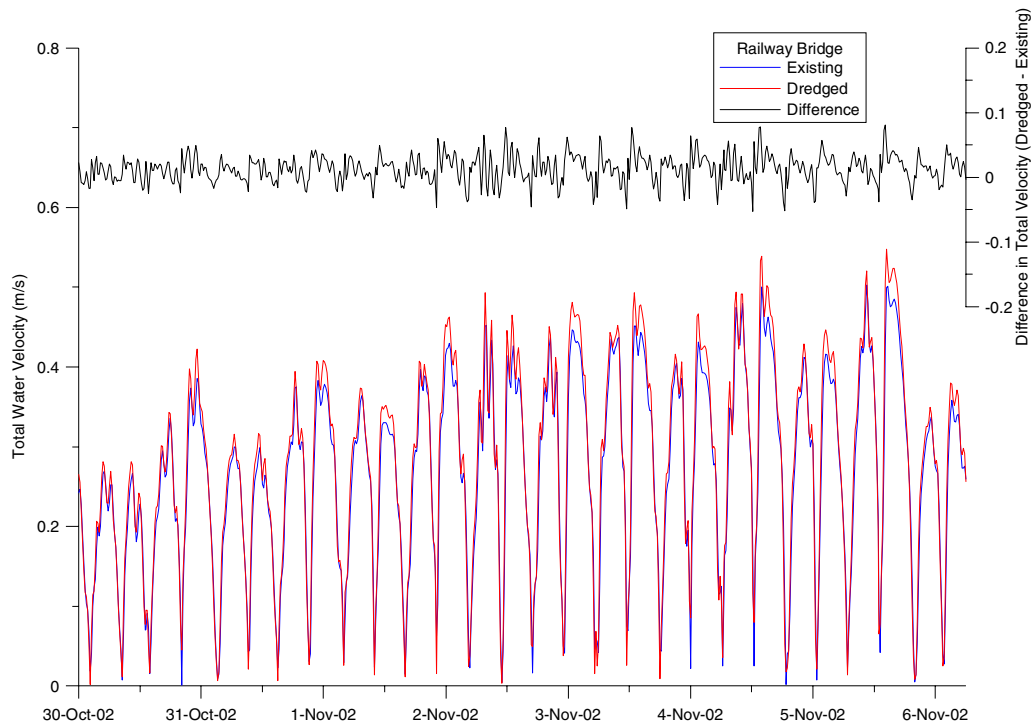


Figure 11: Simulated existing and post-dredging tidal velocities at the Railway Bridge – Day 15 to 22

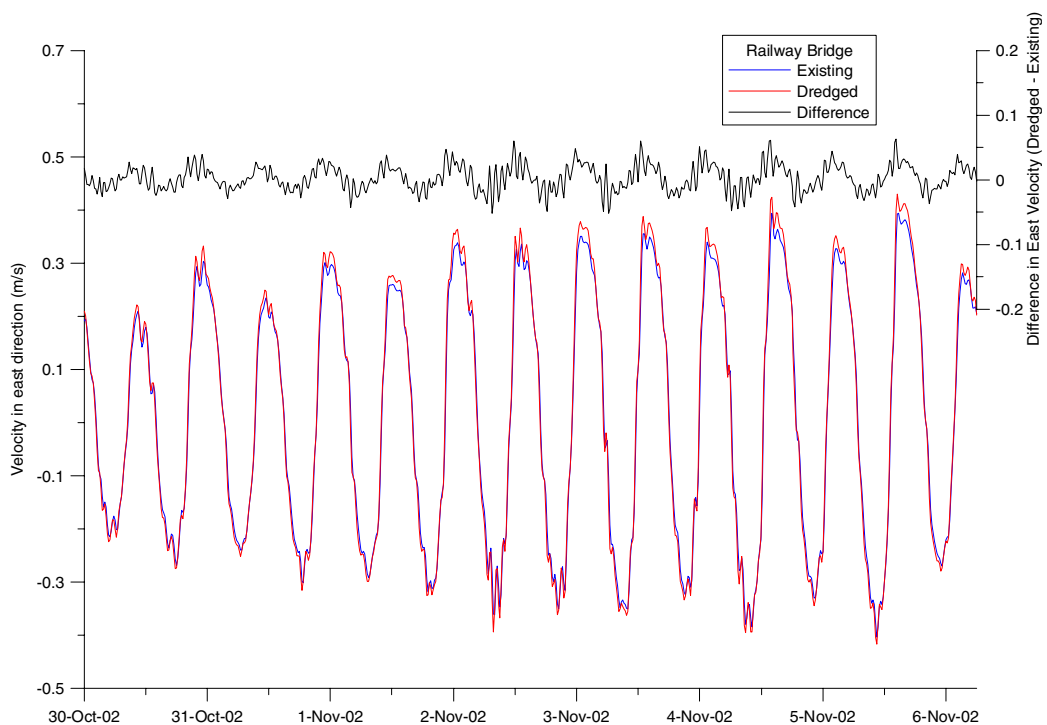


Figure 12: Simulated existing and post-dredging tidal velocities in the east direction at the Railway Bridge – Day 15 to 22

It is evident that the post-dredging velocities would be very slightly higher than under existing conditions at the Railway Bridge around mid-ebb tide.

Note that velocities in the dredged area will reduce substantially after completion of the dredging. The relative effects would be similar to the alteration in flood velocities which is discussed in Section 3.3.3.

It would not be expected that there would be any significant alteration to tidal velocity magnitudes and directions in the port area, such that navigation would be affected.

3.2.4 Flows

Based on the 29 day tidal simulation undertaken, the pre and post dredging flow rates throughout the Hunter estuary are given in **Table 11** (averages) and **Table 12** (maximums). The flows given are the averages across the channel cross section at the locations shown. Note that the maximums given are for the 29 day simulation and are not necessarily the maximum possible tidal flowrates that would occur in the estuary.

Table 11: Predicted pre and post dredging average tidal flow rates in the Hunter estuary

Site	Average Ebb Tide Flow (m ³ /s)		Average Flood Tide Flow (m ³ /s)	
	Existing	Dredged	Existing	Dredged
Ocean Entrance	1122	1132	1049	1054
Entrance to Throsby Creek	47	47	45	45
Main Channel at confluence with Throsby Creek	1011	1021	964	968
Downstream Entrance to South Arm	191	203	180	192
Downstream Entrance to North Arm	751	748	741	738
North Arm near Tomago	235	234	228	225
Tourle St Bridge	96	99	93	100
South Arm near Ash Island Bridge	49	53	57	59
Hexham Bridge	256	255	249	249

Table 12: Predicted pre and post dredging maximum tidal flow rates in the Hunter estuary

Site	Maximum Ebb Tide Flow (m ³ /s)		Maximum Flood Tide Flow (m ³ /s)	
	Existing	Dredged	Existing	Dredged
Ocean Entrance	2811	2880	2680	2703
Entrance to Throsby Creek	158	159	169	156
Main Channel at confluence with Throsby Creek	2531	2591	2468	2503
Downstream Entrance to South Arm	571	659	509	599
Downstream Entrance to North Arm	1890	1887	1870	1879
North Arm near Tomago	453	449	436	431
Tourle St Bridge	264	284	249	267
South Arm near Ash Island Bridge	112	124	143	148
Hexham Bridge	483	484	506	506

It is evident that, post dredging, there would generally be a slight increase in ebb and flood tide flows in the South Arm, with a slight decrease in the North Arm. At Walsh Point, the increase in average South Arm ebb and flood flows in these simulations was about 6%, with a 0.4% decrease in average North Arm ebb and flood flows. In terms of the average North Arm / South Arm flow distribution at Walsh Point, there was only a 1% change. That is, under existing conditions the South Arm took about 20% of the total flow at Walsh Point (on both ebb and flood tides). After dredging, this increased to 21%.

Overall, the modelling results indicate that tidal hydrodynamics would remain virtually unchanged after the proposed dredging. Slightly more tidal flow would pass through the South Arm, with a slightly increased tidal range at locations near the dredged area. However, the magnitudes of these changes would be very small and would not be expected to have any measurable impacts.

3.2.5 Effect of Temporary Sheet Pile Wall

The average and peak mean (cross-section averaged)¹⁹ velocities at Tourle St Bridge and four cross sections along the temporary sheet pile wall (approximately at one-third intervals along its length) over the 29 day tidal simulation are given in **Table 13**, along with corresponding values for existing conditions.

Table 13: Average and peak mean tidal velocities along temporary sheet pile wall location and at Tourle St Bridge for existing conditions and with wall in place

Location	Average Mean Velocity (m/s)		Peak Mean Velocity (m/s)	
	Existing	With Sheet Pile Wall	Existing	With Sheet Pile Wall
Tourle St Bridge	0.19	0.19	0.45	0.44
Upstream end of wall	0.13	0.15	0.35	0.40
One-third along length of wall	0.13	0.16	0.35	0.42
Two-thirds along length of wall	0.05	0.05	0.13	0.15
Downstream end of wall	0.02	0.03	0.06	0.07

It is evident that increases in mean tidal velocities with the temporary sheet pile wall in place would be in the order of 15% along the wall location. Given that mean tidal velocities are less than 0.5m/s at this location, it would not be expected that the increase in velocities would cause significant bank erosion. However, recommendations for monitoring of bank erosion are given with regard to flooding in Section 3.3.1, which would also enable assessment of any tidal effects.

Peak velocity contours for existing conditions and with the temporary sheet pile wall in place are given in **Figure 13** and **Figure 14** respectively. Note that the time snapshot shown is during an ebb tide.

¹⁹ In this case, the terms “average” and “peak” apply to the temporal velocity record, while “mean” refers to spatial averaging.

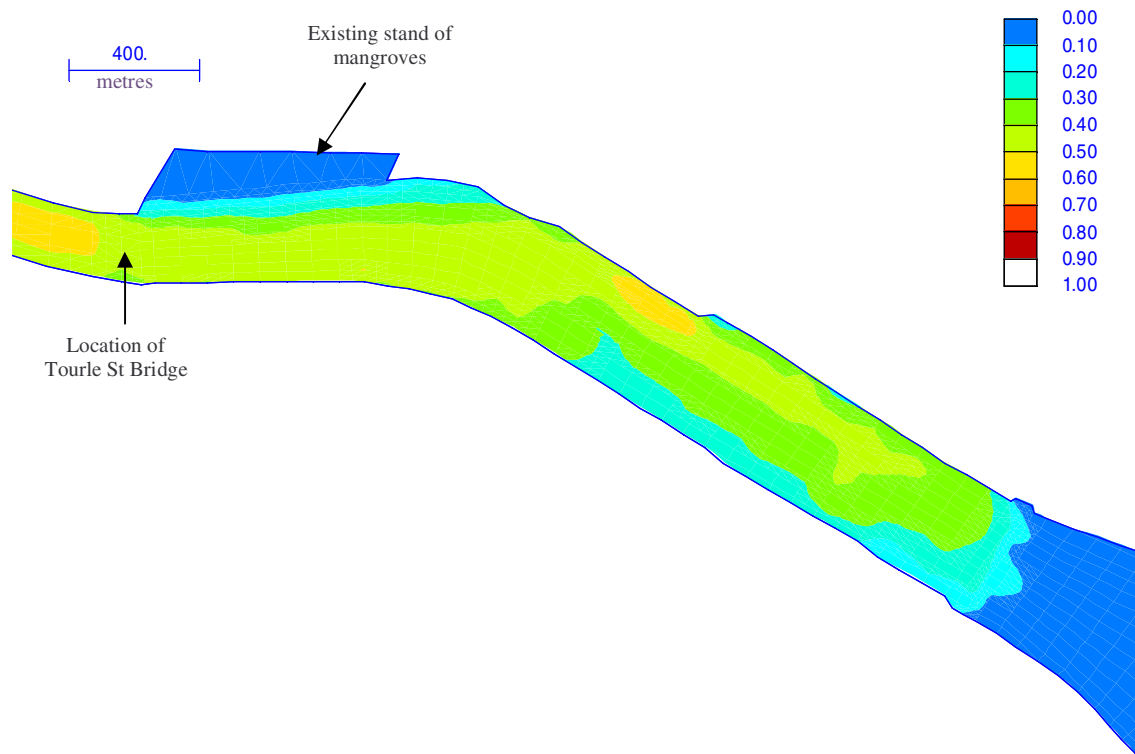


Figure 13: Peak ebb tide velocity contours (m/s) between Tourle St Bridge and Kooragang berths for existing conditions

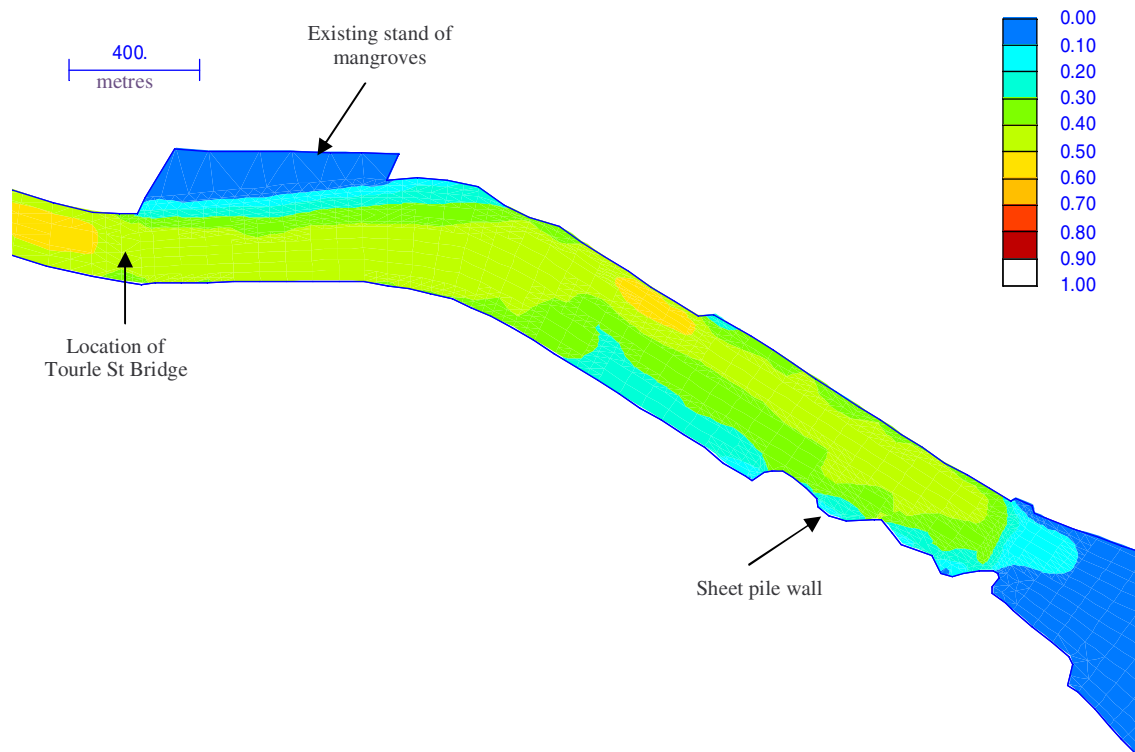


Figure 14: Peak ebb tide velocity contours (m/s) between Tourle St Bridge and Kooragang berths with temporary sheet pile wall in place

It can be seen that effects on tidal velocities with the temporary sheet pile wall in place would be localised and relatively small. It would also therefore be expected that the sheet pile wall would not alter velocities substantially in the downstream port area, such that navigation would be affected. For example, the velocity contours in the port area at the peak ebb flow in the 29 day tidal simulation (as per Figure 13 and Figure 14) are shown in **Figure 15** (existing conditions) and **Figure 16** (temporary sheet pile wall in place), and are virtually identical.

Velocity vectors in the vicinity of the North Arm and South Arm junction (Walsh Point and Stockton Crossing) are shown in **Figure 17** (existing conditions) and **Figure 18** (temporary sheet pile wall in place). The similarity of the current patterns is evident.

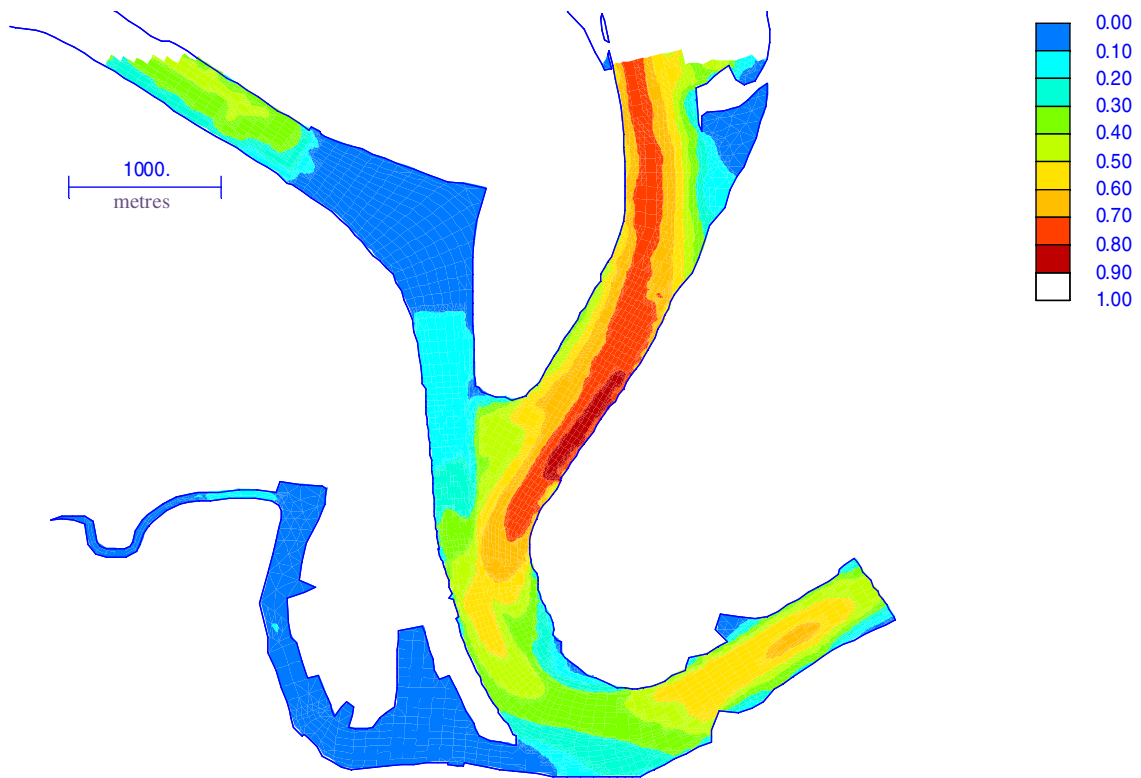


Figure 15: Peak ebb tide velocity contours (m/s) in port area for existing conditions

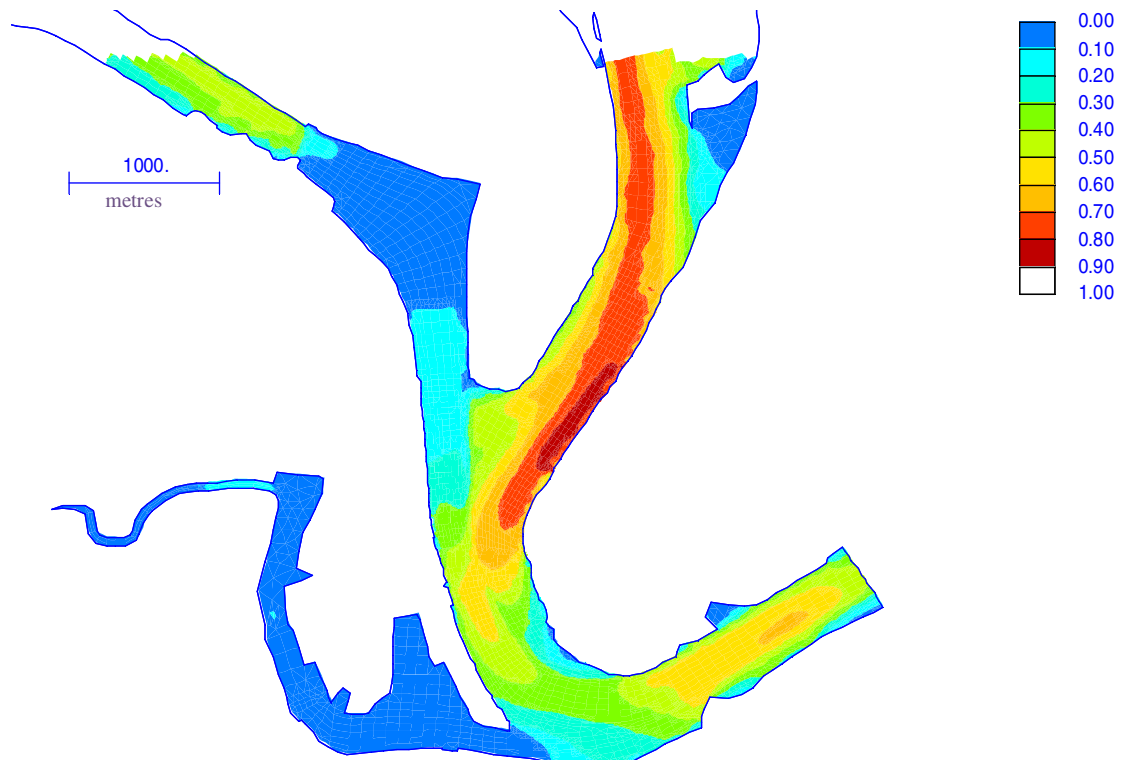


Figure 16: Peak ebb tide velocity contours (m/s) in port area with temporary sheet pile wall in place

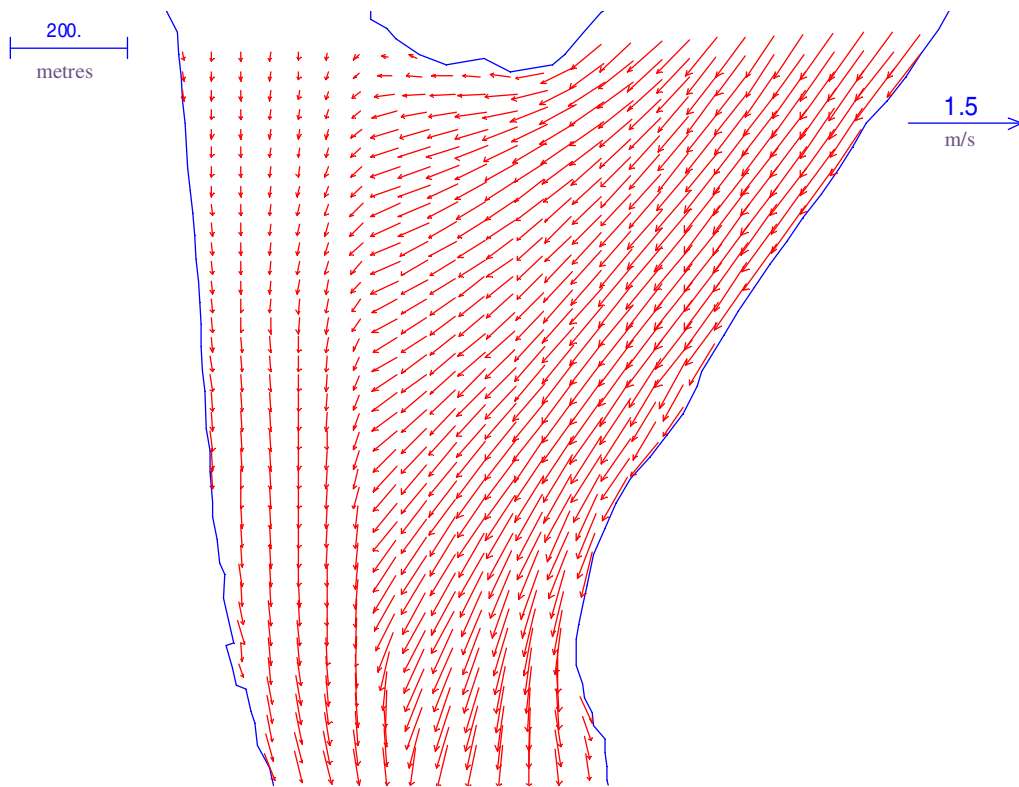


Figure 17: Velocity vectors (m/s) for peak ebb tide in vicinity of Walsh Point (existing conditions)

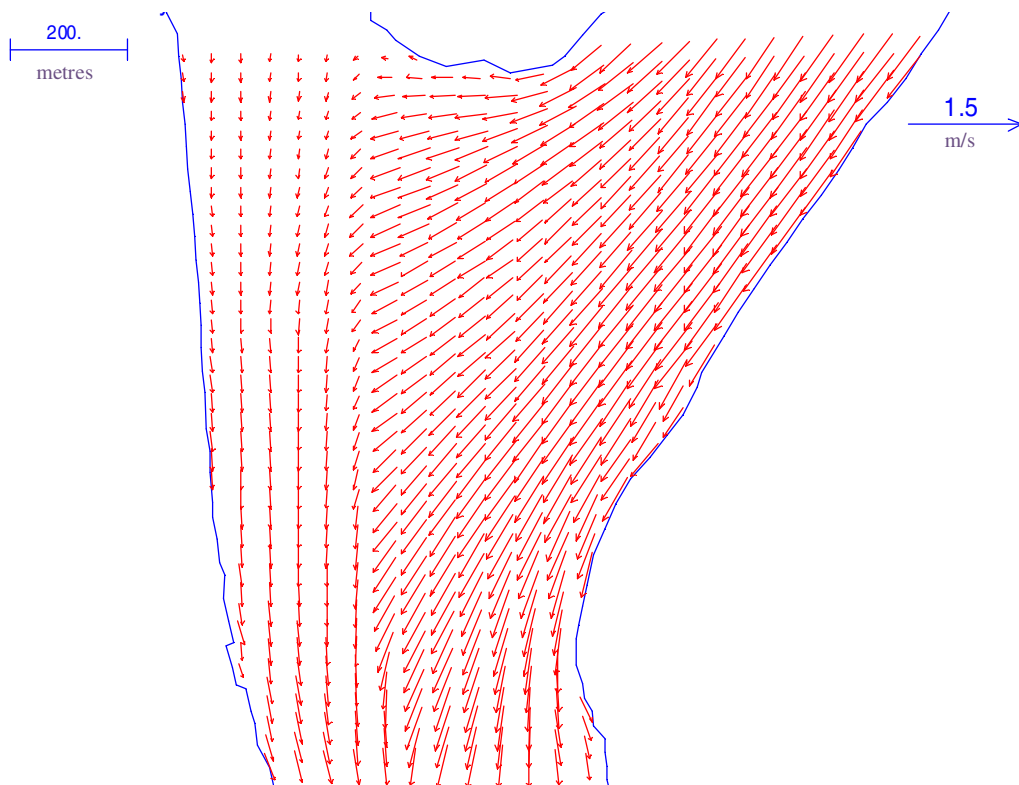


Figure 18: Velocity vectors (m/s) for peak ebb tide in vicinity of Walsh Point (temporary sheet pile wall in place)

3.3 FLOODING

A flood model was developed as described in **Appendix C**. This enabled assessment of various effects on flood behaviour, namely the:

- proposed temporary sheet pile wall (to contain contaminated sediments during dredging operations);
- discharge pipeline transferring dredged sediments to Tomago over Kooragang Island; and,
- the ultimate dredged profile

These aspects are discussed in Sections 3.3.1, 3.3.2 and 3.3.3 respectively.

Design floods as devised in the Lower Hunter Flood Study (PWD, 1994) were simulated for the 1%, 2%, 5% and 10% annual exceedance probability (AEP) events in all cases.

3.3.1 Effect of Temporary Sheet Pile Wall

Simulations were undertaken for existing conditions and with the proposed temporary sheet pile wall in place for the four design floods.

The alteration to the flood profile (peak water levels versus distance) with the temporary sheet pile wall constructed is shown in **Figure 19** (Entrance and North Arm) and **Figure 20** (South Arm). Note that the North Arm is about 2km longer than the South Arm, with the distance to Hexham Bridge given in Figure 19 measured via the North Arm.

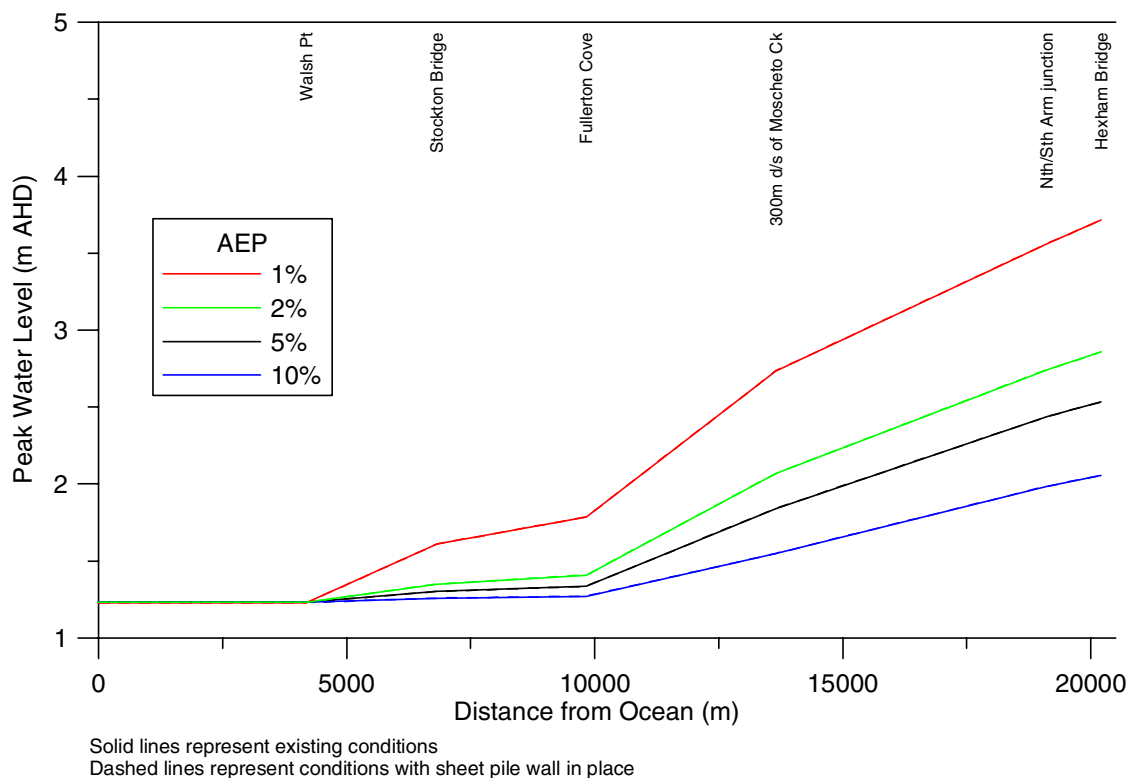


Figure 19: Peak water levels for various AEP floods under existing conditions and with temporary sheet pile wall in place (Entrance and North Arm)

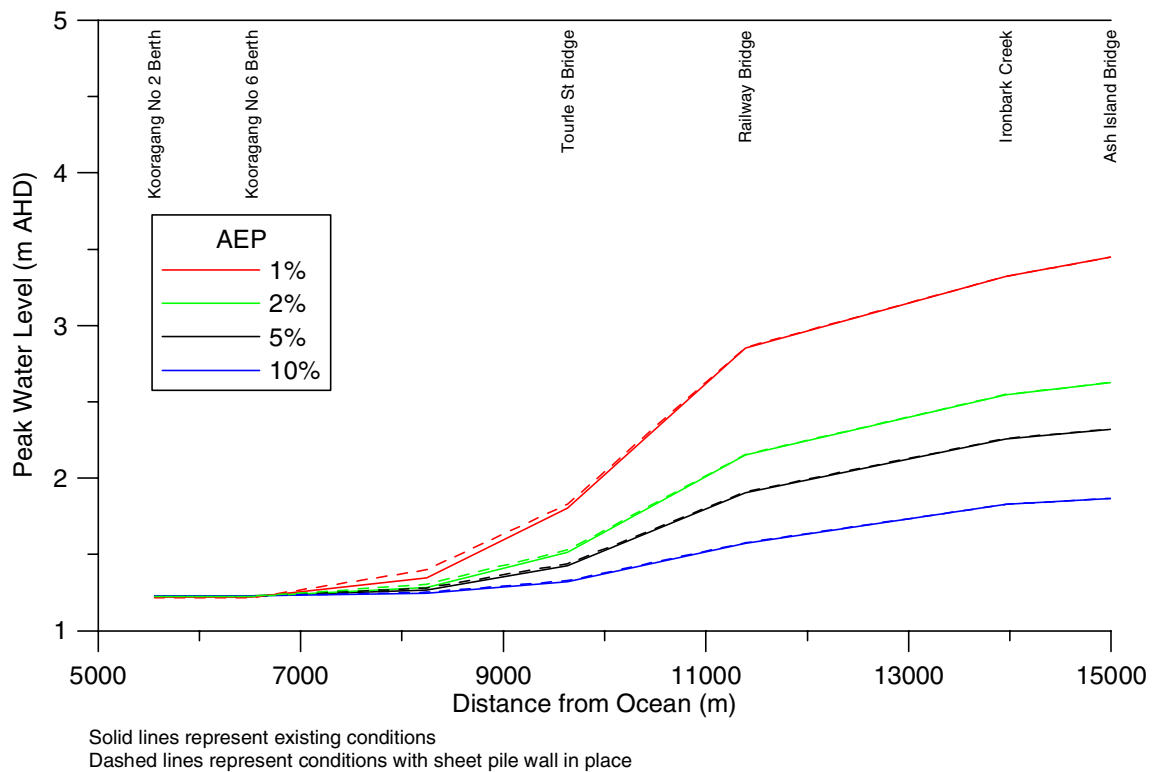


Figure 20: Peak water levels for various AEP floods under existing conditions and with temporary sheet pile wall in place (South Arm)

It is evident that the effect of the temporary sheet pile wall on flood levels would be minimal, and localised to the South Arm. The maximum increase in peak flood levels, midway between Kooragang No 6 Berth and Tourle St Bridge, was 50mm in the 1% AEP event, reducing to 20mm in the 2% event and 7mm in the 10% event. At the Railway Bridge, increases were no greater than 5mm in all simulated events.

It is unlikely that such small increases in flood levels would cause significant adverse affects like damage to property. Flow in the reach of the South Arm affected by the slight increases in levels would be expected to continue as channel flow, with no overbank flow occurring. Further, the proposed sheet pile wall is only expected to be in place for a relatively short period of time (in the order of one year).

With the temporary sheet pile wall in place, the restriction in flow area would cause increases in mean (cross section averaged) velocities along the length of the wall. For the 5% AEP event, peak velocity contours for existing conditions and with the temporary sheet pile wall in place are given in **Figure 21** and **Figure 22** respectively.

The peak mean (cross-section averaged) velocities at Tourle St Bridge and four cross sections along the temporary sheet pile wall (approximately at one-third intervals along its length) for the 5% AEP are given in **Table 14**, along with corresponding values for existing conditions.

Table 14: Peak mean velocities along temporary sheet pile wall location and at Tourle St Bridge for existing conditions and with wall in place (5% AEP flood)

Location	Peak Mean Velocity (m/s)	
	Existing	With Sheet Pile Wall
Tourle St Bridge	1.41	1.40
Upstream end of wall	0.28	0.39
One-third along length of wall	0.18	0.20
Two-thirds along length of wall	0.81	0.97
Downstream end of wall	0.80	0.94

It is evident that increases in mean velocity with the temporary sheet pile wall in place would be in the order of 15% at the downstream (higher velocity) end. The highest velocities would be expected to be against the left hand (northern) bank. It is recommended that an inspection of the northern bank is carried out prior to the installation of the sheet pile wall. The purpose of this would be to identify potential areas that may be susceptible to erosion as a result of increased velocities. If any such areas were identified these may require protection or monitoring while the sheet pile wall is in place. However, given that this bank will be protected with a rock revetment after the completion of dredging, monitoring only may be required given the temporary nature of any erosion that may occur.

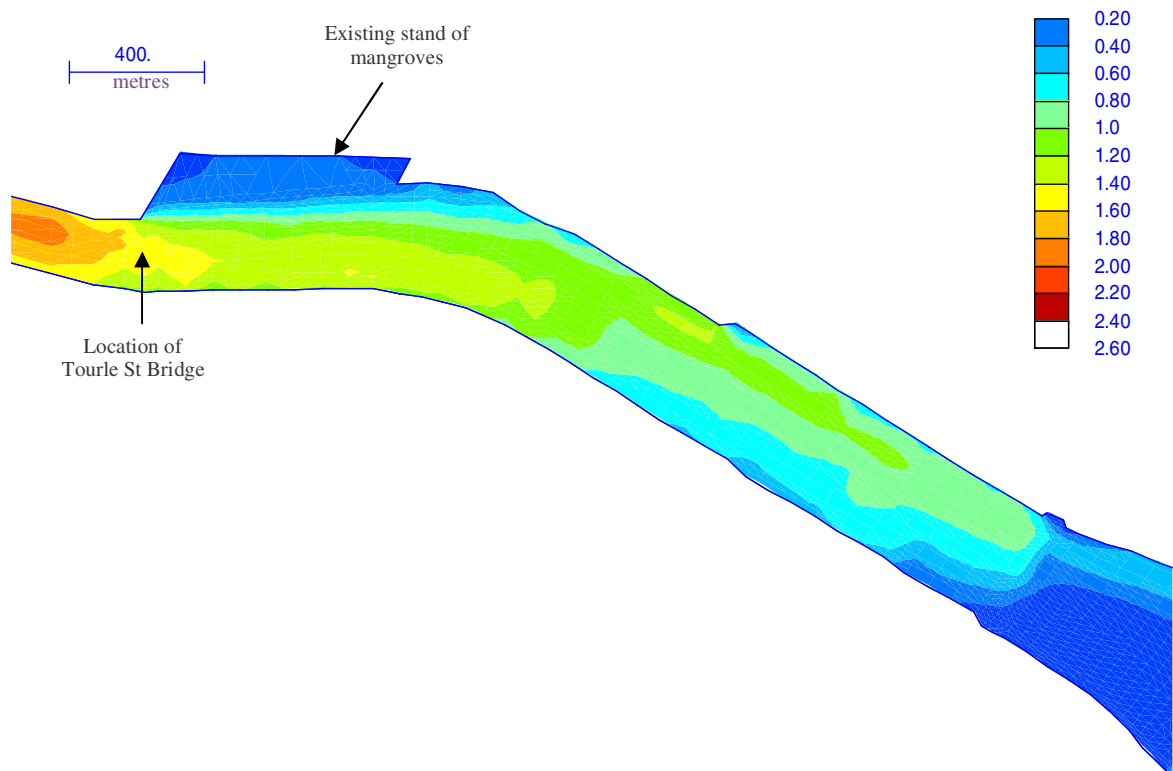


Figure 21: Peak velocity contours (m/s) between Tourle St Bridge and Kooragang berths for existing conditions (5% AEP flood)

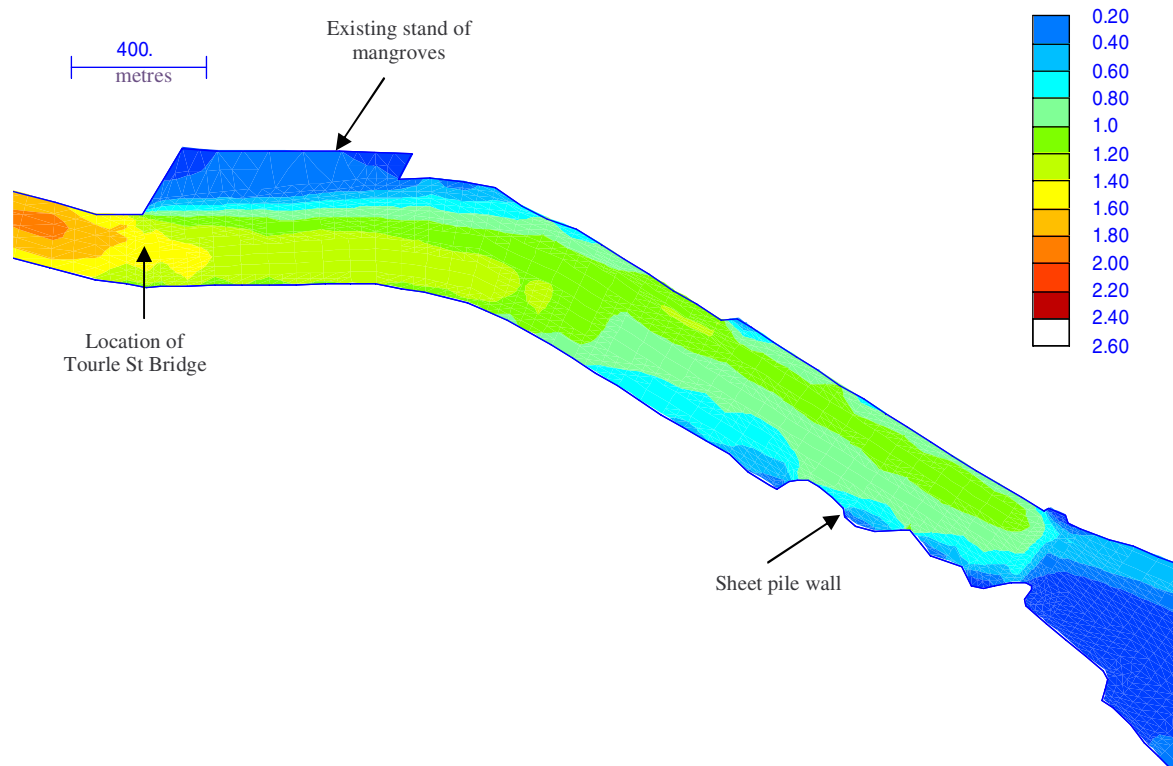


Figure 22: Peak velocity contours (m/s) between Tourle St Bridge and Kooragang berths with temporary sheet pile wall in place (5% AEP flood)

3.3.2 Discharge Pipeline

The dredging and excavation of the South Arm involves the removal and the handling of a total of about 13 million m³ of material. This total includes around 4.5 million m³ of good quality sand, which is located within the dredge footprint beneath the marine silts and clay sediments at the bed surface. This sand is considered suitable for reclamation and filling activities associated with the construction of the proposed Austeel facility at Tomago.

The material would be removed utilising a large cutter suction dredger with a production capacity of approximately 150,000 m³/week to 200,000 m³/week. The sand would be delivered to the Tomago site hydraulically via a discharge pipeline with an estimated diameter of 750 mm. The pipeline would be a temporary structure, required for a period of approximately one year. The preferred route for the discharge pipeline was not determined at the time of completion of this report. For the purposes of this assessment a route was chosen based on a worst case scenario, with the pipeline placed on the existing ground surface.

A two dimensional RMA flood model covering the lower reaches of the Hunter River has previously been used by Patterson Britton to assess flooding scenarios across Kooragang Island. The existing RMA flood model was modified to assess the effects of a discharge pipeline that would traverse across Kooragang Island using a westerly route. In the completion of this assessment it was assumed that the steel pipeline would be effectively impermeable to flood flows. The pipeline was simulated by raising the existing ground levels by the pipeline diameter along the length of the pipe.

Simulations were undertaken for existing conditions and with the pipeline in place for the four design floods. Note that existing ground levels were assumed at the proposed Tomago site on the North Arm (that is no development was simulated).

To compare the sensitivity of the model results to the pipeline height, pipeline diameters of 700 mm and 900 mm were simulated. The 700 mm diameter allows for some settlement of the 750 mm diameter pipe, while the 900 mm diameter assumes the pipeline is raised above ground level. The results for the 900 mm pipe could be considered to be conservative.

The maximum increases in peak water levels as a result of the pipeline construction are shown in **Table 15** for the four design events. These increases would be upstream of the pipeline.

Table 15: Maximum increases in peak water level due to discharge pipeline construction

Flood Event (AEP)	Maximum increase in peak water level (m)	
	700mm pipeline	900mm pipeline
1%	0.09	0.19
2%	0.18	0.27
5%	0.17	0.23
10%	0.09	0.10

It can be seen that over the range of events simulated, peak flood levels increased by up to between about 0.1 and 0.3m. However, the largest increases were localised to just upstream of the pipeline. To illustrate this, contour plots of the increases in peak water level for the 700mm pipeline are shown in **Figure 23** to **Figure 26** for the four design flood events. The results for the 900mm pipeline are provided in **Appendix C**. Note that positive variations represent increases in peak water level due to the pipeline.

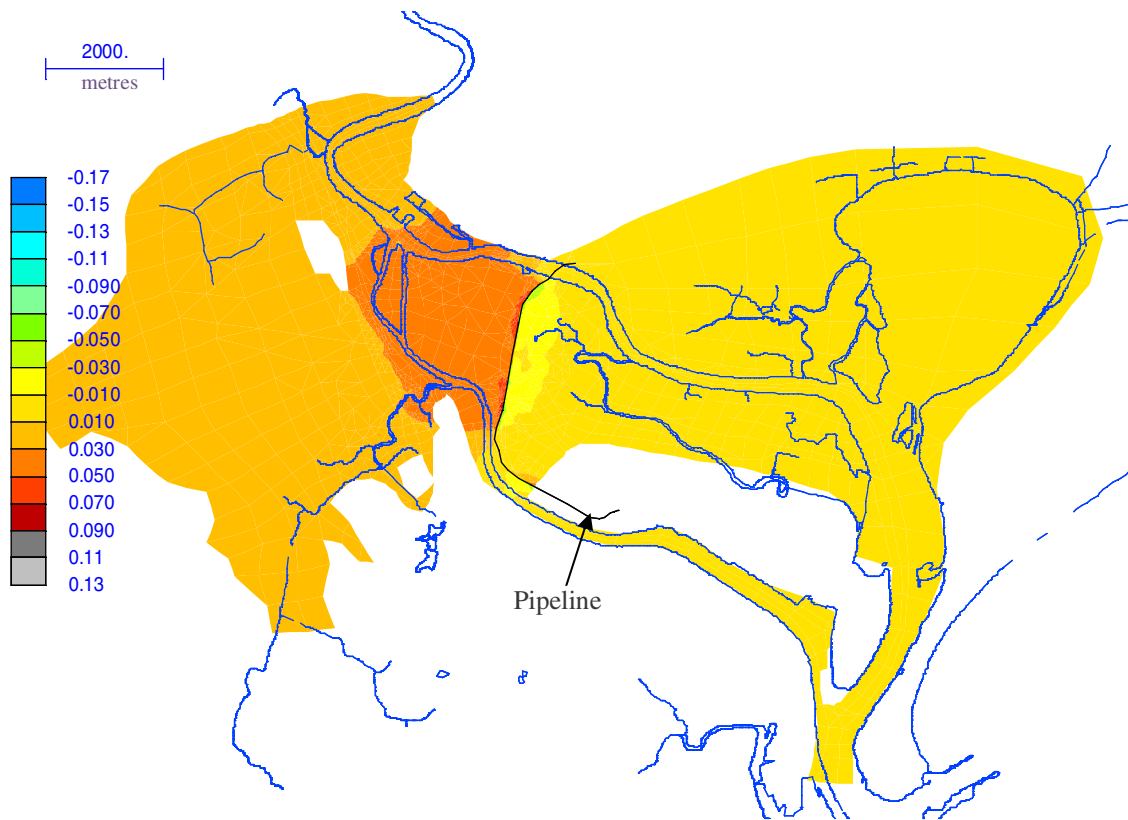


Figure 23: Variation in peak water level (m) due to 700mm pipeline (1% AEP flood)

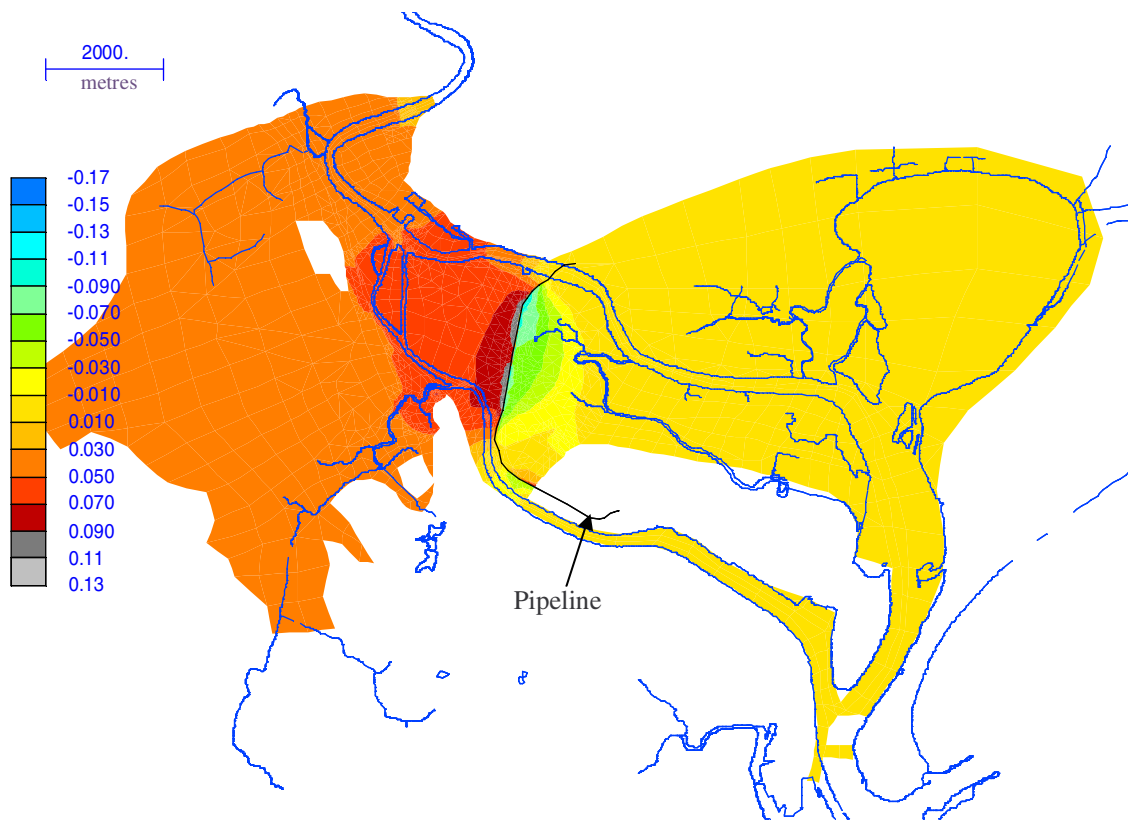


Figure 24: Variation in peak water level (m) due to 700mm pipeline (2% AEP flood)

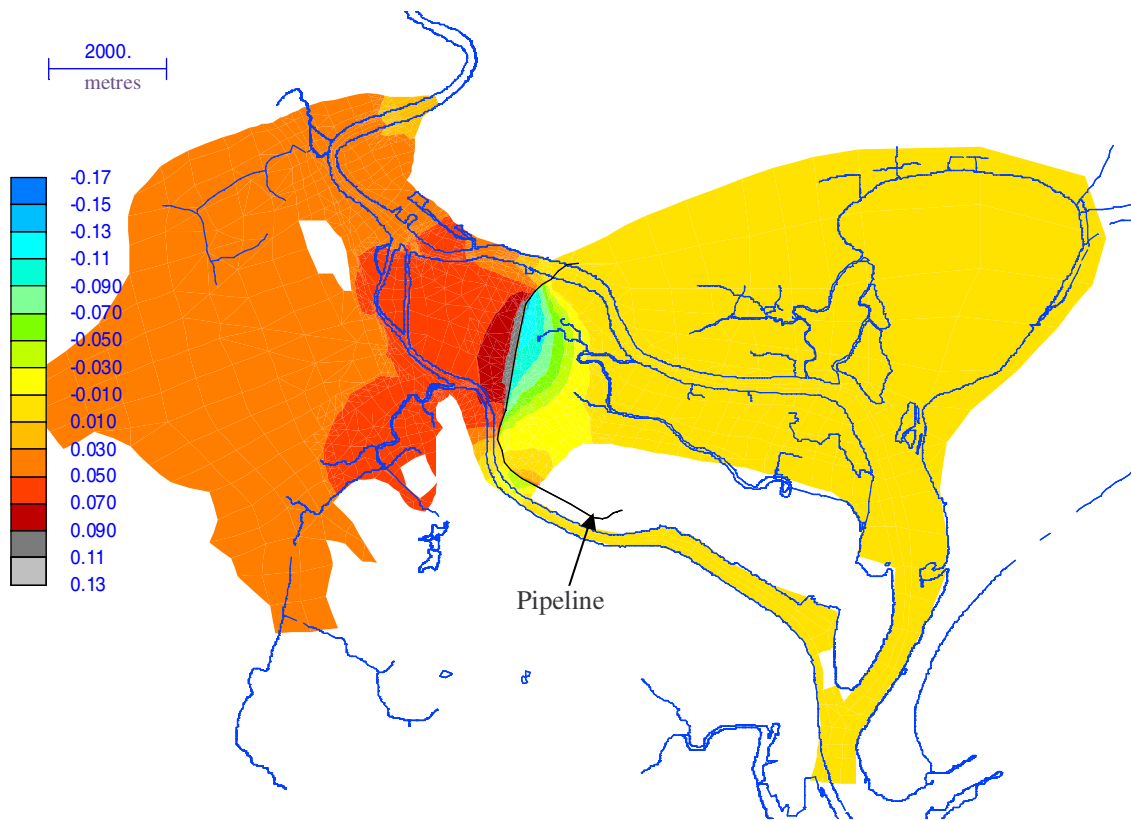


Figure 25: Variation in peak water level (m) due to 700mm pipeline (5% AEP flood)

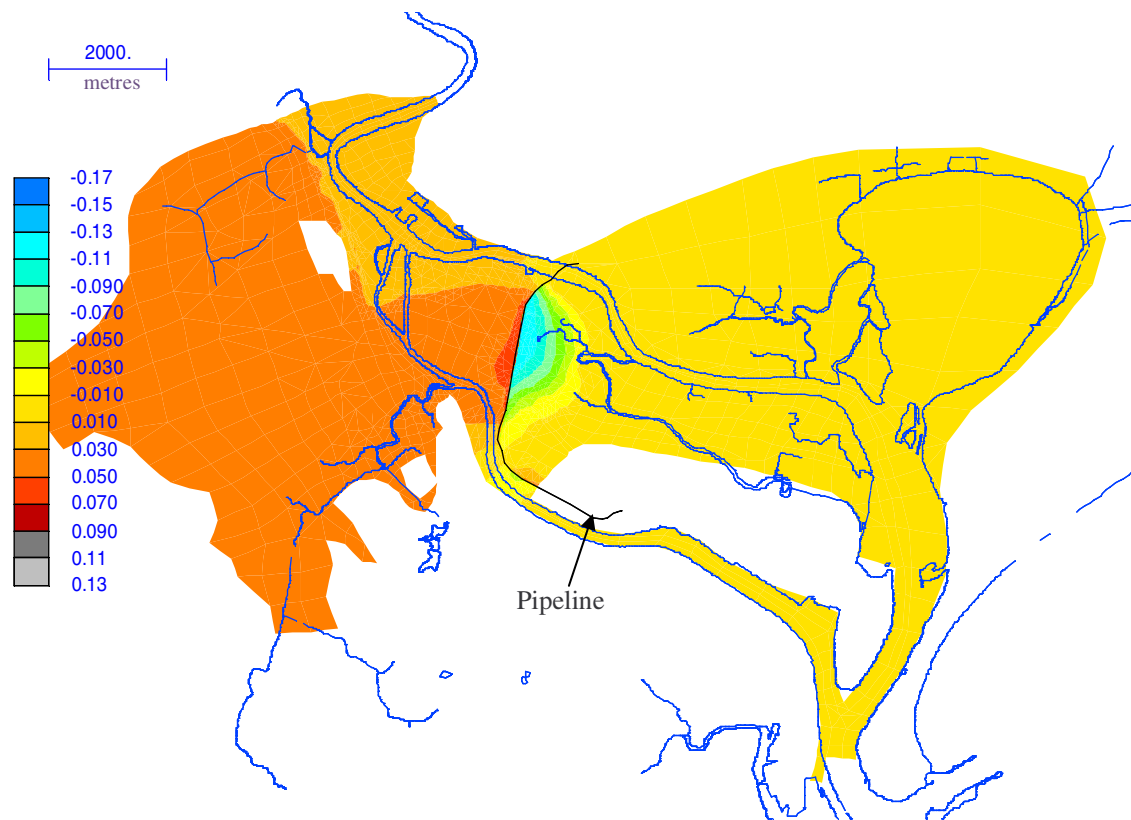


Figure 26: Variation in peak water level (m) due to 700mm pipeline (10% AEP flood)

Based on the assumed pipeline route simulated, it is evident that the largest increases in peak water level would be localised to immediately upstream of the pipeline. In the broad Beresfield, Hexham and Hexham Swamp area, increases in water level were up to about 50mm over all design events, while at Tomago and between Hexham and Sandgate the maximum increase was about 70mm. For the 1% AEP event, maximum increases at these locations were about 30mm and 50mm respectively.

The potential for greater flood damages as a result of the increased water levels cannot be determined simply as information on floor levels was not obtained as part of the Lower Hunter Floodplain Management Study (Patterson Britton & Partners, 2001b). In the Patterson Britton & Partners (2001b) study, it was recognised that existing flooding problems will potentially remain for areas such as Raymond Terrace, Tomago, between Hexham and Sandgate, Beresfield, Tarro, Maryland, Wallsend, and Shortland.

Given that floor levels for habitable areas of dwellings are generally required to be 500mm above the level of the 1% AEP flood in this area, the effect of increased flood levels is considered to be relatively insignificant for development sited according to this requirement.

Note that construction of a raised transport corridor across Kooragang Island itself has been shown to increase flood levels in the vicinity of Hexham by about 20mm for the 1% AEP event (Patterson Britton & Partners, 2003a). It is understood that this long term increase in flood levels would be considered as part of an EIS for the Tomago development. The increase of about 30mm at Hexham due to the pipeline is short-term (in the order of a year) and only marginally larger than the effect of the proposed transport corridor construction.

As stated, the broad-scale increases in peak flood levels in the 1% event, due to the installation of the temporary discharge pipeline, would be in the order of 30-50mm, with net increases only 10-30mm above the long-term effect of any proposed transport corridor (and this conservatively ignores the reduced flood levels as a result of the South Arm dredging). If the potentially increased risk of flood damages due to this increase in levels was considered to be unacceptable, a number of mitigation measures would be possible.

One such measure would be to provide relief floodways under the pipeline at appropriate depressions along the route, for example with culverts. The pipeline could also be embedded further at critical locations to reduce its elevation relative to the ground surface.

3.3.3 Post Dredging Conditions

Simulations were also undertaken for the ultimate post dredging conditions (temporary sheet pile wall removed), for the 1%, 2%, 5% and 10% AEP events. The alteration to the flood profile (peak water levels versus distance) after completion of dredging is shown in **Figure 27** (Entrance and North Arm) and **Figure 28** (South Arm).

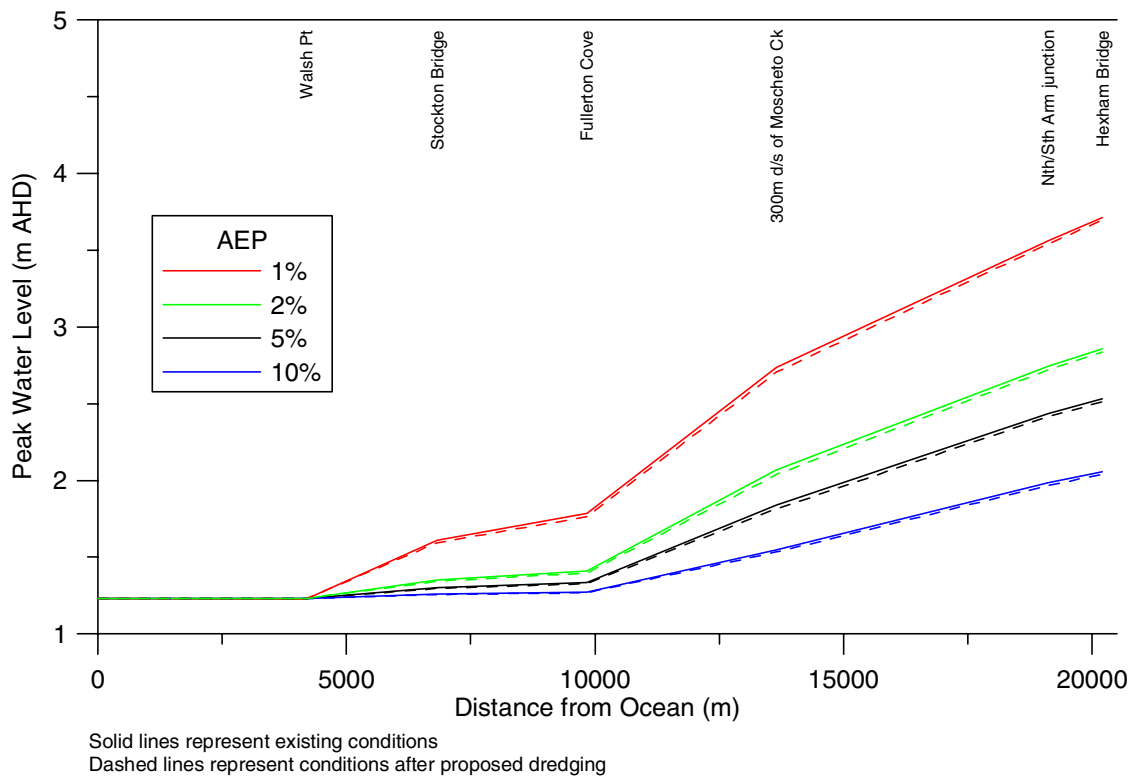


Figure 27: Peak water levels for various AEP floods under existing and post dredging conditions (Entrance and North Arm)

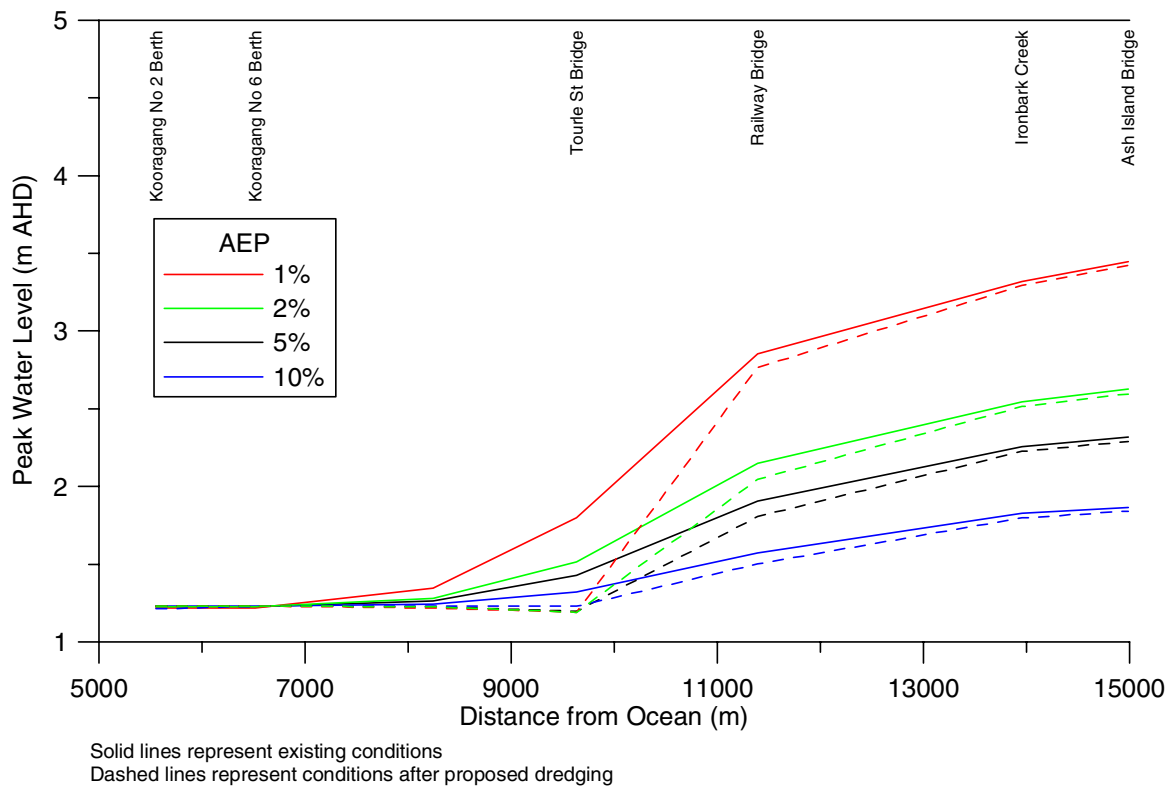


Figure 28: Peak water levels for various AEP floods under existing and post dredging conditions (South Arm)

It is evident that peak water levels would reduce substantially immediately upstream of the dredged area. At Tourle St Bridge, where the greatest effects were noted, the reductions in peak levels were 0.6m, 0.3m, 0.2m and 0.1m for the 1%, 2%, 5% and 10% AEP events respectively. At the Railway Bridge, the reduction was in the order of 0.1m for all simulated events, and at Ironbark Creek, peak levels were about 0.03m lower over these events.

Peak flood levels were also found to slightly reduce in the North Arm and upstream to Hexham. For all simulated events, the reduction in peak levels was about 0.02m at Hexham and 0.03m near Moscheto Creek (except for the 10% AEP event at the latter site, for which levels were about 0.02m lower).

At Fullerton Cove, peak levels were about 0.02m and 0.01m lower for the 1% and 2% AEP events respectively. At Stockton Bridge, peak levels were about 0.015m and 0.007m lower for the 1% and 2% AEP events respectively. For higher AEP events, flood level reductions at these two sites were generally only a few mm.

The proposed dredging thus provides some benefits in terms of slightly reduced flood risk throughout the lower Hunter estuary.

Although the reduction in flood levels within the South Arm would be substantial in the vicinity of Tourle St Bridge, it would not be expected that this would significantly impact on ecosystems such as freshwater wetlands that require inundation from floodwaters. This is because the flood flow currently remains in-bank even up to the 1% AEP event in this area. Proceeding upstream from the South Arm junction with the North Arm at Walsh Point, flows are not overbank until near Ironbark Creek on the south bank and at the Railway Bridge on the north bank. At these upstream locations, the peak water levels would not be substantially altered.

The proposed dredging also has the potential to alter the flow distribution, flood volumes and flood duration. To investigate these aspects, flow hydrographs for the design floods were determined. The approximate locations of cross sections where flow hydrographs were determined are shown in **Figure 29**.

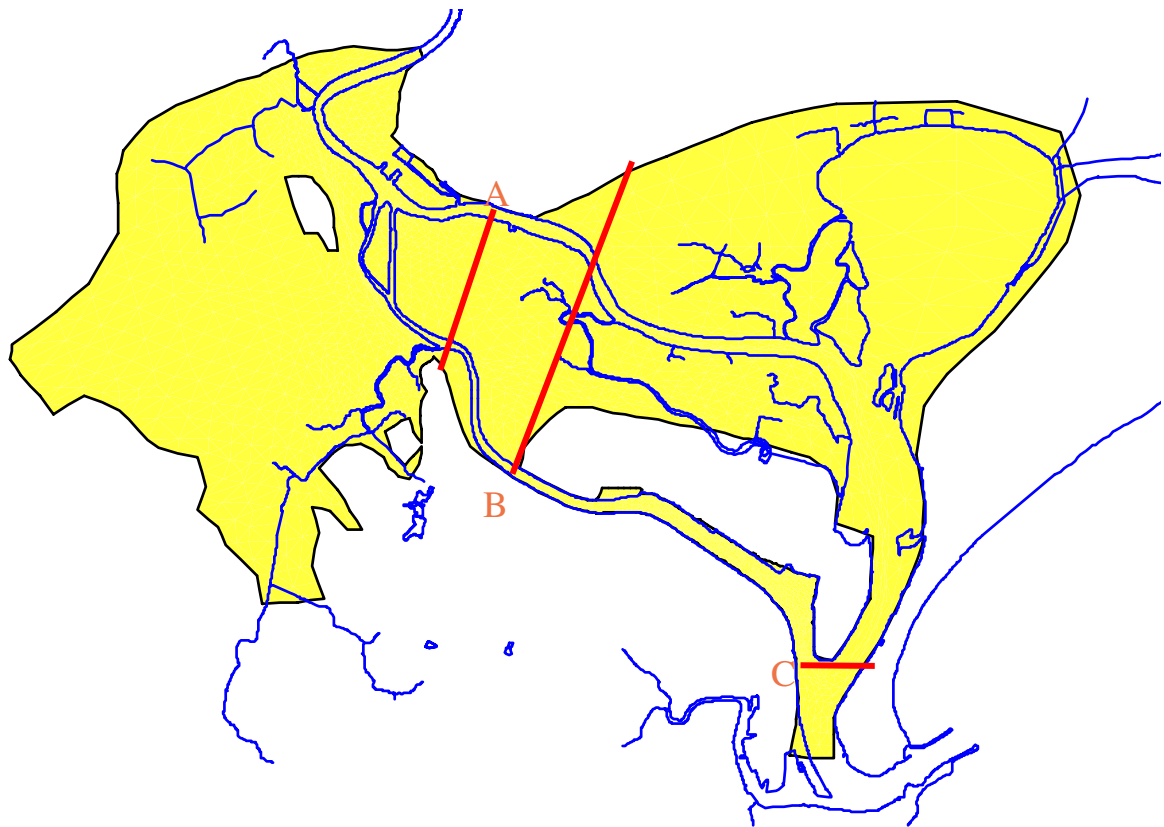


Figure 29: Approximate locations of cross sections for flow hydrograph determination

At Location A, sections were divided into the North Arm, Kooragang Island, South Arm and Ironbark Creek/Hexham Swamp (proceeding north to south), as defined by the river channels and floodplain areas. At Location B, sections were divided into Tomago, North Arm, Kooragang Island and South Arm. At Location C, there were only two sections, for the North Arm and South Arm.

The peak flow and total hydrograph volume at each of these cross sections, for existing and post-dredging conditions, is shown in **Table 16** for the 1% AEP event and **Table 17** for the 10% AEP event.

Table 16: Peak flows and flood hydrograph volumes for the 1% AEP flood, for existing and post dredging conditions (% of total for each section in brackets)

Section	Location	Existing		Post Dredging	
		Peak flow (m ³ /s)	Hydrograph volume (GL)	Peak flow (m ³ /s)	Hydrograph volume (GL)
A	North Arm	1710 (21%)	175 (31%)	1720 (21%)	175 (31%)
A	Kooragang Island	4250 (53%)	234 (42%)	4230 (53%)	233 (42%)
A	South Arm	640 (8%)	57 (10%)	650 (8%)	58 (10%)
A	Hexham Swamp	1390 (17%)	91 (16%)	1390 (17%)	91 (16%)
B	Tomago	2550 (34%)	125 (23%)	2490 (33%)	120 (22%)
B	North Arm	1470 (19%)	167 (31%)	1480 (20%)	166 (31%)
B	Kooragang Island	1650 (22%)	95 (18%)	1590 (21%)	91 (17%)
B	South Arm	1880 (25%)	156 (29%)	2010 (27%)	167 (31%)
C	North Arm	5790 (73%)	385 (70%)	5670 (72%)	375 (68%)
C	South Arm	2130 (27%)	164 (30%)	2250 (28%)	174 (32%)

Table 17: Peak flows and flood hydrograph volumes for the 10% AEP flood, for existing and post dredging conditions (% of each section in brackets)

Section	Location	Existing		Post Dredging	
		Peak flow (m ³ /s)	Hydrograph volume (GL)	Peak flow (m ³ /s)	Hydrograph volume (GL)
A	North Arm	930 (40%)	110 (45%)	930 (40%)	109 (44%)
A	Kooragang Island	750 (32%)	70 (29%)	740 (32%)	70 (28%)
A	South Arm	290 (13%)	33 (13%)	300 (13%)	34 (14%)
A	Hexham Swamp	370 (16%)	32 (13%)	370 (16%)	33 (14%)
B	Tomago	320 (14%)	29 (12%)	310 (13%)	28 (11%)
B	North Arm	900 (39%)	109 (44%)	895 (38%)	109 (43%)
B	Kooragang Island	330 (14%)	32 (13%)	310 (13%)	30 (12%)
B	South Arm	790 (34%)	79 (32%)	840 (36%)	84 (34%)
C	North Arm	1560 (66%)	159 (67%)	1520 (64%)	155 (66%)
C	South Arm	790 (34%)	77 (33%)	840 (36%)	81 (34%)

It is evident that there would be only a small alteration to peak flows and flow volumes during floods as a result of the proposed dredging. After dredging, there would be a tendency for slightly more flow to pass down the South Arm, and slightly less flow to pass across Kooragang Island north of the industrial area. However, in terms of the overall peak flow and flow volume distribution, the alterations are only in the order of 1-2% and can be considered to be insignificant in terms of the overall flooding regime.

Hydrographs for Locations A, B, and C (for existing and post-dredging conditions) are shown in **Figure 30**, **Figure 31** and **Figure 32** respectively for the 1% AEP event, and **Figure 33**, **Figure 34** and **Figure 35** respectively for the 10% AEP event.

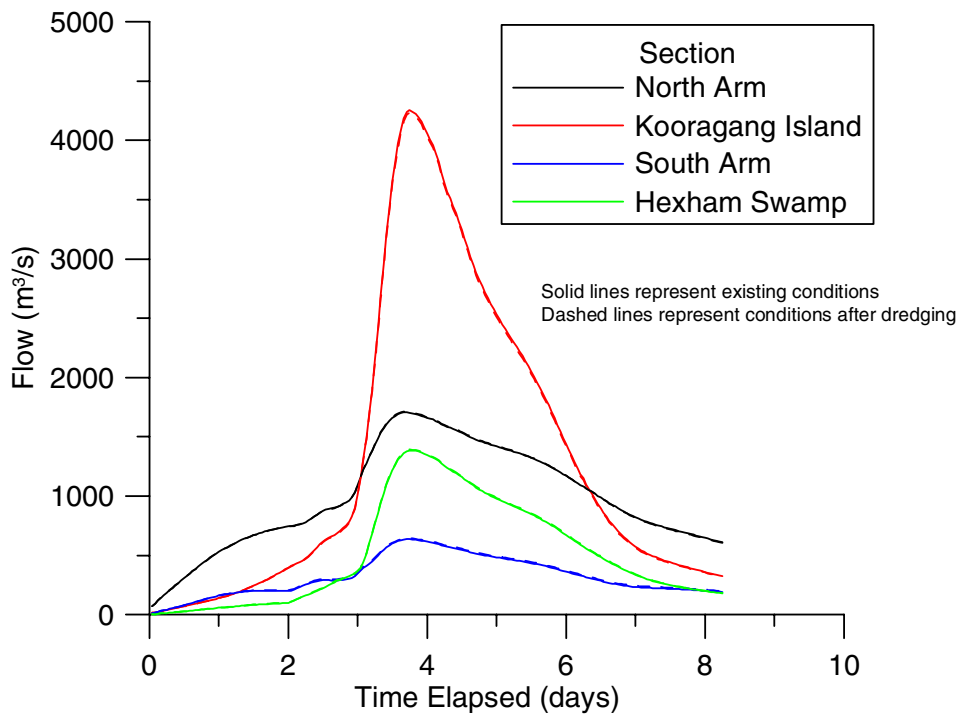


Figure 30: Flow hydrographs for Location A, 1% AEP event

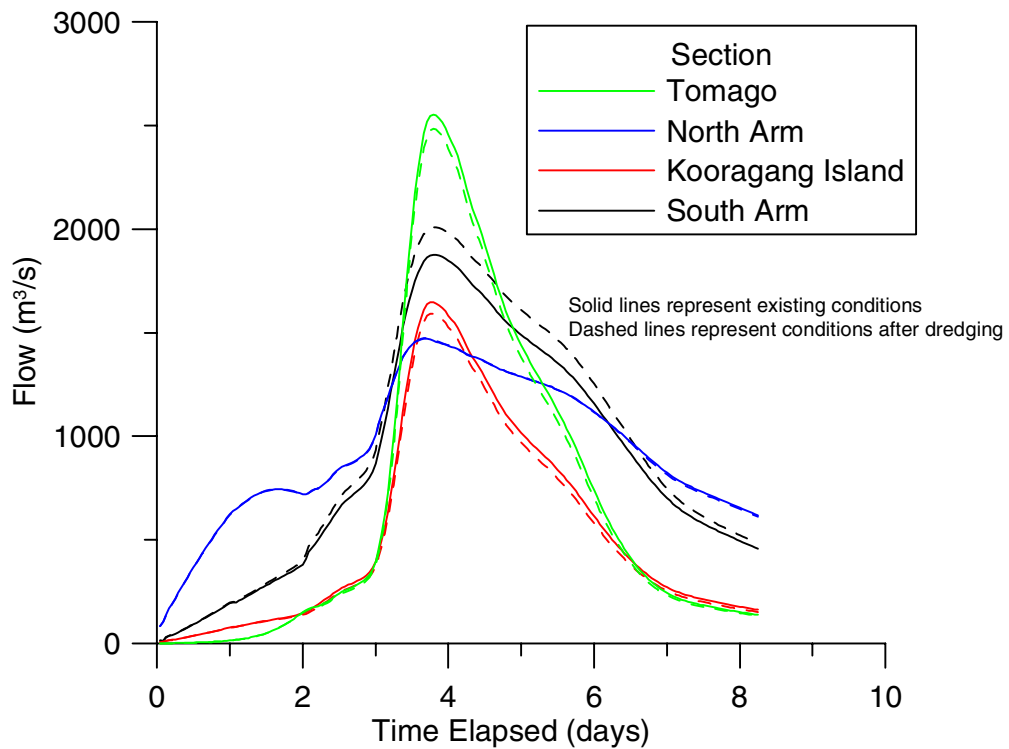


Figure 31: Flow hydrographs for Location B, 1% AEP event

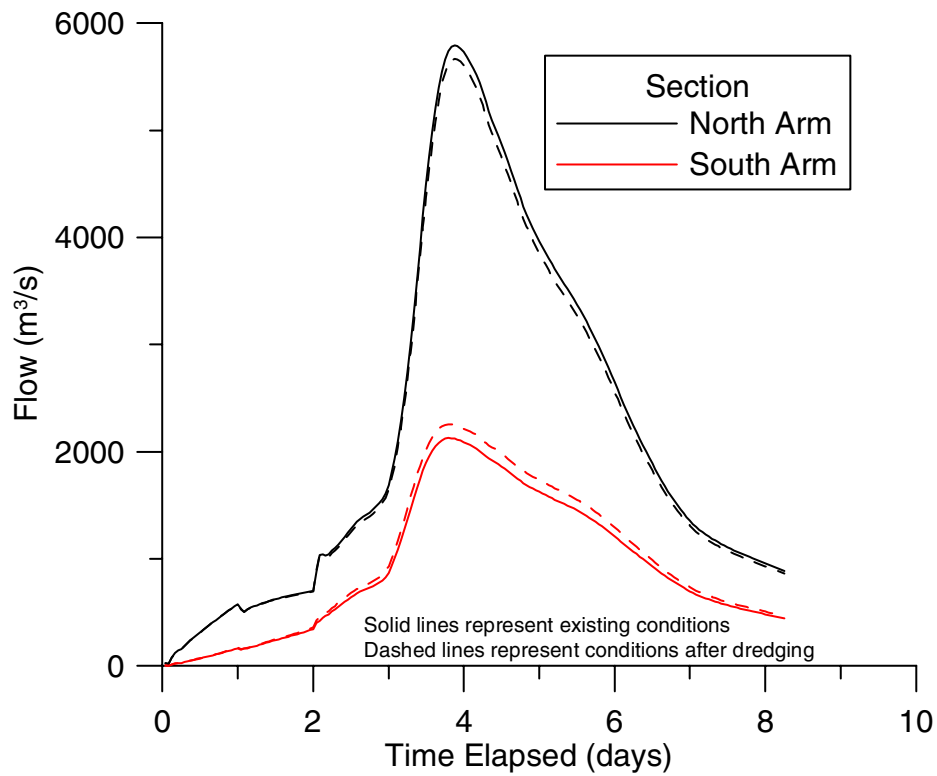


Figure 32: Flow hydrographs for Location C, 1% AEP event

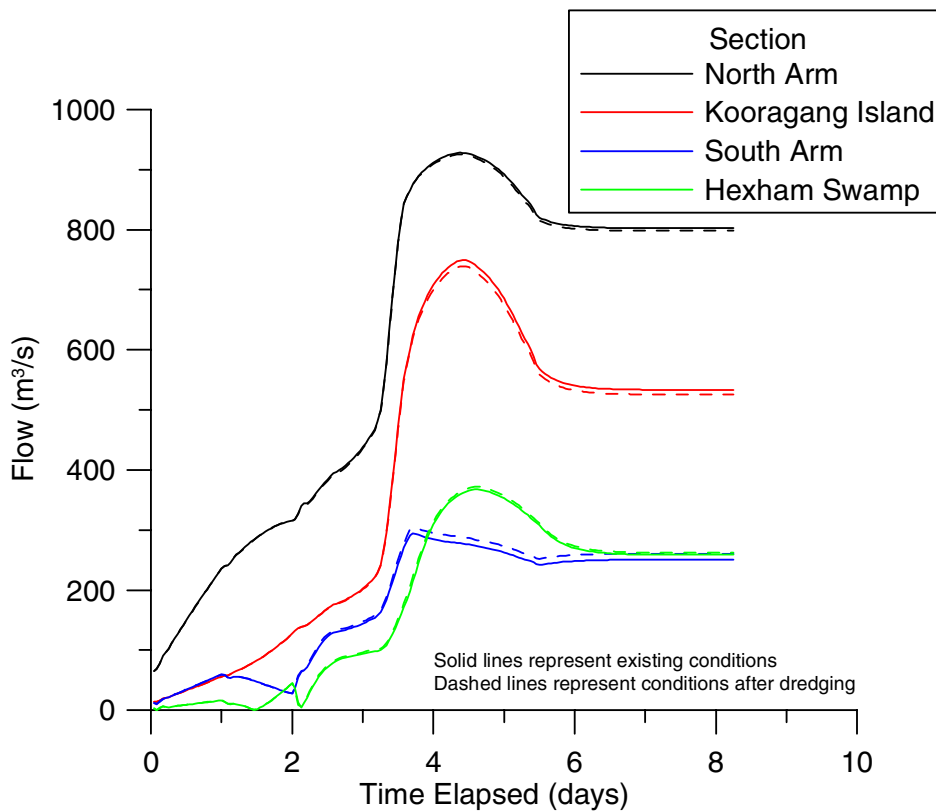


Figure 33: Flow hydrographs for Location A, 10% AEP event

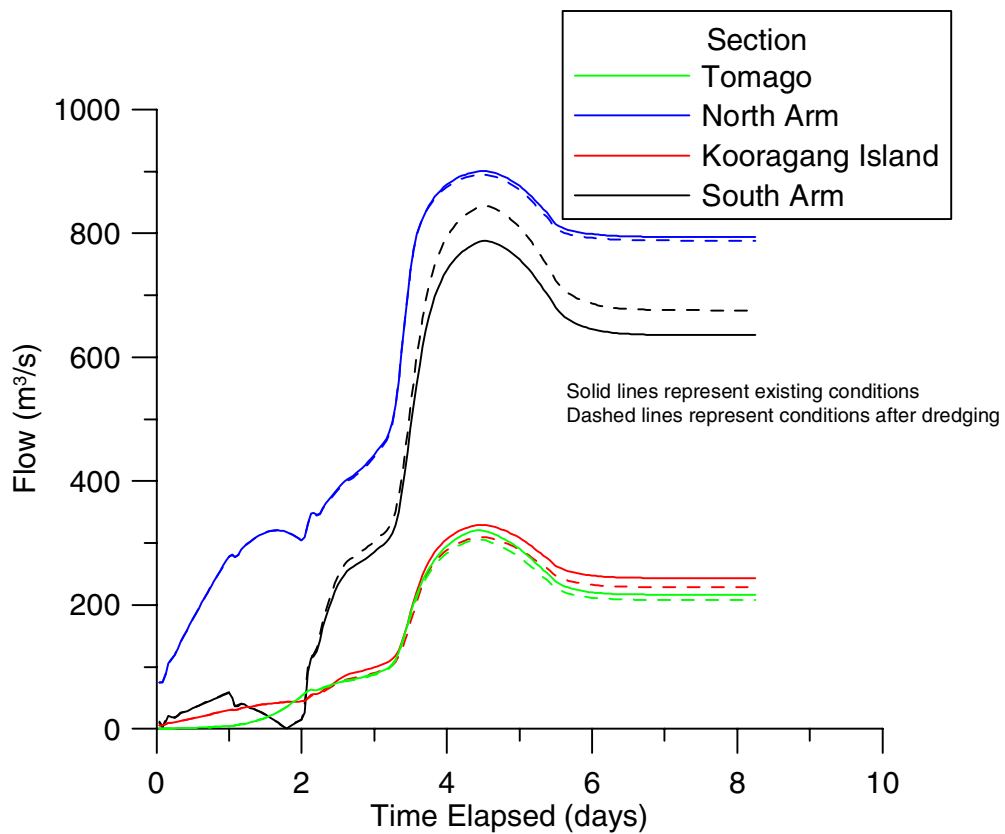


Figure 34: Flow hydrographs for Location B, 10% AEP event

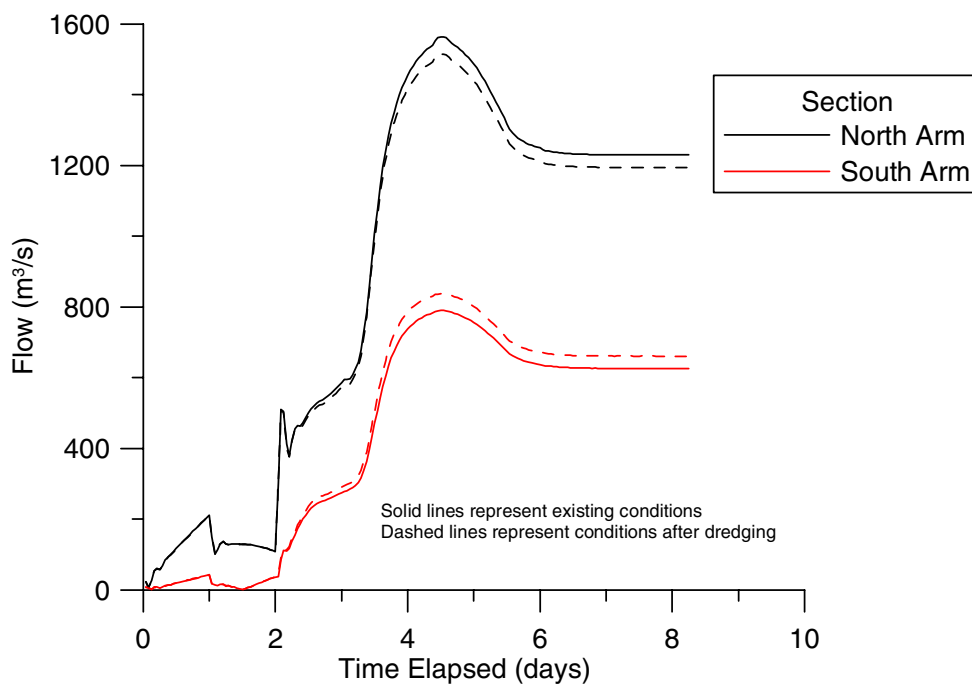


Figure 35: Flow hydrographs for Location C, 10% AEP event

It is again evident that there would be only a slight alteration to flow hydrographs as a result of the proposed dredging. Therefore, there would be virtually no alteration to flood durations, with pre and post dredging flood hydrographs having virtually identical shapes throughout the estuary.

Given that flow rates and volumes would not be substantially altered as a result of the proposed dredging, it can be stated that velocities would not alter substantially, except in areas where the cross sectional area would change. With the dredged section having a larger flow area, velocities would reduce in this area compared to existing conditions.

The peak mean (cross-section averaged) post-dredging velocities at the Railway Bridge, Tourle St Bridge and three cross sections along the dredged profile for the 1% AEP are given in **Table 18**, along with corresponding values for existing conditions.

Table 18: Peak mean velocities along dredged profile and nearby upstream sites for existing and post-dredging conditions (1% AEP flood)

Location	Peak Mean Velocity (m/s)	
	Existing	Post Dredging
Railway Bridge	1.9	2.1
Tourle St Bridge	2.3	3.2
Swinging Basin	1.7	0.5
Midway along proposed -16.5m AHD profile	1.6	0.4
Upstream of Kooragang No. 6 Berth ²⁰	1.1	0.4

It is evident that velocities would reduce substantially in the dredged area after the completion of dredging. At the three sections within the dredged area assessed in **Table 18**, peak velocities reduced by about 65-75%. This would be beneficial in terms of navigation and bank erosion.

Compared to existing conditions, velocities upstream of the dredged area would increase after dredging for a particular AEP flood. At Tourle St Bridge, the peak mean velocity increased by about 40%, while at the Railway Bridge the increase in peak velocity was about 11%. These increases in velocity would be due to the combined effects of increased flow conveyed down the South Arm after dredging, and the reduced flow areas with the reduction in peak water levels.

Bank conditions in the South Arm, proceeding upstream of Tourle St Bridge, should be monitored after significant floods to determine if any new areas of bank erosion have developed as a result of the increased velocities.

3.3.4 Groundwater Characteristics

Given that there would be little alteration to the flooding regime, and also tidal hydrodynamics (Section 3.2), the frequency and duration of inundation for wetland and swamp areas would not be expected to be altered significantly. Therefore, it would not be expected that there would be significant alterations to groundwater characteristics in these wetland and swamp areas, such as the Kooragang Island wetlands and Hexham Swamp.

²⁰ This location is at the upstream limit of the current dredged area.

3.4 SALINITY STRUCTURE

3.4.1 Simulations of Salinity Intrusion

Salinity is a factor that affects the health and distribution of a number of estuarine flora species, including mangroves.

To investigate the potential alteration in salinity regime due to the proposed dredging, simulations were undertaken to investigate saline intrusion over a 29 day period, assuming an initially fresh estuary (0 ppt) and saline oceanic waters of 35ppt, under tidal conditions. These are conservative conditions under which to investigate any changes to salinity regime as freshwater flows (particular floods) have a more significant influence on estuarine salinities than tides as discussed in Section 2.4, and would mask out any variability in salinity intrusion. It would be expected that there would be little alteration to the high freshwater flow salinity regime under post dredging conditions.

The resulting salinity contours at the end of the simulation under existing and dredged conditions are shown in **Figure 36** and **Figure 37** respectively. It is evident that there would be slightly less saline intrusion under the dredged conditions, particularly in the South Arm. Salinity concentrations at the end of the 29 day simulations are tabulated in **Table 19**, along with the average difference in pre and post dredging salinities over the 29 days.

Further details on the salinity simulations are provided in **Appendix D**.

Table 19: Salinity values after 29 day simulation at various locations in estuary for existing and post-dredging conditions

Location	Salinity (ppt) after 29 days		Average difference in salinity pre and post dredging (ppt)
	Existing	Post-Dredging	
Entrance	34.4	34.2	-0.03
Hannell St Bridge, Throsby Creek	33.6	33.3	-0.2
Stockton Crossing	31.1	30.1	-0.6
Walsh Point	29.8	28.0	-1.3
Kooragang No 2 Berth	28.2	25.3	-2.7
Kooragang No 6 Berth	28.0	24.8	-3.3
Tourle St Bridge	26.1	23.7	-2.9
Railway Bridge (South Arm)	24.1	22.3	-2.3
Ironbark Creek entrance	20.0	18.2	-1.3
Stockton Bridge	25.7	24.2	-0.8
Fullerton Cove	21.6	20.4	-0.8
Moscheto Creek	18.2	17.1	-0.6
Tomago	15.7	14.7	-0.5
North Arm and South Arm upstream junction	12.8	12.0	-0.4
Hexham Bridge	10.7	10.1	-0.3
Greenways Creek	4.1	3.9	-0.07
Raymond Terrace	1.1	1.0	-0.01

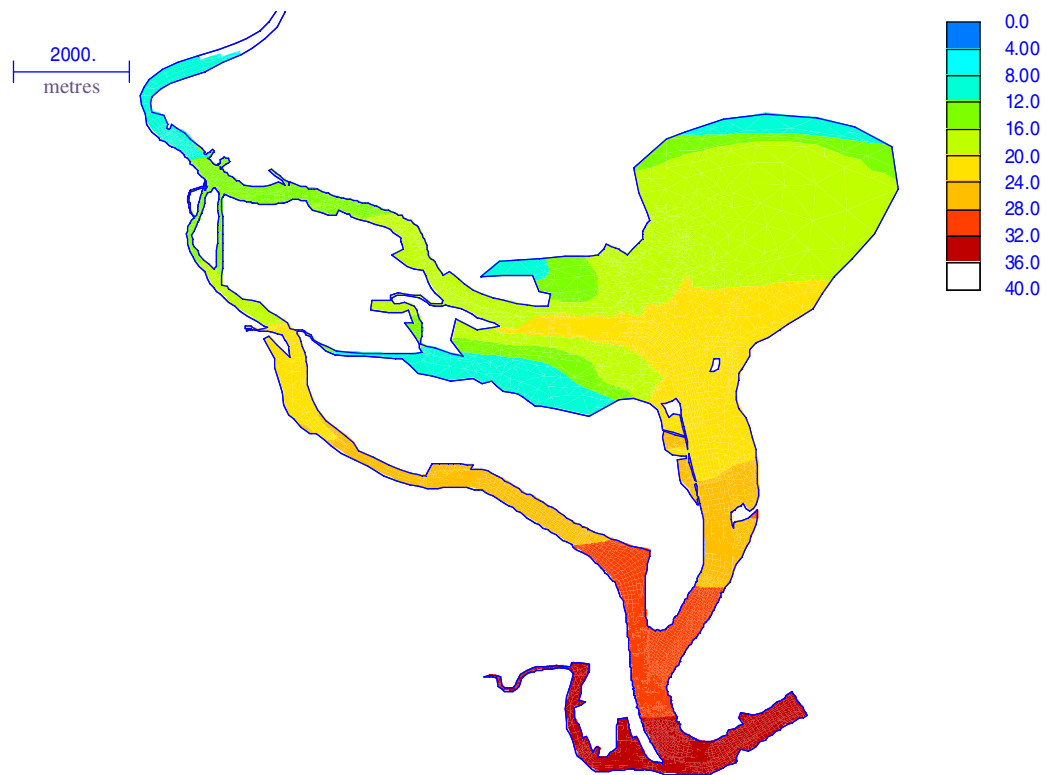


Figure 36: Salinity contours (ppt) after 29 day tidal simulation, assuming initially fresh estuary, for existing conditions

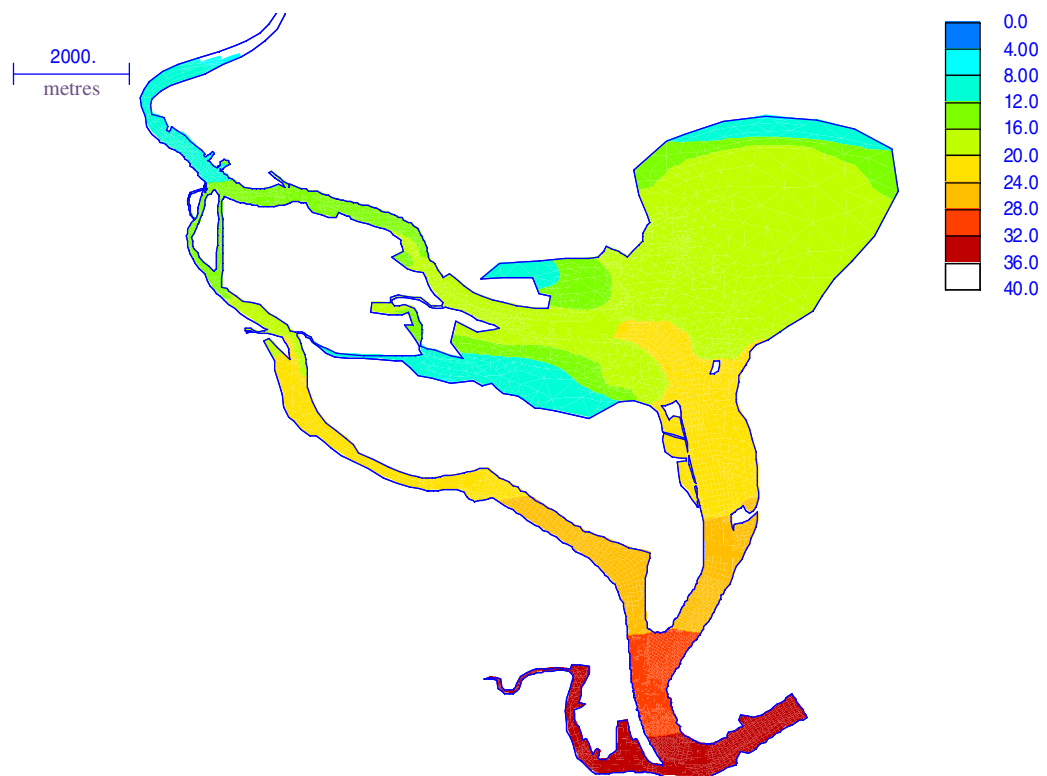


Figure 37: Salinity contours after 29 day tidal simulation, assuming initially fresh estuary, for post-dredging conditions

As is evident, the alteration to the salinity intrusion regime was found to be concentrated near the dredge footprint, from Walsh Point to Ironbark Creek in the South Arm. In this reach, salinity values were (on average) more than 1 ppt lower over the 29 day simulation after dredging. The reduction in salinity intrusion would mainly be caused by reduced tidal velocities in the proposed dredged area.

The temporal variation in salinity over the 29 day simulations is shown in **Figure 38** (for Walsh Point), **Figure 39** (Tourle St Bridge), **Figure 40** (Ironbark Creek), **Figure 41** (Moscheto Creek) and **Figure 42** (Hexham Bridge).

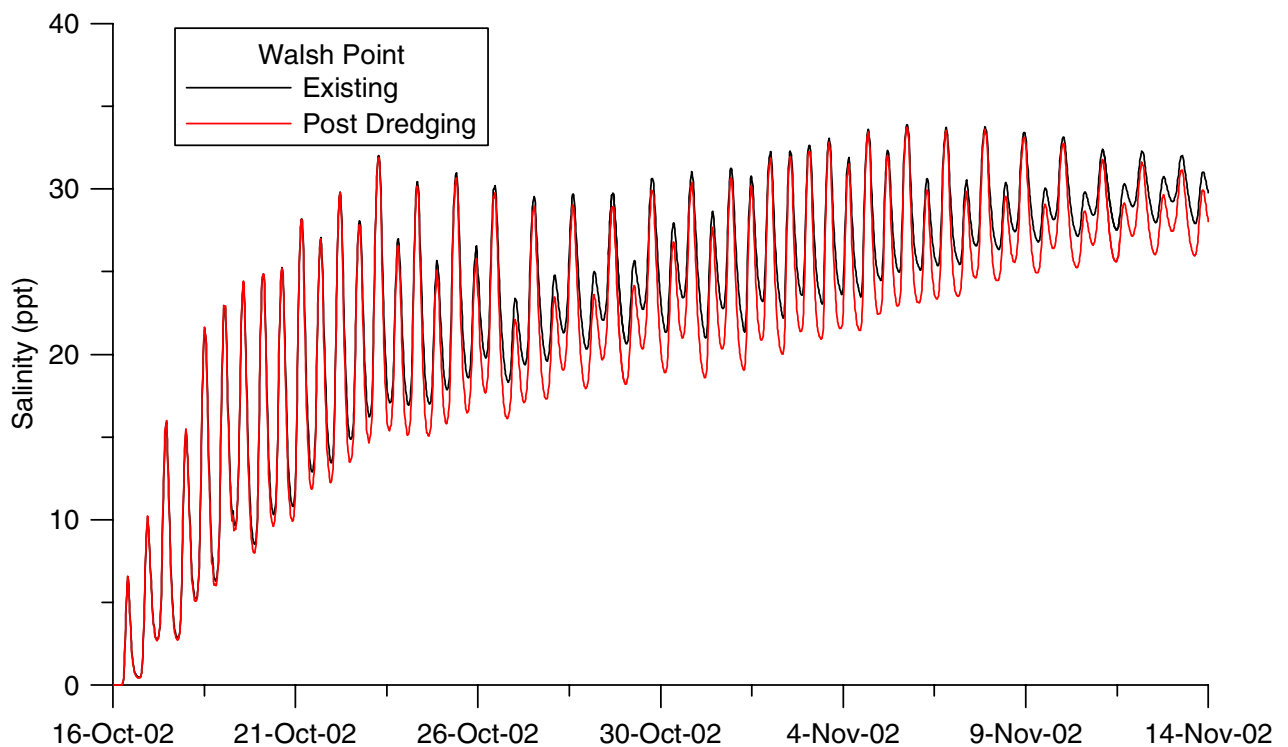


Figure 38: Pre and post dredging variation in salinity at Walsh Point over 29 day simulation

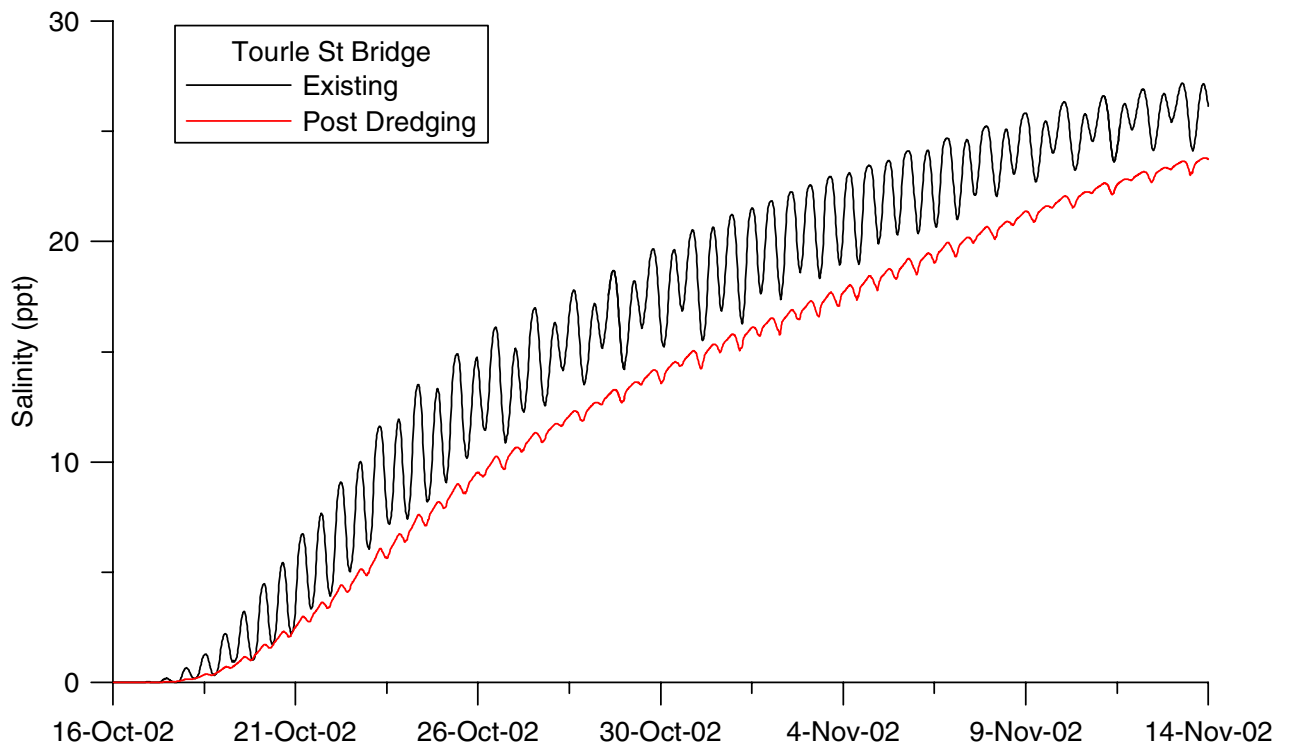


Figure 39: Pre and post dredging variation in salinity at Tourle St Bridge over 29 day simulation

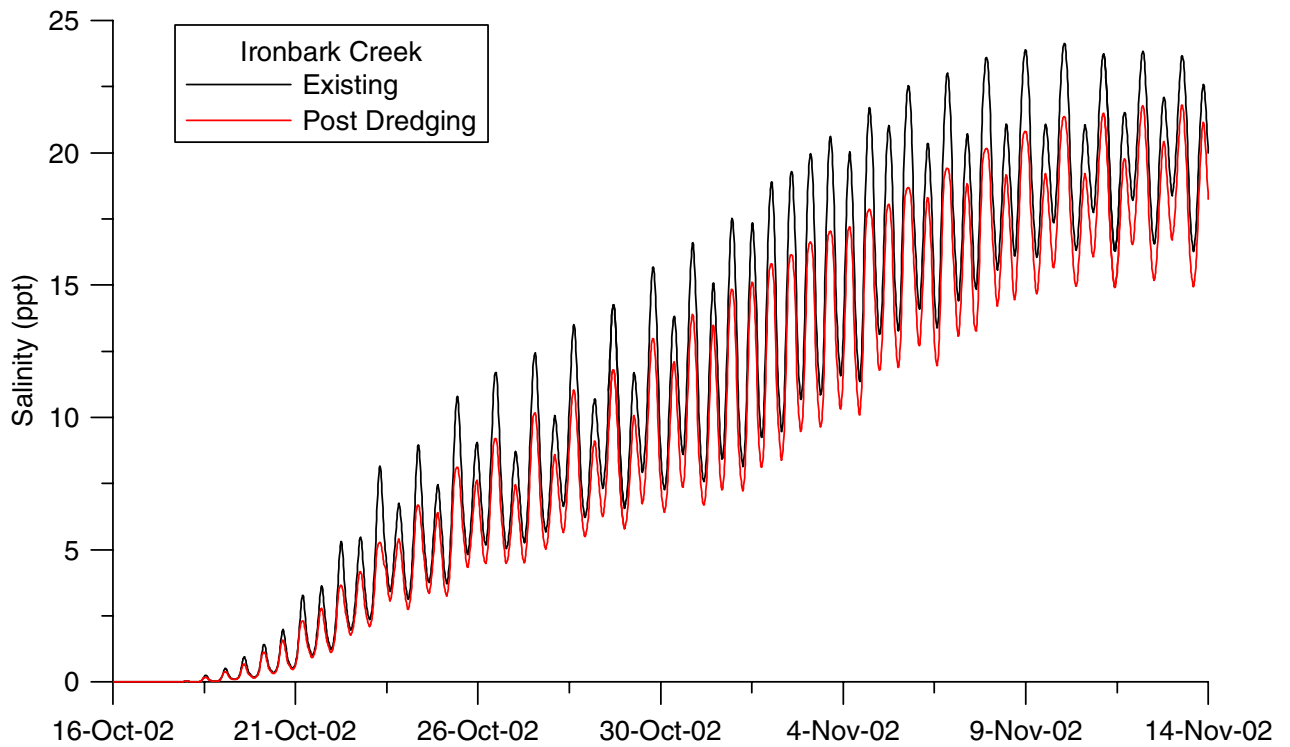


Figure 40: Pre and post dredging variation in salinity at Ironbark Creek over 29 day simulation

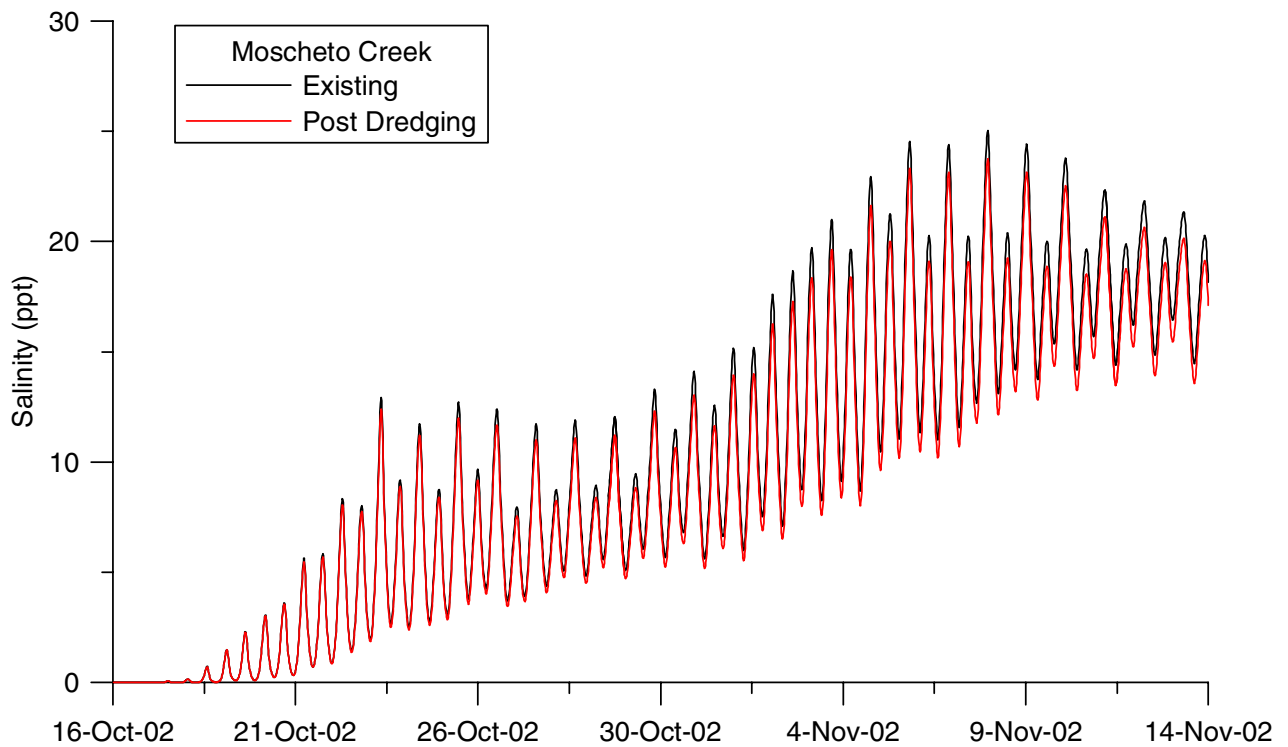


Figure 41: Pre and post dredging variation in salinity at Moschetto Creek over 29 day simulation

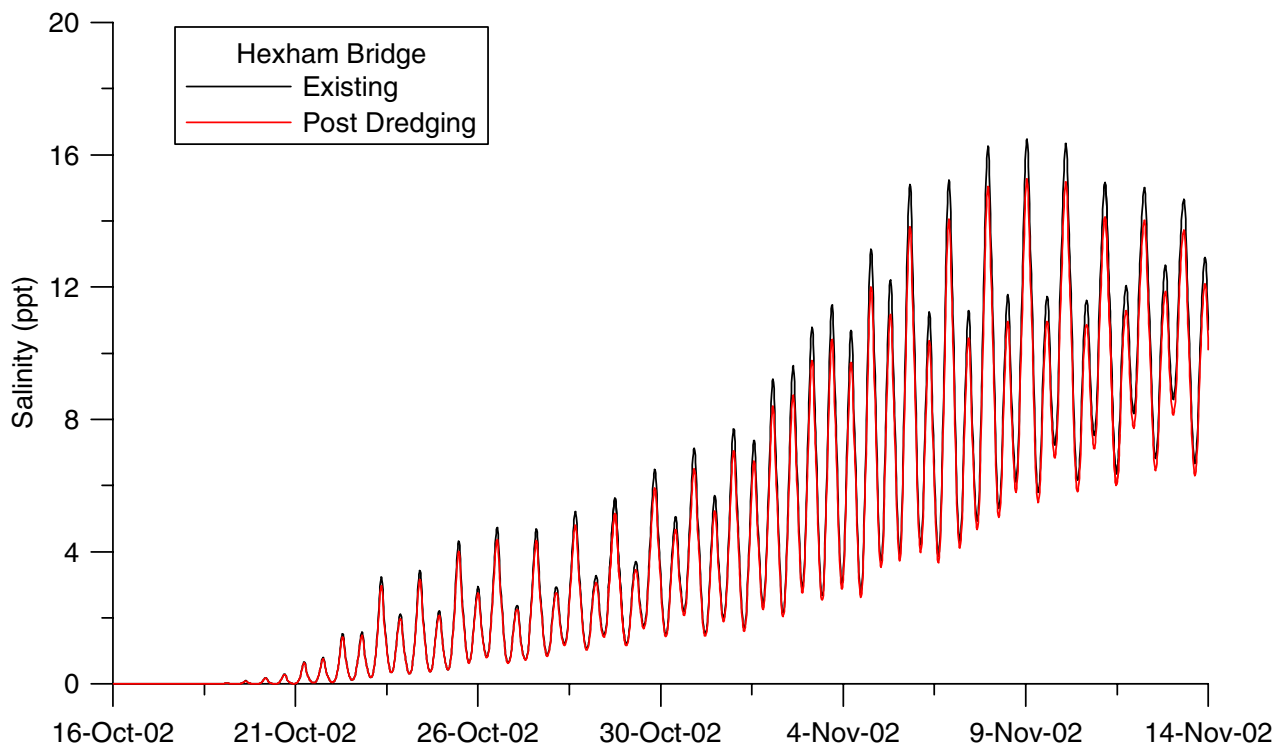


Figure 42: Pre and post dredging variation in salinity at Hexham Bridge over 29 day simulation

It can be seen that there would be only small changes to the salinity regime outside of the Walsh Point to Ironbark Creek reach. The effect of dredging in this reach would be to slightly reduce both the variability in salinity (within and upstream of the dredged area) and upstream intrusion of salinity.

3.4.2 Effect of Altered Salinities on Biota

Flora sensitive to salinity would include mangroves, which are mainly located south of Ironbark Creek on the right bank of the South Arm in this reach, as far downstream as the Railway Bridge. There is also a small stand of mangroves just downstream of Tourle St Bridge, but these would be physically removed as part of the dredging operation.

Mangroves in the Hunter estuary already inhabit a wide variety of areas subject to significantly different salinity regimes, from Stockton to Hexham, indicating their tolerance to a wide range of salinities. Numerous studies of established mangroves in NSW (Hawkesbury River, Lane Cove River, Botany Bay) have found no correlation between mangrove distribution and salinity (Clarke and Allaway, 1993).

Mangroves are tolerant of saline waters, and generally prefer estuarine environments. However, if salinity is altered dramatically, mangroves can exhibit a degree of damage. As reported by Field (1987), for the Grey Mangrove (*Avicennia marina*)²¹, various studies have indicated the optimum salinity for mangrove growth is between about 4 and 18 ppt²². The other species present in the Hunter, the River Mangrove (*Aegiceras corniculatum*), also falls within this range for optimum growth. Therefore, as salinities increase above about 18ppt, growth rates may decline.

Given the wide range of salinities for optimal mangrove growth, it would not be expected that the relatively small predicted post-dredging alteration to salinity intrusion during low freshwater flows would cause significant stress on existing mangrove stands.

Saltmarsh is also potentially sensitive to salinity, although would be expected to survive in higher salinities compared to mangroves. The main factor affecting the zonation of saltmarsh is water availability, related to tidal inundation (Harty and Cheng, 2002). Given that tidal and flood-related inundation would not be expected to alter significantly after dredging, no significant impacts on saltmarsh would be expected.

The structure of fish assemblages has also been shown to be influenced by a range of environmental variables, including salinity (Bishop, 1999). However, when assessing the role of salinity, the complexities introduced by other variables such as turbidity was emphasised. It was also noted that the tolerance of fish to extremes in salinity differs considerably between species.

Bishop (1999) termed biota capable of withstanding wide variations in salinity as “euryhaline”, while those only able to withstand a narrow range were termed “stenohaline”. For the latter, biota only capable of withstanding a narrow range of high salinities were termed “stenohaline-marine”, while those only able to tolerate a narrow range of very low salinities were denoted as “stenohaline-freshwater” species.

²¹ The Grey Mangrove is the dominant mangrove species in the Hunter estuary (MHL, 2002).

²² Note that Field (1987) reported optimum values as percentages of seawater NaCl concentrations, which were assumed here to be equivalent to salinities in ppt relative to an oceanic value of 35ppt.

Given that salinity intrusion would be expected to reduce as a result of the dredging, the species for which available habitat may reduce would be stenohaline-marine. However, since alterations to salinity as a result of the dredging would be minimal in the high salinity range, and given that there still would be abundant high salinity habitat available, the impacts of altered salinity intrusion on fish would not be expected to be significant.

3.4.3 Impact on Proposed Opening of Ironbark Creek Floodgates

Given that the hydrodynamics and salinity intrusion into Hexham Swamp would not be expected to be altered significantly after dredging, there would be little impact from the proposed dredging on the expected outcomes from the proposed opening of the Ironbark Creek floodgates (as discussed in Section 2.8). In fact, the opening of the floodgates themselves would be expected to have substantially more influence on the hydrodynamics and water quality of Hexham Swamp than the proposed dredging.

3.5 WATER QUALITY

3.5.1 Simulation of Pollutant Flushing

The potential for dredging to alter the flushing characteristics of the estuary was assessed by means of the simulation of an arbitrary conservative constituent. In this approach, the entire model network was assumed to have an initial concentration of 100 g/m^3 of this arbitrary pollutant. The reduction of the pollutant concentration with time was observed over a 29 day tidal simulation, as unpolluted oceanic waters mixed in the estuary and diluted the pollutant.

The resulting pollutant concentrations at the end of the simulation under existing and dredged conditions are shown in **Figure 43** and **Figure 44** respectively. Note that the concentration values are equivalent to percentages of the initial pollutant concentration.

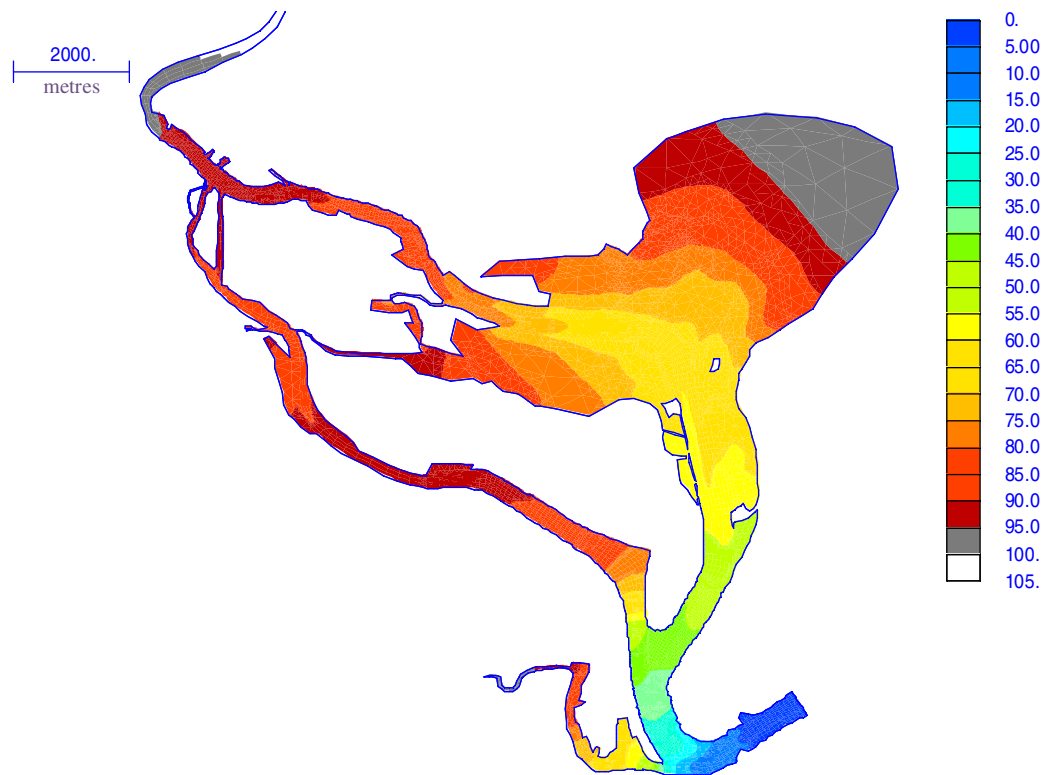


Figure 43: Hypothetical pollutant concentrations (%) relative to initial concentration, after 29 day tidal simulation, for existing conditions (pollutant initially everywhere)

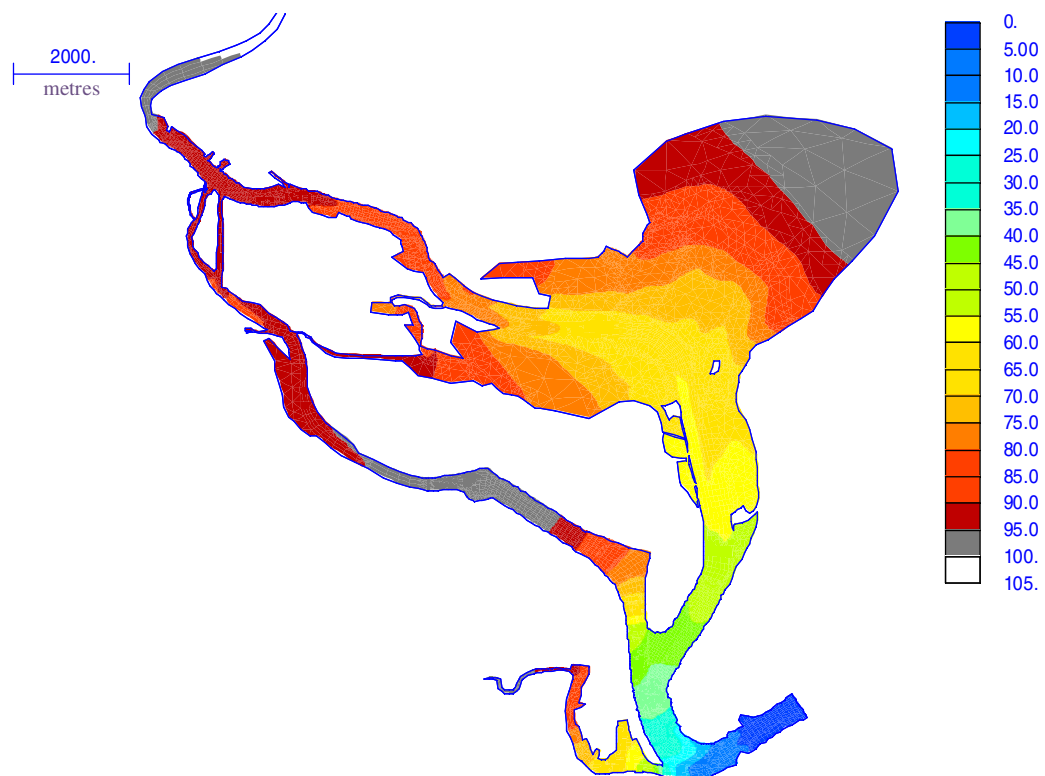


Figure 44: Hypothetical pollutant concentrations (%) relative to initial concentration, after 29 day tidal simulation, for post-dredging conditions (pollutant initially everywhere)

It can be seen that there was slightly less flushing of pollutants in the South Arm under post-dredging conditions, with most other areas of the estuary unaltered. Pollutant concentrations at the end of the 29 day simulations are tabulated in **Table 20**, along with the average difference in pre and post dredging pollutant concentrations over the 29 days.

Table 20: Hypothetical pollutant concentrations after 29 day simulation at various locations in estuary for existing and post-dredging conditions

Location	Pollutant concentration relative to initial (%)		Average difference in concentration pre and post dredging (%)
	Existing	Post-Dredging	
Entrance	2	2	-0.02
Hannell St Bridge, Throsby Creek	91	91	0.00
Stockton Crossing	40	39	-0.4
Walsh Point	48	49	-0.1
Kooragang No 2 Berth	73	74	-0.3
Kooragang No 6 Berth	82	83	0.5
Tourle St Bridge	91	96	1.6
Railway Bridge (South Arm)	90	94	1.0
Ironbark Creek entrance	89	90	0.4
Stockton Bridge	56	56	-0.6
Fullerton Cove	61	60	-0.5
Moscheto Creek	80	80	-0.1
Tomago	89	89	-0.01
North Arm and South Arm upstream junction	93	93	0.00
Hexham Bridge	95	95	0.03

The temporal variation in pollutant concentration at various locations over the 29 day simulations is shown in **Figure 45** (for Walsh Point), **Figure 46** (Tourle St Bridge), **Figure 47** (Ironbark Creek) and **Figure 48** (Moscheto Creek)

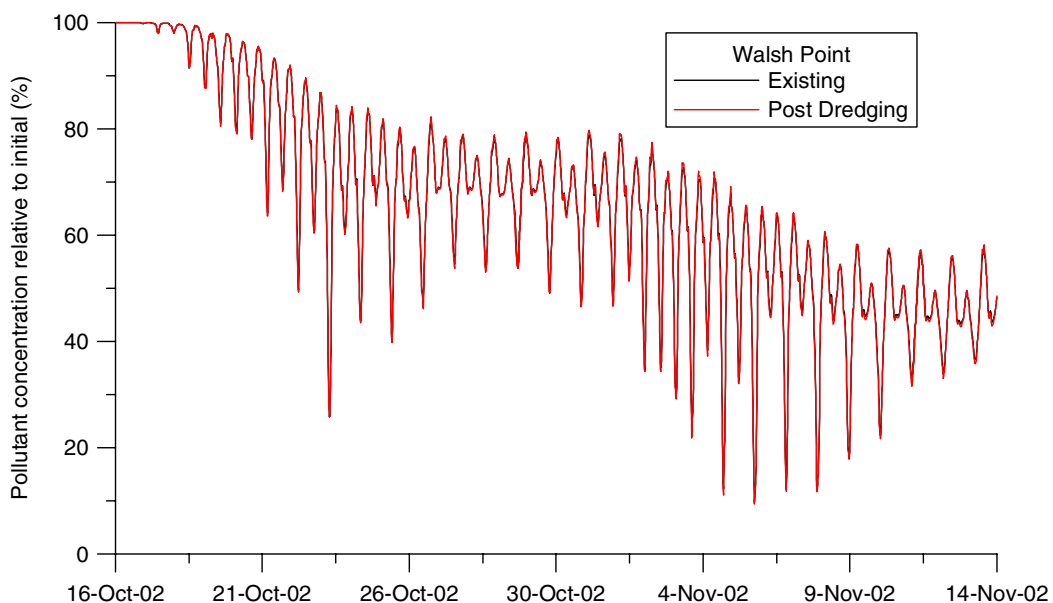


Figure 45: Pre and post dredging variation in hypothetical pollutant concentration at Walsh Point over 29 day simulation

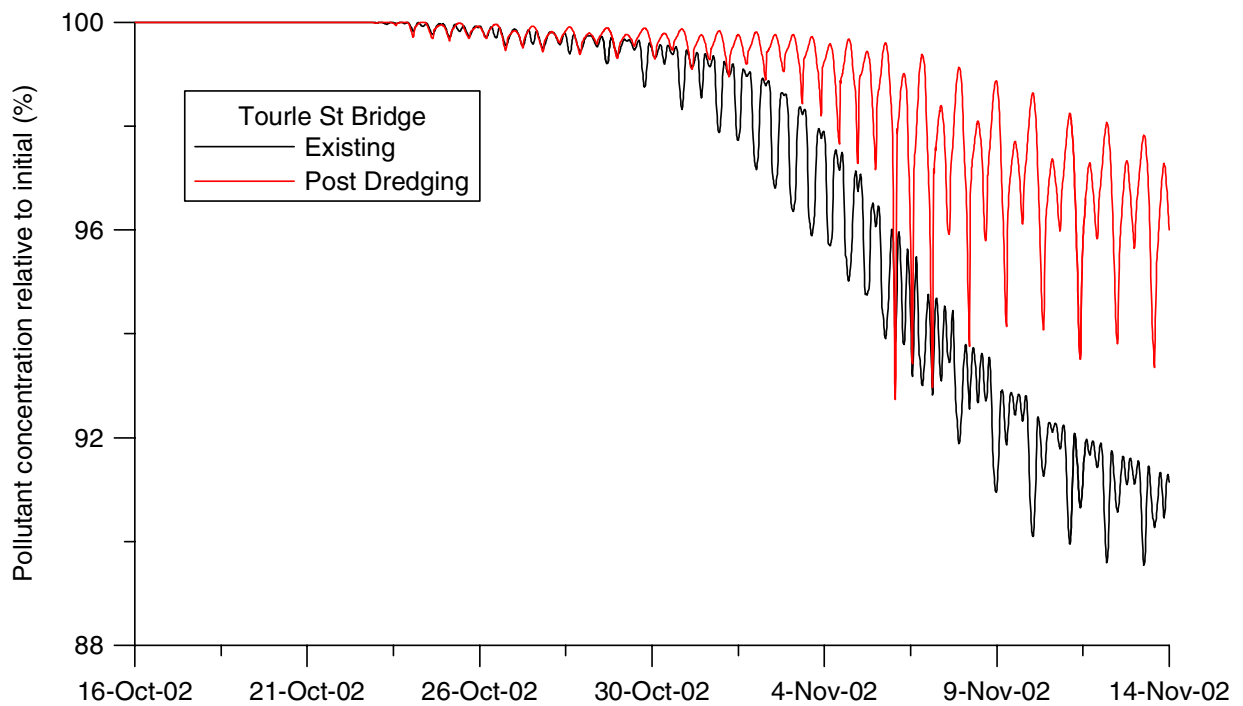


Figure 46: Pre and post dredging variation in hypothetical pollutant concentration at Tourle St Bridge over 29 day simulation

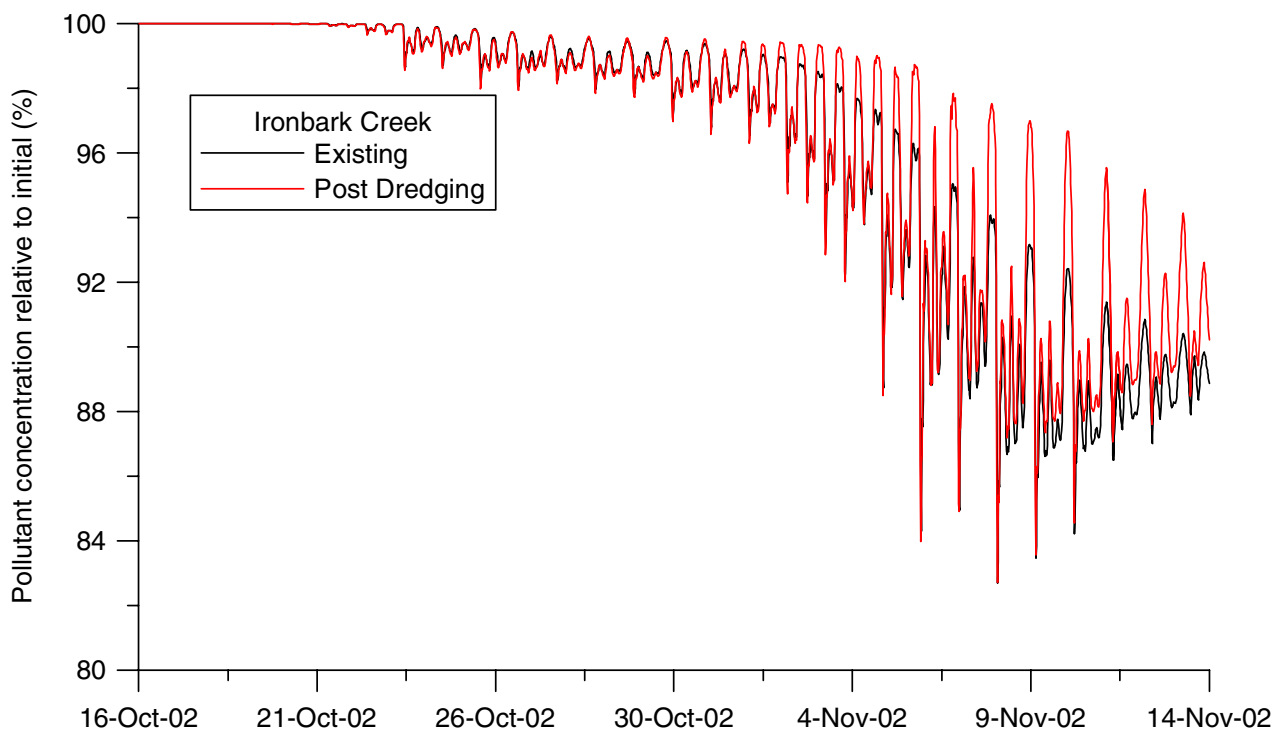


Figure 47: Pre and post dredging variation in hypothetical pollutant concentration at Ironbark Creek over 29 day simulation

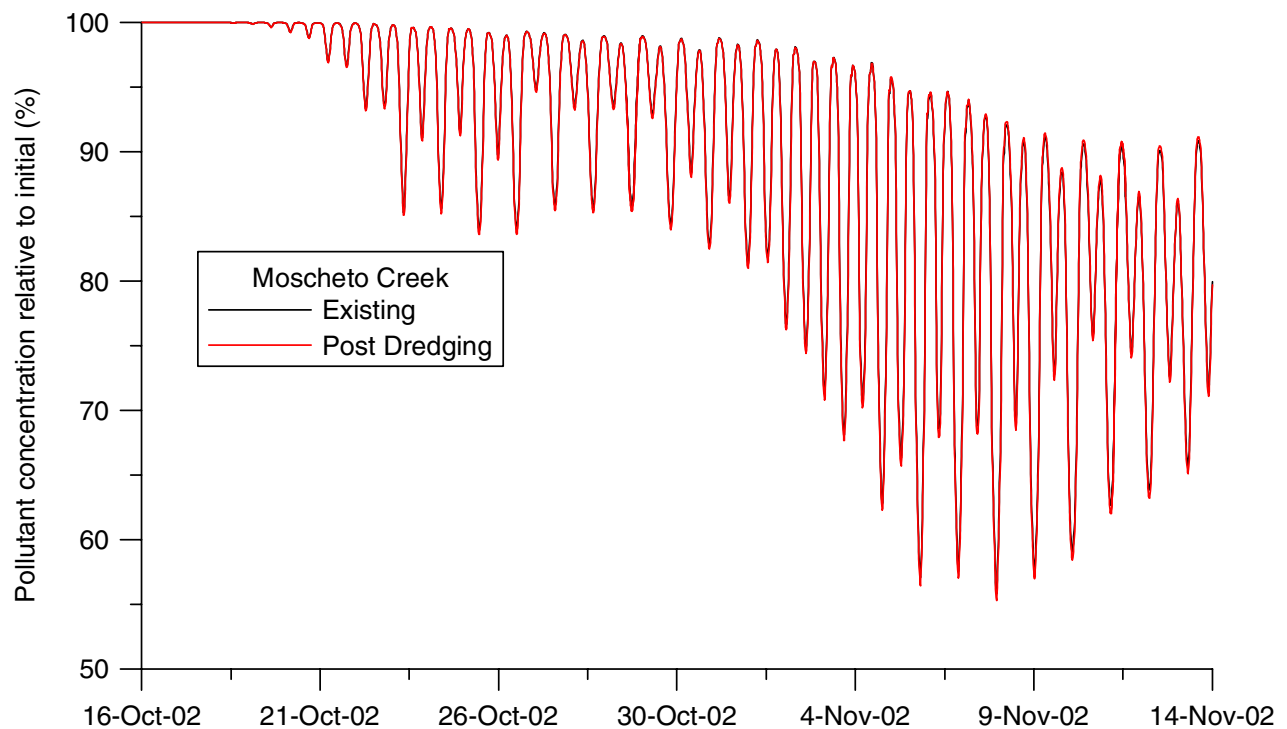


Figure 48: Pre and post dredging variation in hypothetical pollutant concentration at Moscheto Creek over 29 day simulation

It can be seen that the alteration to pollutant flushing characteristics was localised to within the dredged area and just upstream, with changes of only a few percent in concentrations after the 29 day simulations. The additional flushing benefits of spring tides were evident during early November.

3.5.2 Simulation of Pollutant Dispersion

Simulation of an arbitrary conservative constituent released at a constant rate in the South Arm into the ambient water column (assumed to be initially contaminant free) was also undertaken. The pollutant was released around 1.6km downstream of Tourle St Bridge, at a rate of 100 g/s. The reduction of the pollutant concentration with time was observed over a 29 day tidal simulation, as unpolluted ambient waters mixed in the estuary and diluted the pollutant.

The resulting pollutant concentrations at the end of the simulation under existing and dredged conditions are shown in **Figure 49** and **Figure 50** respectively.

It can be seen that pollutant concentrations are higher near the source and spread further upstream under existing conditions. Under post-dredging conditions, the pollutant in the South Arm would be more diluted. This would mainly be due to increased water depths in the vicinity of the pollutant source.

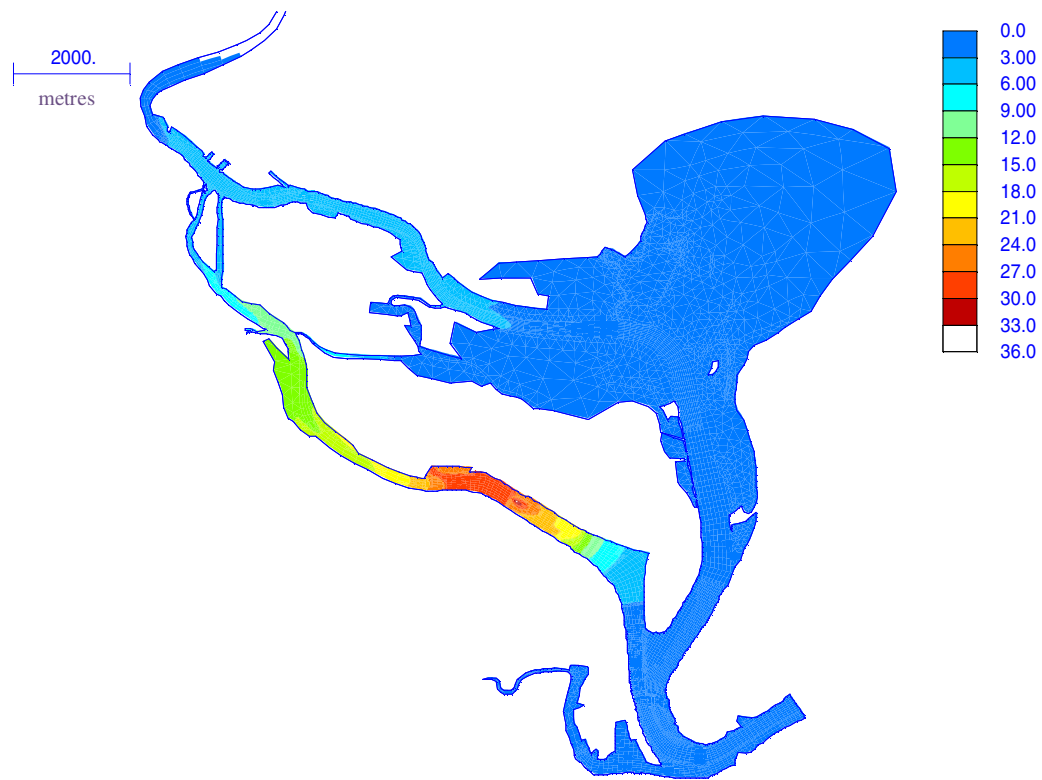


Figure 49: Hypothetical pollutant concentrations (mg/L) after 29 day tidal simulation, for existing conditions (100g/s pollutant source in South Arm)

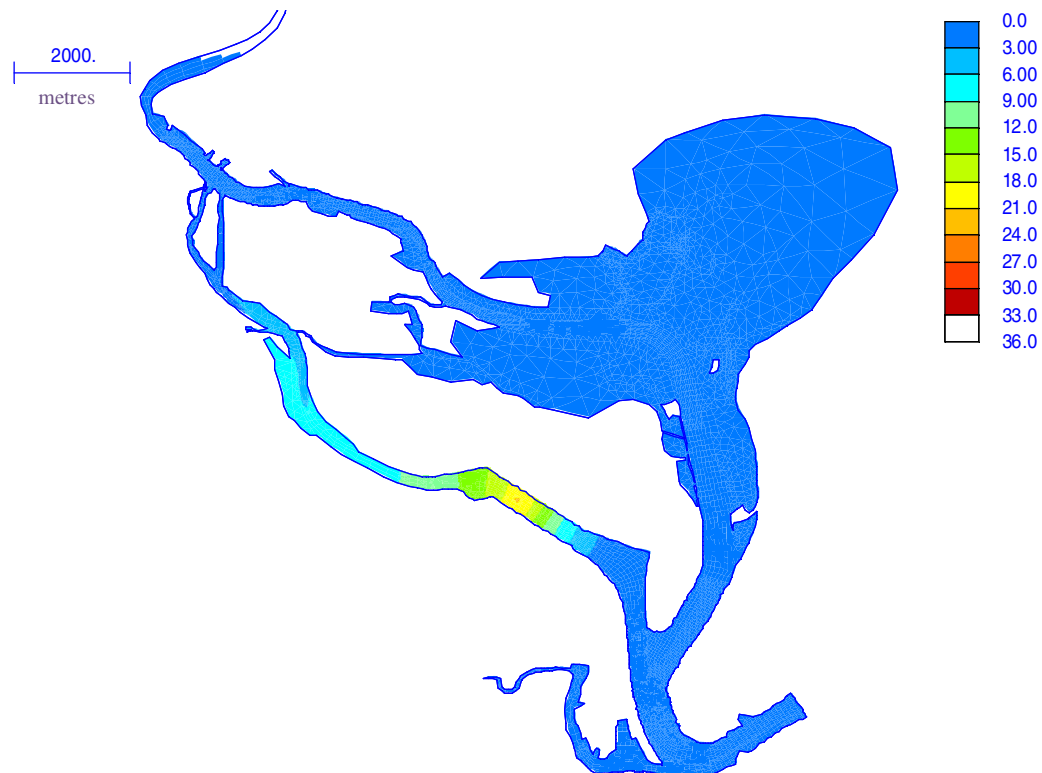


Figure 50: Hypothetical pollutant concentrations (mg/L), after 29 day tidal simulation, for post-dredging conditions (100g/s pollutant source in South Arm)

3.5.3 Effect of Deepening on Water Quality Processes

After dredging, the dredged area itself will be substantially deeper than under existing conditions. This would be expected to potentially alter various water quality processes in this reach, namely:

- there would be a greater likelihood for stratification to occur in the water column after high freshwater flows and as salinity intrudes upstream (before vertical salinity gradients have eroded due to mixing);
- this would coincide with relatively large organic loads depositing on the bed as the result of the freshwater flow (as they do under existing conditions);
- dissolved oxygen levels would reduce in the water column due to the breakdown of this organic material (as they do under existing conditions), potentially reducing the ability of the water column to support aquatic life; and,
- the stratification in the water column, at such times of high freshwater flows, may suppress mixing within this lower layer, exacerbating the reduction in dissolved oxygen, and potentially creating the circumstances leading to the formation of algal blooms; however, limited light penetration due to naturally high turbidity is likely to limit the formation of algal blooms in the Hunter estuary (MHL, 2002).

Dissolved oxygen measurements within the existing dredged areas of the estuary are relatively limited (Sanderson et al, 2001). However, the lower estuary generally has higher dissolved oxygen concentrations.

The measurements of Sanderson et al (2002) indicate that dissolved oxygen levels at depth do reduce substantially after floods. However, the most significant reductions in dissolved oxygen were well upstream of the existing dredged areas in the estuary. In the limited measurements of dissolved oxygen in Sanderson et al (2002), there are no examples of measurements that indicate relatively large dissolved oxygen reductions in the existing deep areas of the port. An example of post-flood dissolved oxygen concentrations in the Hunter estuary, for 16 and 19 March 2002, is shown in **Figure 51**.

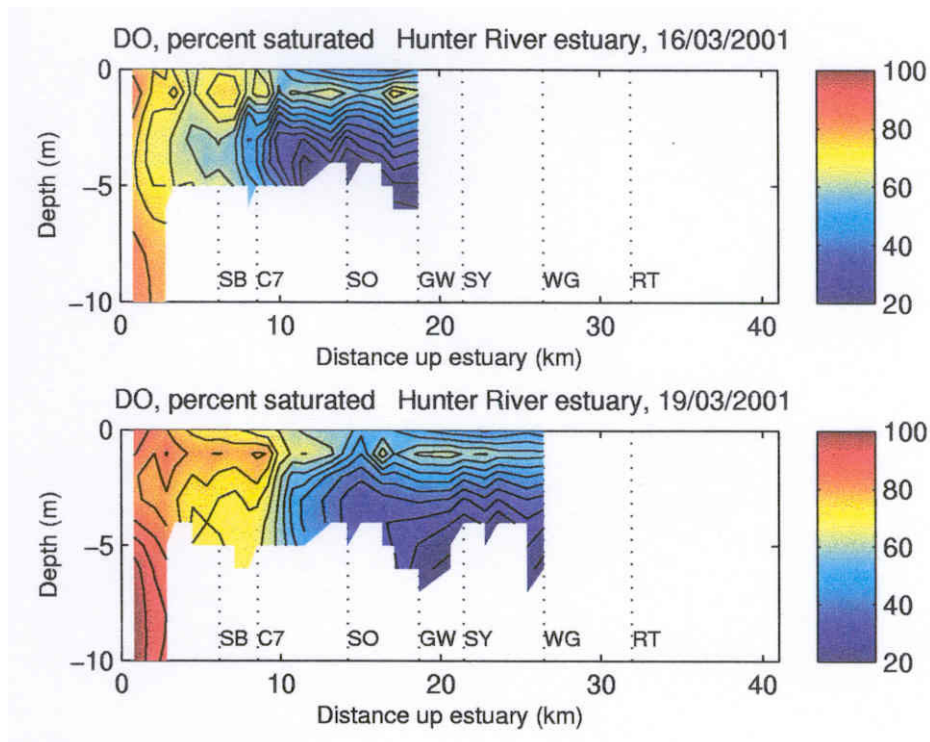


Figure 51: Post-flood dissolved oxygen measurements of Sanderson et al (2002), for two days in March 2001

It is evident that the most significant reductions in dissolved oxygen were upstream of about 10km from the entrance for this event, with concentrations in the order of 20-40% of saturation in this area. Dissolved oxygen concentrations near the entrance were substantially higher, even at a depth of 10m, with no evidence for reduced dissolved oxygen at depth in the downstream areas.

The low dissolved oxygen concentrations from 10km upstream may be related to the freshwater/saltwater interface being at this location²³. For this event, the interface was indeed about 10km upstream on 19 March 2001.

It would be expected that the water quality of the proposed dredged area would be similar to existing dredged areas such as the entrance to Throsby Creek, although even greater mixing would also be likely in the South Arm with the higher velocities. The available evidence suggests that the existing dredged areas have some of the best water quality results in the estuary, most likely since the downstream areas of the estuary have the greatest tidal flushing.

To improve the water quality of the Hunter estuary, a total catchment management approach should continue to be emphasised, with reductions in the sources of sediments and nutrients entering the estuary being the prime focus. This should continue to be implemented in an integrated manner by the responsible authorities such as the Department of Land and Water Conservation, Department of Mineral Resources, Hunter Catchment Management Trust, and

²³ Known as the location of the estuarine turbidity maximum, the freshwater/saltwater interface is typically an area of significant sediment deposition. Deposited particulate matter would promote a reduction in dissolved oxygen concentrations at depth.

Planning NSW (authorities listed as funding recommendations of the Healthy Rivers Commission, 2002).

3.5.4 Local Water Quality Impacts at Dredging Site due to Contamination

General

Available sediment quality data indicates that the fine grained marine silty clays found in the South Arm of the Hunter River are generally contaminated with heavy metals, polycyclic aromatic hydrocarbons (PAH's) and total petroleum hydrocarbons (TPH's), with the highest concentration of contaminants located in an area immediately adjacent to the former BHP Steelworks Site. During dredging, these contaminants could potentially either disperse remaining attached to the sediment or become disassociated from the sediment and disperse in solution.

Investigations into the contaminated sediments indicate that the sediments adjacent to the former BHP steelworks site are toxic to aquatic organisms and thereby unsuitable for unconfined sea disposal. Installation of a temporary sheet pile wall to contain these toxic sediments during dredging is proposed. A detailed description of the contaminated sediments is provided in Patterson Britton & Partners (2003b). In this report it was noted that:

- there would be little release of metals into pore waters and consequently no toxicity to marine organisms due to metals;
- total PAH's appeared to offer the best relationship with observed toxicity; and,
- the lowest total PAH concentration for which any toxicity (response < 80% of control) was observed in two or more bioassays was 75 mg/kg (normalised to 1% TOC²⁴). No toxicity was consistently observed for any bioassay with a total PAH concentration less than 75 mg/kg (normalised to 1% TOC).

Therefore, the temporary sheet pile wall is proposed to be installed along the 75 mg/kg total PAH contour line.

Water Quality Impacts During Dredging Inside the Sheet Pile Wall

In order to assess the potential impact on Hunter River water quality of the proposed dredging inside the sheet pile wall, a water quality sampling and testing program was undertaken during a bulk sediment sampling exercise conducted close to the foreshore of the former BHP Steelworks Site. Details of the water quality testing program and the bulk sediment sampling exercise are provided in GHD-Longmac (2003).

The water quality testing program involved testing of surface water samples taken inside and outside of a turbidity curtain surrounding three zones of sediment removal (representing high, medium and low sediment contamination). The sediment removal was undertaken using a barge mounted excavator.

Comparison of the water quality results from the samples taken immediately outside of the turbidity curtain prior to, during and after bulk sediment sampling indicated that all contaminants

²⁴ TOC is total organic carbon

except total zinc were below ANZECC/ARMCANZ (2000) high reliability trigger values. There was however some evidence that background levels of total zinc were elevated at concentrations close to the ANZECC/ARMCANZ (2000) high reliability trigger value.

Total zinc concentrations inside the turbidity curtain were particularly elevated corresponding to the elevated levels of suspended solids. The impact of elevated levels of total zinc at the dredge site are considered minimal as the turbidity curtain significantly reduces the levels of zinc and other contaminants in the surrounding waters; that is, levels of zinc recorded inside the turbidity curtain were up to 16 times higher than outside the curtain. In the physico-chemical environment of the river, zinc would generally be adsorbed to suspended solids and dilution with surrounding waters would occur. In addition, chemical analysis and toxicity testing of sediment with comparable levels of zinc has shown that zinc is of low bioavailability and is not toxic to sediment-dwelling organisms (CSIRO, 2001a).

The PAH concentration in all the water samples taken inside the turbidity curtain during the bulk sampling were high. However, all naphthalene concentrations were below the high reliability trigger value. Other more toxic PAH's exceed low reliability guidelines inside the turbidity curtain. However, these low reliability guidelines may be overly-conservative and should only be used as an indicative interim working level (ANZECC/ARMCANZ, 2000).

The results of the water quality testing program indicate a turbidity curtain is effective at containing levels of contamination within the water column. Similarly, installation of a sheet pile wall would form a physical barrier further containing contamination levels within the wall.

Consultation with EPA indicates that provision of the temporary sheet pile wall may alone be an adequate mitigation measure to control water quality impacts during dredging of sediments within the sheet pile wall. Depending on the method of dredging used and results of water quality monitoring during the dredging activity, a turbidity curtain could also be installed if necessary around the dredging plant.

Water Quality Impacts During Dredging Outside the Sheet Pile Wall

A series of investigations have been undertaken into the toxicity of the sediments of the South Arm. These investigations have indicated that sulfide, ammonia, cyanide, heavy metals, organochlorine (OC) pesticides, benzene, toluene, ethylbenzene and xylene (BTEXs) are below guideline levels or are not bioavailable to aquatic organisms. It was concluded that these contaminants are therefore not contributing to the toxicity of the Hunter River sediments. As noted above, PAH's appeared to offer the best relationship with observed toxicity.

The 95% upper confidence limit of the mean total PAH concentration for all sediment outside (offshore of) the 75 mg/kg total PAH contour line (normalised to 1% TOC), along which it is proposed to place the sheet pile wall, has been calculated to be 12.9 mg/kg (normalised to 1% TOC). This concentration is below a 15 mg/kg total PAH concentration limit (normalised to 1% TOC) recommended by the CSIRO, based on the available data for the protection of the

ecosystem and human health. In addition, elutriate testing²⁵ of sediment outside the sheet pile wall indicated contaminant concentrations measured in elutriate waters were generally below laboratory detection and would not be an ecological risk (Simpson et al, 2001a,b).

The sediment outside the sheet pile wall is therefore considered not toxic to aquatic organisms and suitable for unconfined sea disposal, which involves release of the sediment through the water column and its deposition on the seabed.

It would therefore be expected that dredging of the sediment outside the sheet pile wall, which would involve some disturbance of sediments into the water column, would not create circumstances that are toxic to aquatic organisms. It is also noted that a number of the dredging activities outside the sheet pile wall involving the soft silty clays would include use of a turbidity curtain (in order to restrict any visible turbidity plume), which would localise any water quality issue.

3.6 SEDIMENT TRANSPORT

3.6.1 Deposition of Suspended Sediment Generated During Dredging

Sediments which are dredged may go into suspension during the dredging process, and release toxic contaminants if already present. Fine material such as clay and silt has the greatest tendency to go into suspension during dredging, and since the fall velocity of these materials is so slow, these particles remain suspended in the water column for a longer time compared with coarse-grained particles (such as sand and gravel) that settle relatively quickly.

The type of dredge used, dredging method, sediment type, and hydrodynamics in the water column determine the degree of sediment suspension and subsequent dispersion (Herbich, 2000).

In the case of the proposed South Arm dredging operations, operation of the Trailing Suction Hopper Dredge (TSHD), dredging the surface silty clays, is considered to be likely to generate the greatest amount of sediment in the water column. Other dredging operations, such as the backhoe dredger on a barge, will be able to be contained within a turbidity curtain to minimise the dispersion of sediment. A TSHD dredging the broken-up stiff clays at depth will also create some additional suspended sediment later in the project, but this is expected to be considerably less than for the surface silty clays.

The stages of dredging with a TSHD that generate suspended sediment include (Pennekamp and Quaak, 1990):

- movement of the suction pipes and suction heads through the water at a velocity in the order of 1-2m/s, suspending sediments near the bed;
- return flow under and along the dredger, especially with low keel clearance;
- propeller wash during manoeuvring of the dredger (far more sediment is suspended in this operation compared to trailing);

²⁵ The elutriate test involves mixing sediment with 4 times its volume of seawater under specified conditions, to estimate the amounts of contaminants that will be released during dredging or during sea disposal (Environment Australia, 2002).

- hopper overflows during the loading process, particularly towards the end of a dredging session when this overflowing mixture would be closer to the concentration of the pumped slurry; and,
- release of any gas from the bed due to disturbance of the sediment.

Based on measurements of TSHD and other dredging operations, Pennekamp et al (1996) provide guidance on the likely mass of sediment (in kg of dry material) that may be resuspended in the water column per cubic metre (in situ) dredged. Most values (termed S) were found to be in the range from 0 to 20 kg/m³. Given that the dry density of the material to be dredged is about 700 kg/m³, an S value of 20 kg/m³ would mean that 3% of the dredged mass would enter the water column as suspended sediment from the sources listed above.

Given that up to about 1,350,000m³ of soft marine silts and clays will be dredged as part of the initial TSHD operation, this is equivalent to a dry mass of 945,000 tonnes. With 3% of this mass estimated to be generated as suspended sediment, there would be about 28,400 tonnes of sediment released into the estuary. Assuming an effective dredging rate of 50,000m³/week (in situ), it would take 27 weeks to complete the dredging operation. The effective average rate of loading of sediment in the water column would thus be about 1740 g/s, for 27 weeks.

For numerical modelling purposes, the suspended solids loading was distributed to 4 locations to represent the spatial extent of dredging. The loading areas were approximately at the upstream and downstream limits of dredging, and at distances about one-third and two-thirds along the length of the dredging. The loading at each of these 4 locations was thus about 435 g/s. No restriction on the migration of sediment from the TSHD operation was applied in the modelling, for example as might be provided in practice by a turbidity curtain installed across the river.

These loadings were applied in the model for a 29 day tidal simulation. Deposited sediment depths at the end of the simulation were scaled by a factor of 6.5 to take account of the dredging period continuing for longer than the 29 day simulation time (that is about 189 effective days).

The extrapolated depths of deposited sediment at the end of the dredging operation are shown in **Figure 52**. Note that deposited depths outside the region shown in Figure 52 were less than 10mm. A zoomed view of deposited depths in the South Arm is provided in **Figure 53**. Predicted suspended sediment concentrations are outlined in Section 3.7. Further details on the sediment transport simulations are provided in **Appendix D**.

Note that these results were derived assuming that the only sediment introduced was as a result of the dredging operation. That is, the “natural” sediment transport within the Hunter River system (which mainly occurs during floods) was not considered, only the additional sediment generated due to dredging. Also, simulations were undertaken using the network for existing conditions. In reality the dredged areas will be getting deeper during the dredging operation. Discussion on future (non-dredged) sediment deposition in the dredged area is given in Section 3.6.3.

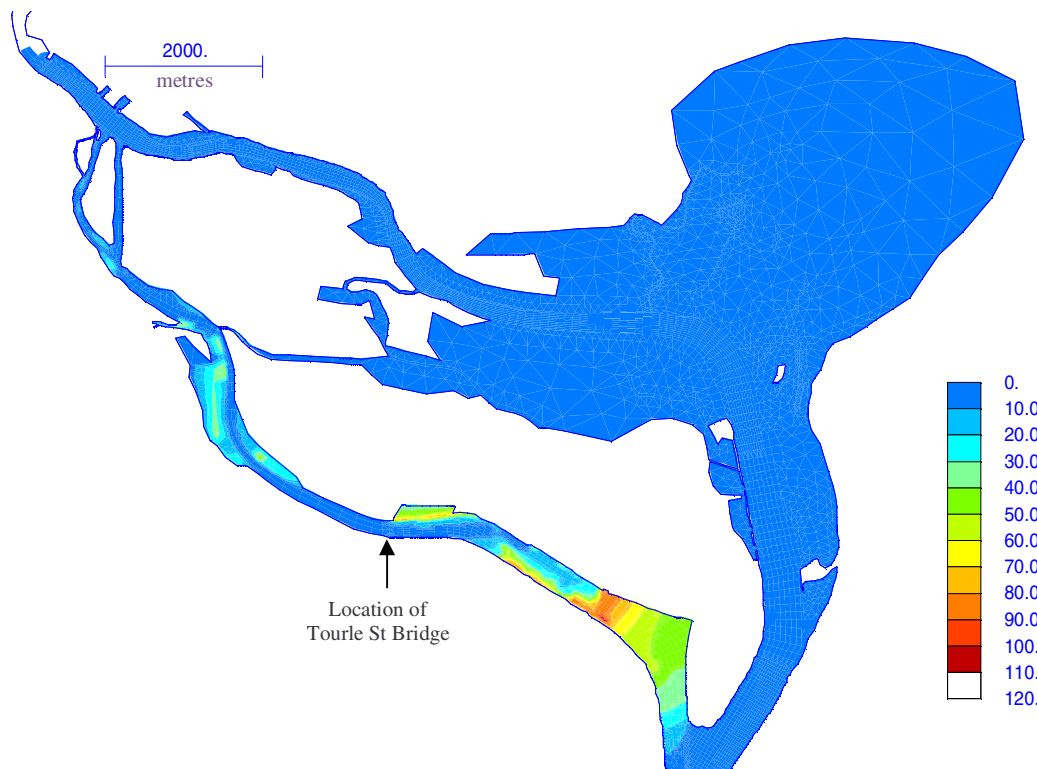


Figure 52: Predicted depths of deposited sediment (mm) at end of dredging operation

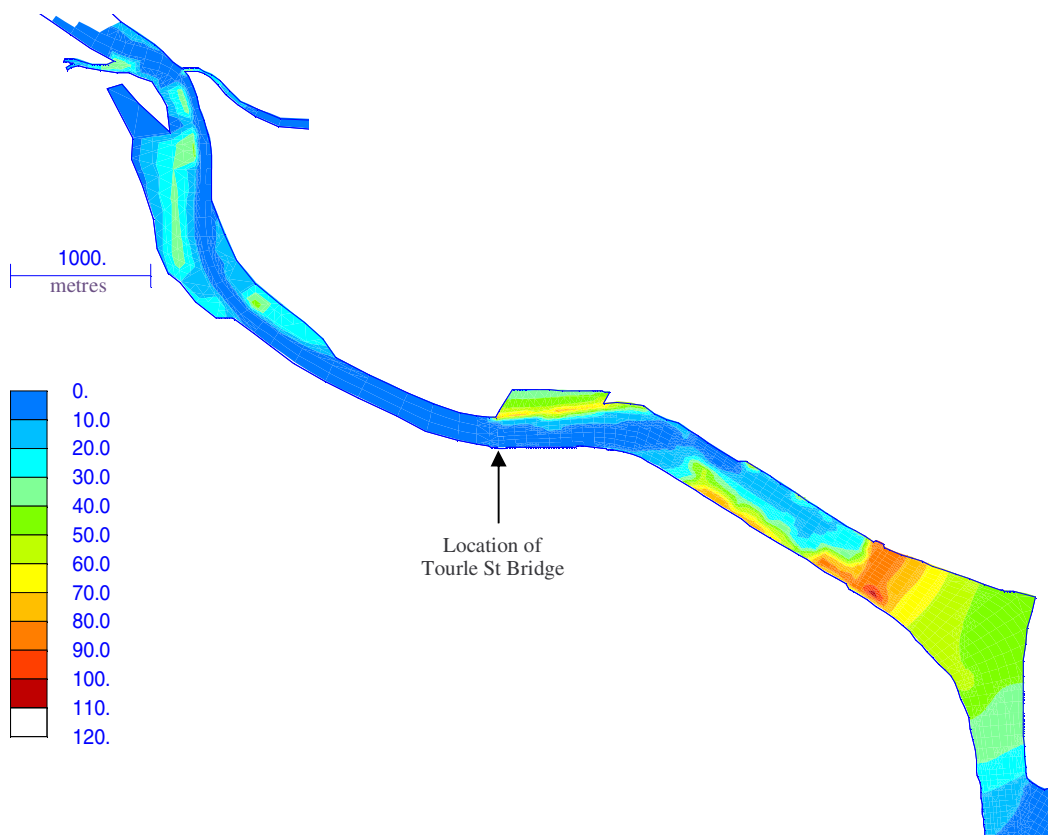


Figure 53: Predicted depths of deposited sediment (mm) at end of dredging operation, in South Arm

In this simulation, a total of 4350 tonnes of sediment was introduced into the model over the 29 days. At the completion of the simulation, about 2755 tonnes of sediment (63% of that introduced) had deposited on the bed and 507 tonnes (12%) of sediment was still in suspension, with the remaining 1088 tonnes (25%) having exited out of the model into the ocean.

Given that only 12% of sediment introduced was predicted to be remaining in suspension at the end of the dredging operation, it can be considered that the deposited sediment depths (as shown in **Figure 52** and **Figure 53**) would be similar to the ultimate post dredging depths (as a result of the dredging operation).

It is evident that most of the suspended sediment would deposit in the existing deepened port area downstream of the proposed dredged area. Newcastle Port Corporation will need to make allowance for this as part of their regular maintenance dredging operations. Sediment would also disperse upstream on flood tides, with deposition of sediment noted in the mangrove areas south of Ironbark Creek in this simulation.

As discussed in Section 2.6, sedimentation is usually beneficial to mangroves, assuming that the sediment buildup is not excessive. From the work of Ellison (1999), deposition on mangrove roots exceeding about 5cm has been shown to cause the death of mangroves (although the mean depth causing death was around 40cm). The depth of sediment buildup at Ironbark Creek is predicted to be in the order of 3-4cm.

It is recommended that monitoring of water quality (particularly turbidity), sediment deposition rates, and the mangrove colonies in the South Arm, especially south of Ironbark Creek, is undertaken during the dredging operations to prompt mitigation measures if required. The mitigation measures would take the form of a floating turbidity barrier(s) installed across the river upstream of the dredge area.

Significant sedimentation can also temporarily smother benthic fauna. However, most benthic species can burrow up through sediment deposited at rates an order of magnitude higher than the expected sedimentation rates estimated here (The Ecology Lab, 2003). Accordingly, benthic fauna would not be expected to be severely impacted by deposited sediments as a result of the proposed dredging.

The modelling undertaken may overestimate the upstream dispersion of sediment as only tidal conditions were considered. Large freshwater flows that may occur would tend to sweep any suspended dredged sediments downstream of the dredged area, either to the existing port area or out to sea.

3.6.2 Pollutant Transport (with Sediment) During Dredging

As discussed in Section 3.5.4, the sediment outside of the temporary sheet pile wall is considered to not be toxic to aquatic organisms. Therefore, it would be expected that dredging (outside of the temporary sheet pile wall) would not generate significant toxic substances into the water column. Consequently, transport of sediment-attached pollutants is not considered to be an issue outside of the sheet pile wall.

Disturbance of sediment on the inside of the temporary sheet pile wall would be contained by the wall during dredging. Depending on the method of dredging used and results of water quality monitoring during the dredging activity, a turbidity curtain could also be installed if necessary around the dredging plant. This would further restrict transport of any pollutants within the area contained by the sheet pile wall (again, see Section 3.5.4).

3.6.3 Effects on Sediment Transport after Completion of Dredging

Given that the South Arm will be deepened between Tourle St Bridge and the existing port area, water velocities will reduce relative to existing conditions. Therefore, “natural” sedimentation of this dredged area would be expected in the future, in a similar manner to the existing deepened port area being a zone of sediment deposition²⁶. As discussed in Section 2.6.3, most sediment deposition in the Hunter estuary would be expected to occur during floods.

There would be no alteration to upstream sediment concentrations as a result of the dredging operation, being affected by catchment processes and other upstream activities remote from the dredging site. That is, the total quantity of sediment travelling down the Hunter River would not be altered, and thus there would be little expected change to the total volume of future annual maintenance dredging requirements of Newcastle Port²⁷.

However, the location and extent of sediment deposition would change, with deposition spread over a greater area than at present. Given that about 30% of the total flood flow of the Hunter River travels down the South Arm (Section 3.3.3), it can be expected that approximately 30% of the sediment load also travels down the South Arm. At present, this sediment would mainly pass through the proposed dredge areas and be deposited within the existing Port areas downstream. However, after the South Arm dredging operation, these deepened areas would be expected to capture most of the sediment that previously passed downstream into the existing Port.

Therefore, an allowance of about 30% of the current maintenance dredging requirement will need to be made for future maintenance dredging of the areas deepened as part of the proposed South Arm dredging operations, with a commensurate reduction in dredging requirements for the existing Port area. The future maintenance dredging in the South Arm would be expected to be particularly concentrated to areas just downstream of the Tourle St Bridge.

3.6.4 Bed Stability Upstream of Tourle St Bridge

At the upstream limit of the proposed dredging in the South Arm near Tourle St Bridge, the dredged area (at a bed elevation of about -14.5m AHD) must link with the existing bed of the river (with a bed elevation of between about -2 and -3m AHD).

²⁶ Cohesive sediment deposition is also affected by salinity, in particular the position of the fresh/saline interface.

²⁷ Note however that there may initially be an increased maintenance dredging requirement in the Port after completion of the South Arm dredging operation, due to deposition of the dredged (as opposed to “natural”) sediments (see Section 3.6.1). Also, given that there would be more extensive deepened areas after the completion of the South Arm dredging, the trapping efficiency of the Port would be slightly enhanced. However, given the relative areas involved, it is not considered that any more than an additional 10% of sediment would be captured compared to present. Future management of bank and catchment erosion may reduce sediment loads.

Concerns were raised about the stability of the bed in this area, and the potential for the slope between the existing and dredged areas to adjust over time in order to maintain a more stable profile. This was seen to potentially impact on the stability of Tourle St Bridge.

In order to provide bed stability at the junction between the existing and dredged sections, it is proposed that a rock berm will be constructed at a slope of 1:1. This has been denoted as the “western submerged batter”. Further details on this structure are provided in a *Position Paper on Dredging Layout and Batter Profiles* prepared by GHD.

The western submerged batter is also designed to arrest an accidental ship impact for a fully laden Panamax size vessel travelling at 0.2m/s. This would prevent such a ship from impacting on the Tourle St Bridge.

3.7 FISH, PRAWNS AND OYSTERS

Dredging has the potential to suspend sediments and increase turbidity in the water column, which may impact on fish, prawns and oysters. Based on the suspended sediment simulations undertaken as described in Section 3.6.1, suspended sediment concentrations as a result of the dredging, at the end of the 29 day tidal simulation, are shown in **Figure 54**. Note that suspended sediment concentrations outside the region shown were less than 10mg/L.

It is evident that the suspended sediment concentrations in this simulation are in the order of about 40 to 90 mg/L near the dredging operation.

However, it has been observed that turbidity levels in the estuary are already high (Section 2.5), generally related to catchment erosion. At the mean flow in the Hunter River, it has been predicted that the suspended sediment concentration at Hexham would be about 40 mg/L (see Section 2.6.3). This is not dissimilar to the concentrations predicted to occur in much of the dredged area during the dredging operations.

The impacts of these concentrations on fish, prawns and oysters is difficult to quantify (The Ecology Lab, 2003). As discussed in Section 2.5, impacts of high suspended sediment concentrations on fish could include affecting their foraging behaviour (perhaps creating a barrier to movement), and abrading their protective mucus coats, thereby increasing their susceptibility to disease, clogging gill filaments, or causing suffocation. Oyster populations in the estuary already appear to be limited by high turbidity (Section 2.7).

Therefore, with the understanding that suspended sediment concentrations are already high in the Hunter estuary, the approach to the uncertainty of impacts on these species would be to employ monitoring and turbidity curtains during some of the dredging operations which have the potential to cause particularly significant turbidity, and to only monitor at other times.

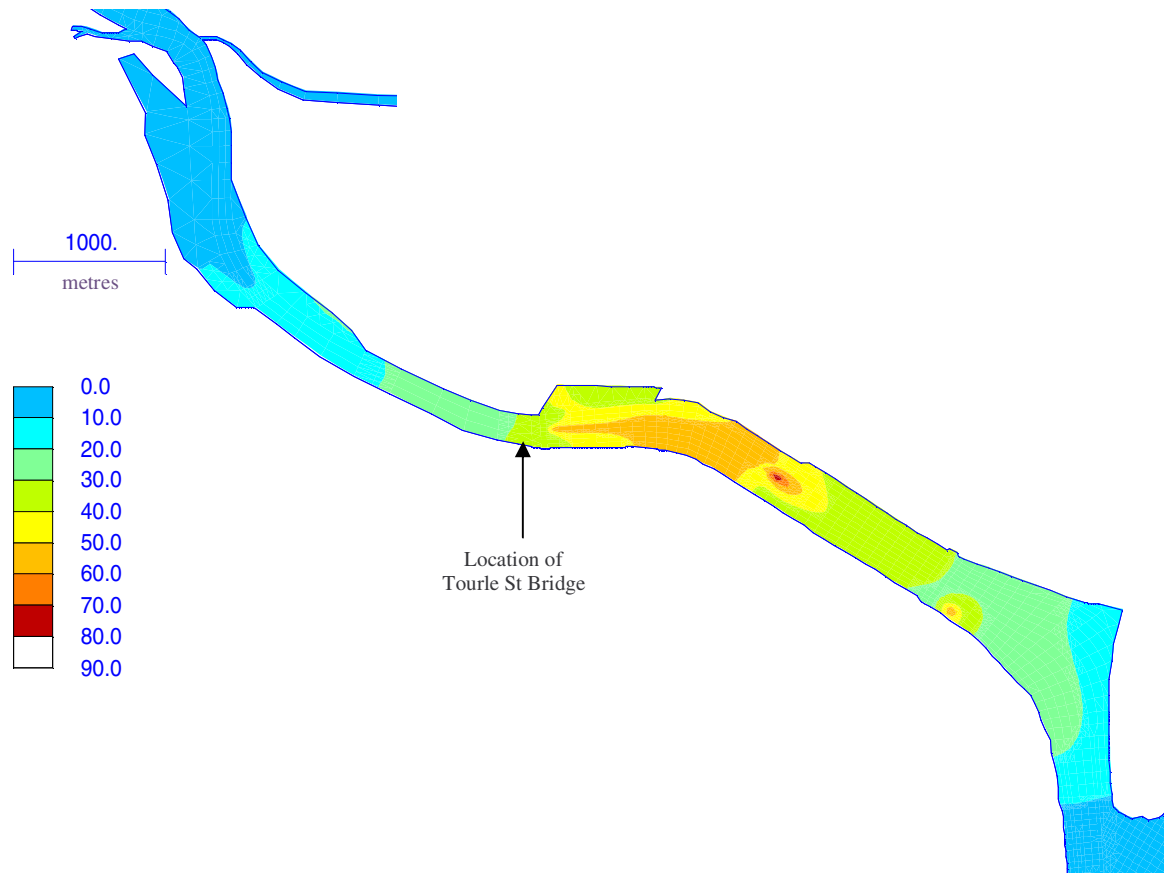


Figure 54: Suspended sediment concentrations (mg/L) at end of 29 day tidal simulation

4 RECOMMENDED MITIGATION MEASURES

4.1.1 Summary of Impacts

To summarise Section 3, the following potential impacts were determined for the proposed South Arm dredging. It was found that, after dredging:

- there would not be a significant alteration to tidal hydrodynamics (water levels, tidal planes, velocities outside the proposed dredged area, and flows); slightly more tidal flow would pass through the South Arm, with a slightly increased tidal range at locations near the dredged area, but the magnitudes of these changes would be very small and would not be expected to have any measurable impacts;
- there would be a localised and substantial reduction in peak flood levels in the South Arm in the vicinity of Tourle St Bridge (0.6m in the 1% AEP event);
- there would be a slightly reduced flood risk throughout the lower Hunter estuary;
- ecosystems relying on flood inundation would not be significantly impacted;
- the flood flow distribution, flood volumes and flood duration would only be slightly altered;
- velocities within the proposed dredged area would reduce substantially, providing benefits in terms of ease of navigation and reduced bank erosion;
- flood velocities in the South Arm upstream of Tourle St Bridge would increase, with a predicted 40% increase at Tourle St Bridge and 11% increase at the Railway Bridge;
- groundwater characteristics in wetland and swamp areas would not be expected to change significantly;
- salinity intrusion would be slightly reduced, particularly into the South Arm, although this would not be expected to significantly impact on biota such as mangroves, saltmarsh and fish;
- there would be slightly less flushing of pollutants in the South Arm, which was not considered significant;
- there may be a greater tendency for stratification and depletion of dissolved oxygen concentrations at depth in the deepened areas, although the available evidence suggested that this does not occur in the existing dredged areas of the port; and,
- there would be a requirement for the periodic maintenance dredging of the South Arm dredged area, particularly just downstream of Tourle St Bridge.

During dredging operations, sediment may go into suspension, creating two potential impacts, namely:

- elevated suspended sediment concentrations in the water column potentially harming aquatic life such as fish; and,
- eventual deposition of the suspended sediment in lower velocity locations such as mangroves and deep port areas; excess deposition of sediment may stress or kill mangroves.

The sediment deposition predicted in the mangrove areas south of Ironbark Creek are around the magnitude at which sedimentation has been observed to potentially become a concern to mangroves.

Dispersion of pollutants in the sediments suspended as part of the dredging operations was not considered to be a significant issue given that a temporary sheet pile wall would be installed to provide a physical barrier to isolate the contaminated material in the vicinity of the former BHP Steelworks site. In addition, dredging inside the temporary sheet pile wall may also be conducted within a turbidity barrier where dictated by the results of monitoring. Dredging of material outside the wall would not be expected to generate significant toxic substances into the water column, based on extensive research on sediment toxicity as reported in Patterson Britton & Partners (2003b).

The effect of the temporary sheet pile wall which is proposed to contain contaminated sediments during dredging was also assessed in terms of tidal and flood hydrodynamics. It was found that:

- mean tidal and flood velocities would increase by about 15% along the localised wall location;
- there would be a small localised increase in peak water levels during floods, affecting the reach from the wall upstream to the Railway Bridge, the maximum increase in levels was about 50mm for the 1% AEP event, but it was not expected that the increases in levels would lead to significant flood damages.

Assessment of the effect on flooding of a temporary discharge pipeline delivering sand to Tomago was also undertaken for an assumed westerly route. For the 1% AEP event, increases in peak flood levels in the Hexham and Tomago area were about 30mm and 50mm respectively. This was found to only be 10-30mm larger than the increase in flood levels due to the construction of a potential permanent transport corridor to Tomago.

4.1.2 Mitigation Measures

The measures recommended to mitigate the potentially significant impacts listed in Section 4.1.1 are discussed below.

Related to potential excess deposition of sediment upstream of Tourle St Bridge due to settling of sediments suspended during dredging, it is recommended that water quality (particularly turbidity), sediment deposition rates, and the mangrove colonies in the South Arm, particularly south of Ironbark Creek, are monitored during the dredging operations to prompt mitigation measures if required. The mitigation measures would take the form of a floating turbidity barrier(s) installed across the river upstream of the dredge area.

Newcastle Port Corporation will also need to make allowance for additional sedimentation in the existing port during the South Arm dredging project, as part of their regular maintenance dredging operations.

Turbidity curtains would be used in conjunction with various dredging operations, to minimise the dispersion of suspended sediment. For example, turbidity curtains would be employed during the operation of a backhoe dredge and barges in the removal of 600,000m³ of marine silts and clays to create a temporary access channel and temporary swing basin.

As discussed in Section 4.1.1, a temporary sheet pile wall would be employed to contain contaminated sediments. With the temporary sheet pile wall in place, mean tidal and flood

velocities would be expected to increase by about 15% in the vicinity of the wall, with the highest velocities against the northern bank. It is recommended that an inspection of the northern bank is carried out prior to the installation of the temporary sheet pile wall. The purpose of this would be to identify potential areas that may be susceptible to erosion as a result of increased velocities. If any such areas were identified these may require protection or monitoring while the sheet pile wall is in place. However, given that this bank would be protected with a rock revetment after the completion of dredging, only monitoring may be required given the temporary nature of any erosion that may occur.

Similarly, flood velocities upstream of Tourle St Bridge would be expected to increase after dredging. It is recommended that bank conditions in the South Arm, proceeding upstream of Tourle St Bridge, should be monitored after significant floods to determine if any new areas of bank erosion have developed as a result of the increased velocities.

The potential for a temporary discharge pipeline (across Kooragang Island to Tomago) to cause increased flood damages should be further assessed once the final pipeline route is confirmed. However, this should be weighed against the short-term placement of the pipeline and the reduction in flood levels which would occur after the completion of dredging, which is a benefit of the works.

It is recommended that a comprehensive water quality program is implemented, as agreed with the EPA, to assess water quality impacts of the proposed dredging. This program should be started in the order of 12 months prior to the works commencing if possible, to gather pre-dredging water quality data.

5 CONCLUSIONS

The potential impacts of the proposed South Arm dredging on hydrodynamics, flooding and water quality were assessed.

It was found that there would not be significant impacts on tidal hydrodynamics.

With regard to flooding, it was found that the general flood flow distribution, volumes and duration would not be altered by a significant amount. It was estimated that there would be a localised and substantial reduction in peak flood levels in the South Arm in the vicinity of Tourle St Bridge (0.6m in the 1% AEP event), and a slightly reduced flood risk throughout the lower Hunter estuary. These benefits were not expected to cause significant impacts on ecosystems relying on flood inundation.

Flood velocities in the South Arm upstream of the dredged area were predicted to increase, with the recommendation that bank stability be monitored, particularly between Tourle St Bridge and the Railway Bridge. Tidal and flood velocities in the dredged area were estimated to substantially reduce, providing benefits in terms of ease of navigation and reduced bank erosion.

Flood levels upstream to the Railway Bridge were predicted to marginally increase as a result of the installation of a temporary sheet pile wall (for a period of about one year) to contain contaminated sediments in the vicinity of the former BHP Steelworks site during the dredging activities. This slight increase in flood levels was not expected to lead to significant flood damages.

With the temporary sheet pile wall in place, mean tidal and flood velocities would be expected to increase by about 15% in the vicinity of the wall, with the highest velocities against the northern bank. It was recommended that the stability of this bank be monitored while the wall was in place.

Assessment of the effect on flooding of a temporary discharge pipeline delivering sand to Tomago was also undertaken for an assumed westerly route. For the 1% AEP event, increases in peak water levels in the Hexham and Tomago area were found to only be 10-30mm larger than the increase in water levels due to the construction of a proposed permanent transport corridor to Tomago.

Salinity intrusion was predicted to slightly reduce, although not to the extent of significantly impacting on mangroves, saltmarsh and fish.

It was also envisaged that there may be a greater tendency for stratification and depletion of dissolved oxygen concentrations at depth in the deepened areas, although the available evidence suggested that this does not occur in the existing dredged areas of the port. The existing dredged areas have some of the best water quality results in the estuary, most likely since the downstream areas of the estuary have the greatest tidal flushing.

There would be a requirement for the periodic maintenance dredging of the South Arm dredged area, particularly just downstream of Tourle St Bridge. This would be expected to be commensurate with a reduction in the maintenance dredging requirements of the existing Port area.

During dredging operations, it was predicted that elevated suspended sediment concentrations may potentially harm aquatic life such as fish, although the Hunter estuary was noted as already having high suspended sediment concentrations. Turbidity curtains would be used in conjunction with various dredging operations, to minimise the dispersion of suspended sediment. Dispersion of pollutants in the sediments suspended as part of the dredging operations was not considered to be a significant issue.

Deposition of sediment in sensitive areas such as mangroves south of Ironbark Creek was also considered to be around the magnitude at which concerns may be raised. It was recommended that water quality (particularly turbidity), sediment deposition rates, and the mangrove colonies in the South Arm, particularly south of Ironbark Creek, were monitored during the dredging operations to prompt mitigation measures if required. The mitigation measures would take the form of a floating turbidity barrier(s) installed across the river upstream of the dredge area.

It was envisaged that Newcastle Port Corporation would need to make allowance for additional sedimentation in the port (during the South Arm dredging project) as part of their regular maintenance dredging operations.

6 REFERENCES

- Australian and New Zealand Environment and Conservation Council [ANZECC] and Agriculture and Resource Management Council of Australia and New Zealand [ARMCANZ] (2000), *Australian and New Zealand Guidelines for Fresh and Marine Water Quality, Volume 1, The Guidelines (Chapters 1-7)*, October, ISBN 09578245 0 5
- Bishop, KA (1999), “Characterisation of Fish Communities and Habitats within the Upper Arms of the Richmond River Estuary with emphasis on the Potential Effects of Altered Salinity Structure as arising from Freshwater Extraction in the Upper Estuary (Preliminary Desktop Analysis)”, November 25, Appendix B in Peirson, WL; Bishop, KA; Nittim, R and MJ Chadwick (1999), “An Investigation of the Potential Ecological Impacts of Freshwater Extraction from the Richmond River Tidal Pool”, *WRL Technical Report 99/51*, Water Research Laboratory, Manly Vale, November
- Clarke, PJ and WG Allaway (1993), “The regeneration niche of the grey mangrove (*Avicennia marina*): effects of salinity, light and sediment factors on establishment, growth and survival in the field”, *Oecologia*, Volume 93, Issue 4, pp. 548-556.
- Department of Public Works NSW [DPW] (1967), “Newcastle Harbour Siltation Investigation”, *Report No. 114*, Harbours and Rivers Branch, Manly Hydraulic and Soils Laboratory, in conjunction with the Hydraulic Research Station, Wallingford, period of investigation February 1962 to September 1967
- Ellison, Joanna C (1999), “Impacts of Sediment Burial on Mangroves”, *Marine Pollution Bulletin*, Volume 37, Issues 8-12, December, pp. 420-426
- Environment Australia (2002), *National Ocean Disposal Guidelines for Dredged Material*, Commonwealth of Australia, Canberra, May, ISBN 0 642 54831 5
- Evans, Glen (2003), Hunter Catchment Management Trust, personal communication
- Field, CD (1987), “Salt Tolerance in Mangroves”, *Proceedings, Mangrove Ecosystems of Asia and the Pacific: Status, Exploitation and Management, Research for Development Seminar on the Mangrove Ecosystem*, 18-25 May 1985, Townsville, CD Field and AJ Dartnall (editors), Australian Institute of Marine Science, Townsville, ISBN 0642115230, pp. 278-285
- GHD-Longmac (2003), *Proposed Extension of Shipping Channels, Port of Newcastle, Results of Bulk Sampling and Testing Program*
- Harty, Christopher and Dominic Cheng (2002), “Ecological assessment and strategies for the management of mangroves in Brisbane Water – Gosford, New South Wales, Australia”, *Landscape and Urban Planning*, Issue 950, In Press, Corrected Proof, available online 11 September 2002

Healthy Rivers Commission (2002), *Independent Inquiry into Hunter River System*, May, Final Report

Herbich, John B (2000), *Handbook of Dredging Engineering*, Second Edition, McGraw-Hill, New York

Lynch, Peter and Jenny Burchmore (2002), *Fishcare - Our Mangrove Forests Fishnote DF/30*, online at <http://www.fisheries.nsw.gov.au/conservation/habitats/mangroves.htm>, edited by HT Johnson

Manly Hydraulics Laboratory [MHL] (1995), "Hunter River Data Collection 9 October 1995", *MHL Report 750*

Manly Hydraulics Laboratory [MHL] (2002), "Hunter Estuary Processes Study", *Draft Report MHL 1095*, NSW Department of Public Works and Services, for Newcastle City Council, December, ISBN 0 7347 4163 4

McLoughlin, LC (2000), "Estuarine wetlands distribution along the Parramatta River, Sydney, 1788-1940: implications for planning and conservation", *Cunninghamia*, Volume 6, No. 3, ISSN 07279620, p579-610

Patterson Britton & Partners (1989), *Mobility Study, Dumped Dredge Spoil, Port of Newcastle*, December, for MSB Hunter Ports Authority, J585/R330

Patterson Britton & Partners (1996), *Lower Hunter Valley Floodplain Management Study, Assessment of Strategic Options for Community Consultation*, Issue No. 1, October, for Newcastle City Council and Port Stephens Council

Patterson Britton & Partners (2001a), *Lower Hunter River Port Lands Development – Tomago Lands Site Flooding Assessment*, Draft, Issue No. 1, June, for The Premiers Department, rp3480cjd010522

Patterson Britton & Partners (2001b), *Lower Hunter Floodplain Management Study, Volume B – Planning Implementation Study*, Issue No. 5, November, for Newcastle City Council and Port Stephens Council

Patterson Britton & Partners (2003a), *Lower Hunter River Port Lands Development – Haul Road Assessment*, March, for The Premiers Department, lr3480cjd030307-Modelling Haul Road-Iss2.doc

Patterson Britton & Partners (2003b), *Proposed Extension of Shipping Channels, Port of Newcastle, Sediment Quality Data*, Issue No. 2, March

Pennekamp, Joh GS; Epskamp, RJC; Rosenbrand, WF; Mullié, A; Wessel, GL; Arts, T and IK Deibel (1996), "Turbidity Caused by Dredging; Viewed in Perspective", *Terra et Aqua*, Number 64, September, International Association of Dredging Companies, Netherlands, ISSN 0376-6411, pp. 10-27

- Pennekamp, JGS and MP Quaak (1990), "Impact on the Environment of Turbidity Caused by Dredging", *Terra et Aqua*, Number 42, April, International Association of Dredging Companies, Netherlands, ISSN 0376-6411, pp. 10-20
- Public Works Department [PWD] (1994), *Lower Hunter Flood Study (Green Rocks to Newcastle)*, for Newcastle City Council and Port Stephens Council, August, Report No. PWD 91077, ISBN 07305 86472
- Saintilan, Neil and Robert J Williams (1999), "Mangrove transgression into saltmarsh environments in southeast Australia, *Global Ecology and Biogeography*, Volume 8, No. 2, March, Blackwell Science Ltd, ISSN 1466822X, p117-124
- Sanderson, Dr Brian G and Dr Anna M Redden (2001), *Hunter River Estuary Water Quality Data Review and Analysis*, report submitted to Manly Hydraulics Laboratory, Centre for Sustainable Use of Coasts and Catchments, University of Newcastle, December
- Sanderson, Dr Brian; Redden, Dr Anna and Matthew Smith (2002), *Salinity Structure in the Hunter River Estuary*, report submitted to Newcastle City Council and Manly Hydraulics Laboratory, Centre for Sustainable Use of Coasts and Catchments, University of Newcastle, January
- Simpson, SL; King, CK; Adams, MS and JL Stauber (2001a), "Chemical and Ecotoxicological Testing of Dredged Sediment from Newcastle Harbour: South Arm Master Plan Dredge Area", *CSIRO Centre for Advanced Analytical Chemistry, Report No: ET/IR400R*, June
- Simpson, SL; King, CK; Adams, MS; Stauber, JL and GE Batley (2001b), "Chemical and Ecotoxicological testing of Dredged Sediment from Newcastle Harbour: MPT Stage 2/K7 Area" *CSIRO Centre for Advanced Analytical Chemistry, Report No: ET/IR401R*, June
- The Ecology Lab (2003), Sophie Diller, Environmental Scientist, personal communication
- Thomas, Christopher and Bruce Druery (1996), "Geomorphology of the Lower Hunter River, NSW, Managing the Legacy of the Past", *23rd Hydrology and Water Resources Symposium, Proceedings, Volume 2*, Hobart, 21-24 May, pp. 463-470
- Umwelt (2002), *Shifting Sands at Stockton Beach*, for Newcastle City Council, June, in association with SMEC, Report No. 1411/RO4/V2
- West, RJ; Thorogood, C; and RJ Williams (1983), "Environmental stress causing mangrove 'dieback' in NSW", *Australian Fisheries*, Volume 42, No. 8, August

APPENDIX A: THE RMA MODEL SUITE

TABLE OF CONTENTS

Page No.

A1	INTRODUCTION	1
A2	GENERAL INFORMATION ON THE RMA SUITE	2
	A2.1 TWO DIMENSIONAL HYDRODYNAMIC MODEL, RMA-2	2
	A2.2 WATER QUALITY MODEL, RMA-11	2
A3	RMA MODEL DEVELOPMENT	4
A4	USAGE OF THE RMA MODEL SUITE	5
A5	CONCLUSIONS	7
A6	REFERENCES	8

A1 INTRODUCTION

A finite element numerical model of the Hunter River estuary was constructed utilising the RMA model suite.

In this Appendix, general details on the RMA model suite are given in Section A2. The RMA model has been established for decades, and a history of the development of the model is provided in Section A3.

The RMA model is also used throughout the world, and a non-exhaustive list of studies in which it has been applied and users of the model is provided in Section A4.

Conclusions are given in Section A5, with references provided in Section A6.

A2 GENERAL INFORMATION ON THE RMA SUITE

The RMA model suite consists of one, two and three dimensional models for flow in estuaries and streams. It includes the two and three dimensional hydrodynamic models RMA-2 and RMA-10 respectively, and the water quality model RMA-11.

In the hydrodynamic models, the Reynolds form of the Navier Stokes equations are solved together with the volume continuity equations.

The model is finite element, with a mesh (consisting of nodes joined to form quadrilateral or triangular elements) representing the bathymetry of the region of interest. The finite element network is unstructured, allowing variable resolution throughout the system.

To simulate areas of the system that do not remain wet during the entire tidal cycle (such as sand banks, mud flats and mangrove areas), a subsurface flow analogy is used where flow in the drying area is treated as a low porosity region when the water surface elevation drops below the ground level (Roig and King, 1988).

A2.1 TWO DIMENSIONAL HYDRODYNAMIC MODEL, RMA-2

RMA-2 is designed to simulate transient flow and water depth in prototype systems that can be approximated with either the depth-integrated two-dimensional or area-integrated one-dimensional shallow water equations. The model incorporates a fully non-linear solution of the governing equations including terms for convective inertia, pressure gradient, turbulent viscosity, bed and bank friction, wind stresses and Coriolis forces.

The RMA-2 model was used in this study for the hydrodynamic simulations. This simulated depth-averaged conditions.

A2.2 WATER QUALITY MODEL, RMA-11

RMA-11 is a finite element water quality model for simulation of three-dimensional estuaries, bays, lakes and rivers. It is also capable of simulating one and two-dimensional approximations to systems either separately or in combined form. It is designed to accept input of velocities and depths from either the two-dimensional hydrodynamic model, RMA-2, or the three-dimensional stratified flow model, RMA-10. Results in the form of velocities and depth from the hydrodynamic models are used in the solution of the advection diffusion constituent transport equations. Additional terms for each constituent represent source or sinks and growth or decay.

Water quality interactions that can be accounted for in the RMA model include:

- Temperature with a full atmospheric heat budget at the water surface;
- Biochemical Oxygen Demand (BOD) and Dissolved Oxygen (DO);
- The nitrogen cycle (including organic nitrogen, ammonia, nitrite and nitrates);
- The phosphorous cycle (including organic phosphorous and phosphates);

- Algae growth and decay (as Chlorophyll-A);
- Cohesive suspended sediment;
- Non-cohesive suspended sediment such as sand;
- Arbitrary conservative or non-conservative constituents that may be linked to each other;
- Coliforms with related decay; and,
- Salinity

Each individual constituent is appropriately linked to derive growth and decay based on current concentrations. Additional terms represent benthic and sediment sources and sinks.

A3 RMA MODEL DEVELOPMENT

As described by King (1993), development of the RMA model suite was initially sponsored by the US Army Corps of Engineers in the 1970's. In early developments, two dimensional models were developed for both laterally averaged (King et al, 1973) and depth averaged (Norton et al, 1973) approximations. This was pioneering work as it was the first application of finite element models (which had originally been developed for structural analysis) for water resources problems.

The Resource Management Associates (RMA) company was formed in 1974 (in California) as an outworking of the early model development. Hence the model names RMA-2 etc were coined. The company included Ian King, the primary developer of the RMA models, as an associate.

Following this, work proceeded on improving the solution capacity and efficiency together with accumulating experience from applications where calibration and verification in field situations was stressed (see Norton and King, 1978, for example).

As computing power improved, in 1979, the Waterways Experiment Station, Coastal Engineering Research Center, US Army Corps of Engineers, contracted RMA to develop three dimensional finite element models for flow and sediment transport. When completed, this work was reported in King (1982) and Ariathurai (1983).

Ian King joined the University of California, Davis in 1983 as a Professor of Civil and Environmental Engineering. The model continued to be improved, including refinements in the computational techniques to improve model speed and resource requirements, and inclusion of additional options. This was reported in King (1988).

The RMA company of California continues to provide water resources consulting services. Model development is largely controlled by Ian King, who moved to Australia and formed the Resource Modelling Associates company in 1999.

A4 USAGE OF THE RMA MODEL SUITE

The RMA model has been used in thousands of estuary and floodplain studies throughout the world. Examples of major studies where the model suite has been applied include:

- the Sydney Deepwater Outfalls Environmental Monitoring Programme;
- Hong Kong harbour;
- Lake Macquarie Estuary Processes Study;
- Manly Lagoon, New South Wales;
- Darwin Harbour and Mary River, Northern Territory;
- Hawkesbury River, New South Wales;
- Hunter River, New South Wales;
- Moreton Bay, Brisbane;
- San Francisco Bay, California;
- the Sacramento and Columbia River system, USA;
- Galveston Bay, Texas;
- New York Harbour, East River and Kensico Reservoir, New York;
- Delaware Bay, Delaware;
- St Lawrence River and Lower Hudson's Bay, Ontario Canada.

A non-exhaustive list of users of the RMA suite includes the following:

- Government Agencies:
 - California Department of Water Resources;
 - Department of Lands, Planning and Environment, Northern Territory;
 - Manly Hydraulics Laboratory, Sydney, Australia;
 - National Institute for Water and Atmospheric Research, New Zealand;
 - National Research Laboratory, Ottawa, Canada;
 - US Army Corps of Engineers;
 - US Navy Research Laboratory.
- Universities and Research Organisations:
 - University of New South Wales;
 - Griffith University, Brisbane, Queensland;
 - University of Aachen, Germany;
 - University of Auckland, New Zealand;
 - Warsaw Institute of Technology, Poland;
 - Bristol University, UK;
 - Cambridge University, UK;
 - Cairo University, Egypt;
 - University of California, Davis;
 - University of Connecticut;
 - Asian Institute of Technology, Thailand;
 - Coastal Engineering Research and Development Institute, Seoul, South Korea;
 - Seoul Development Institute, Seoul, South Korea;

- Korean Institute of Construction Technology, Seoul, South Korea;
- Consultants:
 - Australia – Patterson Britton & Partners, Paterson Consultants, Ports and Harbours Ltd, SMEC, Webb Mckeown, WBM Oceanics;
 - Canada – Acres International, Golder Associates, SNC Lavalin;
 - South Africa – Watermeyer Prestedge Retief;
 - UK – Hydraulic Research (Wallingford);
 - USA – Aubrey Consultants, EA Consultants, Foster Wheeler Environmental Corporation, Hydromat, Lawler Matusky and Skelly, McEwan Consulting, Najarian and Associates, Simons and Associates; Woods Hole Group.

A5 CONCLUSIONS

The RMA model suite consists of one, two and three dimensional finite element models for flow in estuaries and streams. It includes the two and three dimensional hydrodynamic models RMA-2 and RMA-10 respectively, and the water quality model RMA-11.

The RMA model suite has been developed for many decades and applied in thousands of estuary studies throughout the world.

It can be considered as a robust modelling tool suitable for the simulation of hydrodynamics and water quality in the Hunter estuary.

A6 REFERENCES

Ariathurai, CR (1983), *Two and Three Dimensional Models for Sediment Transport*, report prepared by Resource Management Associates, Lafayette, California, for the US Army Corps of Engineers Waterways Experiment Station, Vicksburg, Mississippi

King, Ian P (1993), “Sydney Deepwater Outfalls Environmental Monitoring Program Post Commissioning Phase, RMA-10, A Finite Element Model for Three-Dimensional Density Stratified Flow”, *Australian Water and Coastal Studies Interim Report 93/01/04*, January

King, IP; Norton, WR and GT Orlob (1973), *A Finite Element Solution for Two-Dimensional Density Stratified Flow*, report prepared by Water Resources Engineers, Walnut Creek, California, for the US Department of the Interior, Office of Water Resources Research

King, IP (1982), *A Finite Element Model for Three Dimensional Flow*, report prepared by Resource Management Associates, Lafayette, California, for the US Army Corps of Engineers Waterways Experiment Station, Vicksburg, Mississippi

King, IP (1988), *A Finite Element Model for Three Dimensional Hydrodynamic Systems*, report prepared by Resource Management Associates, Lafayette, California, for the US Army Corps of Engineers Waterways Experiment Station, Vicksburg, Mississippi

Norton, WR and IP King (1978), “Recent Application of RMA’s Finite Element Models for Two Dimensional Hydrodynamics and Water Quality”, *Finite Elements in Water Resources*, Proceedings of the Second International Conference, Imperial College, London, July, edited by CA Brebbia, Pentech Press, London

Norton, WR; King, IP and GT Orlob (1973), *A Finite Element Model for Lower Granite Reservoir*, report prepared by Water Resources Engineers, Walnut Creek, California, for the US Army Corps of Engineers, Walla Walla, Washington

Roig, LC and IP King (1988), “Two-Dimensional Finite Element Models for Flood Plains and Tidal Flats”, *International Conference on Computational Methods in Flow Analysis*, Okayama, Japan, September

APPENDIX B: DEVELOPMENT, CALIBRATION AND VERIFICATION OF TIDAL HYDRODYNAMIC MODEL

TABLE OF CONTENTS

	Page No.
B1 INTRODUCTION	1
B2 AVAILABLE DATA USEFUL FOR MODELLING	2
B2.1 WATER LEVEL INFORMATION	2
B2.2 RAINFALL DATA	3
B2.3 FRESHWATER FLOW DATA	3
B2.4 WATER QUALITY DATA	4
B3 DEVELOPMENT OF TIDAL HYDRODYNAMIC MODEL	5
B3.1 MODEL EXTENT	5
B3.2 FINITE ELEMENT NETWORK	6
B3.3 BATHYMETRY	9
B3.4 ROUGHNESS	13
B3.5 BOUNDARY CONDITIONS	13
B4 MODEL CALIBRATION AND VERIFICATION	14
B4.1 STATISTICS FOR EVALUATING SIMULATION OUTPUTS	14
B4.2 CALIBRATION	15
B4.3 VERIFICATION	31
B5 CONCLUSIONS	43
B6 REFERENCES	44

LIST OF FIGURES

Page No.

FIGURE B1: EXAMPLE OF LIMITED EXCHANGE UPSTREAM OF IRONBARK CREEK FLOODGATES	6
FIGURE B2: FINITE ELEMENT NETWORK OF THE HUNTER RIVER ESTUARY	7
FIGURE B3: FINITE ELEMENT NETWORK OF THE HUNTER RIVER ESTUARY, DOWNSTREAM OF HEXHAM	8
FIGURE B4: FINITE ELEMENT NETWORK OF THE HUNTER RIVER ESTUARY, ENTRANCE AREA	9
FIGURE B5: ASSUMED MANGROVE AND SALTMARSH AREAS IN FINITE ELEMENT NETWORK (LIGHT GREEN)	11
FIGURE B6: ADOPTED HUNTER RIVER ESTUARY BATHYMETRY (M AHD), DOWNSTREAM OF HEXHAM	12
FIGURE B7: ADOPTED HUNTER RIVER ESTUARY BATHYMETRY (M AHD), IN PORT AREA	12
FIGURE B8: FLOWS IN HUNTER, WILLIAMS AND PATERSON RIVER BEFORE AND DURING CALIBRATION PERIOD	16
FIGURE B9: DOWNSTREAM (PILOT STATION) WATER LEVEL FOR CALIBRATION SIMULATION	17
FIGURE B10: WATER LEVELS MEASURED IN LOWER HUNTER ESTUARY FOR DAY 1-7 OF CALIBRATION	18
FIGURE B11: WATER LEVELS MEASURED IN LOWER HUNTER ESTUARY FOR DAY 7-15 OF CALIBRATION	18
FIGURE B12: WATER LEVELS MEASURED IN LOWER HUNTER ESTUARY FOR DAY 15-22 OF CALIBRATION	19
FIGURE B13: WATER LEVELS MEASURED IN LOWER HUNTER ESTUARY FOR DAY 22-29 OF CALIBRATION	19
FIGURE B14: SIMULATED AND OBSERVED PILOT STATION WATER LEVEL FOR DAY 1-7 OF CALIBRATION	20
FIGURE B15: SIMULATED AND OBSERVED PILOT STATION WATER LEVEL FOR DAY 7-15 OF CALIBRATION	21
FIGURE B16: SIMULATED AND OBSERVED PILOT STATION WATER LEVEL FOR DAY 15-22 OF CALIBRATION	21
FIGURE B17: SIMULATED AND OBSERVED PILOT STATION WATER LEVEL FOR DAY 22-29 OF CALIBRATION	22
FIGURE B18: SIMULATED AND OBSERVED STOCKTON WATER LEVEL FOR DAY 1-7 OF CALIBRATION	22
FIGURE B19: SIMULATED AND OBSERVED STOCKTON WATER LEVEL FOR DAY 7-15 OF CALIBRATION	23
FIGURE B20: SIMULATED AND OBSERVED STOCKTON WATER LEVEL FOR DAY 15-22 OF CALIBRATION	23
FIGURE B21: SIMULATED AND OBSERVED STOCKTON WATER LEVEL FOR DAY 22-29 OF CALIBRATION	24
FIGURE B22: SIMULATED AND OBSERVED IRONBARK CK WATER LEVEL FOR DAY 1-7 OF CALIBRATION	24
FIGURE B23: SIMULATED AND OBSERVED IRONBARK CK WATER LEVEL FOR DAY 7-15 OF CALIBRATION	25

LIST OF FIGURES

Page No.

FIGURE B24: SIMULATED AND OBSERVED IRONBARK CK WATER LEVEL FOR DAY 15-22 OF CALIBRATION	25
FIGURE B25: SIMULATED AND OBSERVED IRONBARK CK WATER LEVEL FOR DAY 22-29 OF CALIBRATION	26
FIGURE B26: SIMULATED AND OBSERVED HEXHAM WATER LEVEL FOR DAY 1-7 OF CALIBRATION	26
FIGURE B27: SIMULATED AND OBSERVED HEXHAM WATER LEVEL FOR DAY 7-15 OF CALIBRATION	27
FIGURE B28: SIMULATED AND OBSERVED HEXHAM WATER LEVEL FOR DAY 15-22 OF CALIBRATION	27
FIGURE B29: SIMULATED AND OBSERVED HEXHAM WATER LEVEL FOR DAY 22-29 OF CALIBRATION	28
FIGURE B30: MEASURED AND SIMULATED TIDAL PLANES IN LOWER HUNTER ESTUARY DURING CALIBRATION, VERSUS DISTANCE UPSTREAM FROM THE ENTRANCE	29
FIGURE B31: FLOWS IN HUNTER, WILLIAMS AND PATERSON RIVER BEFORE AND DURING VERIFICATION PERIOD	31
FIGURE B32: DOWNSTREAM (PILOT STATION) WATER LEVEL FOR VERIFICATION SIMULATION	32
FIGURE B33: WATER LEVELS MEASURED IN LOWER HUNTER ESTUARY FOR DAY 1-7 OF VERIFICATION	33
FIGURE B34: WATER LEVELS MEASURED IN LOWER HUNTER ESTUARY FOR DAY 7-15 OF VERIFICATION	33
FIGURE B35: WATER LEVELS MEASURED IN LOWER HUNTER ESTUARY FOR DAY 15-22 OF VERIFICATION	34
FIGURE B36: WATER LEVELS MEASURED IN LOWER HUNTER ESTUARY FOR DAY 22-29 OF VERIFICATION	34
FIGURE B37: SIMULATED AND OBSERVED PILOT STATION WATER LEVEL FOR DAY 1-7 OF VERIFICATION	35
FIGURE B38: SIMULATED AND OBSERVED PILOT STATION WATER LEVEL FOR DAY 7-15 OF VERIFICATION	36
FIGURE B39: SIMULATED AND OBSERVED PILOT STATION WATER LEVEL FOR DAY 15-22 OF VERIFICATION	36
FIGURE B40: SIMULATED AND OBSERVED PILOT STATION WATER LEVEL FOR DAY 22-29 OF VERIFICATION	37
FIGURE B41: SIMULATED AND OBSERVED STOCKTON WATER LEVEL FOR DAY 1-7 OF VERIFICATION	37
FIGURE B42: SIMULATED AND OBSERVED STOCKTON WATER LEVEL FOR DAY 7-15 OF VERIFICATION	38
FIGURE B43: SIMULATED AND OBSERVED STOCKTON WATER LEVEL FOR DAY 15-22 OF VERIFICATION	38
FIGURE B44: SIMULATED AND OBSERVED STOCKTON WATER LEVEL FOR DAY 22-29 OF VERIFICATION	39
FIGURE B45: SIMULATED AND OBSERVED HEXHAM WATER LEVEL FOR DAY 1-7 OF VERIFICATION	39

LIST OF FIGURES

Page No.

FIGURE B46: SIMULATED AND OBSERVED HEXHAM WATER LEVEL FOR DAYS 7-15 OF VERIFICATION	40
FIGURE B47: SIMULATED AND OBSERVED HEXHAM WATER LEVEL FOR DAY 15-22 OF VERIFICATION	40
FIGURE B48: SIMULATED AND OBSERVED HEXHAM WATER LEVEL FOR DAY 22-29 OF VERIFICATION	41

LIST OF TABLES

Page No.

TABLE B1:	WATER LEVEL DATA OBTAINED FOR THE LOWER HUNTER ESTUARY	2
TABLE B2:	RAINFALL DATA OBTAINED IN HUNTER RIVER CATCHMENT	3
TABLE B3:	WATER QUALITY DATA OBTAINED FOR THE ENTRANCE TO IRONBARK CREEK	4
TABLE B4:	RAINFALL DURING CALIBRATION PERIOD, 16 OCTOBER 2002 TO 14 NOVEMBER 2002	16
TABLE B5:	MEASURED AND SIMULATED TIDAL PLANES IN LOWER HUNTER ESTUARY DURING CALIBRATION	28
TABLE B6:	STATISTICAL COMPARISON OF SIMULATED AND OBSERVED WATER LEVELS IN LOWER HUNTER ESTUARY DURING CALIBRATION PERIOD	30
TABLE B7:	RAINFALL DURING VERIFICATION PERIOD, 25 JUNE 2002 TO 24 JULY 2002	31
TABLE B8:	STATISTICAL COMPARISON OF SIMULATED AND OBSERVED WATER LEVELS IN LOWER HUNTER ESTUARY DURING VERIFICATION PERIOD	41

B1 INTRODUCTION

A two-dimensional tidal hydrodynamic and water quality model of the Hunter River estuary was developed as a convenient tool to assess the impacts of the proposed South Arm dredging works.

In this Appendix, the development, calibration and verification of the tidal hydrodynamic model is described. The finite element RMA model suite was used in this investigation. General information on this model is given in **Appendix A**.

In Section B2, the available data useful for modelling is described, including water levels, rainfall, freshwater flows and water quality data.

Details of the development of the RMA model for this study is given in Section B3, including information on model extents, the finite element network, bathymetry, roughness and boundary conditions.

Hydrodynamic calibration and verification of the Hunter River tidal estuary model is described in Section B4.

Finally, conclusions are given in Section B5 and references are provided in Section B6.

B2 AVAILABLE DATA USEFUL FOR MODELLING

Numerical modelling is dependent on the availability of suitable data in order to:

- define boundary conditions, such as downstream tides or upstream flows, to drive the model;
- enable comparison of simulation outputs with corresponding recorded values to assist in calibration and verification of the model; and,
- determine additional processes that may be influencing the model results.

The available data useful for modelling of the Hunter River estuary is outlined in this Section.

B2.1 WATER LEVEL INFORMATION

There are four sites within the lower Hunter River estuary (downstream of Hexham) where water levels have been recorded over the long-term, namely at:

- Newcastle Pilot Station;
- Stockton Bridge;
- the entrance to Ironbark Creek; and,
- just upstream of Hexham Bridge

Data was obtained for these sites from Newcastle Port Corporation (Pilot Station) and the Department of Public Works and Services, Manly Hydraulics Laboratory (other three sites) as detailed in **Table B1**.

Table B1: Water level data obtained for the lower Hunter estuary

Site	Data Coverage	Frequency
Newcastle Pilot Station	1 January 2001 (0000) to 22 December 2002 (2359)	1 minute ¹
Stockton Bridge	1 January 2001 (0000) to 1 January 2003 (0000)	15 minutes ²
Ironbark Creek	1 May 1998 (0800) to 16 May 2002 (1200), then 8 August 2002 (1700) to 15 January 2003 (0500)	Hourly ³
Hexham Bridge	1 January 2001 (0000) to 6 January 2003 (0415)	15 minutes ⁴

Data has been collected at these sites since May 1992 (Pilot Station⁵), 11 December 1984 (Stockton), 1 May 1998 (Ironbark Creek), and 12 June 1985 (Hexham Bridge).

¹ There were 9645 missing data values over the period of data coverage. With 1038240 possible values this was a data recovery of 99.1%.

² There was complete data recovery over the period of data coverage (70081 data values).

³ There were 628 missing data values over the period of data coverage. With 39258 possible values this was a data recovery of 98.4%.

⁴ There were 310 missing data values over the period of data coverage. With 70578 possible values this was a data recovery of 99.6%.

B2.2 RAINFALL DATA

Water levels within the Hunter River are sensitive to rainfall-runoff. However, given that the tidal model generated for this study was driven predominantly by downstream water levels, it was necessary to simulate periods of minimal rainfall-induced freshwater flow so that recorded and simulated water levels had a reasonable match.

To determine when runoff was likely to be elevating water levels within the Hunter River, rainfall data was obtained for a number of sites distributed throughout the Hunter River catchment as detailed in **Table B2**. Data was obtained for these sites from the Bureau of Meteorology (BOM). The data obtained was daily rainfalls to 9am at each site, from 1 January 2001 to 24 December 2002 (unless otherwise stated).

Table B2: Rainfall data obtained in Hunter River catchment

Site	BOM Number	Data Recovery (%)	Note
Murrurundi Post Office	61051	100.0	
Newcastle Nobbys Signal Station	61055	82.4	
Williamtown RAAF	61078	100.0	
Chichester Dam	61151	99.9	Data ends 31/10/02
Muswellbrook (Lindisfarne)	61168	99.5	Data ends 30/9/02
Total	61250	99.9	
Singleton Water Board	61371	89.9	Data ends 26/11/02
Maitland Visitors Centre	61388	99.9	
Ulan Post Office	62036	100.0	

B2.3 FRESHWATER FLOW DATA

Flow data was obtained for the following three stations, covering the Hunter River and its two main tributaries:

- Williams River @ Glen Martin (Mill Dam Falls), No. 210010;
- Hunter River @ Greta, No. 210064; and
- Paterson River @ Gostwyck, No. 210079

The data was obtained from the Department of Land and Water Conservation for all of 2001 and 2002, with daily flows provided.

This enabled the baseflow component to be input into the RMA model as an upstream boundary condition, and provided further confirmation that freshwater flows were low as was appropriate in the tidal model.

⁵ Digital data collection commenced in May 1992. Prior to this, hard copy graphs plotted by mechanical tide gauges are available back to 1925 (Randall, 2003).

B2.4 WATER QUALITY DATA

Water quality data collected at the entrance to Ironbark Creek was obtained over the same period as the water level measurements outlined in Section B2.1, namely 1 May 1998 (0800) to 16 May 2002 (1200), then 8 August 2002 (1700) to 15 January 2003 (0500). The data was obtained from the Department of Public Works and Services, Manly Hydraulics Laboratory.

The variables in the data set and data recovery for each variable is outlined in **Table B3**.

Table B3: Water quality data obtained for the entrance to Ironbark Creek

Variable	Data Recovery (%)
Conductivity (mS/cm)	99.8
Salinity (ppt)	99.9
Temperature (°C)	99.5
pH	99.9
Dissolved Oxygen (% saturation)	96.8
Dissolved Oxygen (mg/L)	97.3
Turbidity (NTU)	46.6 ⁶

⁶ Turbidity data was only collected from 5 July 2000 at 1700.

B3 DEVELOPMENT OF TIDAL HYDRODYNAMIC MODEL

B3.1 MODEL EXTENT

The tidal limits in the Hunter estuary have been determined by Manly Hydraulics Laboratory (2002) as listed below:

- Oakhampton (Hunter River);
- Seaham (Williams River);
- Gostwyck (Paterson River);
- Testers Hollow (Wallis Creek);
- Dagworth Bridge (Fishery Creek, also known as Swamp Creek);
- Minmi Road (Ironbark Creek);
- Alexandria Park (Throsby Creek);
- Griffiths Road (Styx Creek); and,
- Broadmeadow Racecourse (Cottage Creek).

For this study of the Hunter River estuary, the upstream model extents in plan were generally to these perceived tidal limits, namely in the Hunter, Williams and Paterson Rivers. However, with the limited exchange within Wallis and Fishery Creek and Ironbark Creek due to floodgates, these systems (upstream of the floodgates) were not included in the final finite element network.

Sensitivity testing was undertaken with Wallis Creek, Fishery Creek and Ironbark Creek included in the network, incorporating details of the floodgate structures. It was found that there were negligible changes in results for the purposes of this investigation with these systems included.

An example of the limited exchange upstream of the Ironbark Creek floodgates is shown in **Figure B1**, with relatively turbid waters upstream and clearer waters downstream.

Styx Creek and Cottage Creek were not included in the model as these were negligible in terms of the tidal hydrodynamics of the estuary as a whole. The section of Throsby Creek upstream of Maitland Road was also not included for the same reason. These three reaches are all developed urban stormwater systems.



Figure B1: Example of limited exchange upstream of Ironbark Creek floodgates

The downstream model extent was to the ocean at the eastern end of the entrance training walls.

The model was designed as an estuarine representation only, so the top of bank was the vertical elevation limit to the bathymetry. That is, floodplain areas were not included in this model (except for mangrove areas). Mangrove areas identified from aerial photography and 1:25,000 scale topographic maps in the study region were included in the model, as they would be expected to be regularly tidally inundated.

B3.2 FINITE ELEMENT NETWORK

Based on the model extents outlined in Section B3.1, the finite element network developed for the Hunter River estuary is shown in **Figure B2**. The model was constructed based on ISG coordinates (NSW Integrated Survey Grid, Zone 56/1).

A zoomed view of the network downstream of Hexham is provided in **Figure B3**, while the network near the entrance (including Throsby Creek, the South Arm upstream to Tourle St Bridge and the North Arm to Fern Bay) is shown in **Figure B4**.

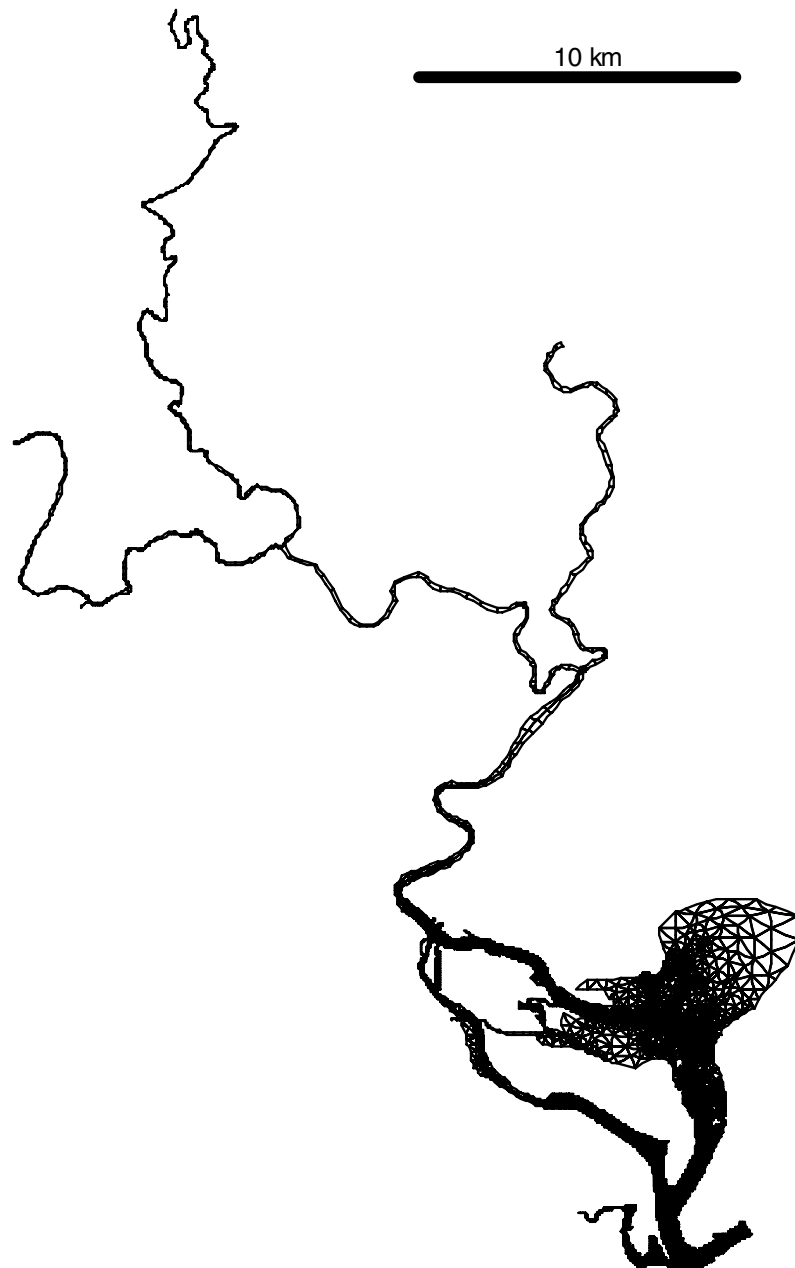


Figure B2: Finite element network of the Hunter River estuary

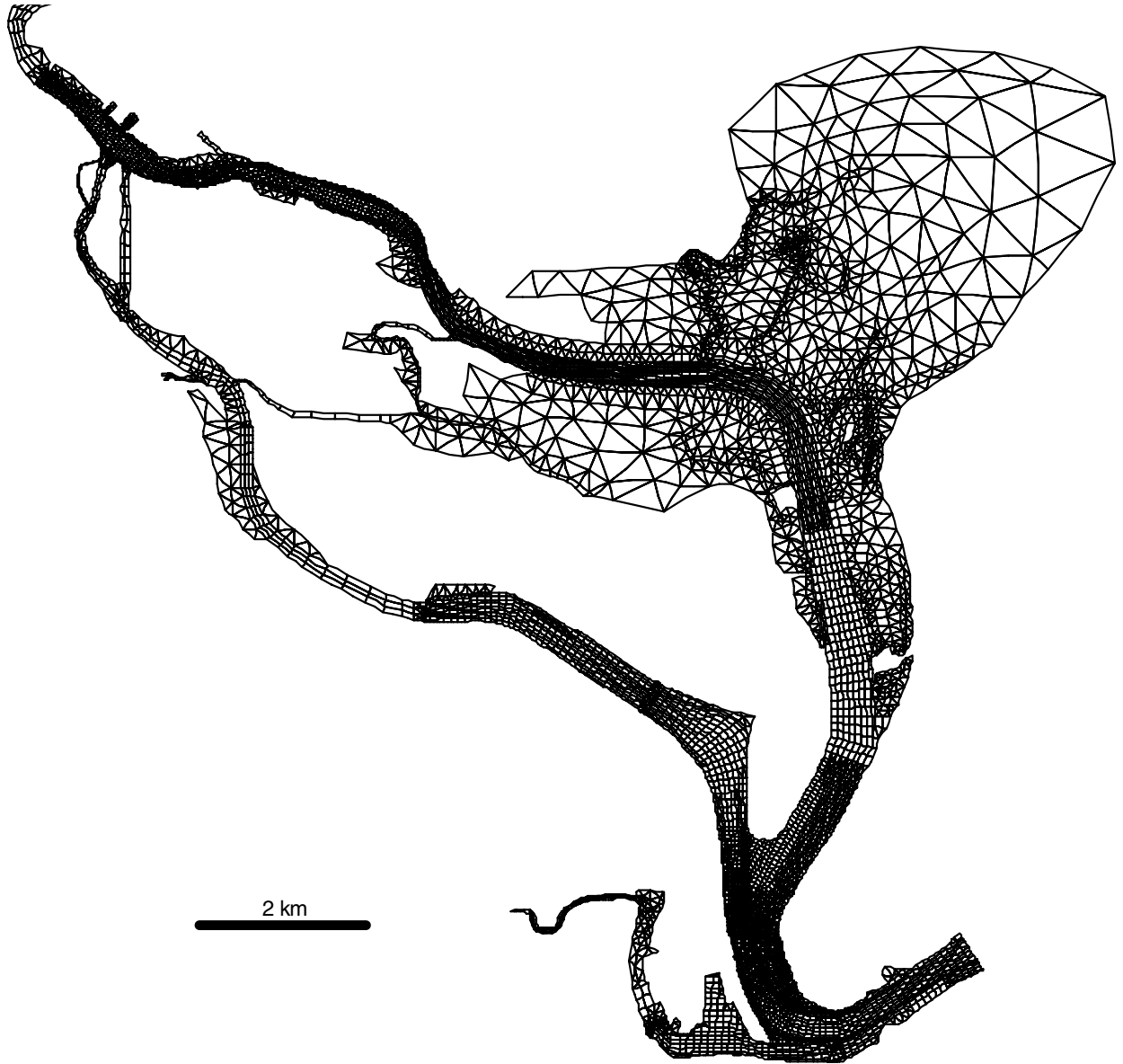


Figure B3: Finite element network of the Hunter River estuary, downstream of Hexham

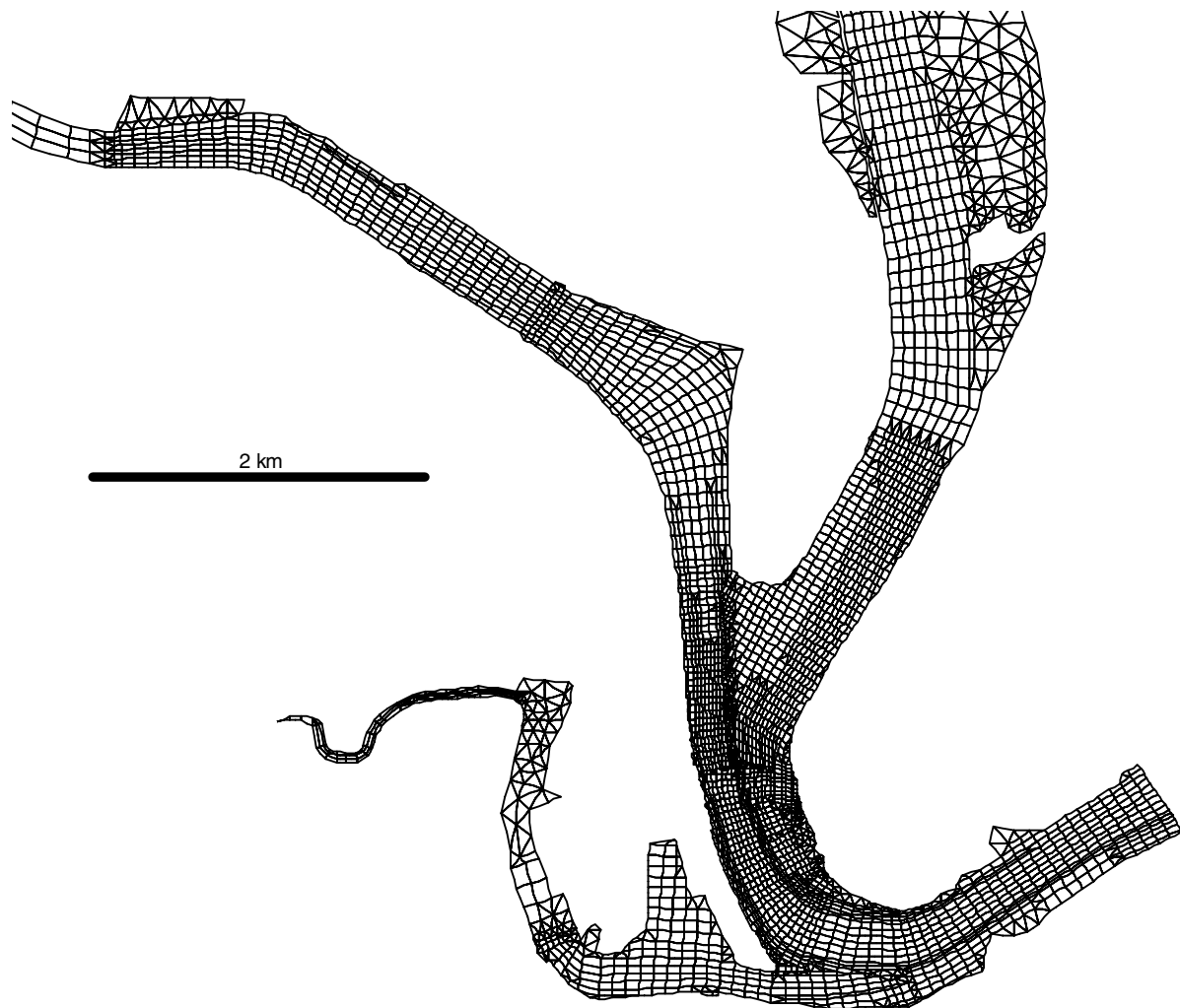


Figure B4: Finite element network of the Hunter River estuary, entrance area

B3.3 BATHYMETRY

The bed elevations in the RMA model network were derived from a number of sources. Detailed Newcastle Port Corporation hydrographic soundings were available for much of the study area downstream of Hexham Bridge, namely:

- North Arm, from Hexham Bridge to Stockton Bridge, completed in December 1997;
- South Arm, from Tourle Bridge to Kooragang No 6 Berth, completed in March 2001;
- North Arm, downstream of Stockton Bridge, completed in October 2001; and,
- Port Hunter and Throsby Creek, completed in 2002.

The soundings were approximately every 0.3m, providing a total of about 1.15 million bathymetric sounding points. Note that this data was supplied to Newcastle Harbour Tide Gauge Datum, and converted to AHD by subtracting 1.01m.

Australian Hydrographic Service AUS Charts were used to define the bathymetry outside of the coverage of the Newcastle Port Corporation soundings. These comprised:

- AUS 208⁷ to define bed elevations upstream of the dredged areas in Throsby Creek (upstream of Throsby Basin);
- AUS 208 to define bed elevations in the sand and mud flat areas near Stockton Bridge; and,
- AUS 207⁸ to define bed elevations in Fullerton Cove, and upstream of Tourle St Bridge in the South Arm.

These AUS Charts were also used to define the channel fringes in conjunction with 1:25,000 scale topographic maps.

Reference was also made to an existing tidal model of the Hunter estuary derived by Patterson Britton & Partners (1999a) as part of the Newcastle Harbour Environmental Improvement Plan study undertaken for Hunter Water Corporation.

Upstream of Hexham Bridge, bathymetric information was relatively sparse, comprising cross sections spaced tens of metres apart. This data was sourced from a variety of reports, including Patterson Britton & Partners (1993, 1994, 1995a, 1995b, 1999b, 2000). In Patterson Britton & Partners (1993), the information was presented as depths, areas and other hydraulic information at the location of cross sections in the model used for the PWD (1994) Flood Study.

Areas of mangrove and saltmarsh inhabitation generally did not have bathymetric information available. These areas were identified from 1:25,000 scale topographic maps and 1:12,000 scale aerial photographs⁹. Mangroves are typically found at elevations from just above low tide to mean high tide (so they are regularly tidally inundated), while saltmarsh usually extends from mean high to high-high tide levels (Burchett et al, 1999). Therefore, bed elevations for mangrove areas were set at between about -0.3 and 0.5m AHD, while saltmarsh areas were set at elevations up to 1m AHD.

The most extensive areas of mangroves and saltmarsh noted included:

- Fullerton Cove and the islands to the west (Smiths, Wallis and Dunns Island), and proceeding upstream along the left¹⁰ (north bank) of the North Arm;
- parts of Kooragang Island (especially the north-east, in the vicinity of Mangrove Creek and upstream along the right or south bank of the North Arm);
- south of Ironbark Creek on the right bank of the South Arm;
- between Ash Island Bridge and Ironbark Creek on the left bank of the South Arm; and,
- on the left and right bank of the North Arm in patches near Tomago.

⁷ AUS 208 is 1:7,500 scale and entitled "Australia – East Coast , New South Wales, Newcastle Harbour". The edition used was dated 29 October 1999 (New Edition, originally published 1972).

⁸ AUS 207 is 1:25,000 scale and entitled "Australia – East Coast , New South Wales, Approaches to Newcastle". The edition used was dated 21 July 2000 (New Edition, originally published 1993). An earlier edition (24 June 1988) was also used to provide additional bathymetric information at the north of Fullerton Cove.

⁹ Note that the extent of mangroves appeared to be overestimated on the 1:25,000 scale topographic maps. For example, Smiths Island would appear to be dominated by saltmarsh from aerial photography, yet was denoted as being mangrove covered on the topographic map.

¹⁰ The left and right banks are denoted as if looking downstream.

Of these, saltmarsh areas were most extensive on the islands to the west of Fullerton Cove and on the more inland areas of Kooragang Island.

The assumed mangrove and saltmarsh areas are shown as light green in **Figure B5**. Dark green areas represent the main channel. Note that only a portion of the finite element network is shown.

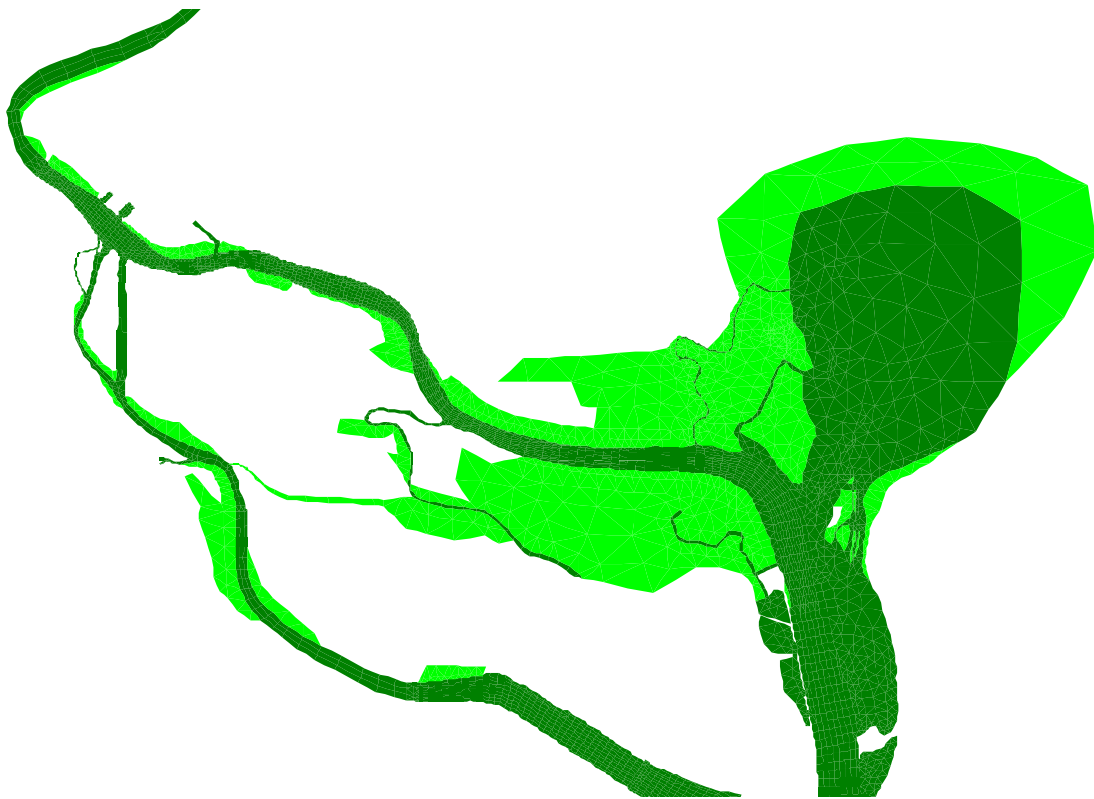


Figure B5: Assumed mangrove and saltmarsh areas in finite element network (light green)

A contour plan of the adopted bathymetry in the Hunter River estuary is shown in **Figure B6** for the area downstream of Hexham, and in **Figure B7** for the entrance port area.

Note that the adopted bathymetry is a particular snapshot of historical conditions and does not take account of any variations since or before that time due to sediment transport or dredging. It is therefore possible that the model bathymetry is at variance with the conditions occurring at particular times prior to or after the dates of the bathymetric surveys. However, it is known that no capital dredging (that is dredging beyond maintenance requirements) has been undertaken since the dates of the adopted Newcastle Port Corporation bathymetry.

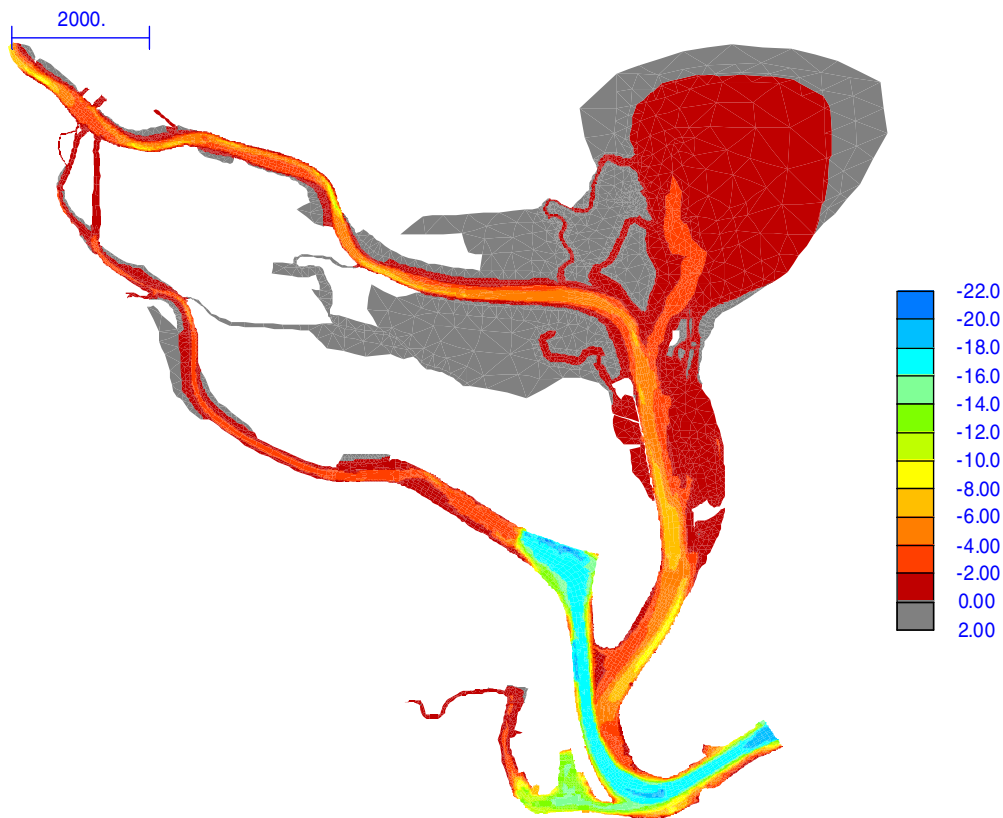


Figure B6: Adopted Hunter River estuary bathymetry (m AHD), downstream of Hexham

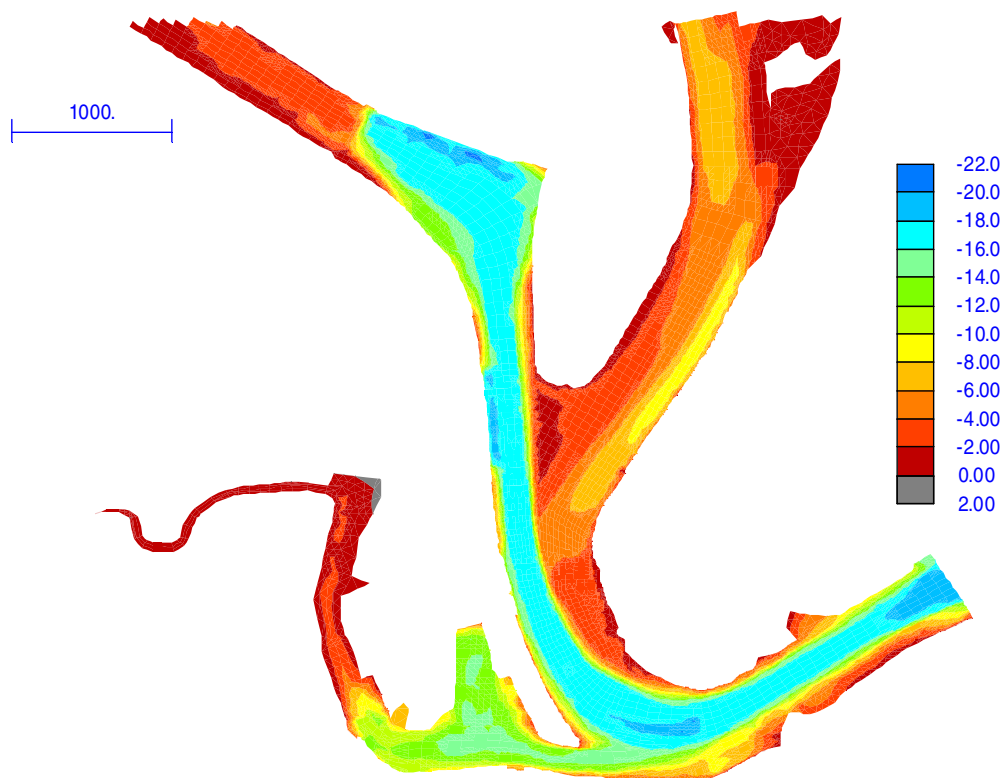


Figure B7: Adopted Hunter River estuary bathymetry (m AHD), in port area

B3.4 ROUGHNESS

Manning's n roughness values were derived based on typical values in the literature. For the natural channel sections, which were assumed generally clean and straight (as opposed to winding and weedy), an n value of 0.025 was adopted as per Chow (1959).

For mangrove areas, an n value of 0.08 was adopted, within the range recommended by Chow (1959), and used for other recent studies in mangrove areas such as Horton and King (1999a, b, c). Results were not sensitive to the mangrove n selected in the range of 0.07-0.09.

B3.5 BOUNDARY CONDITIONS

Typically, boundary conditions are applied as input flows at the upstream ends of the model and varying (or constant) water levels at the downstream end (tailwater) of the model. In the case of tidal-only simulations, the upstream flows are zero or a small baseflow, and almost all water movement is generated by the varying downstream tailwater.

For this study, the flows measured in the Hunter River at Greta, Williams River at Glen Martin, and Paterson River at Gostwyck (Section B2.3) were used as upstream boundary conditions. Given that simulations were undertaken during periods of low freshwater flow, incorporation of these baseflows had very little influence on the hydrodynamics of the Hunter estuary. They were included for completeness.

The downstream boundary condition applied for this study utilised the Newcastle Pilot Station data. The small (negligible) difference in amplitude and phase between the Pilot Station and the downstream boundary of the model was ignored.

The Pilot Station site would include most processes affecting the water level at the oceanic entrance to the Hunter River, such as:

- tide; and
- storm surge (barometric and wind setup¹¹).

Wave setup, the superelevation of the mean water level caused by wave action alone, was not considered to be necessary to include at this site. Wave setup is related to the conversion of the kinetic energy of wave motion to quasi-steady potential energy. It is manifested as a decrease in water level prior to breaking, with a maximum set down at the break point; from the break point the mean water surface slopes upward to the point of intersection with the shore (Coastal Engineering Research Center, 1984).

However, in the case of river entrances like the Hunter, wave setup at the entrance, where the depth is finite, is less than the wave setup at a beach, where the depth tends to zero (Dunn et al, 2001). Any potential wave setup effects were therefore ignored for this study.

¹¹ It was assumed that the Pilot Station site experienced similar regional wind setup to the open coast.

B4 MODEL CALIBRATION AND VERIFICATION

To calibrate and verify the RMA numerical model, an attempt was made to match recorded and simulated water levels at the Pilot Station, Stockton Bridge, Ironbark Creek and Hexham Bridge (where available). Both the calibration and verification simulations covered a neap/spring tidal cycle of 29 days, with an additional start up allowance of one day to ensure washout of initial conditions.

The calibration and verification results are outlined in Sections B4.2 and B4.3 respectively. Prior to this, in Section B4.1, the statistical parameters used to evaluate the success of the calibration and verification are outlined.

B4.1 STATISTICS FOR EVALUATING SIMULATION OUTPUTS

There are a number of statistical measures that can be used to compare simulation outputs with observed (actual) values (Yang, 1997). Most statistics outlined in this Section were derived from this source.

The *absolute maximum error* is the absolute value of the maximum deviation between the simulated and observed values.

Root-mean-square (RMS) error is a measure of the deviation of the simulated variable from its observed value, and is given by:

$$\text{RMS error} = \sqrt{\frac{1}{n} \sum_{i=1}^n (\hat{y}_i - y_i)^2}$$

where \hat{y}_i is the simulated value, y_i is the observed value, and n is the number of data points.

RMS percent error is given by:

$$\text{RMS percent error} = \sqrt{\frac{1}{n} \sum_{i=1}^n \left(\frac{\hat{y}_i - y_i}{y_i} \right)^2}$$

Mean error is defined as:

$$\text{mean error} = \frac{1}{n} \sum_{i=1}^n (\hat{y}_i - y_i)$$

Mean percent error is given by:

$$\text{mean percent error} = \frac{1}{n} \sum_{i=1}^n \left(\frac{\hat{y}_i - y_i}{y_i} \right)$$

The mean error and mean percent error are useful indicators of systematic bias¹².

The *correlation coefficient*, ρ , is an indicator of how the simulated and observed values are related, and is given by:

$$\rho = \frac{\sum_{i=1}^n (\hat{y}_i - \bar{\hat{y}})(y_i - \bar{y})}{n\hat{\sigma}\sigma}$$

where $\bar{\hat{y}}$ and $\hat{\sigma}$ are the mean and standard deviation respectively of the simulated values, and \bar{y} and σ are the mean and standard deviation respectively of the observed values. The closer that ρ is to 1, the better the performance of the simulation model.

The RMS percent error and mean percent error can only be used where all observed data points are non-zero. Another simulation statistic, related to the RMS percent error, that does not have this restriction is *Theil's inequality coefficient* (U), which is defined as:

$$U = \frac{\text{rms error}}{\sqrt{\frac{1}{n} \sum_{i=1}^n \hat{y}_i^2 + \frac{1}{n} \sum_{i=1}^n y_i^2}}$$

U always has values between 0 and 1. If $U=0$, the simulated values are identical to the observed values (perfect fit). If $U=1$, the simulation fit is as bad as it could be.

U can be decomposed into three components termed the *proportions of inequality*. These break the simulation error down into its characteristic sources, namely:

- U_M , the *bias proportion*, a measure of systematic error;
- U_S , the *variance proportion*, an indication of the model's ability to replicate the degree of variability in the observed values; and,
- U_C , the *covariance proportion*, a measure of unsystematic error.

Definition of these components is given in Yang (1997). The sum of these three components equals 1. Ideally, U_M and U_S should be close to 0 and U_C should be close to 1.

If U_M exceeds 0.1 or 0.2, this implies the existence of a systematic bias. A high value of U_S is an indication that there is a large fluctuation in the simulated values that is not present in the observed data, or vice versa.

B4.2 CALIBRATION

The 29-day period from 16 October 2002 to 14 November 2002 was chosen for calibration. This was a suitable period for simulation as there were few days of rainfall during this time.

¹² Systematic bias is a non-random difference between the simulated and observed values, for example, caused by a particular process not being accounted for in the model, or recording equipment malfunction.

The total rainfall that fell at nine sites throughout the Hunter catchment during the calibration period is shown in **Table B4**.

Table B4: Rainfall during calibration period, 16 October 2002 to 14 November 2002

Site	Rainfall (mm)	Note
Murrurundi Post Office	0.2	
Newcastle Nobbys Signal Station	0.2	
Williamtown RAAF	2.6	
Chichester Dam	12.0	14 days missing in record
Muswellbrook (Lindisfarne)	-	No data
Total	0.6	
Singleton Water Board	1.3	2 days missing in record
Maitland Visitors Centre	0.8	
Ulan Post Office	0	

As confirmation of the lack of rainfall in the calibration period, the flows in the Hunter River at Greta, Williams River at Glen Martin, and Paterson River at Gostwyck that occurred during the calibration simulation (and for 4 days prior) are shown in **Figure B8**.

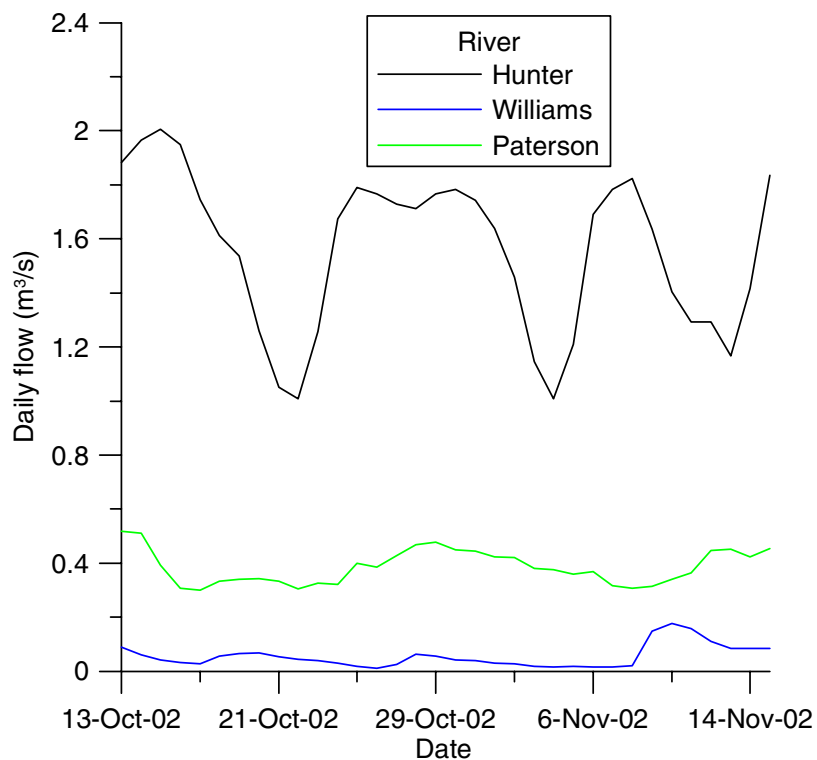


Figure B8: Flows in Hunter, Williams and Paterson River before and during calibration period

The Pilot Station water level used as the downstream boundary condition for the calibration simulation is shown in **Figure B9**. The Pilot Station water level is also shown along with the water levels recorded at Stockton Bridge, Ironbark Creek and Hexham Bridge during this period, in **Figure B10** to **Figure B13** in 7.25 day intervals.

Note that after significant analysis and model sensitivity testing, Patterson Britton approached Manly Hydraulics Laboratory (in February 2003) with a request to check the datum for the supplied data at Hexham Bridge. This was prompted by the inconsistency of the water level record at Hexham compared to the other available data.

Manly Hydraulics Laboratory checked the Hexham Bridge gauge datum, and found that the data supplied for Hexham Bridge was indeed not correctly surveyed in relation to AHD¹³. Davidson (2003) advised that the originally supplied data should be shifted downwards by 50mm to provide levels to AHD.

All comparisons between model results and measured data (at Hexham Bridge) presented in this report are based on the data shifted downwards by 50mm.

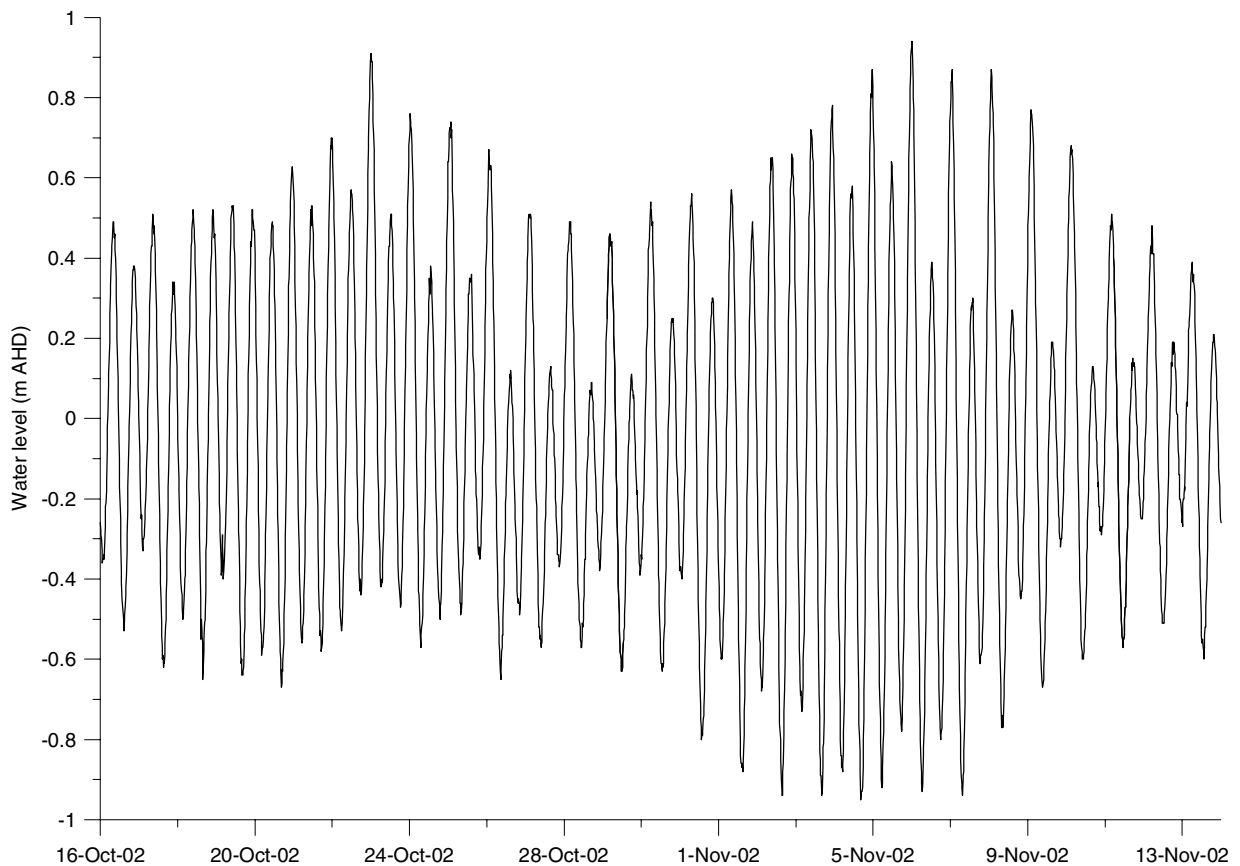


Figure B9: Downstream (Pilot Station) water level for calibration simulation

¹³ It was noted that the error may have been caused by tide boards that had shifted due to boats mooring to them.

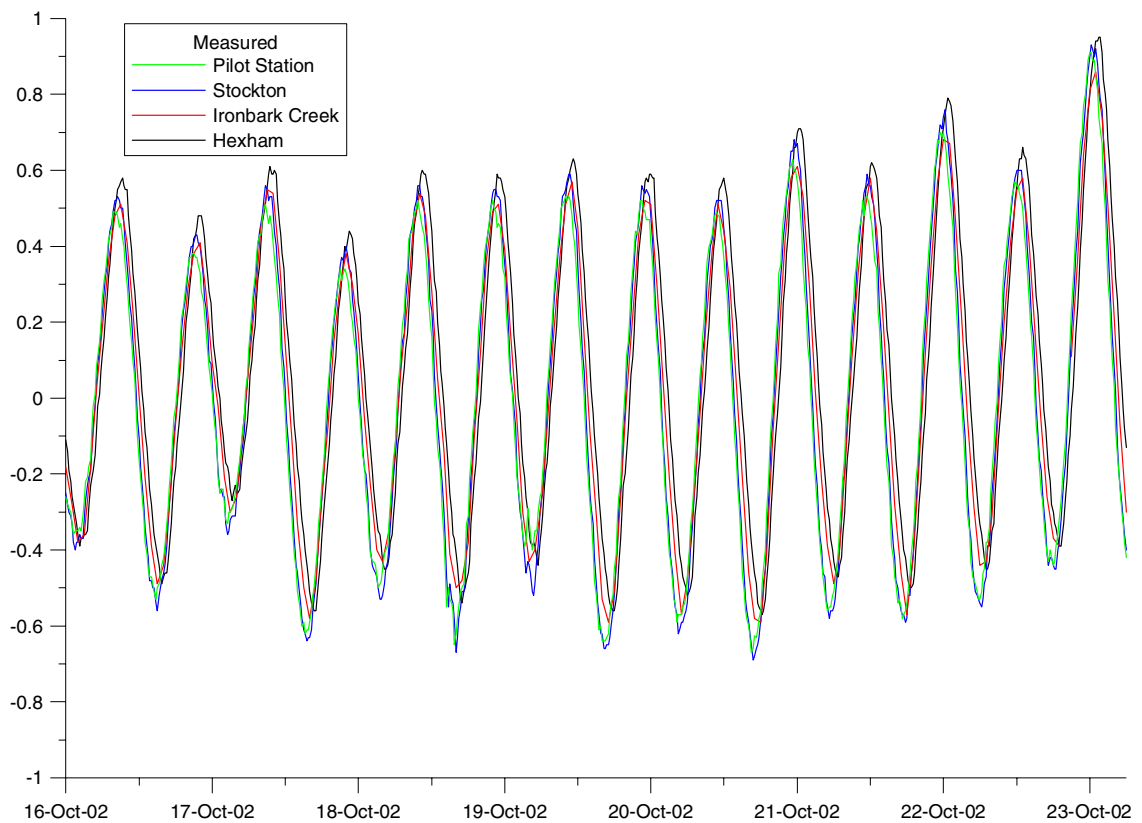


Figure B10: Water levels measured in lower Hunter estuary for day 1-7 of calibration

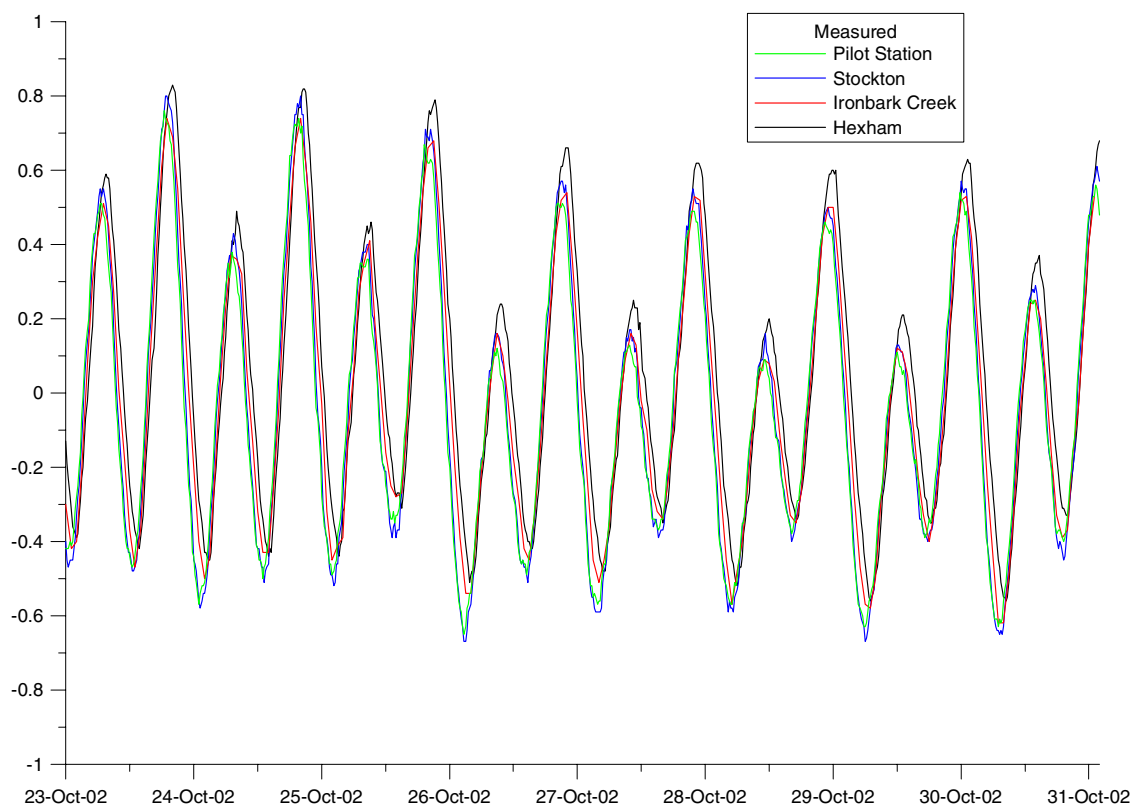


Figure B11: Water levels measured in lower Hunter estuary for day 7-15 of calibration

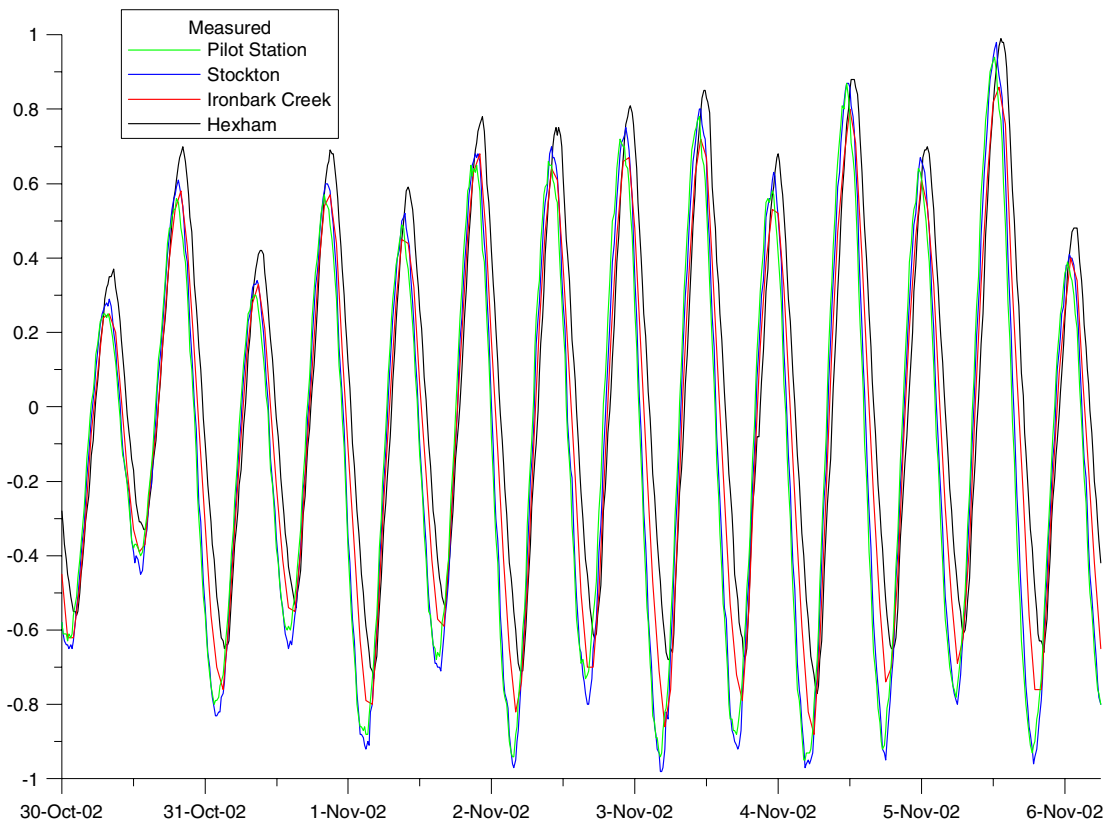


Figure B12: Water levels measured in lower Hunter estuary for day 15-22 of calibration

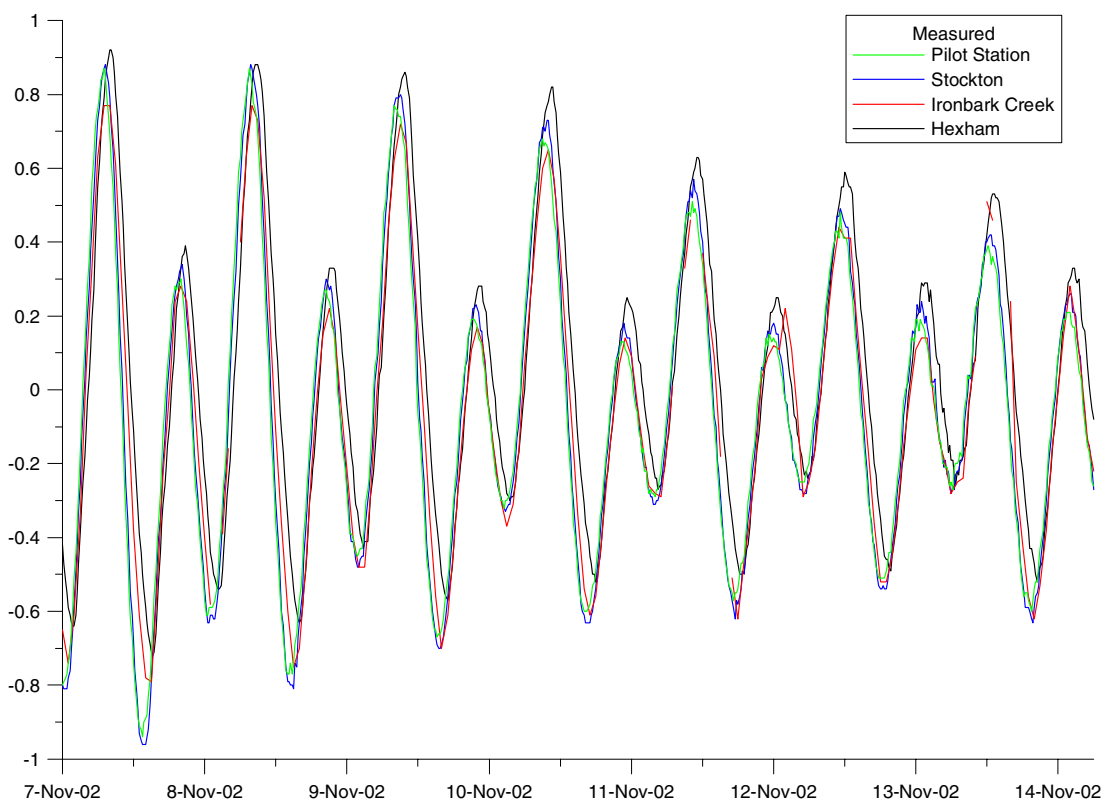


Figure B13: Water levels measured in lower Hunter estuary for day 22-29 of calibration

The measurements indicate that water levels at Stockton Bridge were generally slightly amplified relative to the Pilot Station, while water levels at Ironbark Creek were generally slightly attenuated relative to the Pilot Station¹⁴. The lag in the tide moving upstream is also evident.

The measurements at Hexham are unusual in that high and low tide is consistently higher than the three downstream stations.

A comparison of simulated and observed water levels during the calibration period is given as detailed below in 7.25 day increments:

- Pilot Station, **Figure B14 to Figure B17**;
- Stockton Bridge, **Figure B26 to Figure B29**;
- Ironbark Creek, **Figure B18 to Figure B21** (which includes some gaps in the measured data in the latter Figure); and,
- Hexham Bridge, **Figure B22 to Figure B25**.

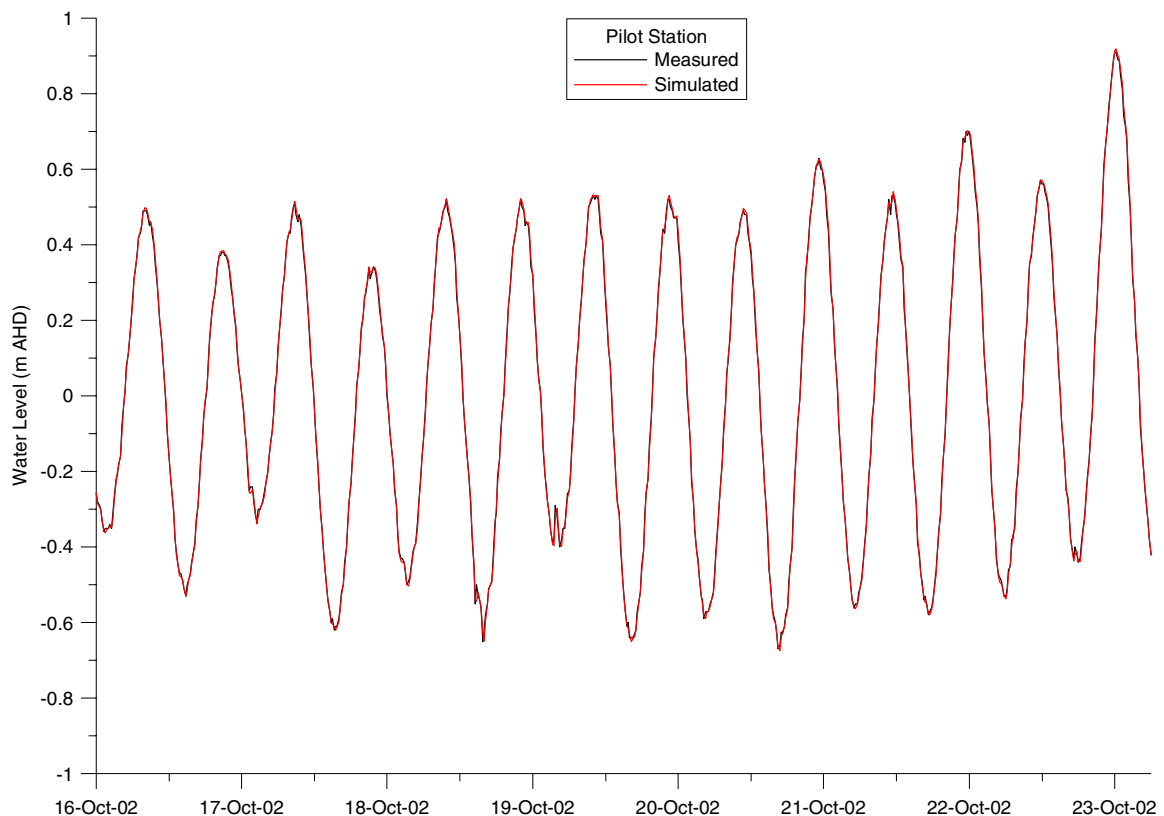


Figure B14: Simulated and observed Pilot Station water level for day 1-7 of calibration

¹⁴ Tidal amplification refers to high tide getting higher and low tide getting lower proceeding upstream (this is often related to estuary narrowing). Tidal attenuation refers to high tide getting lower and low tide getting higher proceeding upstream (this is often related to shallowing and friction).

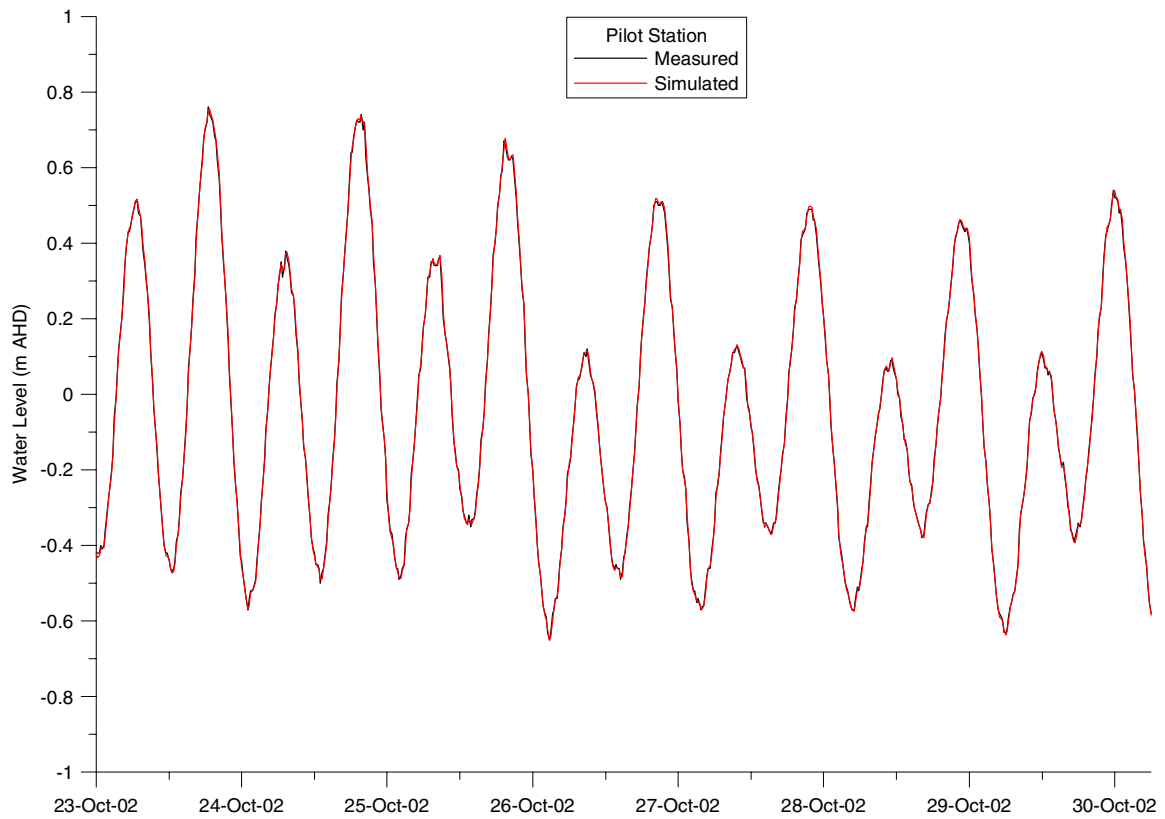


Figure B15: Simulated and observed Pilot Station water level for day 7-15 of calibration

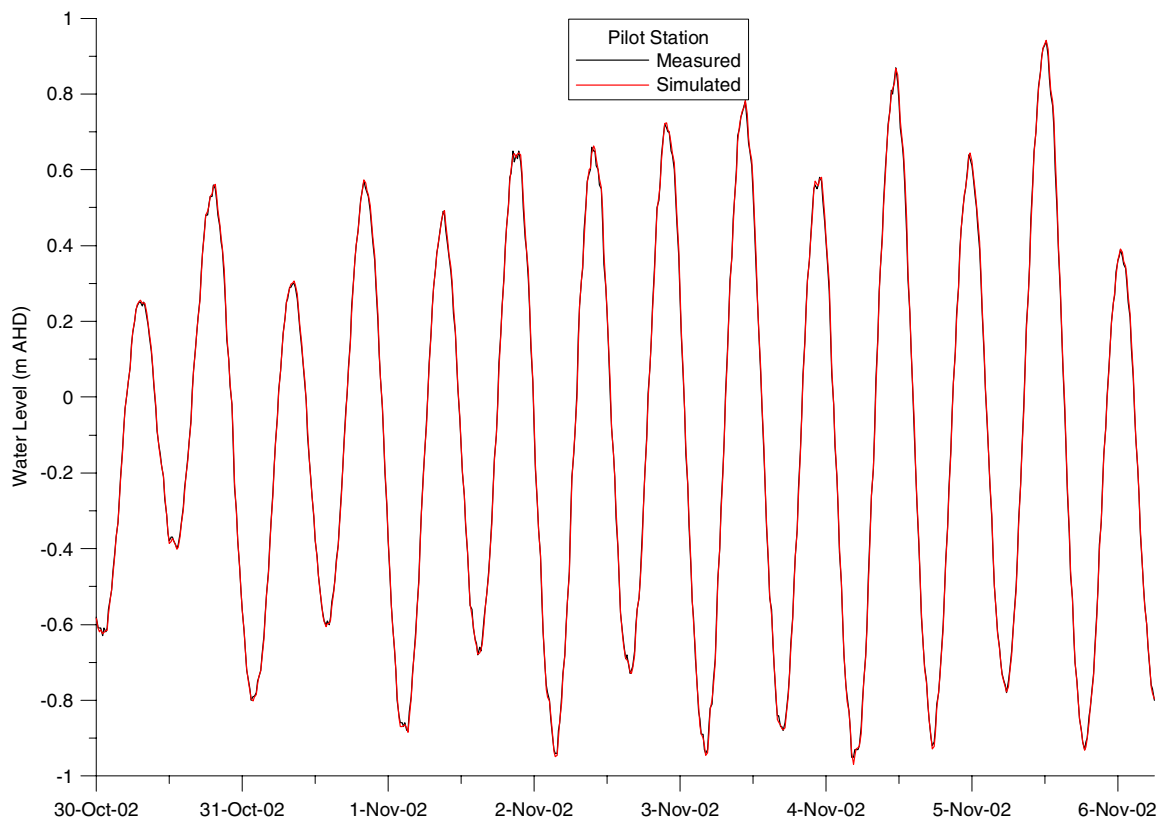


Figure B16: Simulated and observed Pilot Station water level for day 15-22 of calibration

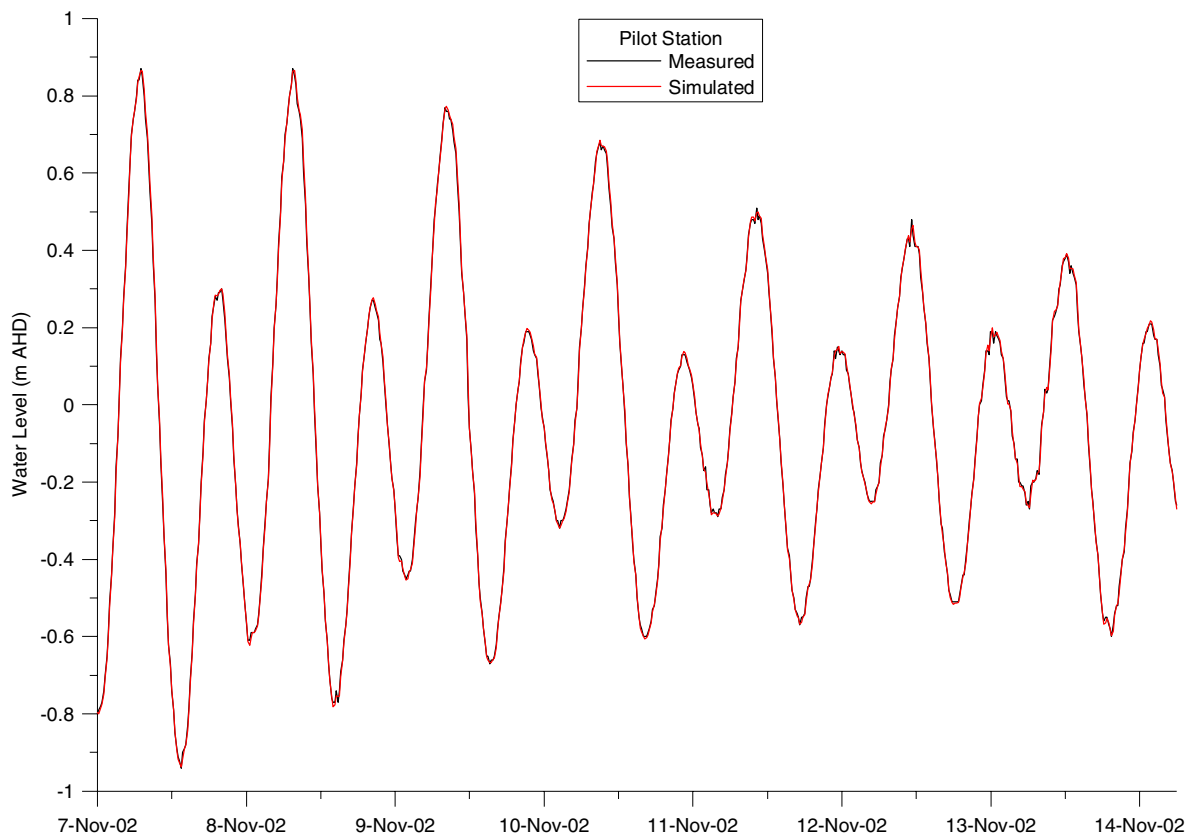


Figure B17: Simulated and observed Pilot Station water level for day 22-29 of calibration

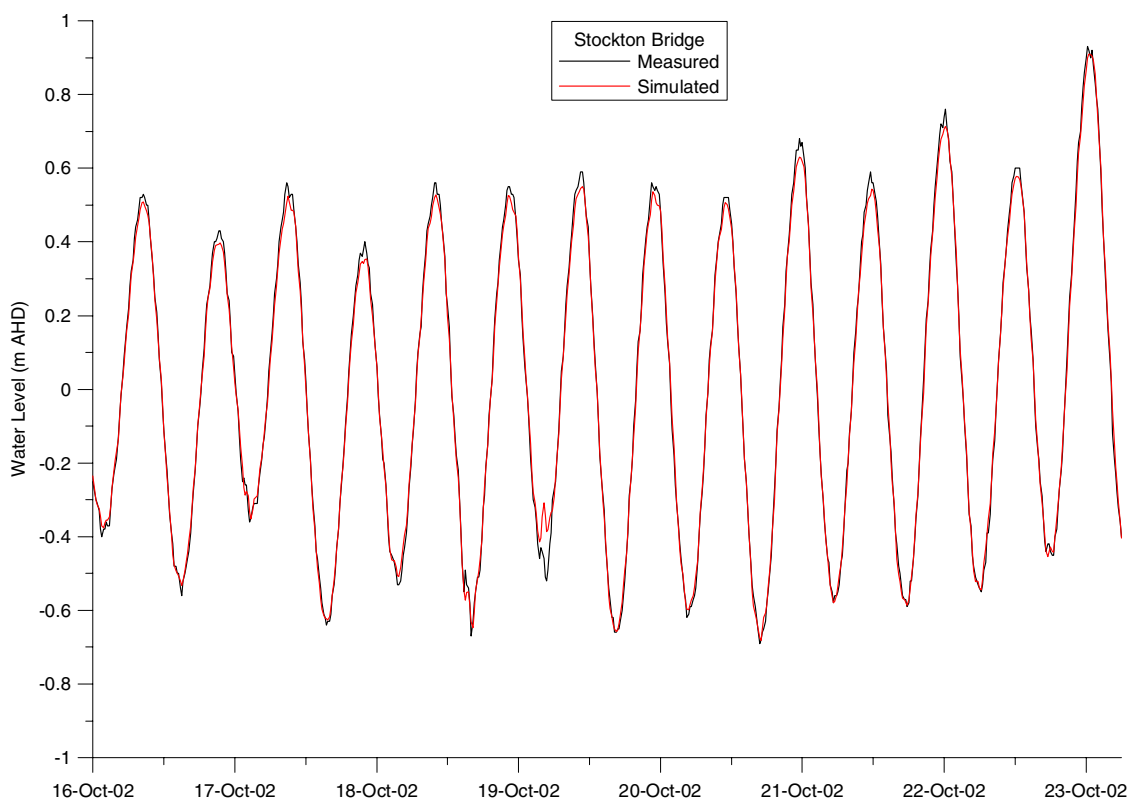


Figure B18: Simulated and observed Stockton water level for day 1-7 of calibration

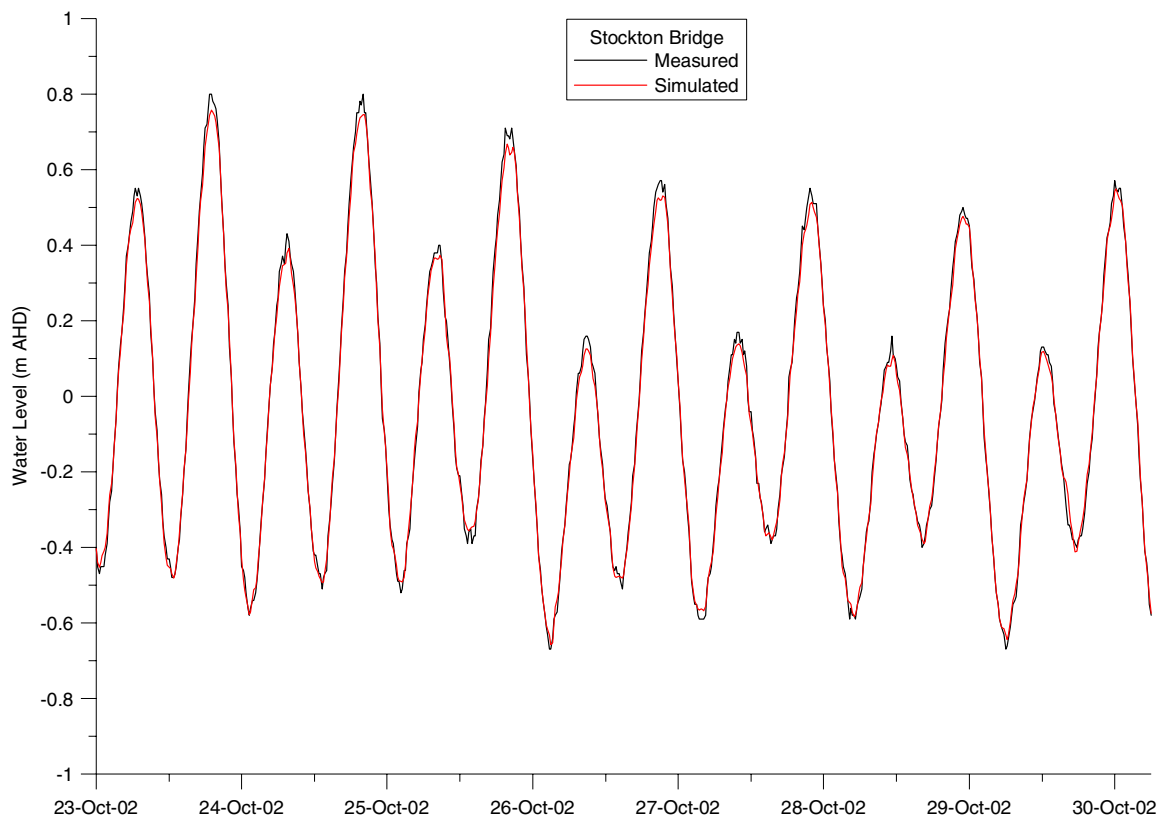


Figure B19: Simulated and observed Stockton water level for day 7-15 of calibration

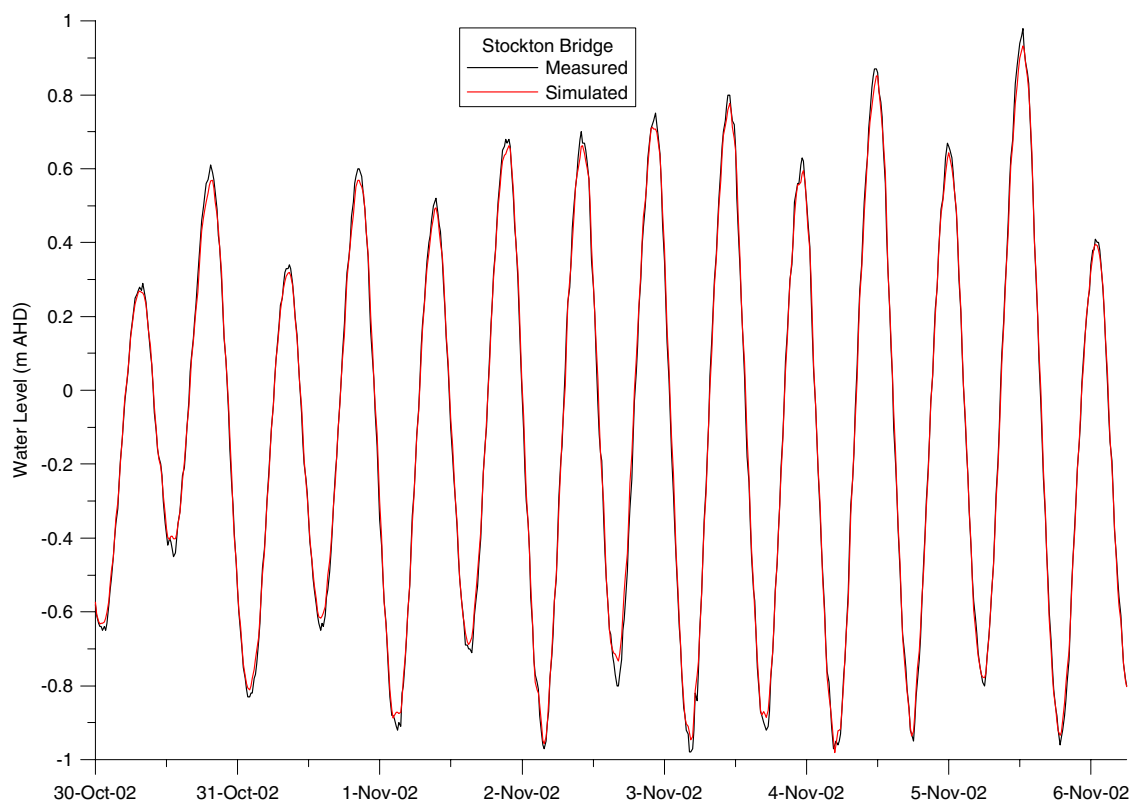


Figure B20: Simulated and observed Stockton water level for day 15-22 of calibration

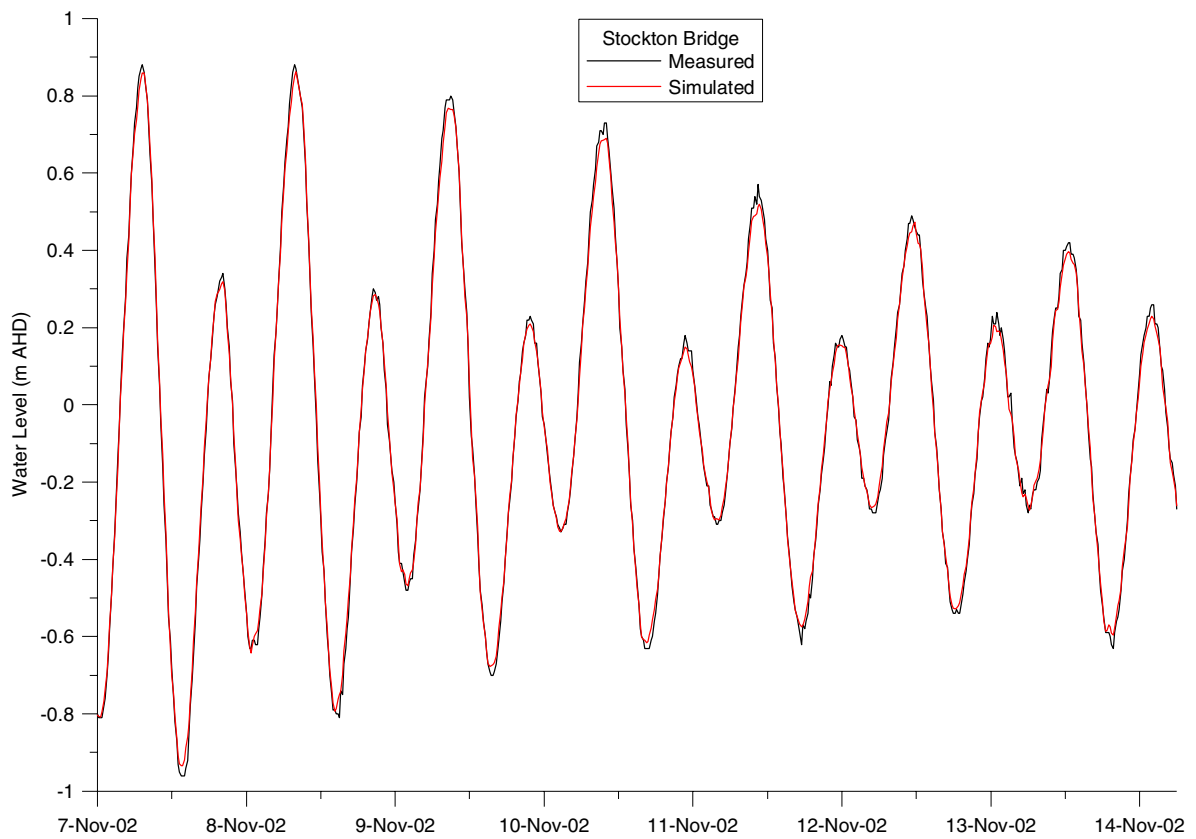


Figure B21: Simulated and observed Stockton water level for day 22-29 of calibration

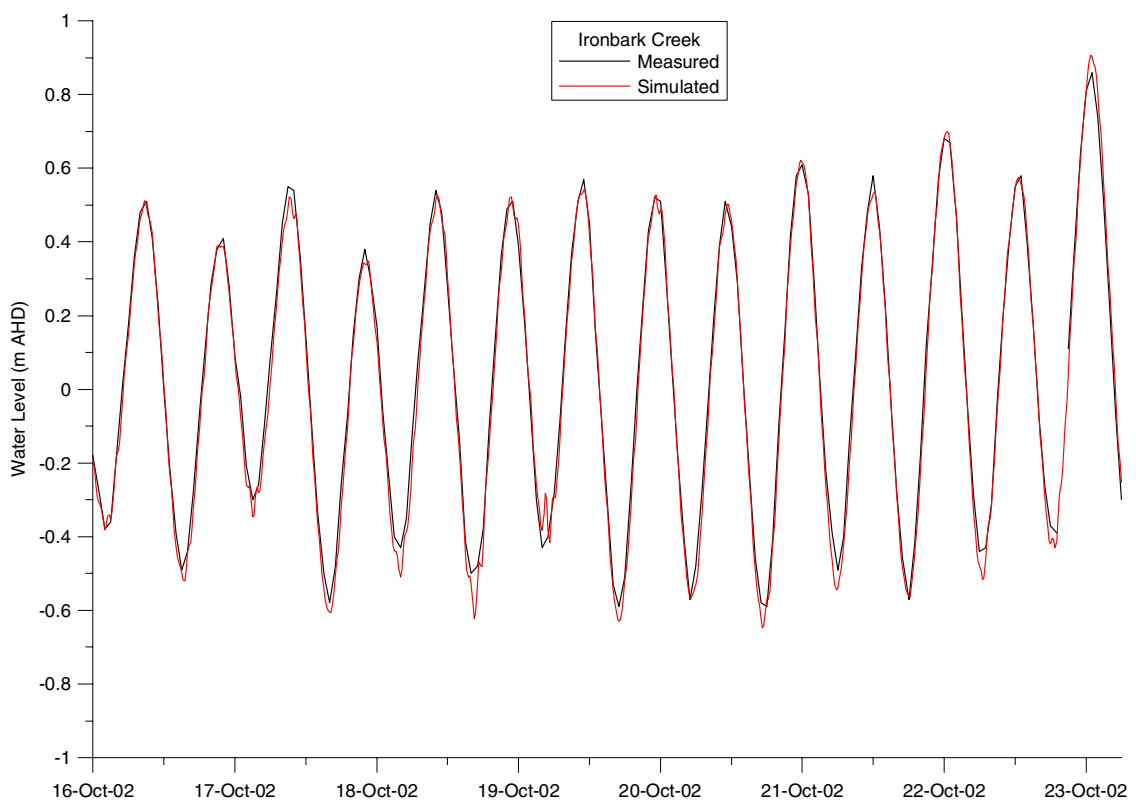


Figure B22: Simulated and observed Ironbark Ck water level for day 1-7 of calibration

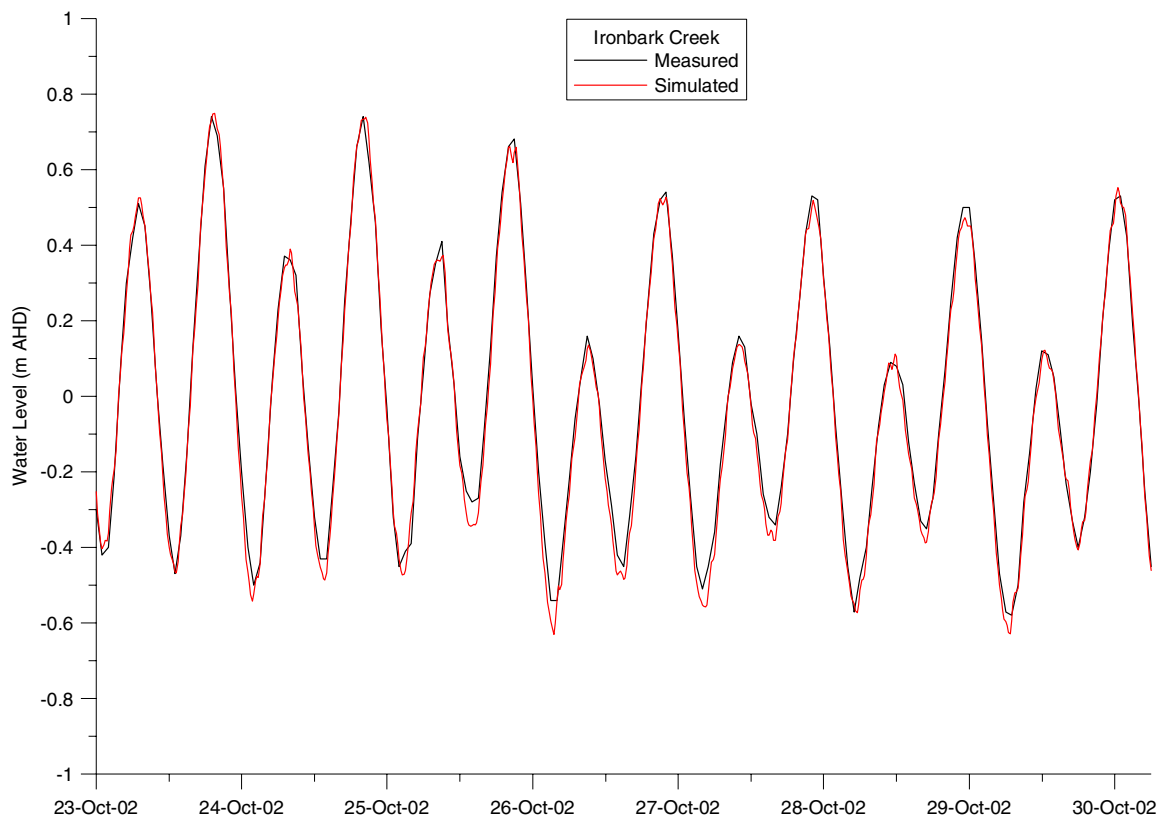


Figure B23: Simulated and observed Ironbark Ck water level for day 7-15 of calibration

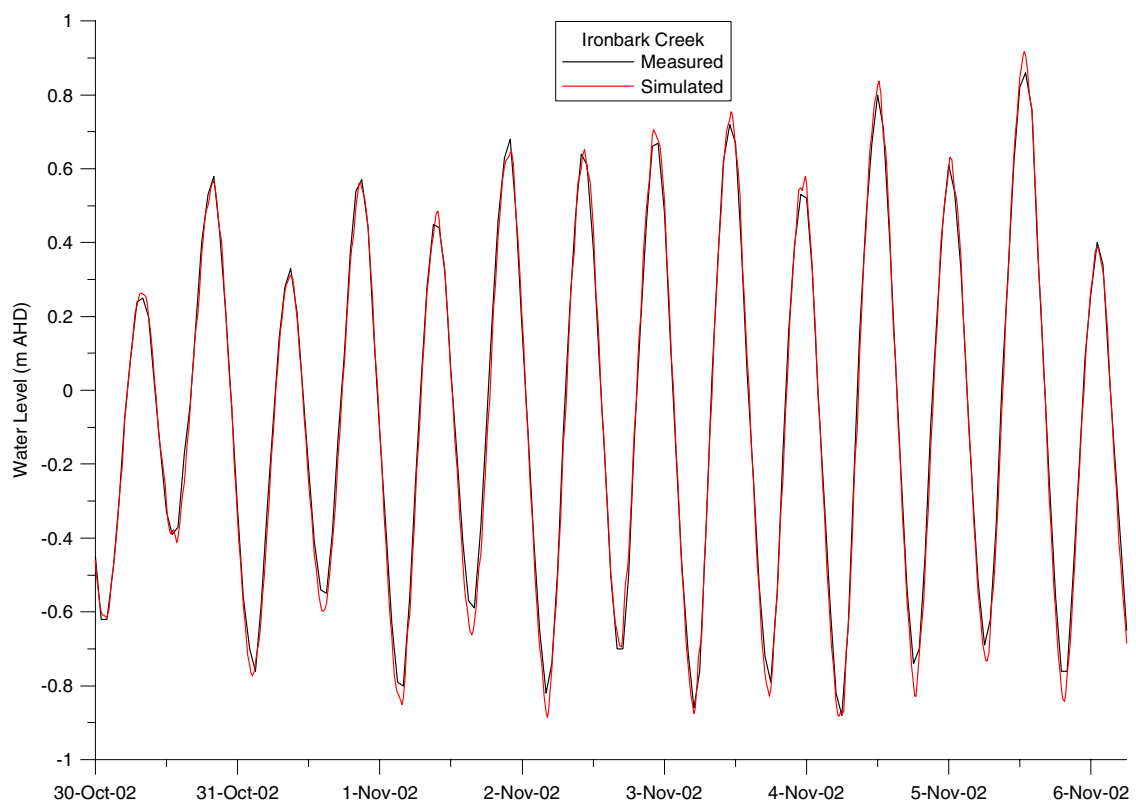


Figure B24: Simulated and observed Ironbark Ck water level for day 15-22 of calibration

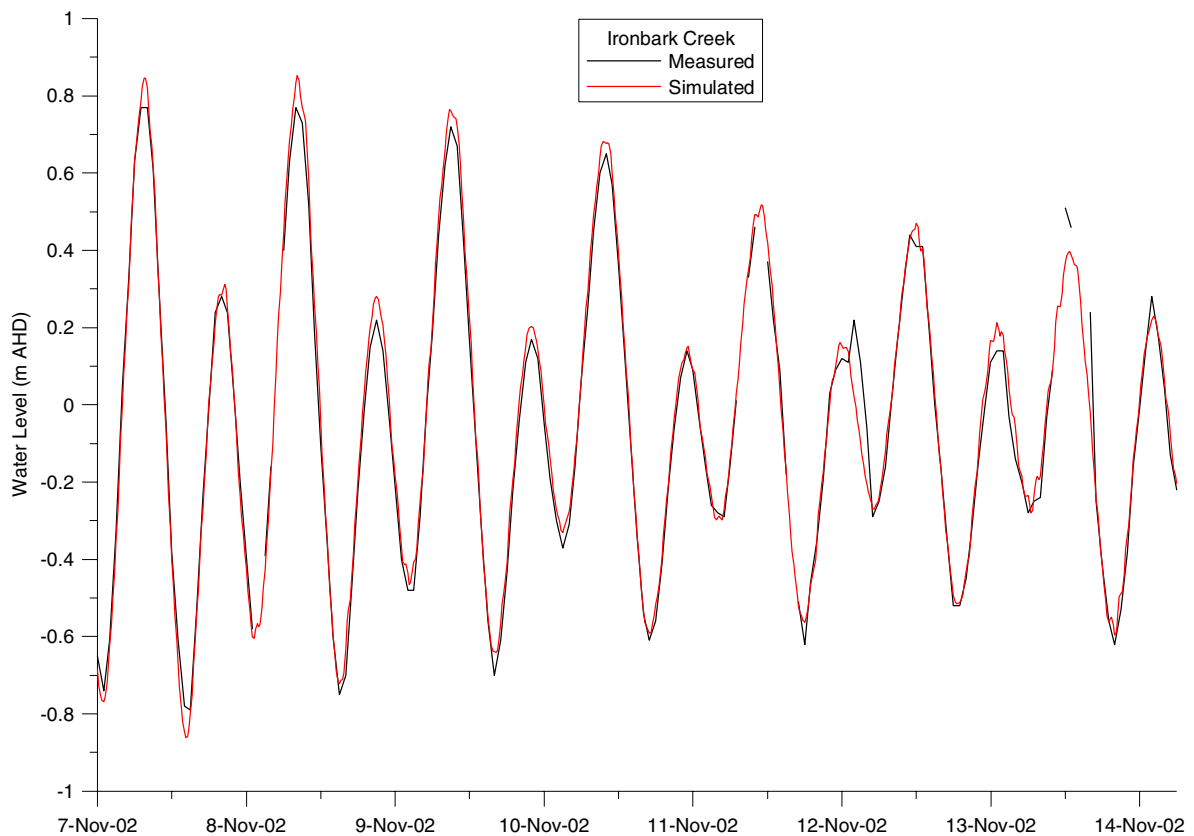


Figure B25: Simulated and observed Ironbark Ck water level for day 22-29 of calibration

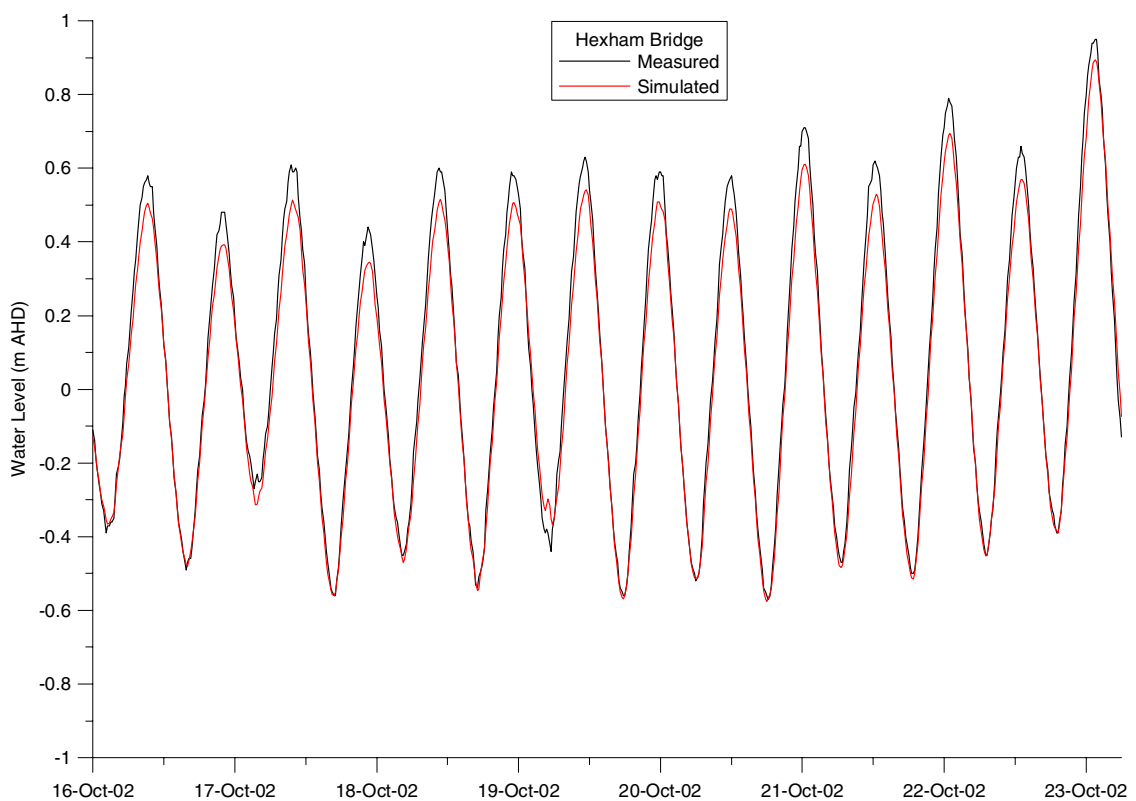


Figure B26: Simulated and observed Hexham water level for day 1-7 of calibration

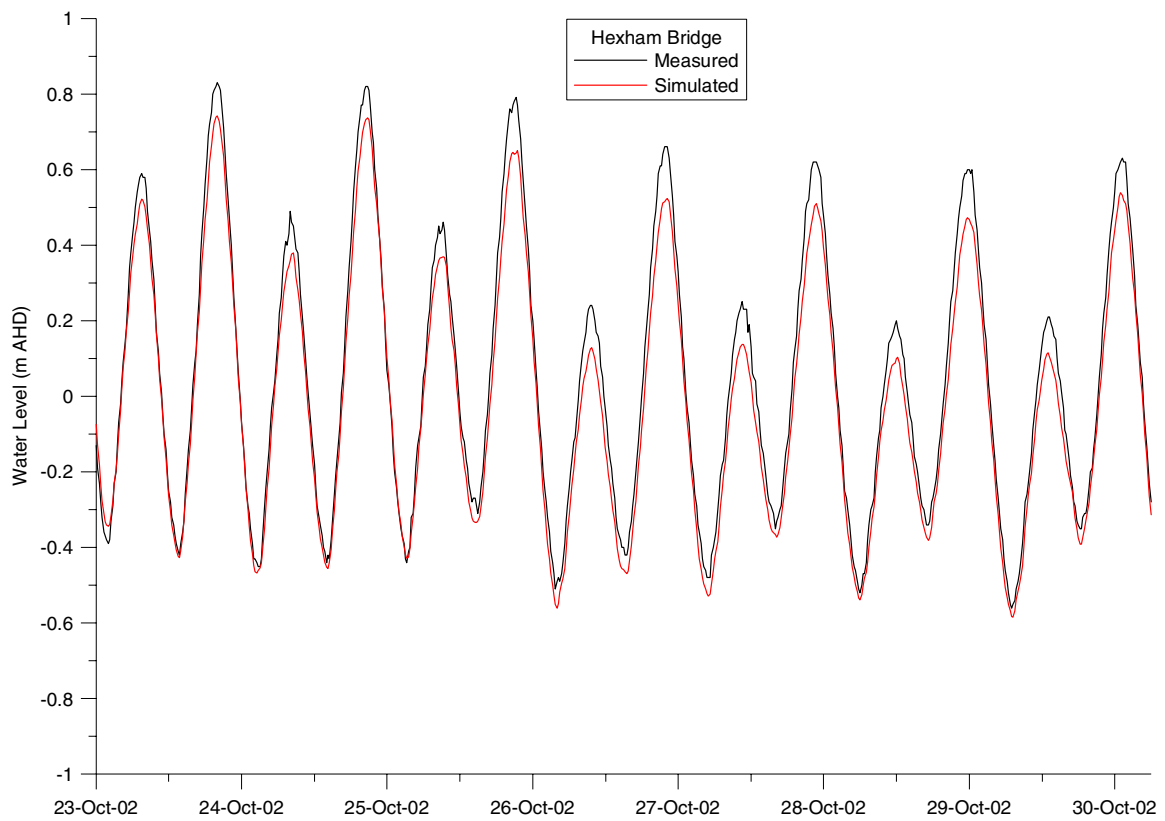


Figure B27: Simulated and observed Hexham water level for day 7-15 of calibration

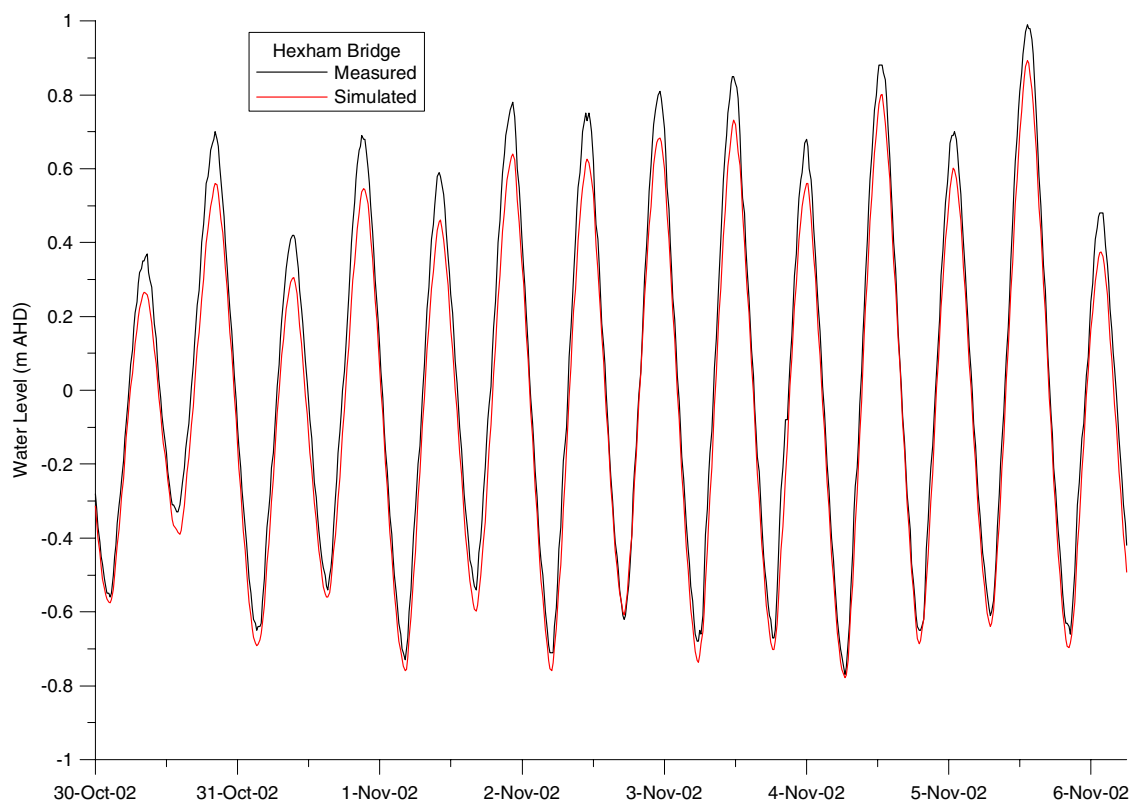


Figure B28: Simulated and observed Hexham water level for day 15-22 of calibration

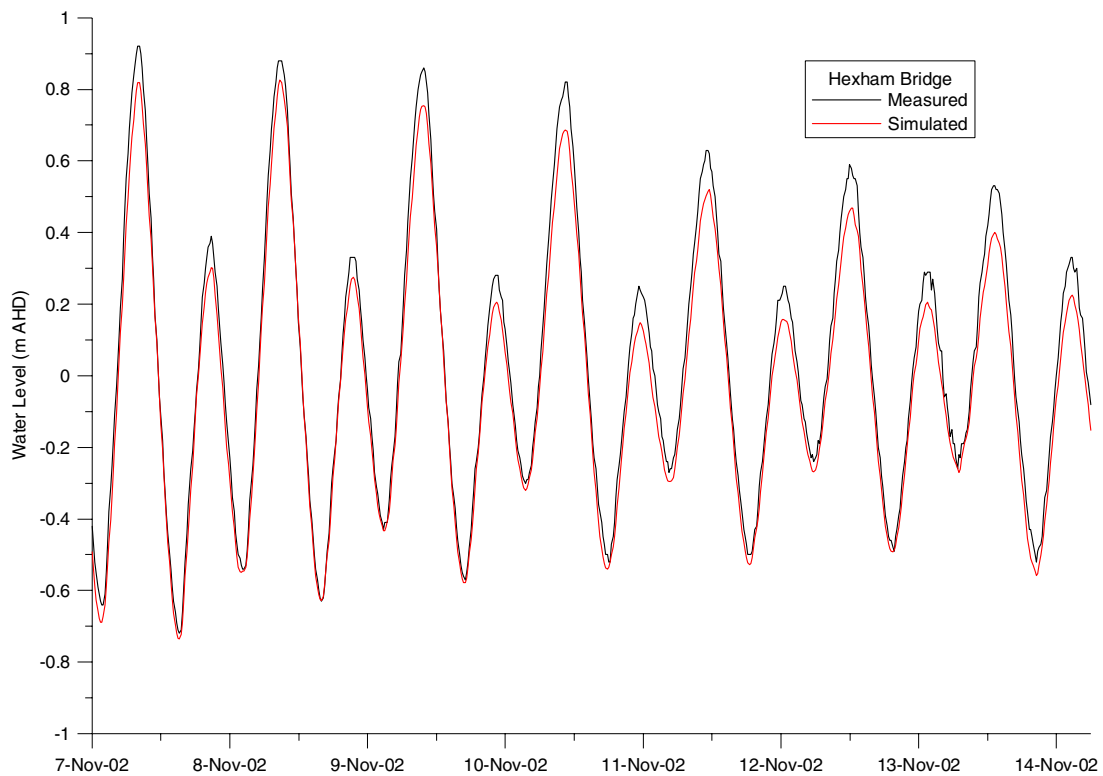


Figure B29: Simulated and observed Hexham water level for day 22-29 of calibration

A comparison of the measured and simulated tidal planes at the Pilot Station, Stockton Bridge, Ironbark Creek and Hexham Bridge is given in **Table B5**. This information is also presented graphically with distance upstream from the entrance in **Figure B30**.

Table B5: Measured and simulated tidal planes in lower Hunter estuary during calibration

Tidal Plane	Pilot Station		Stockton Bridge		Ironbark Creek		Hexham Bridge	
	Measured	Simulated	Measured	Simulated	Measured	Simulated	Measured	Simulated
HHWSS	0.963	0.970	0.999	0.968	0.943	0.950	1.011	0.899
MHWS	0.601	0.606	0.629	0.609	0.589	0.595	0.654	0.559
MHW	0.468	0.473	0.495	0.477	0.476	0.473	0.543	0.451
MHWN	0.335	0.339	0.361	0.345	0.362	0.350	0.432	0.343
MSL	-0.047	-0.047	-0.044	-0.048	-0.017	-0.027	0.048	-0.011
MLWN	-0.430	-0.432	-0.45	-0.440	-0.396	-0.405	-0.336	-0.365
MLW	-0.562	-0.566	-0.584	-0.572	-0.509	-0.527	-0.446	-0.473
MLWS	-0.695	-0.700	-0.718	-0.704	-0.623	-0.649	-0.557	-0.582
ISLW	-0.954	-0.960	-0.982	-0.961	-0.876	-0.903	-0.812	-0.824
MHWS-MLWS	1.296	1.306	1.346	1.313	1.212	1.244	1.211	1.141
MHWN-MLWN	0.765	0.771	0.811	0.785	0.757	0.755	0.768	0.708
MHW-MLW	1.030	1.039	1.079	1.049	0.985	1.000	0.989	0.924
HHWSS-ISLW	1.918	1.930	1.981	1.929	1.818	1.853	1.824	1.723

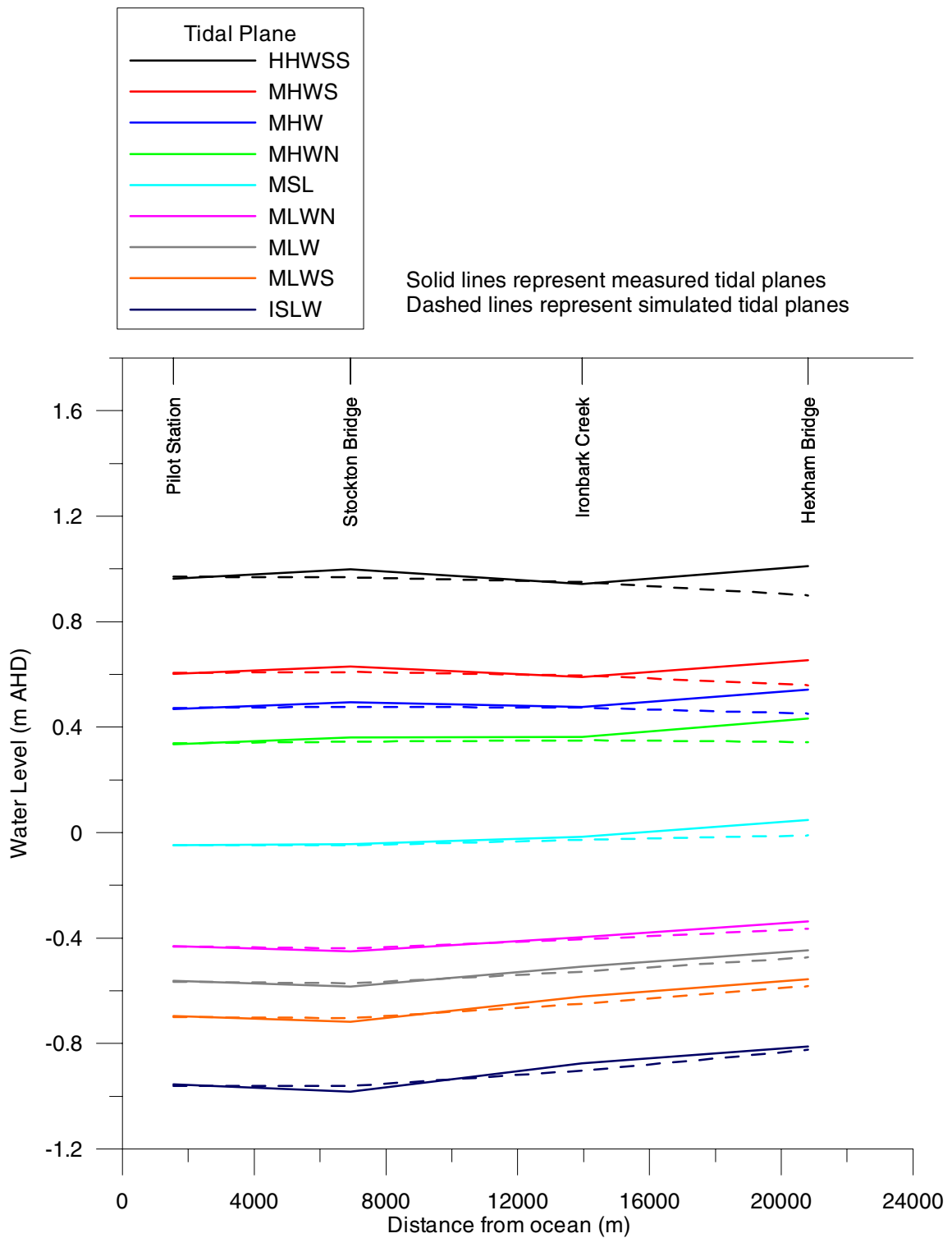


Figure B30: Measured and simulated tidal planes in lower Hunter estuary during calibration, versus distance upstream from the entrance

Based on Section B4.1, statistical measures of the comparison between the calibration simulation output and observed water level at the Pilot Station, Stockton Bridge, Ironbark Creek and Hexham Bridge are given in **Table B6**.

Table B6: Statistical comparison of simulated and observed water levels in lower Hunter estuary during calibration period

Statistic	Pilot Station	Stockton Bridge	Ironbark Creek	Hexham Bridge
Absolute Maximum Error (m)	0.044	0.169	0.262	0.179
RMS Error (m)	0.010	0.022	0.037	0.070
Mean Error (m)	0.000	-0.003	-0.010	-0.058
Correlation Coefficient, ρ	1.000	0.999	0.996	0.996
Theil's Inequality Coefficient, U (m)	0.012	0.026	0.047	0.092
Theil's Inequality Coefficient, U (%)	1.2	2.6	4.7	9.2
Bias Proportion, U_M	0.002	0.017	0.072	0.689
Variance Proportion, U_S	0.102	0.254	0.026	0.101
Covariance Proportion, U_C	0.896	0.729	0.902	0.210

It is evident that there was an excellent fit between the simulated and measured water levels at the Pilot Station, Stockton Bridge and Ironbark Creek. The correlation coefficient was very close to 1 and Theil's Inequality Coefficient was less than 5% at these sites, with the proportions of inequality indicating that the simulation error was essentially unsystematic.

There was an excellent fit between the simulated and measured water levels at Hexham Bridge, except at the peaks, although the correlation coefficient was still a very acceptable 0.996. The simulated peaks were consistently lower than those measured, reflected in the simulated tidal planes for MSL, MHW, MHWS and HHWSS being lower than those recorded at Hexham, and the bias proportion for Hexham being relatively large. It is not clear what would have caused this result, especially given the consistency of the simulated and observed water levels at the nearby Ironbark Creek. Possible causes may be:

- Limitations of measuring equipment.
- Coarsely defined bathymetry upstream of Hexham Bridge. Widely spaced cross sectional surveys were used to define bed elevations in this reach, and it was found that model results were sensitive to the levels chosen. This sensitivity may partly be due to the formation of standing waves in the Williams River, which is dependent on bathymetry. As noted by Sanderson et al (2002), the weir at Seaham acts as a reflective barrier, and may lead to the generation of standing waves in the river.
- Non-representative tidal limits. The upstream limits of the model were based on the observations of MHL (2002), but the accuracy of these limits, and applicability to the calibration period, is not known. It was found that the model results were sensitive to the limits chosen.
- Variance of the surveyed bathymetry to the bed conditions existing at the time of the calibration. For example, the North Arm bathymetry was derived from a survey in 1997. It is possible that some sedimentation has occurred since that time. Also, given the regular maintenance dredging, bed elevations in the port area may vary depending on the status of this dredging and deposited sediment, although fluctuations in bed elevations (relative to the mean depth) would be small.
- Coarsely defined bathymetry in Fullerton Cove and the South Arm upstream of Tourle St Bridge. The model bed elevations in these areas were based on AUS Charts, which provide relatively coarse soundings. Some areas in the AUS Charts do not appear to have altered in the 20 last years with any new survey information, although this cannot be confirmed.
- Assumed bathymetry of mangrove and saltmarsh areas.

B4.3 VERIFICATION

The 29-day period from 25 June 2002 to 24 July 2002 was chosen for verification. This was a suitable period for simulation as there were few days of rainfall during this time.

The total rainfall that fell at nine sites throughout the Hunter catchment during the verification period is shown in **Table B7**. There was complete data coverage at these sites during this period.

Table B7: Rainfall during verification period, 25 June 2002 to 24 July 2002

Site	Rainfall (mm)
Murrurundi Post Office	4
Newcastle Nobbys Signal Station	9
Williamstown RAAF	2.4
Chichester Dam	1.4
Muswellbrook (Lindisfarne)	0.0
Total	0.2
Singleton Water Board	0.0
Maitland Visitors Centre	0.0
Ulan Post Office	11.8

As confirmation of the lack of rainfall in the calibration period, the flows in the Hunter River at Greta, Williams River at Glen Martin, and Paterson River at Gostwyck that occurred during the calibration simulation (and for 4 days prior) are shown in **Figure B31**.

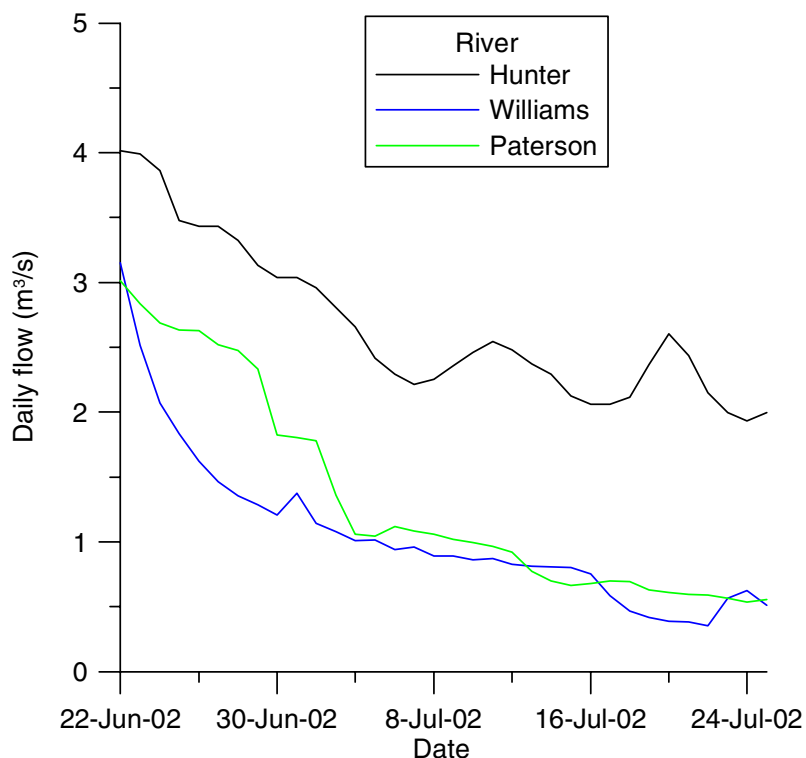


Figure B31: Flows in Hunter, Williams and Paterson River before and during verification period

The Pilot Station water level used as the downstream boundary condition for the verification simulation is shown in **Figure B32**. The Pilot Station water level is also shown along with the water levels recorded at Stockton Bridge and Hexham Bridge during this period, in **Figure B33** to **Figure B36** in 7.25 day blocks. Note that no data was available for Ironbark Creek during the verification period. The correction advised by Davidson (2003) again was applied to the Hexham data as per the calibration period.

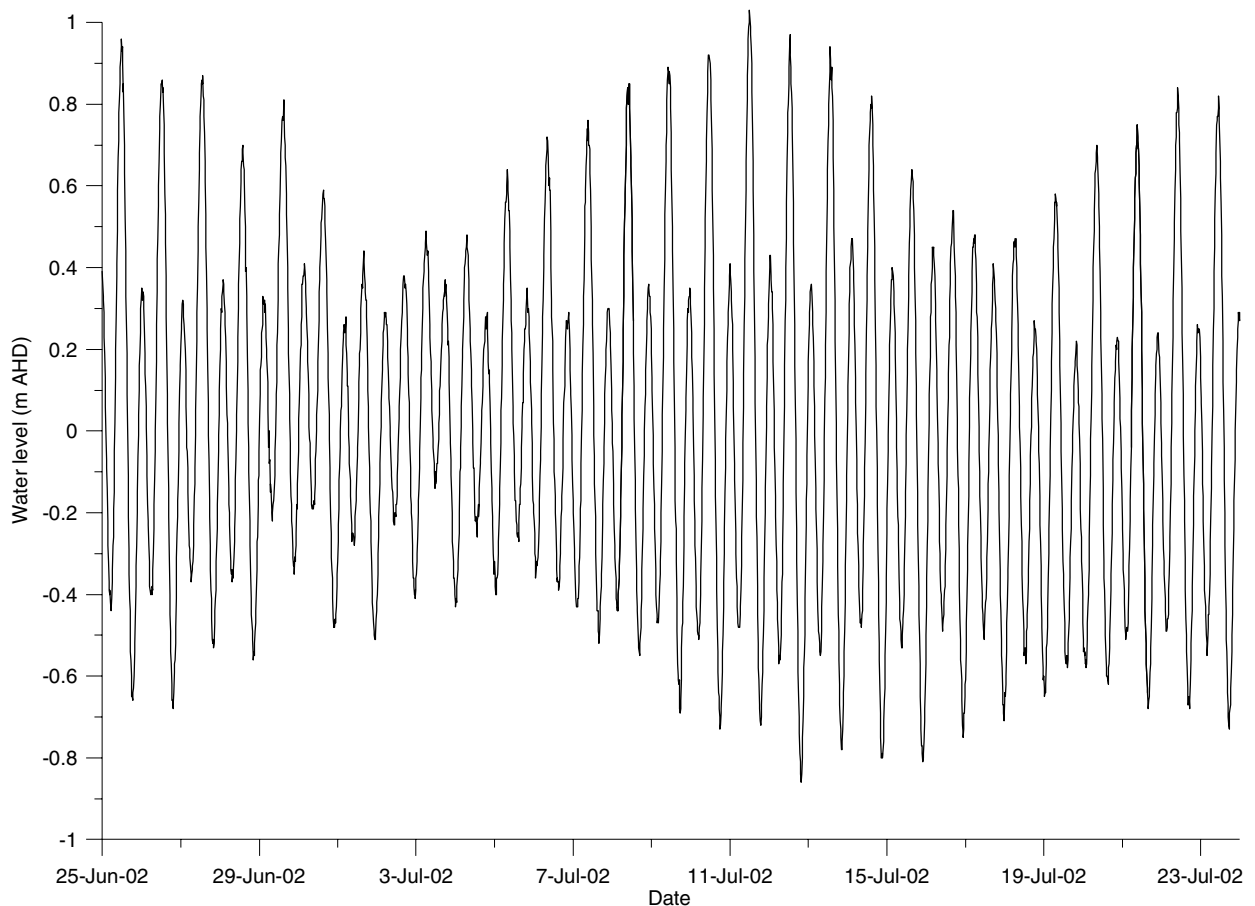


Figure B32: Downstream (Pilot Station) water level for verification simulation

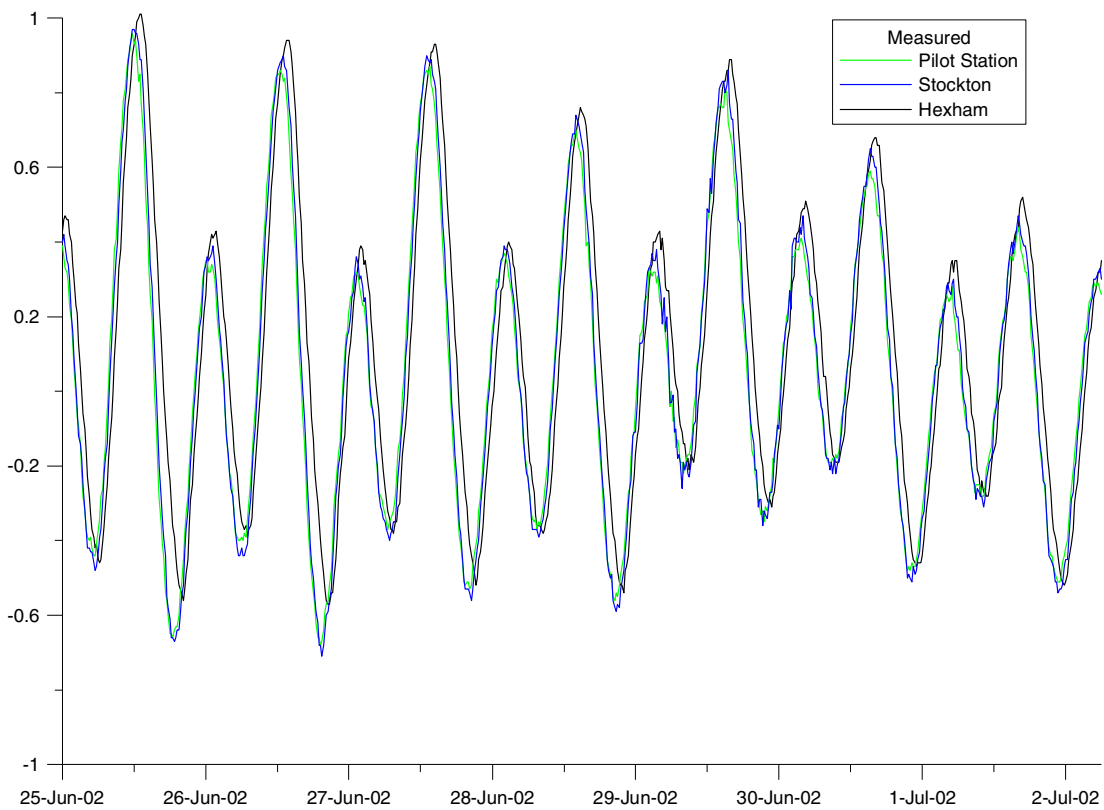


Figure B33: Water levels measured in lower Hunter estuary for day 1-7 of verification

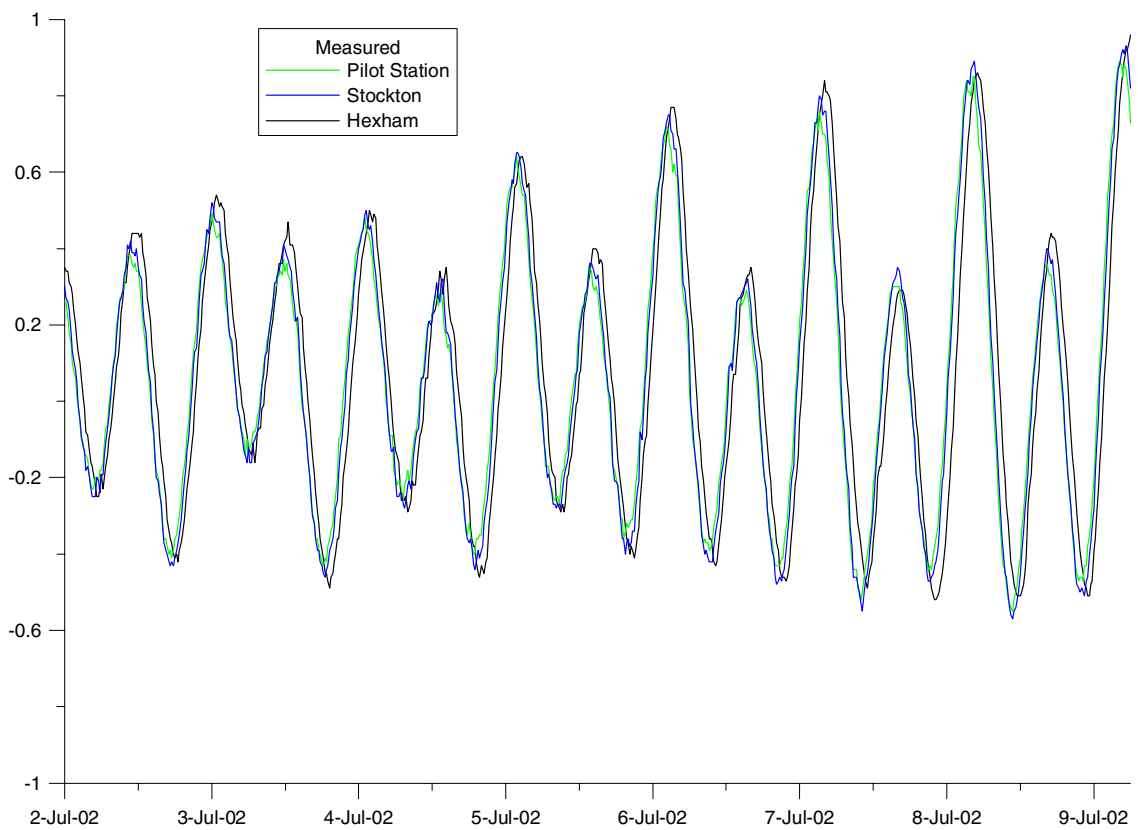


Figure B34: Water levels measured in lower Hunter estuary for day 7-15 of verification

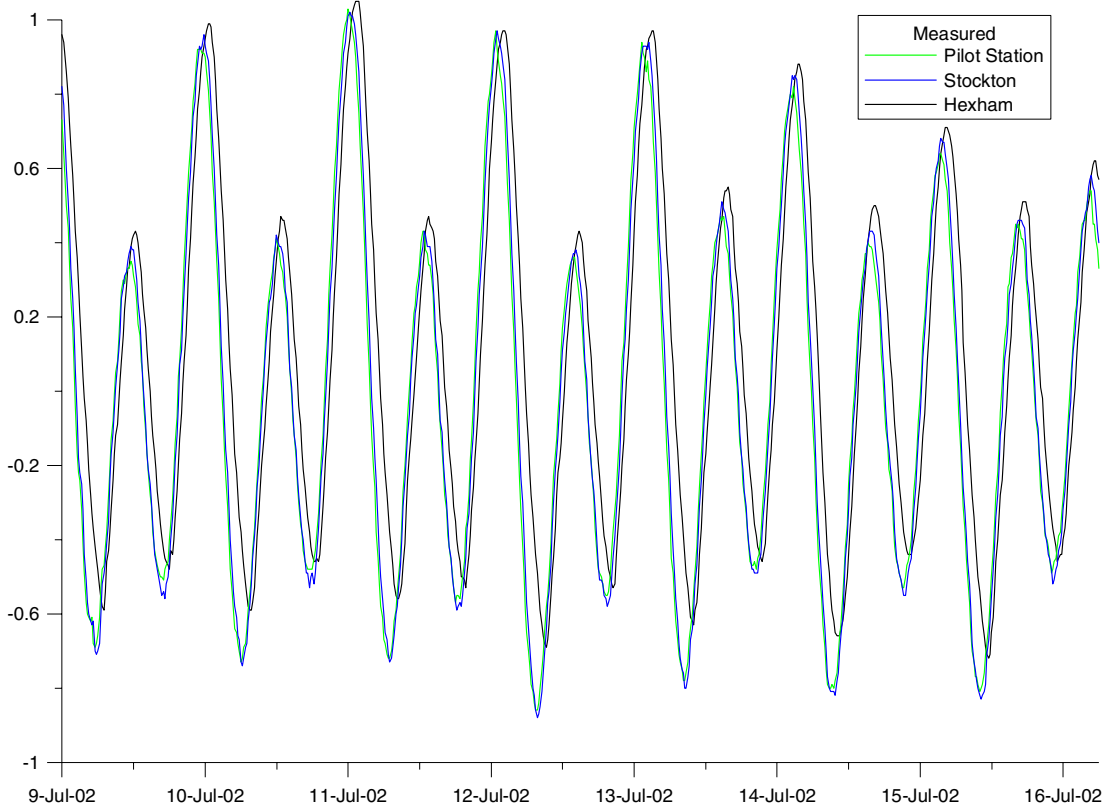


Figure B35: Water levels measured in lower Hunter estuary for day 15-22 of verification

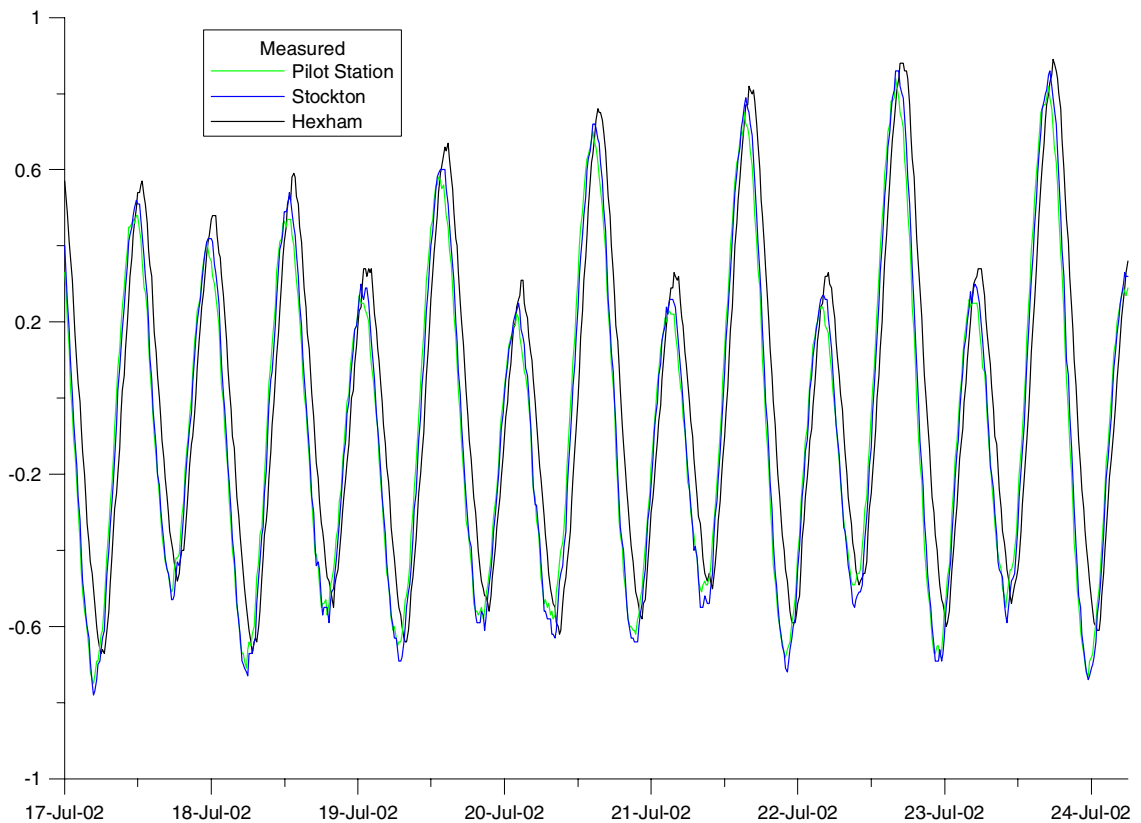


Figure B36: Water levels measured in lower Hunter estuary for day 22-29 of verification

As per the calibration period, the measurements indicate that water levels at Stockton Bridge were generally slightly amplified relative to the Pilot Station. The lag in the tide moving upstream is also evident. Again, the measurements at Hexham are unusual in that high and low tide is generally higher than the two downstream stations.

A comparison of simulated and observed water levels during the verification period is given as detailed below in 7.25 day increments:

- Pilot Station, **Figure B37 to Figure B40**;
- Stockton Bridge, **Figure B41 to Figure B44**; and,
- Hexham Bridge, **Figure B45 to Figure B48**.

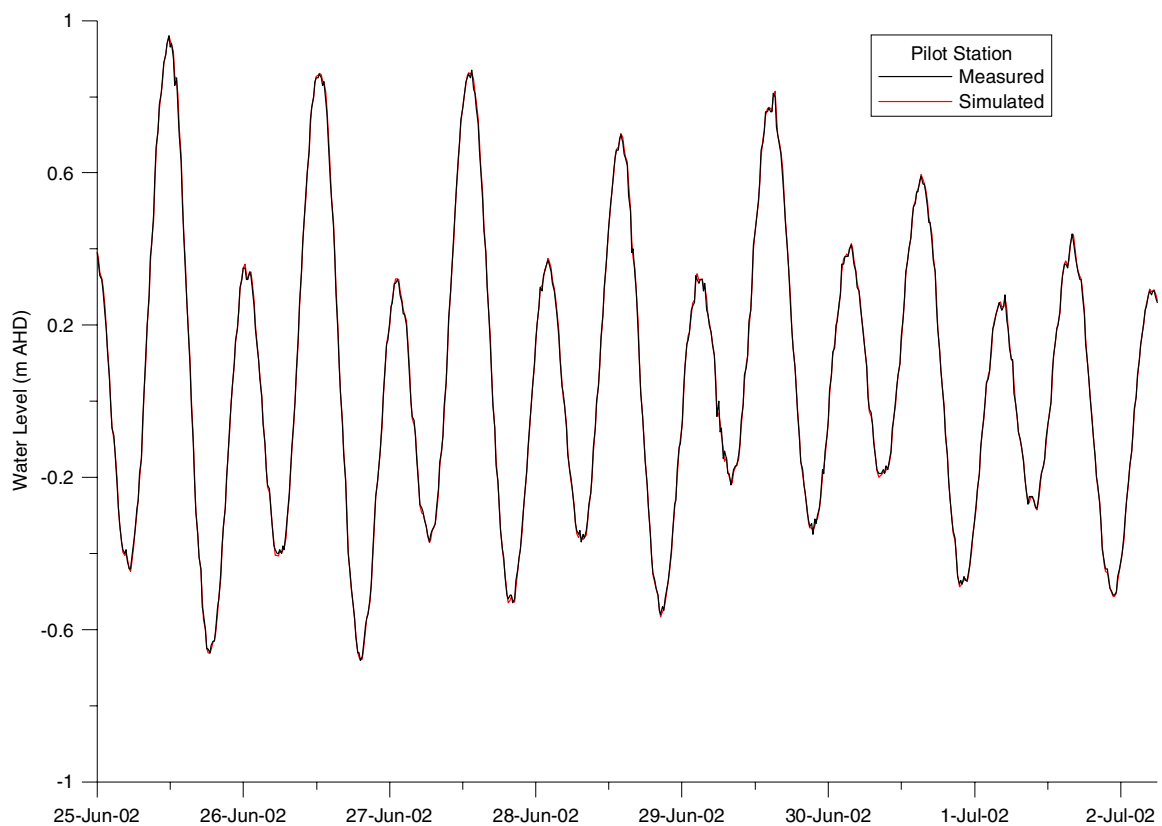


Figure B37: Simulated and observed Pilot Station water level for day 1-7 of verification

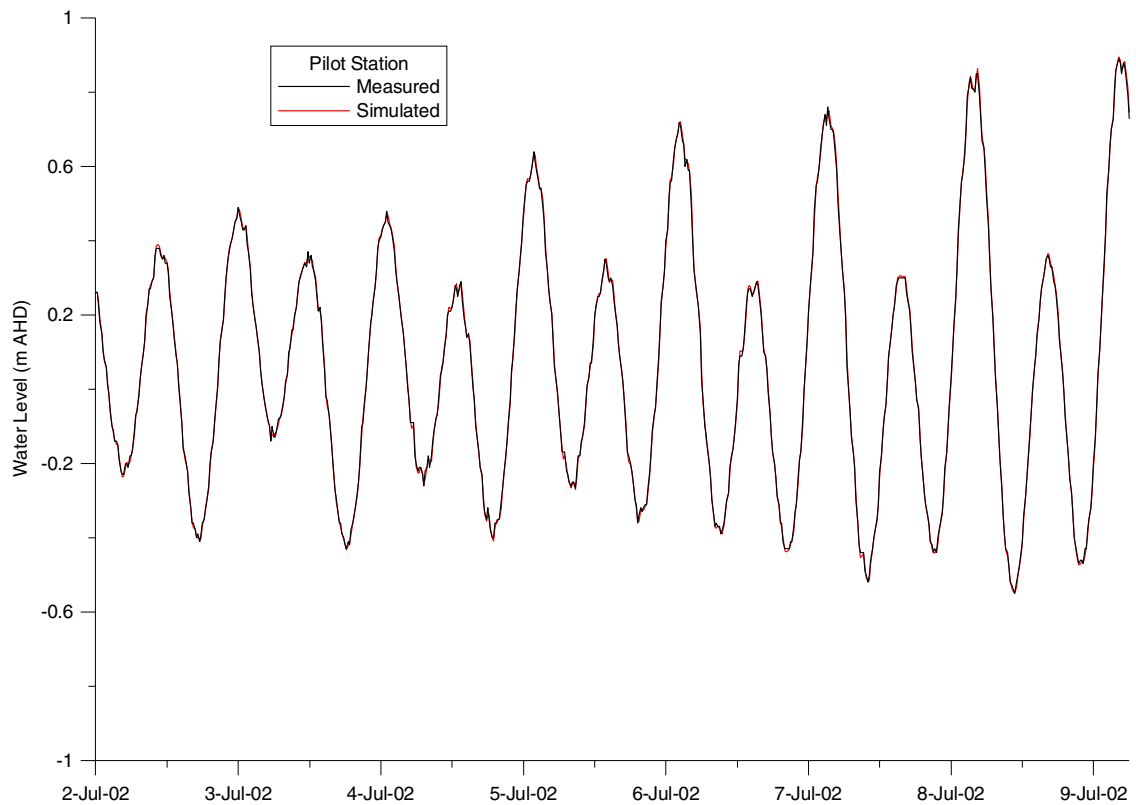


Figure B38: Simulated and observed Pilot Station water level for day 7-15 of verification

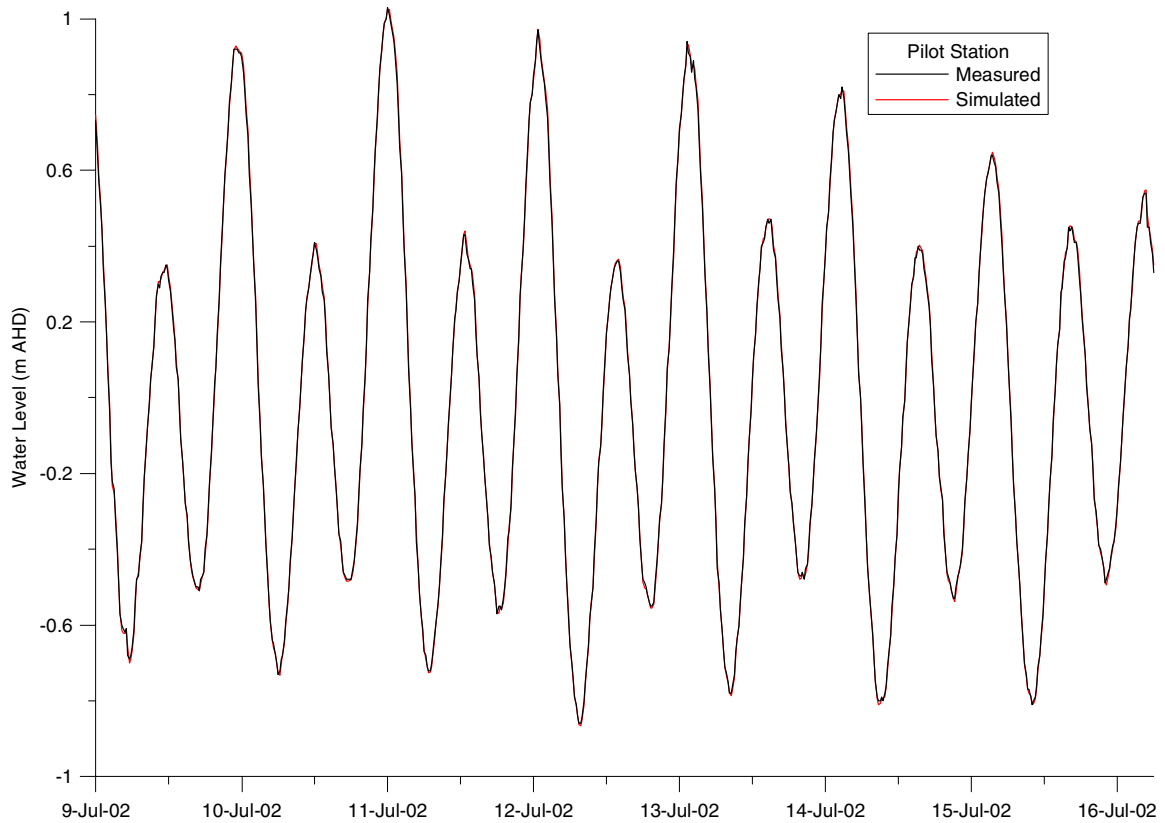


Figure B39: Simulated and observed Pilot Station water level for day 15-22 of verification

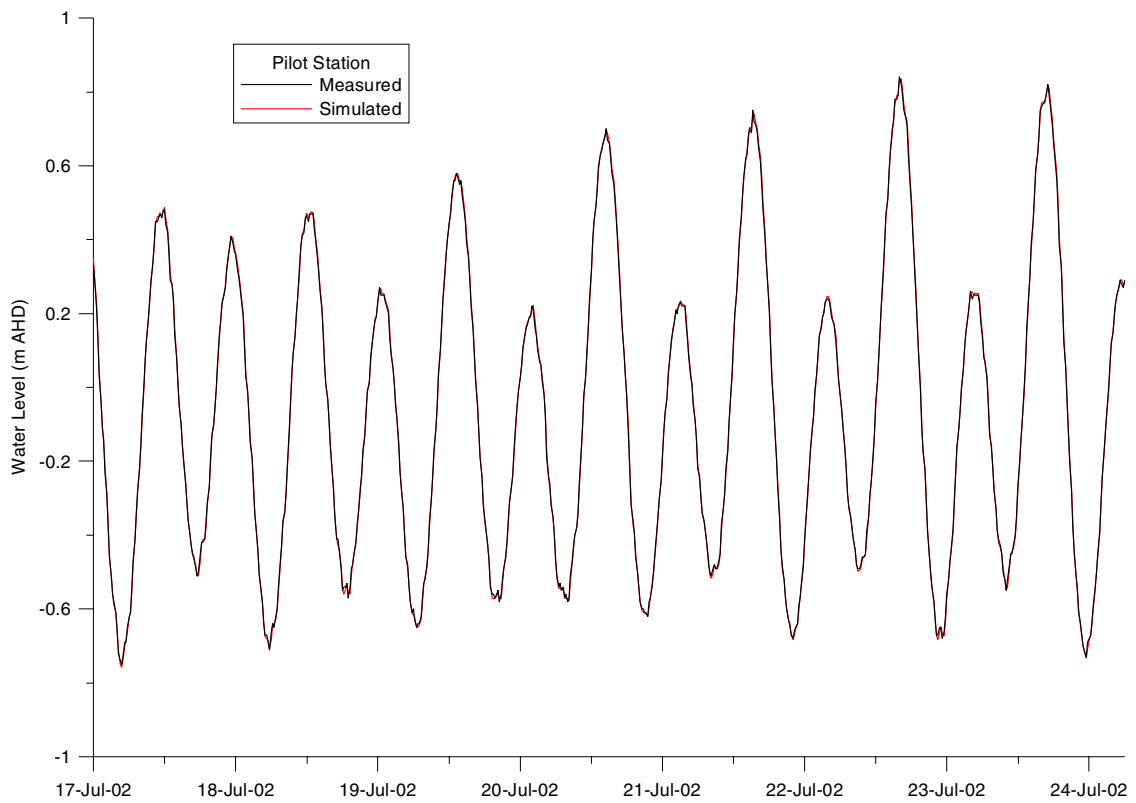


Figure B40: Simulated and observed Pilot Station water level for day 22-29 of verification

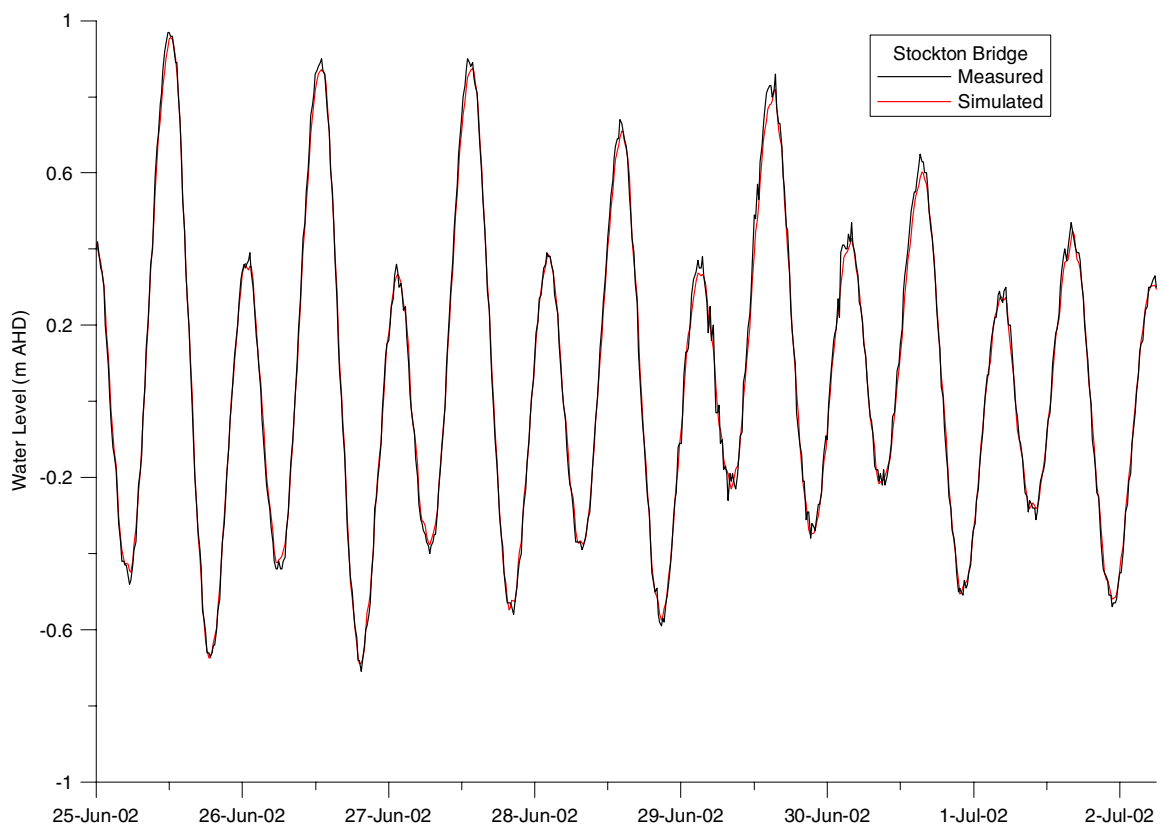


Figure B41: Simulated and observed Stockton water level for day 1-7 of verification

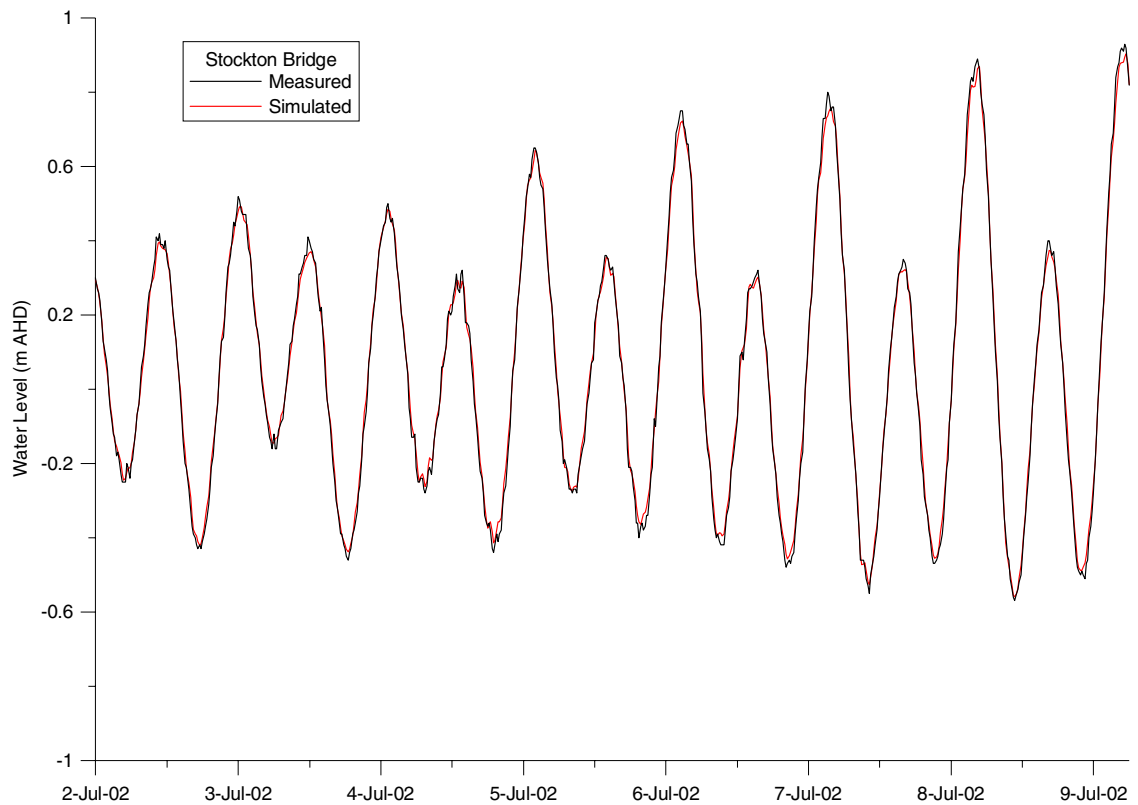


Figure B42: Simulated and observed Stockton water level for day 7-15 of verification

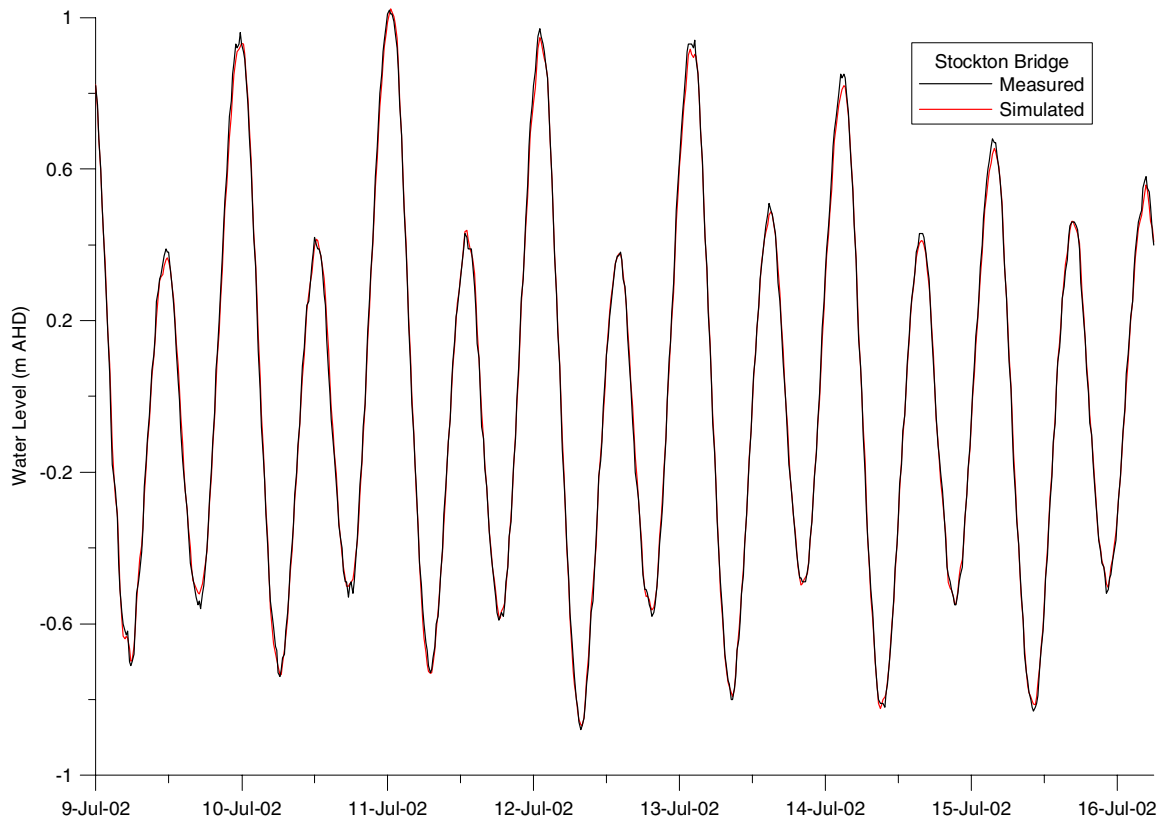


Figure B43: Simulated and observed Stockton water level for day 15-22 of verification

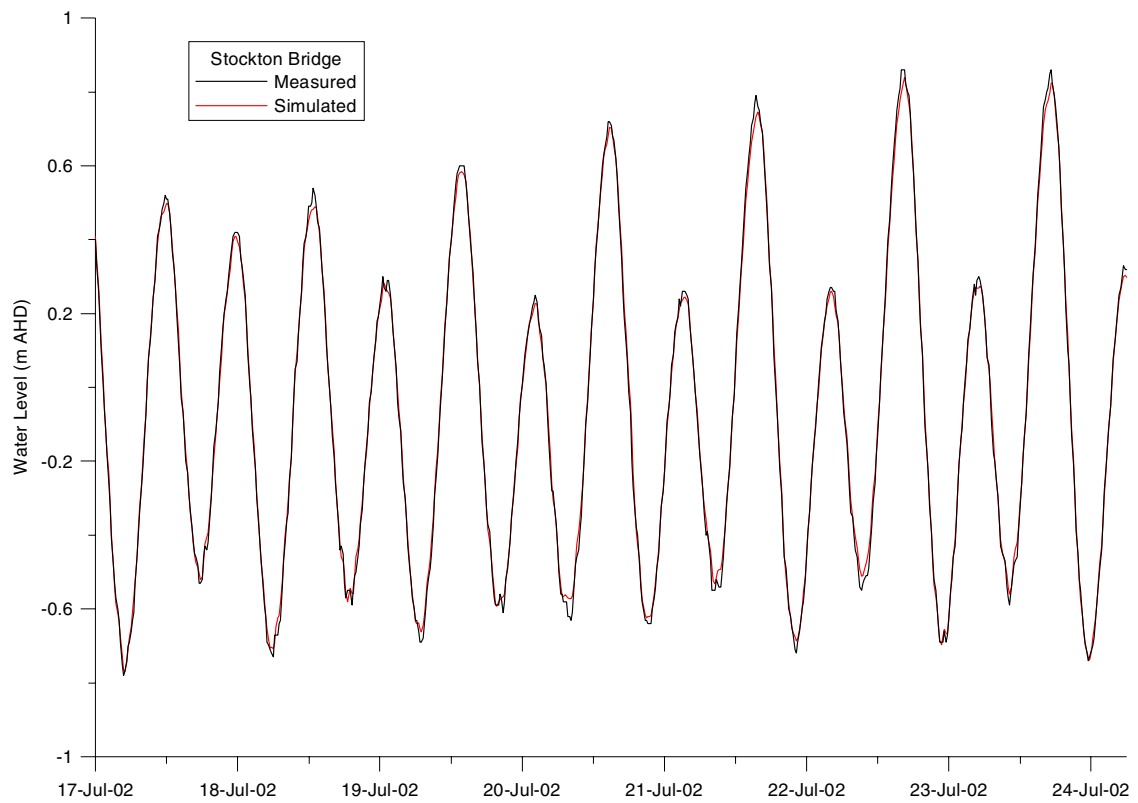


Figure B44: Simulated and observed Stockton water level for day 22-29 of verification

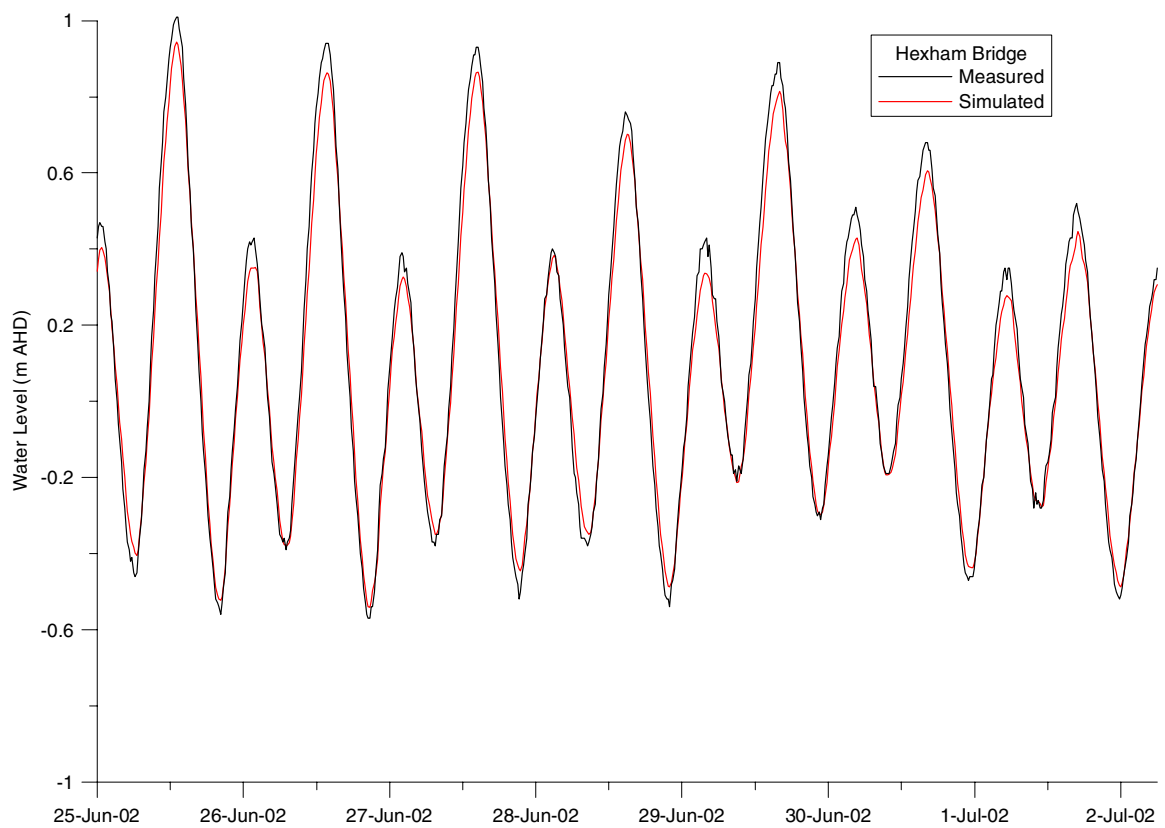


Figure B45: Simulated and observed Hexham water level for day 1-7 of verification

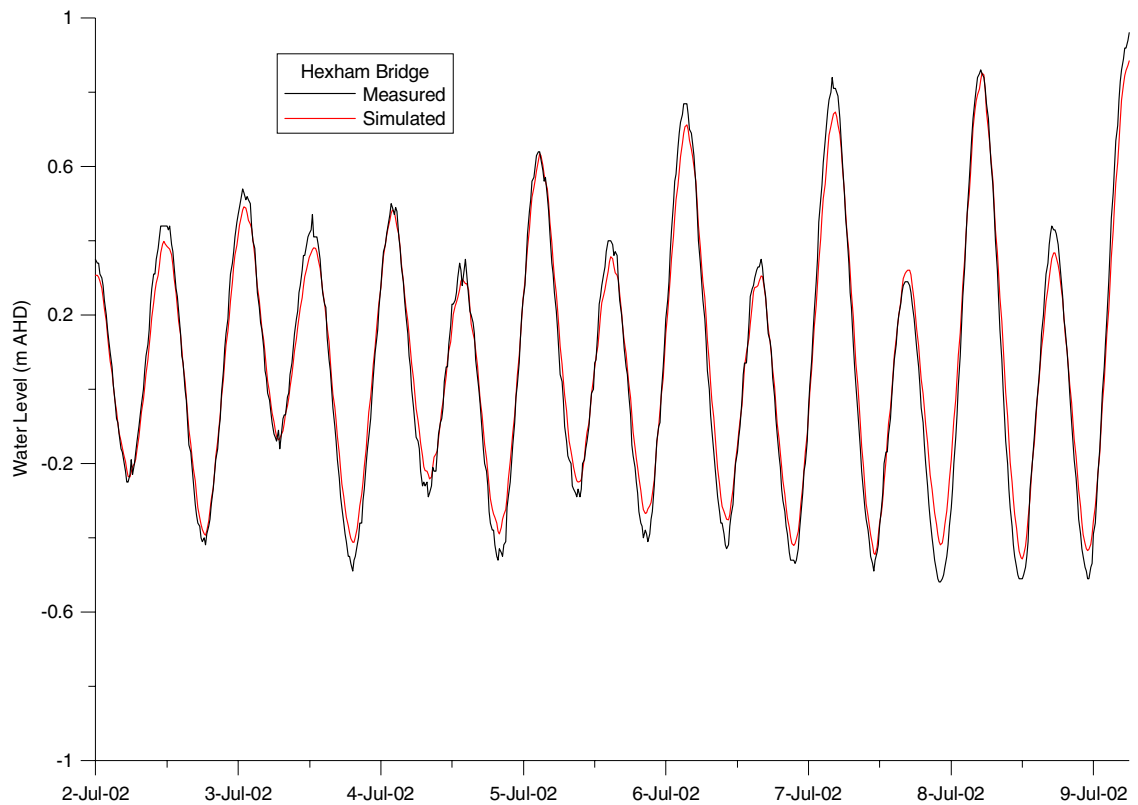


Figure B46: Simulated and observed Hexham water level for days 7-15 of verification

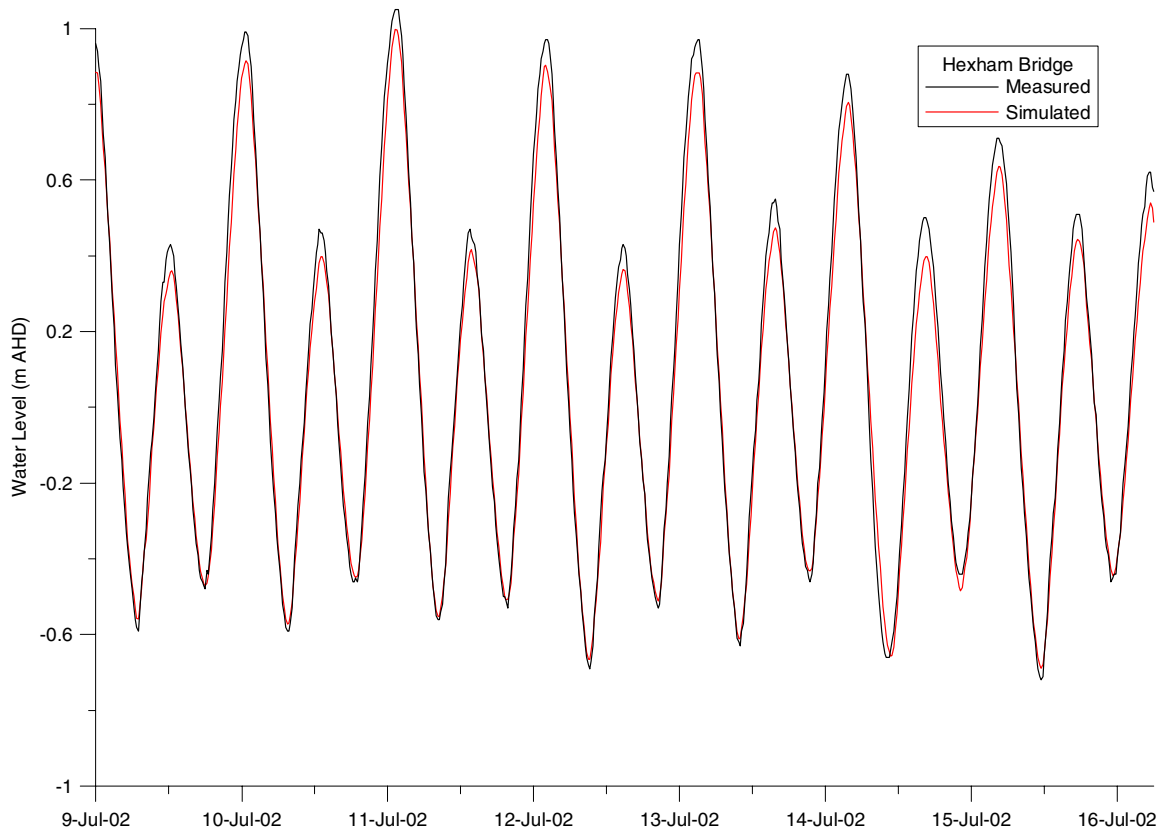


Figure B47: Simulated and observed Hexham water level for day 15-22 of verification

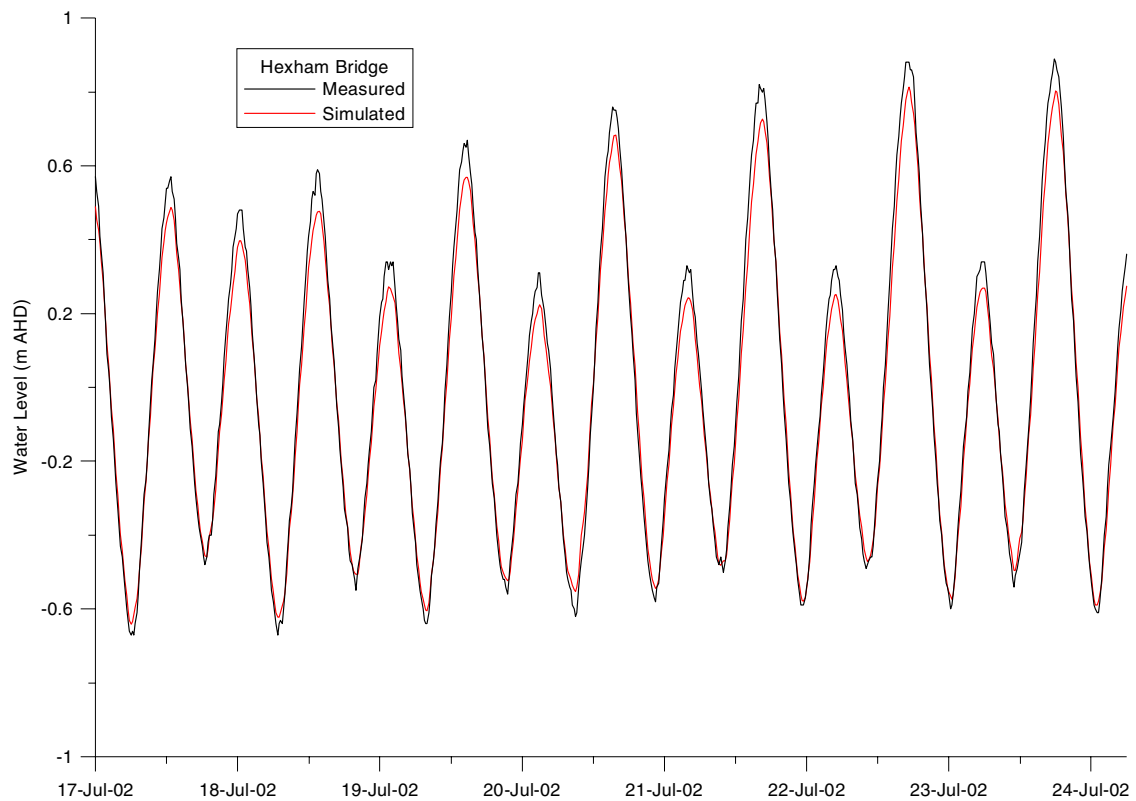


Figure B48: Simulated and observed Hexham water level for day 22-29 of verification

Based on Section B4.1, statistical measures of the comparison between the verification simulation output and observed water level at the Pilot Station, Stockton Bridge and Hexham Bridge are given in **Table B8**.

Table B8: Statistical comparison of simulated and observed water levels in lower Hunter estuary during verification period

Statistic	Pilot Station	Stockton Bridge	Hexham Bridge
Absolute Maximum Error (m)	0.036	0.102	0.144
RMS Error (m)	0.010	0.021	0.056
Mean Error (m)	0.000	0.000	-0.016
Correlation Coefficient, ρ	1.000	0.999	0.994
Theil's Inequality Coefficient, U (m)	0.012	0.026	0.071
Theil's Inequality Coefficient, U (%)	1.2	2.6	7.1
Bias Proportion, U_M	0.002	0.000	0.085
Variance Proportion, U_S	0.096	0.180	0.373
Covariance Proportion, U_C	0.902	0.820	0.541

It is evident that there was an excellent fit between the simulated and measured water levels at the Pilot Station and Stockton Bridge. The correlation coefficient was very close to 1 (1.000 and 0.999 for the two stations respectively) and Theil's Inequality Coefficient was less than 3% at these sites, with the proportions of inequality indicating that the simulation error was essentially unsystematic.

There was an excellent fit between the simulated and measured water levels at Hexham Bridge, except at the peaks, although the correlation coefficient was still a very acceptable 0.994. The simulated peaks were generally lower than those measured, reflected in the variance proportion for Hexham being relatively large.

B5 CONCLUSIONS

The RMA-2 model set up for the Hunter estuary has been shown to reasonably match observed hydrodynamics at four sites in the lower estuary, for two 29-day (calibration and verification) periods.

The model is therefore considered to be suitable for the simulation of tidal behaviour in the Hunter estuary, in the absence of rainfall generating significant freshwater flows leading to overbank inundation. This is acceptable for the purpose of assessing the impacts of the proposed South Arm dredging works under tidal conditions.

B6 REFERENCES

Burchett, MD; Pulkownik, A; Grant, C and G Macfarlane (1999), “Rehabilitation of Saline Wetlands, Olympics 2000 Site, Sydney (Australia), I: Management Strategies Based on Ecological Needs Assessment”, *Marine Pollution Bulletin*, Volume 37, Issues 8-12, December 1998, pp. 515-525

Chow, Ven Te (1959), *Open Channel Hydraulics*, McGraw-Hill Book Company

Coastal Engineering Research Center (1984), *Shore Protection Manual*, Volumes 1 and 2, Fourth Edition, Department of the Army, Waterways Experiment Station, Corps of Engineers, Vicksburg, Mississippi

Davidson, Peter (2003), Manly Hydraulics Laboratory, personal communication

Dunn, Scott L; Nielsen, Peter; Madsen, Per A and Peter Evans (2001), “Wave Setup in River Entrances”, *Coastal Engineering 2000, Conference Proceedings*, 27th International Conference on Coastal Engineering, 16-21 July, Sydney, Australia, edited by Billy L Edge, American Society of Civil Engineers, Virginia, ISBN 0784405492, Volume 4, pp. 3432-3445

Horton, PR and IP King (1999a), “Hydrodynamic and Water Quality Modelling of Darwin Harbour Using RMA”, *Water Research Laboratory Technical Report 99/03*, for the Northern Territory Department of Lands, Planning and Environment

Horton, PR and IP King (1999b), “RMA Modelling of the Disposal of Sediments from Darwin Naval Base”, *Water Research Laboratory Technical Report 99/16*, for Gutteridge Haskins and Davey, May

Horton, PR and IP King (1999c), “RMA Modelling of the Disposal of Sediments from the Outer Marina of Cullen Bay, Darwin”, *Water Research Laboratory Technical Report 99/17*, for the Northern Territory Department of Lands, Planning and Environment, June

Manly Hydraulics Laboratory [MHL] (2002), “Hunter Estuary Processes Study”, *MHL Report 1095*, Draft, December, NSW Department of Public Works and Services, DPWS Report No 01010, ISBN 0 7347 4163 4

Patterson Britton & Partners (1993), *Lower Hunter Flood Mitigation Scheme Levee Bank Restoration Project: Hydrodynamic Parameters and River Bed Scour Potential*, July, for the Hunter Catchment Management Trust, including Corrigendum

Patterson Britton & Partners (1994), *Hunter Valley Flood Mitigation: Detailed Bend Investigation, Site P20 (Woodville)*, in association with Resource Management Associates, September, for the Hunter Catchment Management Trust, Job 1690, Report 1079

Patterson Britton & Partners (1995a), *Hunter Valley Flood Mitigation: 3D Bend Investigation, Site H21 (Green Rocks)*, in association with Resource Management Associates, January, for the Hunter Catchment Management Trust, Job 1690, Report 1128

Patterson Britton & Partners (1995b), *Hunter Valley Flood Mitigation: 3D Bend Investigation, Site H50 (McKimms Corner, Glenarvon)*, in association with Resource Management Associates, February, for the Hunter Catchment Management Trust, Job 1690, Report 1144

Patterson Britton & Partners (1999a), *Newcastle Harbour Environmental Improvement Plan, Sewer System and Environmental Modelling*, Issue No. 1, October, for Hunter Water Corporation, rp3300nh-dmc991008-HWC-NH-EIP.doc

Patterson Britton & Partners (1999b), *Riverside Park Revetment Reconstruction, Raymond Terrace, Concept Design Report*, Issue No. 2, March, for Port Stephens Council, Job 3136, Report 1967

Patterson Britton & Partners (2000), *Hunter River Bank Stabilisation Sites H1, H3, H4, H5, H8, H9, H11, H13*, Issue No. 1, March, for the Department of Public Works and Services, rp3587bmdec000228

Public Works Department [PWD] (1994), *Lower Hunter Flood Study (Green Rocks to Newcastle)*, for Newcastle City Council and Port Stephens Council, August, Report No. PWD 91077, ISBN 07305 86472

Randall, Bass (2003), Port Surveyor, Newcastle Port Corporation, personal communication

Sanderson, Dr Brian; Redden, Dr Anna and Matthew Smith (2002), *Salinity Structure in the Hunter River Estuary*, report submitted to Newcastle City Council and Manly Hydraulics Laboratory, Centre for Sustainable Use of Coasts and Catchments, University of Newcastle, January

Yang, Qi (1997), "Statistics for Evaluating Simulation Models", online at <http://hippo.mit.edu/products/mitsim/node176.html>

APPENDIX C: DEVELOPMENT OF FLOOD MODEL

TABLE OF CONTENTS

Page No.

C1	INTRODUCTION	1
C2	DEVELOPMENT OF FLOOD MODEL	2
C3	DISCHARGE PIPELINE SIMULATIONS	3
C4	CONCLUSIONS	7
C5	REFERENCES	8

LIST OF FIGURES

Page No.

FIGURE C1: FINITE ELEMENT NETWORK FOR SIMULATION OF EFFECT OF DISCHARGE PIPELINE, SHOWING LOCATION OF PROPOSED PIPELINE	3
FIGURE C2: VARIATION IN PEAK WATER LEVEL (M) DUE TO 900MM PIPELINE (1% AEP FLOOD)	4
FIGURE C3: VARIATION IN PEAK WATER LEVEL (M) DUE TO 900MM PIPELINE (2% AEP FLOOD)	4
FIGURE C4: VARIATION IN PEAK WATER LEVEL (M) DUE TO 900MM PIPELINE (5% AEP FLOOD)	5
FIGURE C5: VARIATION IN PEAK WATER LEVEL (M) DUE TO 900MM PIPELINE (10% AEP FLOOD)	5

C1 INTRODUCTION

A flood model was developed to enable assessment of various aspects of the proposed South Arm Dredging project on flood behaviour of the region, namely the:

- temporary sheet pile wall (to contain contaminated sediments during dredging operations);
- temporary discharge pipeline transferring dredged sediments to Tomago over Kooragang Island; and,
- the ultimate dredged profile.

Results and discussions on these aspects have been provided in the main report. In this Appendix, additional supplementary information is given.

Background information on the development of the flood model is provided in Section C2.

In Section C3, additional information on the modelling undertaken of the discharge pipeline is provided. Note that the pipeline impacts were assessed based on an assumed potential westerly corridor route to Tomago, and are thus only preliminary results. The exact route was not determined at the time of completion of this report.

Conclusions are given in Section C4 and references are listed in Section C5.

C2 DEVELOPMENT OF FLOOD MODEL

The flood model used in this investigation had been developed as part of previous studies of flood behaviour in the Hunter region, namely Patterson Britton & Partners (2001a, 2001b, 2002, 2003a, 2003b). These studies were all undertaken for the Premiers Department.

As described in Patterson Britton & Partners (2001a), the flood model was originally developed covering both arms of the Hunter River from Hexham Bridge to the entrance together with Kooragang Island, Tomago and Fullerton Cove. Due to subsequent revisions and additional requirements this initial model was then expanded upstream to Purgatory Creek, across Hexham Swamp and up to Raymond Terrace.

A detailed spot height survey undertaken by the Department of Public Works and Services for previous Kooragang Island and Hexham Swamp studies was used in development of the model floodplain elevations. Flood hydrographs were derived from PWD (1994) as an upstream boundary condition and a 1.2m AHD water level was used as a downstream boundary condition¹. The PWD (1994) study found that tidal variation had little effect on upstream flood levels for large floods.

¹ The PWD (1994) study reports that the most likely Port Newcastle flood level for the 1% AEP event is 1.2m AHD.

C3 DISCHARGE PIPELINE SIMULATIONS

As discussed in the main report, the effect on flooding of a possible pipeline delivering dredged sand to Tomago was assessed.

The model network used for simulation of the discharge pipeline is shown in **Figure C1**.

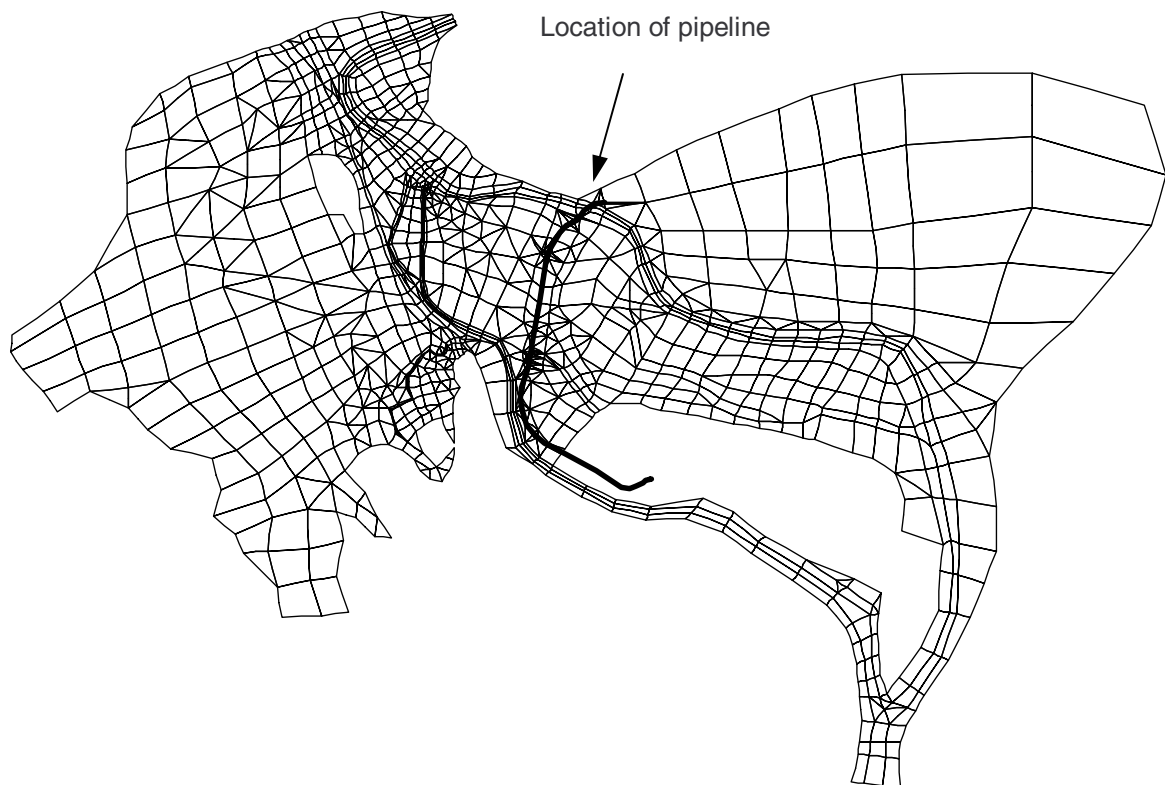


Figure C1: Finite element network for simulation of effect of discharge pipeline, showing location of proposed pipeline

Contours of increases in peak water level due to the pipeline were presented in the main report for the 700mm diameter pipe. The results for the 900mm pipeline are shown below in **Figure C2** to **Figure C5** for the 1%, 2%, 5% and 10% AEP events respectively. Note that positive variations represent increases in water level due to the pipeline.

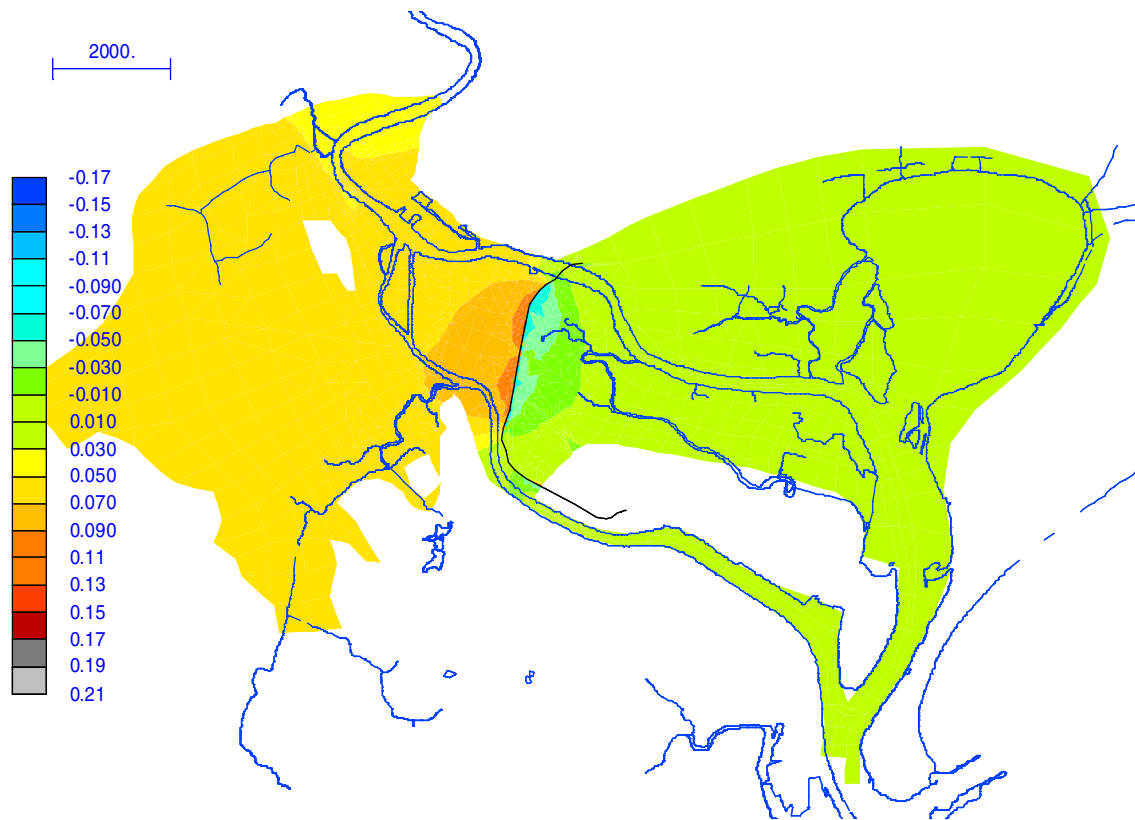


Figure C2: Variation in peak water level (m) due to 900mm pipeline (1% AEP flood)

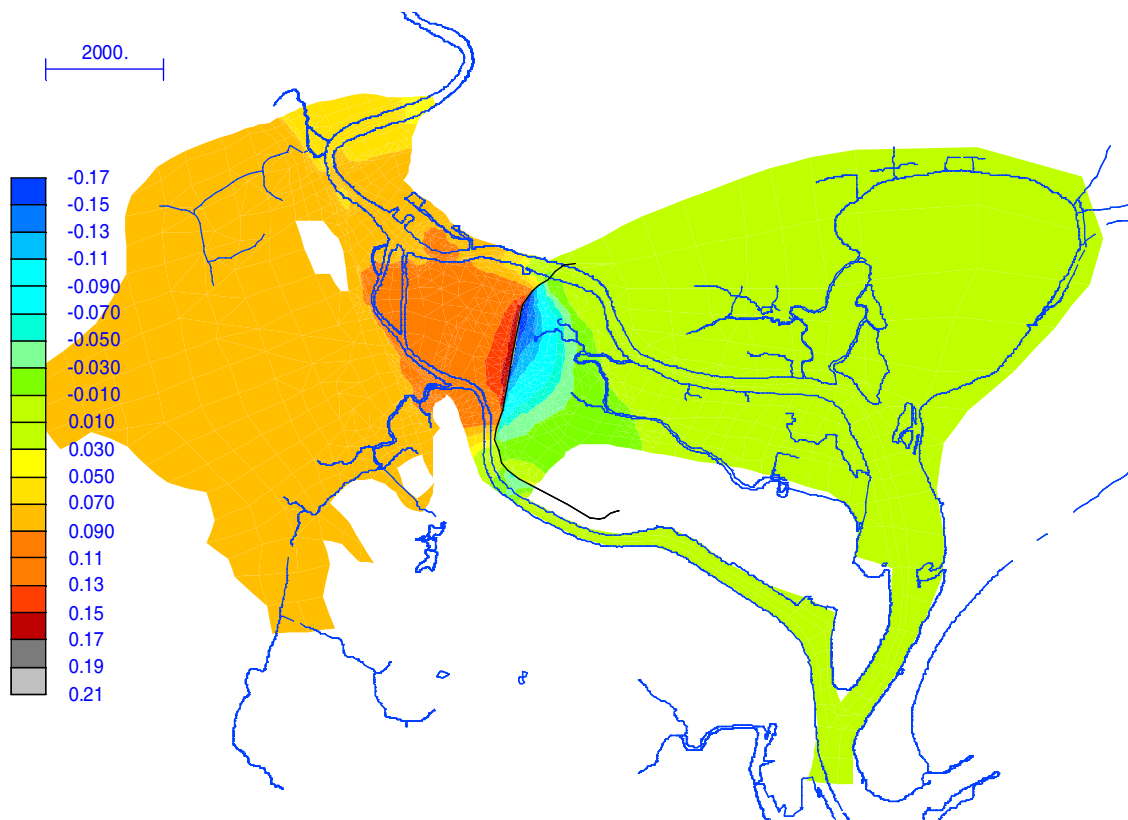


Figure C3: Variation in peak water level (m) due to 900mm pipeline (2% AEP flood)

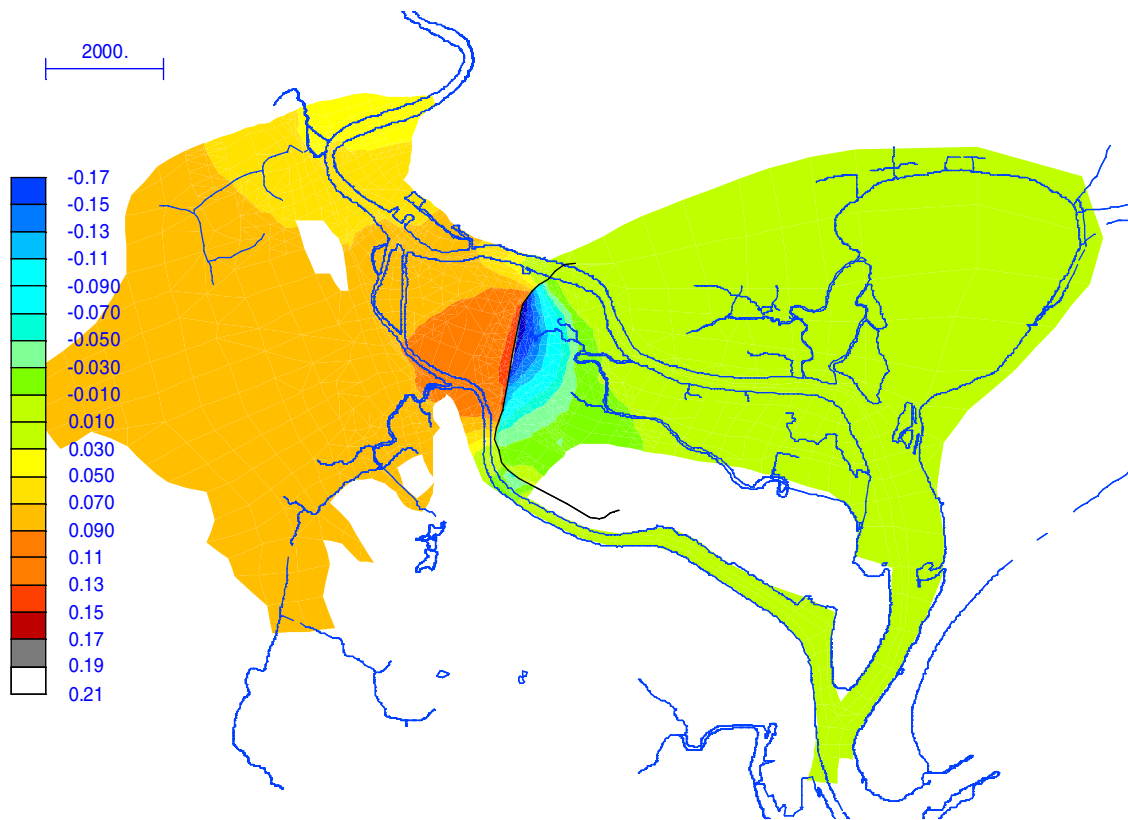


Figure C4: Variation in peak water level (m) due to 900mm pipeline (5% AEP flood)

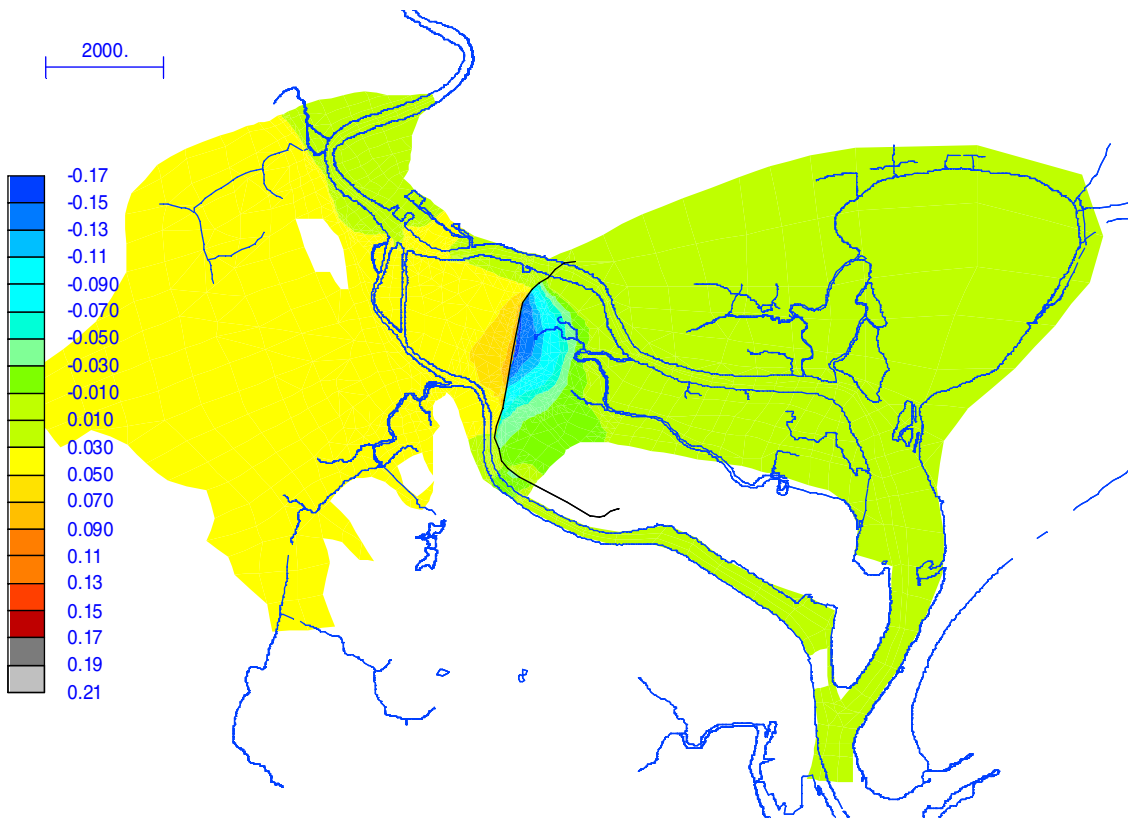


Figure C5: Variation in peak water level (m) due to 900mm pipeline (10% AEP flood)

It is evident that the largest increases in peak water level would be localised to immediately upstream of the pipeline. In the broad Beresfield, Hexham and Hexham Swamp area, increases in water level were up to about 90mm over all design events, while at Tomago and between Hexham and Sandgate the maximum increase was about 110mm. For the 1% AEP event, maximum increases at these locations were about 70mm and 90mm respectively.

C4 CONCLUSIONS

A flood model was developed of the lower Hunter estuary based on previous work by Patterson Britton & Partners.

This model was used to assess the potential effects on flooding from various aspects of the proposed South Arm Dredging project.

C5 REFERENCES

Patterson Britton & Partners (2001a), *Lower Hunter River Port Lands Developments*, Issue No. 1, January, for The Premiers Department, rp3480jmf010130finalreport

Patterson Britton & Partners (2001b), *Lower Hunter River Port Lands Development – Tomago Lands Site Flooding Assessment*, Draft, Issue No. 1, June, for The Premiers Department, rp3480cjd010522

Patterson Britton & Partners (2002), *Lower Hunter River Port Lands Development – Haul Road Assessment*, November, for The Premiers Department, lr3480cjd021108-Modelling Haul Road.doc

Patterson Britton & Partners (2003a), *Lower Hunter River Port Lands Development – Haul Road Assessment, Addendum*, February, for The Premiers Department, lr3480cjd030226-Modelling Haul Road - Addendum.doc

Patterson Britton & Partners (2003b), *Lower Hunter River Port Lands Development – Haul Road Assessment*, March, for The Premiers Department, lr3480cjd030307-Modelling Haul Road-Iss2.doc

Public Works Department [PWD] (1994), *Lower Hunter Flood Study (Green Rocks to Newcastle)*, for Newcastle City Council and Port Stephens Council, August, Report No. PWD 91077, ISBN 07305 86472

APPENDIX D: WATER QUALITY SIMULATIONS (SALINITY AND SEDIMENT TRANSPORT)

TABLE OF CONTENTS

Page No.

D1	INTRODUCTION	1
D2	SALINITY SIMULATIONS	2
D3	SEDIMENT TRANSPORT SIMULATIONS	3
	D3.1 INTRODUCTION	3
	D3.2 HUNTER ESTUARY SEDIMENT PROPERTIES	4
	D3.3 OTHER STUDIES OF SEDIMENT PROPERTIES	4
	D3.4 GENERAL MODEL PARAMETERS	5
	D3.5 COHESIVE SEDIMENT PARAMETERS	5
	D3.5.1 Settling Velocity	5
	D3.5.2 Bed Roughness	5
	D3.5.3 Deposition	6
	D3.5.4 Resistance to Erosion	8
	D3.5.5 Suspending Water	9
	D3.6 NON-COHESIVE SEDIMENT PARAMETERS	10
	D3.7 SUMMARY OF PARAMETERS AND SENSITIVITY TESTING	10
	D3.7.1 Best Estimate	10
	D3.7.2 Sensitivity Testing	11
	D3.8 RESULTS OF SIMULATIONS	11
	D3.8.1 Deposition Favourable (Cohesive Sediment)	11
	D3.8.2 Suspension Favourable (Cohesive Sediment)	14
	D3.8.3 Non Cohesive Sediment	16
	D3.8.4 Discussion	17
	D3.9 INTERPRETATION OF RESULTS	18
D4	CONCLUSIONS	19
D5	REFERENCES	20

LIST OF FIGURES

Page No.

FIGURE D1: PREDICTED DEPTHS OF DEPOSITED COHESIVE SEDIMENT (MM) AT END OF DREDGING OPERATION FOR DEPOSITION FAVOURABLE SCENARIO	12
FIGURE D2: PREDICTED DEPTHS OF DEPOSITED COHESIVE SEDIMENT (MM) AT END OF DREDGING OPERATION FOR DEPOSITION FAVOURABLE SCENARIO, IN SOUTH ARM	13
FIGURE D3: COHESIVE SUSPENDED SEDIMENT CONCENTRATIONS (MG/L) AT END OF 29 DAY TIDAL SIMULATION FOR DEPOSITION FAVOURABLE SCENARIO	13
FIGURE D4: PREDICTED DEPTHS OF DEPOSITED COHESIVE SEDIMENT (MM) AT END OF DREDGING OPERATION FOR SUSPENSION FAVOURABLE SCENARIO	14
FIGURE D5: PREDICTED DEPTHS OF DEPOSITED COHESIVE SEDIMENT (MM) AT END OF DREDGING OPERATION FOR SUSPENSION FAVOURABLE SCENARIO, IN SOUTH ARM	15
FIGURE D6: COHESIVE SUSPENDED SEDIMENT CONCENTRATIONS (MG/L) AT END OF 29 DAY TIDAL SIMULATION FOR SUSPENSION FAVOURABLE SCENARIO	15
FIGURE D7: ARBITRARY PREDICTED DEPTHS OF DEPOSITED NON-COHESIVE SEDIMENT (MM) AT END OF DREDGING OPERATION, IN SOUTH ARM	16
FIGURE D8: ARBITRARY NON-COHESIVE SUSPENDED SEDIMENT CONCENTRATIONS (MG/L) AT END OF 29 DAY TIDAL SIMULATION	17

LIST OF TABLES

Page No.

TABLE D1:	FALL VELOCITIES DETERMINED FOR DARWIN HARBOUR SAMPLES AS REPORTED IN HORTON AND KING (1999A, B)	4
TABLE D2:	DRY DENSITIES AND CRITICAL SHEAR STRESSES FOR EROSION FOR SELECTED BULK DENSITIES IN RMA-11	9
TABLE D3:	PARAMETERS SELECTED FOR “BEST ESTIMATE” COHESIVE AND NON-COHESIVE SEDIMENT TRANSPORT SIMULATIONS	10
TABLE D4:	PARAMETERS SELECTED FOR DEPOSITION AND SUSPENSION FAVOURABLE SENSITIVITY TESTS IN COHESIVE SEDIMENT	11

D1 INTRODUCTION

A variety of water quality simulations were undertaken to investigate the effects of the proposed dredging of the South Arm.

In this Appendix, further details are provided on two aspects of this modelling, namely the salinity simulations (Section D2) and sediment transport simulations (Section D3).

Conclusions are given in Section D4, with references listed in Section D5.

D2 SALINITY SIMULATIONS

The movement of salt in the Hunter estuary under tidal conditions is essentially dependent on two factors, namely:

- the hydrodynamics of the estuary; and,
- the eddy-diffusivity of the salt, a measure of the rate of diffusion of the salt within the estuary.

Sanderson et al (2002) estimated eddy-diffusivities of about $100 \text{ m}^2/\text{s}$ for the Hunter River downstream of Raymond Terrace, $60 \text{ m}^2/\text{s}$ for the Hunter upstream of Raymond Terrace, and $3 \text{ m}^2/\text{s}$ for the Williams River. The relatively low value of eddy-diffusivity for the Williams River was considered to be due to the reflectivity of the Seaham weir, which may be generating a standing wave in the river, and therefore weaker tidal currents.

These values of eddy-diffusivities were used in the RMA model.

The validity of these eddy-diffusivities was evident by investigating the available salinity data at Ironbark Creek. Two flood events, in February and March 2002, reduced the salinity at Ironbark Creek to close to 0 ppt. In both cases, the salinity at Ironbark Creek after about 29 days had increased to between 22-25 ppt.

In the case of the simulation of existing conditions undertaken as outlined in the main report, a similar scenario was investigated. That is, the saline intrusion into the estuary with 0 ppt initially was simulated over a period of 29 days. The salinity at Ironbark Creek after this period was 20 ppt, similar to the measured pattern (taking account that hydrodynamics in the two periods were not identical).

D3 SEDIMENT TRANSPORT SIMULATIONS

D3.1 INTRODUCTION

In the RMA-11 model, simulation of sediment transport is undertaken by modelling cohesive sediment (denoted as “mud”) and non-cohesive sediment (denoted as “sand”) separately. This is reasonable given the inhomogeneous nature of this sediment. Sand and mud generally behave as entirely separate populations when suspended in a water column. The differentiation between non-cohesive and cohesive sediment is usually based on a grain size of 75 µm (0.075mm), the sand portion having coarser grains than 75 µm.

The behaviour of estuarine bed sediments is extremely complicated and therefore parameterisation of this behaviour involves simple representations. This is particularly true for cohesive sediments where electrochemical bonding plays a significant role in settling behaviour.

Cohesive sediment tends to flocculate when it comes into contact with water having a salinity exceeding 1 ppt, increasing settling velocities by an order of magnitude compared to rates in freshwater. In order for flocculation to occur once the water is saline, individual particles need to come in close proximity to other particles. For this reason the settling velocity of cohesive sediment in estuarine waters is usually closely related to the suspended sediment concentration, with larger concentrations lead to greater flocculation and faster settling velocities. The available literature shows, however, that the precise details of the relationship can vary widely from estuary to estuary.

Flocculation also depends on the turbulence of the flow. Small amounts of turbulence can assist with flocculation by bringing particles together, whereas large amounts of turbulence tend to break up the flocs.

The approach used in this study was to rely on relevant literature based on measurements of Australian sediments (where possible) to determine the sediment properties to be input into the model, including work undertaken in Darwin by Horton and King (1999a, b). Comparison with other recent similar studies was also made. These included a study of Brisbane River and Moreton Bay (McEwan, 1998) and an investigation of Upper Newport Bay in California by the US Army Corps of Engineers (1997).

In subsequent sections, details on the parameters and methodology for the sediment transport simulations are provided. In Section D3.2, an outline of the sediment data collected in the Hunter estuary is given, including fall velocities of the mud fraction in seawater. A more comprehensive sediment data set is outlined in Section D3.3, mainly based on studies of the fate of dredged sediments in Darwin Harbour.

In Section D3.4, the general parameters chosen for input into the model are outlined, with specific details on cohesive sediment in Section D3.5 and non-cohesive sediment in Section D3.6. A summary of the selected parameters is given in D3.7, along with details of sensitivity testing undertaken.

Results of “deposition favourable” and “suspension favourable” cohesive sediment simulations are given in Section D3.8, along with non-cohesive sediment modelling outputs and a discussion on the results. Further interpretation of the results is provided in Section D3.9

D3.2 HUNTER ESTUARY SEDIMENT PROPERTIES

As noted in the main report (Section 2.6.1), Patterson Britton & Partners (1989) reported that the settling velocity of two Hunter estuary mud samples (in seawater) was between 0.01 and 0.05 mm/s. The Department of Public Works (1967) also reported a rate of 0.7mm/s for Hunter estuary silts in seawater. These are the only known measurements of fall velocities for Hunter estuary cohesive sediments in saline water.

Recent data on sediments in the Hunter estuary has also been collected as outlined in Patterson Britton & Partners (2003). For samples in the sand range (0.075mm to 2.36mm), the average d_{50} was 0.27mm, with a standard deviation of 0.09mm.

D3.3 OTHER STUDIES OF SEDIMENT PROPERTIES

In Horton and King (1999a, b), RMA model simulations of the movement of sediments dredged in Darwin Harbour were outlined, at Cullen Bay and Darwin Naval Base respectively. These studies included measurement of the fall velocities of the mud fraction in seawater as reported in Nielsen (1999a, b). Fall velocities were measured in seawater as salinity has a strong influence on the flocculation of clay and silt particles (the settling rate is much slower in freshwater).

The Cullen Bay samples had sand and mud in approximately equal proportions. The average d_{90} for the mud fraction was 0.069 mm¹, with a standard deviation of 0.001. The average d_{50} for the sand fraction was 0.20 mm, with a standard deviation of 0.046².

The Darwin Naval Base samples were about 75% mud and 25% sand. The average d_{90} for mud was 0.035 mm, with a standard deviation of 0.007. The average d_{50} for sand was 0.16 mm, with a standard deviation of 0.032. At both sites, the particle density was approximately 2640 kg/m³.

The fall velocities measured for the Cullen Bay and Darwin Naval Base samples are summarised in **Table D1**.

Table D1: Fall velocities determined for Darwin Harbour samples as reported in Horton and King (1999a, b)

Location	Mud		Sand	
	Average Fall Velocity (mm/s)	Standard Deviation	Average Fall Velocity (mm/s)	Standard Deviation
Cullen Bay	0.037	0.032	30	5
Darwin Naval Base	0.060	0.078	23	11

¹ The d_{90} value is the grain size that 90% of particles are finer than.

² The d_{50} value is the median grain size.

The average fall velocity for the Cullen Bay samples falls near the middle of the range of fall velocities measured in Hunter estuary sediments by Patterson Britton (Section D3.2). For the purposes of this investigation, it was therefore considered valid to use the range of properties of the Cullen Bay sediments to parameterise the Hunter estuary sediments.

D3.4 GENERAL MODEL PARAMETERS

In RMA-11, horizontal diffusion coefficients were applied in the direction of flow. For the longitudinal direction they were computed from element size and velocity magnitude, and scaled by input values. The transverse coefficients were defined as a further factor times the longitudinal value.

Given that there was no known calibration data to estimate diffusion coefficients, scale factors were chosen to be as small as possible while retaining model stability. The values chosen were 0.1 in the longitudinal direction and a further multiplier of 0.1 in the transverse direction (0.2 for non-cohesive sediment).

D3.5 COHESIVE SEDIMENT PARAMETERS

D3.5.1 Settling Velocity

A constant settling velocity was used for all nodes. Based on the sediment testing outlined in Section D3.3, the average settling velocity at Cullen Bay of 0.037 mm/s was chosen. However, given the wide variability in measured fall velocities, sensitivity testing was undertaken using a minimum value of 0.0048 mm/s (lower bound within one standard deviation of mean of measurements) and a maximum value of 0.069 mm/s (upper bound within one standard deviation of mean of measurements).

D3.5.2 Bed Roughness

For a rough bed, as part of the Rouse equation for suspended sediment distribution in a fully developed turbulent flow (used in RMA-11), Ariathurai (1982) showed that the shear velocity, U_* , could be computed from:

$$\frac{u}{U_*} = \frac{2.3}{k} \log_{10} \left(12.27 \frac{h}{k_s} \right) \quad (1)$$

where u is the local velocity, k is Von Karman's constant (generally equal to 0.4 and chosen to be so for this study), h is the depth of flow and k_s is the roughness height.

For a smooth bed (k_s less than or equal to 0.0001 m in RMA-11), U_* can be computed from:

$$\frac{u}{U_*} = \frac{2.3}{k} \log_{10} \left(3.32 \frac{hU_*}{\nu} \right) \quad (2)$$

where ν is the kinematic viscosity.

The shear velocity U_* is not a real velocity but is related to the actual fluid velocity which gives rise to a shear stress. The bed shear stress (τ_b) can be calculated as:

$$\tau_b = \rho_w U_*^2 \quad (3)$$

where ρ_w is the density of the suspending water.

The bed height roughness for the Rouse distribution calculation (k_s in Equation 1) mainly consists of grain roughness (k_{sg}) and form roughness (k_{sf}) generated by pressure forces acting on the bed forms. For a given bed material size, k_s is not a constant, but depends on flow conditions such as depth and velocity which affects the bed form dimensions. Generally, k_s values decrease with increasing velocities because bed forms are washed out at large velocities.

In a current field only (ignoring waves), experimental research has shown that k_{sg} is largely related to the largest particles of the top layer of the bed, typically parameterised as d_{90} , the grain size that 90% of particles are finer than. A relationship proposed by van Rijn (1982) is:

$$k_{sg} = 3d_{90} \quad (4)$$

Based on the sediment testing for Cullen Bay outlined in Section D3.1, where the average d_{90} of the mud was 0.069 mm, k_{sg} is equal to 2.08×10^{-4} m. Thus it can be estimated that k_s is not less than 2.08×10^{-4} m.

There is little known information on form roughness in the Hunter estuary as related to ripples and dune bed forms, so it is difficult to estimate this component of the roughness height. It was considered that the bed was generally flat without major bed forms. It is typically assumed that form roughness in cohesive sediments is negligible as the beds are hydraulically smooth; overall, k_s values are typically in the range of 0.0001 to 0.001 m (van Rijn, 1989).

Given that cohesive and non-cohesive sediments are considered separately in RMA-11, k_s was chosen to be 2.08×10^{-4} m (equal to the cohesive grain roughness value). However, given the uncertainty in this estimate, sensitivity testing was undertaken with k_s values of 0 (smooth bed) and 0.002 m, the latter cited in McEwan (1998). Note that typical measured values of k_s in non-cohesive sediments when ripples and dunes are present are in the order of 0.025 m (van Rijn, 1989).

D3.5.3 Deposition

Deposited sediment properties are a function of depth. Newly-deposited sediment is generally less dense and more easily scoured than sediments which have been covered and have begun to consolidate. RMA-11 represents the variation in bed properties as a series of thin fixed layers over a variable thickness stratum. Sediment is always deposited into the top layer (Layer 1). As the top layer fills, sediment is shifted down to the lower layers, with the bottom layer able to grow indefinitely. When scour occurs, the upper layers are removed first.

Consolidation is a process of floc compaction under the influence of gravity forces with a simultaneous expulsion of pore water and a gain in shear strength (or cohesion) of the bed material. Generally, three consolidation stages of settled muds are recognised (van Rijn, 1989):

- initial stage (days) - the flocs in a freshly deposited layer are grouped in an open structure with a large pore volume; bulk densities are typically 1000-1050 kg/m³ after one day and 1050-1150 kg/m³ after one week;
- secondary stage (weeks) - the pore volume between the flocs is further reduced and small thin vertical pipes (drains) are formed allowing pore water to escape; bulk densities are typically 1150-1250 kg/m³ after one month; and,
- final stage (years) - pore volume is further reduced and flocs are broken down; bulk densities are typically 1250-1350 kg/m³ after one year and 1350-1400 kg/m³ after 10 years.

For this study, the model was configured to allow up to 2 layers of deposited material to form, once the thickness of the top deposited layer reached 0.005 m. In recent studies, McEwan (1998) used 2 layers in a study of Brisbane River and Moreton Bay, with the top layer having a bulk density of 1120 kg/m³. The US Army Corps of Engineers (1997), in a 6 layer model, used a similar top layer bulk density of 1105 kg/m³. These bulk density values are all in the range given above for a deposit of about 1 weeks age, relevant for the study of dredged sediment settling in this investigation.

There are no known available measurements of bulk density in the Hunter estuary for freshly deposited sediments, let alone such measurements of the variation in bulk density with depth, to encourage the use of greater than 2 layers in RMA-11. A top layer bulk density of 1120 kg/m³ was selected. The particle density of sediment material used was 2640 kg/m³.

The bulk density of the second layer was chosen to be 1250 kg/m³. This is similar to the bottom layer bulk densities of 1269 and 1250 kg/m³ used by the U.S. Army Corps of Engineers (1997) and McEwan (1998) respectively in recent studies.

Deposition of cohesive sediment occurs when the bed shear stress falls below a critical value for deposition, denoted as τ_{bd} (Krone, 1962). It has been observed that there are up to three distinct phases in the deposition process depending on the suspended sediment concentration:

- a period of slow deposition due to hindered settling at high suspended sediment concentrations (greater than about 10,000 mg/L).
- a period of more rapid deposition (due to flocculation) at suspended sediment concentrations in the order of 300-10,000 mg/L
- a period of very slow deposition at suspended sediment concentrations less than about 300 mg/L

For the second phase above (concentrations from 300-10,000 mg/L) it has been shown that there is a minimum bed stress (τ_{bdmin}) below which all sediment particles are deposited on the bed yielding a maximum deposition rate. There is also a maximum bed stress (τ_{bdmax}) above which all sediment particles or flocs just remain in suspension yielding a zero deposition rate. Mehta and Partheniades (1975) found τ_{bdmin} was approximately 0.2 N/m² and τ_{bdmax} was approximately 1 N/m² for kaolinite in distilled water.

For the third phase above (concentrations less than 300 mg/L), Krone (1962) found that no net deposition occurs when the bed shear stress exceeds 0.06 N/m^2 . This value was used in a previous study of Hunter estuary sediment transport, namely the Department of Public Works (1967).

Given that it is most likely the dredged spoil will be at suspended concentrations much less than 300 mg/L once dispersed (as supported by the modelling results and also limited suspended sediment measurements in the Hunter estuary), the critical shear stress for deposition was chosen to be 0.06 N/m^2 . Other values quoted in recent studies include 0.04 N/m^2 for Moreton Bay in Brisbane (McEwan, 1998) and 0.08 N/m^2 for Upper Newport Bay in California (US Army Corps of Engineers, 1997). Sensitivity testing was undertaken using these lower and upper values.

D3.5.4 Resistance to Erosion

For erosion to occur in cohesive sediments, the electro-chemical bond between cohesive particles must first be broken. This occurs when a critical shear stress for erosion is exceeded.

The resistance of a cohesive bed to erosion by flowing water depends on a number of factors, including the depth of the deposit. As described in Section D3.5.3, RMA-11 represents the variation in bed properties as a series of thin fixed layers over a variable thickness stratum. The greater the depth within the bed, the greater the overburden pressure and the greater the resistance to erosion.

At bed shear stresses just above the critical value, erosion occurs particle by particle; this process is called *surface erosion*. At higher levels of stress, however, the bulk shear strength of the bed may be exceeded (Ariathurai, 1982). The portion of a bed in such a state is susceptible to *mass erosion*, so as the bed shear exceeds the critical shear stress of that portion of the bed, it fails totally and is instantly suspended in clusters or lumps.

In RMA-11, to model the transport process it is necessary to know the critical shear stress for erosion and the bulk density of each layer, as well as the erosion rate if the erosive mechanism is surface erosion. The erosion rate for *surface erosion* (S_e), defined as a mass rate of erosion per unit area, may be written as (Partheniades, 1963):

$$S_e = M \left(\frac{\tau_b}{\tau_{ce}} - 1 \right) \quad \tau_b \geq \tau_{ce} \quad (5)$$

where τ_b is the bed shear stress, τ_{ce} is the critical shear stress for erosion and M is an erodibility constant with SI units of $\text{kg}/(\text{m}^2\text{s})$.

The M constant typically varies between 0.00001 and $0.0004 \text{ kg}/(\text{m}^2\text{s})$ for natural muds. McEwan (1998) used a value of $0.00015 \text{ kg}/(\text{m}^2\text{s})$ which was adopted for this study.

The erosion rate for *mass erosion* is simply the mass eroded per unit bed area divided by a characteristic time in which erosion occurs. To calculate the mass eroded per unit bed area, the thickness of a layer is multiplied by a dry density (ρ_d) to give a dry mass per unit area, where ρ_d is defined as:

$$\rho_d = \frac{\rho_s(\rho_b - \rho_w)}{\rho_s - \rho_w} \quad (6)$$

and ρ_b is the bulk (wet or moist) density of the layer, ρ_w is the density of the suspending water (1025 kg/m³, see Section D3.5.5) and ρ_s is the solid (particle) density (2640 kg/m³, see Section D3.5.3). The mass used in defining dry density is the mass of the sediment, which is what is suspended when erosion occurs.

In both regimes (*surface* and *mass* erosion), erosion occurs when the shear stress at the bed exceeds the critical shear stress for erosion (τ_{ce}). In RMA-11, *surface erosion* only occurs on the bottom layer, and all other layers are considered to be unconsolidated and undergoing *mass erosion*.

There are no generally accepted relationships to calculate τ_{ce} based on sediment parameters. Hence the determination of τ_{ce} should be based on laboratory tests using natural mud or in situ field tests. However, it was considered that τ_{ce} measurements were beyond the scope of this study. Values of τ_{ce} for soft deposits typically range from 0.01 to 2.5 N/m² (van Rijn, 1989).

In the case of the selected bulk densities for this study, the corresponding dry densities (calculated from Equation 6) and typical τ_{ce} values for natural mud in saline water (van Rijn, 1989) are shown in Table D2.

Table D2: Dry densities and critical shear stresses for erosion for selected bulk densities in RMA-11

Layer	Bulk Density (kg/m ³)	Dry Density (kg/m ³)	τ_{ce} range(N/m ²)
1	1120	155	0.03-0.6 (0.2 typical)
2	1250	366	0.1-2.5 (0.6 typical)

Otsubo and Muraoko (1988) performed many tests to determine the critical shear stresses of natural muds. For *surface erosion* (representative of Layer 2 above), τ_{ce} ranged from 0.05-0.5 N/m², while for *mass erosion* (Layer 1), τ_{ce} ranged from 0.1-1 N/m².

Based on field measurements cited in McEwan (1998), a τ_{ce} value of 0.08 N/m² for the top layer was adopted for this study. However, given the uncertainty in this estimate, sensitivity testing was undertaken for values of 0.03 and 0.6 N/m², the lower and upper limits specified by van Rijn (1989).

For the bottom layer, McEwan (1998) cited a τ_{ce} value of 0.25 N/m². This value was adopted for this study. However, given the uncertainty in this estimate, sensitivity testing was undertaken for values of 0.1 and 2.5 N/m², the lower and upper limits specified by van Rijn (1989).

D3.5.5 Suspending Water

The suspending water was assumed to be saline with a salinity of 35 ppt. The density of this water at a temperature of 20°C is 1025 kg/m³ while the kinematic viscosity is 1.06×10⁻⁶ m²/s (Lide, 1996). These values were chosen to be input into the model.

D3.6 NON-COHESIVE SEDIMENT PARAMETERS

The method of sand sediment transport chosen to be used in RMA-11 for this study was based on the work of Ackers and White (1973). The main parameters to be selected in this approach are the median grain size, d_{50} , and the settling (fall) velocity.

Based on the sediment testing outlined in Section D3.2, the average d_{50} of 0.27 mm measured for the Hunter sand fraction was chosen to be used in RMA-11.

Fall velocities of non-cohesive sediment can be approximately predicted analytically for a given grain size, assuming the drag coefficient is in the Stokes region (Reynolds number less than unity). According to van Rijn (1989), the terminal fall velocity of a non-spherical sediment particle (w_s) is given by:

$$w_s = \frac{10\nu}{d} \left[\left(1 + \frac{0.01(s-1)gd^3}{\nu^2} \right)^{0.5} - 1 \right] \quad 100 < d < 1000 \mu m \quad (7)$$

where d is $0.8 \times d_{50}$ ($0.00027m$ in this case)³, ν is the kinematic viscosity (about $1.06 \times 10^{-6} m^2/s$ for water at 20°C), g is the gravitational acceleration (approximately $9.8 m/s^2$) and s is the particle relative density (given previously as 2.64). From Equation 7, w_s is thus 0.028 m/s. This settling velocity was chosen to be used in RMA-11.

Given the lack of calibration data, the grain shape factor, a calibration parameter, was selected to be the default of 0.7. Similarly, the characteristic length factors for deposition and erosion were selected to be 1 and 10 respectively. These factors are multipliers in the calculation of the time for sediment to settle (equal to depth divided by settling velocity) or re-suspend (equal to depth divided by water velocity).

D3.7 SUMMARY OF PARAMETERS AND SENSITIVITY TESTING

D3.7.1 Best Estimate

A summary of the “best estimate” sediment parameters is given in **Table D3**.

Table D3: Parameters selected for “best estimate” cohesive and non-cohesive sediment transport simulations

Parameter	Cohesive Sediment Value	Non-Cohesive Sediment Value
Settling velocity (mm/s)	0.037	28
Median grain size (mm)	-	0.27
Bed height roughness k_s (m)	0.00021	-
Critical shear stress for deposition (N/m ²)	0.06	-
Critical shear stress for erosion τ_{ce} (N/m ²) for top layer	0.08	-
Critical shear stress for erosion τ_{ce} (N/m ²) for bottom layer	0.25	-

³ The factor of 0.8 is included as a multiplier to take account that sediment in suspension is generally finer than the deposited material, given that the bed sediments are what is sampled for the purposes of grain size calculations.

D3.7.2 Sensitivity Testing

Due to the wide variation in the values of some sediment parameters, sensitivity testing was undertaken for cohesive sediment. This was attempted to give an indication of the range in results that could be expected. Two sensitivity tests were undertaken, namely:

- a *deposition* favourable test, in which parameters were selected in order to favour the faster deposition of sediment and to favour deposited material remaining on the bed; and,
- a *suspension* favourable test, in which parameters were selected in order to favour the slower deposition of sediment and to favour deposited material being eroded and re-suspended.

The parameters selected in each of these scenarios are shown in **Table D4**.

Table D4: Parameters selected for deposition and suspension favourable sensitivity tests in cohesive sediment

Parameter	Deposition Favourable Value	Suspension Favourable Value
Settling velocity (mm/s)	0.069	0.0048
Bed height roughness k_s (m)	0	0.002
Critical shear stress for deposition (N/m ²)	0.04	0.08
Critical shear stress for erosion τ_{ce} (N/m ²) for top layer	0.6	0.03
Critical shear stress for erosion τ_{ce} (N/m ²) for bottom layer	2.5	0.1

D3.8 RESULTS OF SIMULATIONS

The results for the best estimate cohesive sediment simulation were presented in the main report. The results for the deposition favourable cohesive sediment simulation are given in Section D3.8.1, with the suspension favourable cohesive sediment results provided in Section D3.8.2 (both using the parameters outlined in Section D3.7). The results for non-cohesive sediment are given in Section D3.8.3.

In all three simulations exactly the same hydrodynamics and sediment loads were applied as per the main report. That is, the suspended solids loading was distributed to 4 locations, each at 435 g/s, and applied in the model for a 29 day tidal simulation. Again, deposited sediment depths at the end of the simulation were scaled by a factor of 6.5.

Note that the non-cohesive sediment simulation was a purely arbitrary scenario with no particular relation to predicted dredging conditions and generated non-cohesive suspended sediment rates. It was undertaken to illustrate the significant difference between the behaviour of non-cohesive and cohesive sediment.

D3.8.1 Deposition Favourable (Cohesive Sediment)

For the deposition favourable cohesive sediment simulation, the extrapolated depths of deposited sediment at the end of the dredging operation are shown in **Figure D1**. Note that deposited depths

outside the region shown in Figure D1 were less than 10mm. A zoomed view of deposited depths in the South Arm is provided in **Figure D2**.

Predicted suspended sediment concentrations as a result of the dredging, at the end of the 29 day tidal simulation, are shown in **Figure D3**. Note that suspended sediment concentrations outside the region shown were less than 10mg/L.

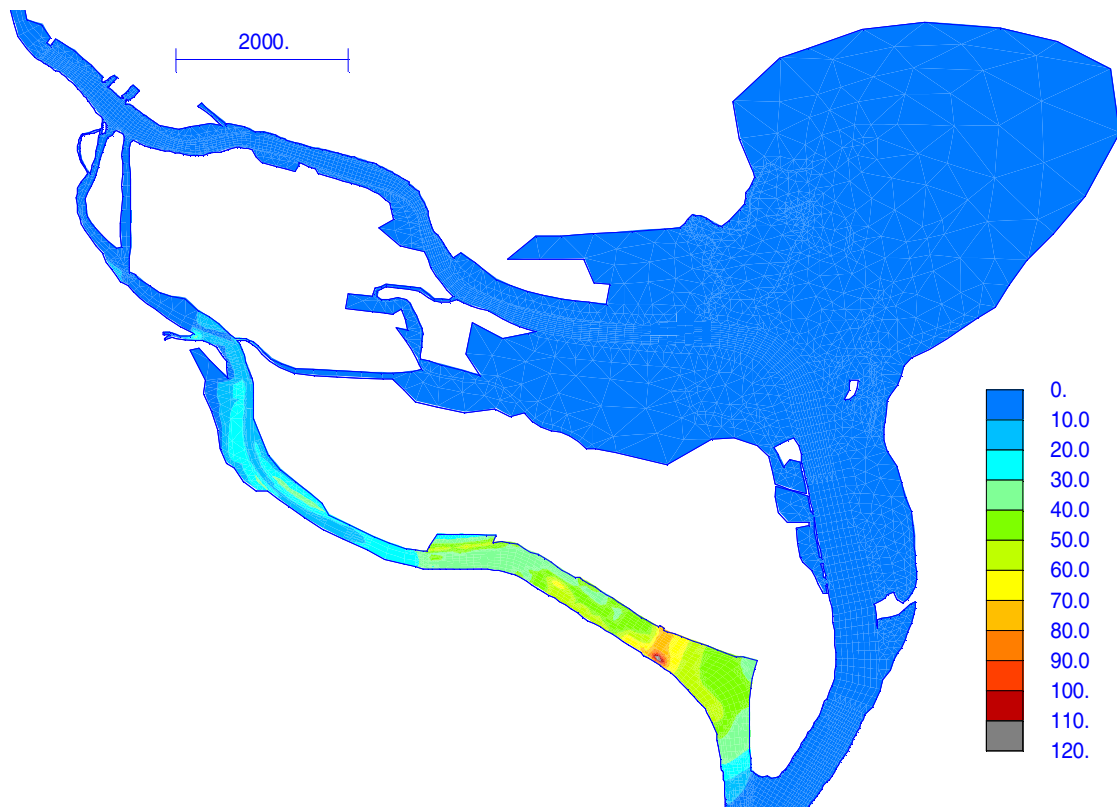


Figure D1: Predicted depths of deposited cohesive sediment (mm) at end of dredging operation for deposition favourable scenario

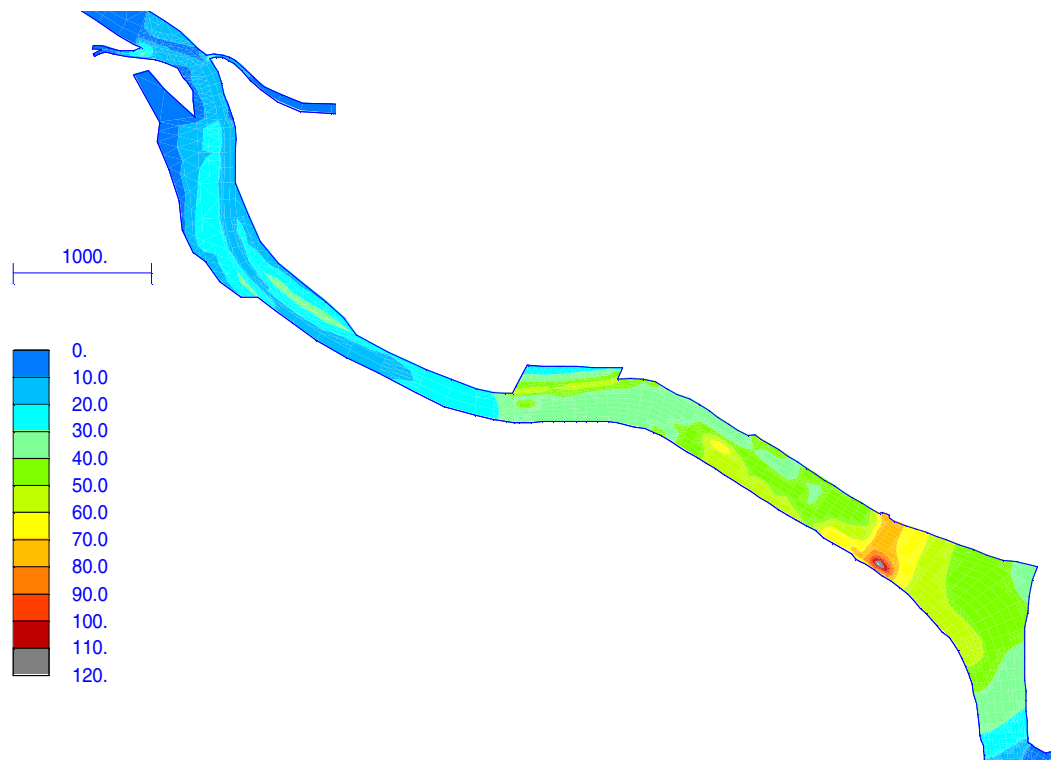


Figure D2: Predicted depths of deposited cohesive sediment (mm) at end of dredging operation for deposition favourable scenario, in South Arm

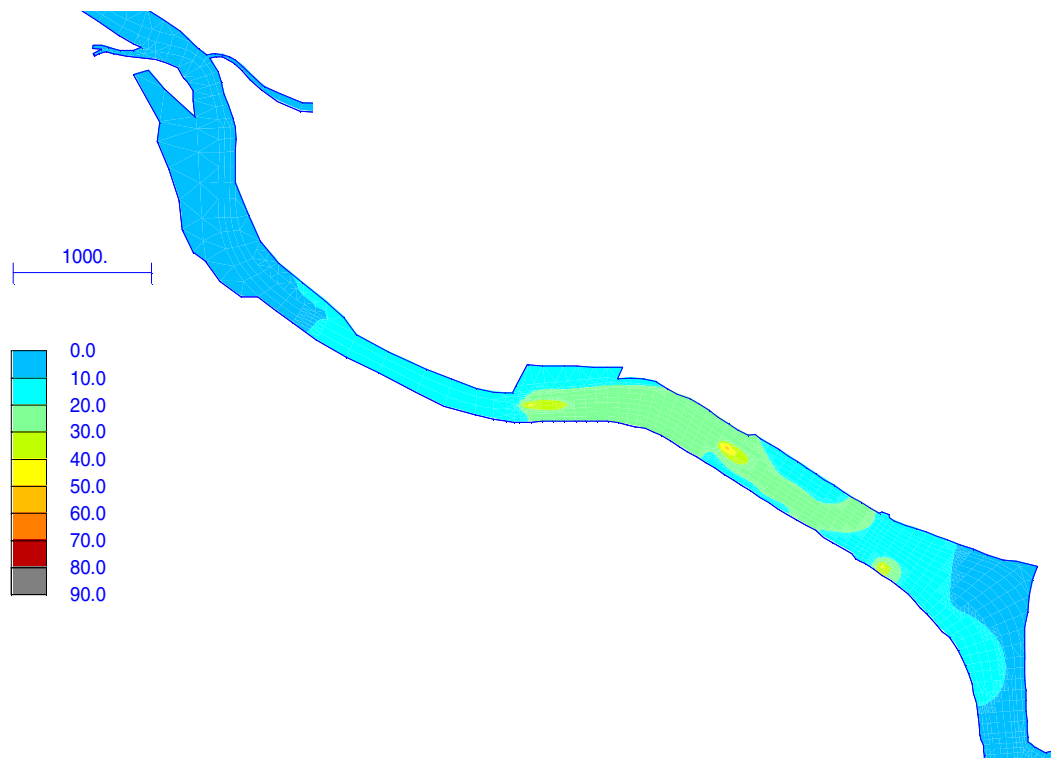


Figure D3: Cohesive suspended sediment concentrations (mg/L) at end of 29 day tidal simulation for deposition favourable scenario

In this simulation, a total of 4350 tonnes of sediment was introduced into the model over the 29 days. At the completion of the simulation, about 3176 tonnes of sediment (73% of that introduced) had deposited on the bed and 228 tonnes (5%) of sediment was still in suspension, with the remaining 946 tonnes (22%) having exited out of the model into the ocean.

D3.8.2 Suspension Favourable (Cohesive Sediment)

For the suspension favourable cohesive sediment simulation, the extrapolated depths of deposited sediment at the end of the dredging operation are shown in **Figure D4**. Note that deposited depths outside the region shown in Figure D4 were less than 10mm. A zoomed view of deposited depths in the South Arm is provided in **Figure D5**.

Predicted suspended sediment concentrations as a result of the dredging, at the end of the 29 day tidal simulation, are shown in **Figure D6**. Note that suspended sediment concentrations outside the region shown were less than 10mg/L.



Figure D4: Predicted depths of deposited cohesive sediment (mm) at end of dredging operation for suspension favourable scenario

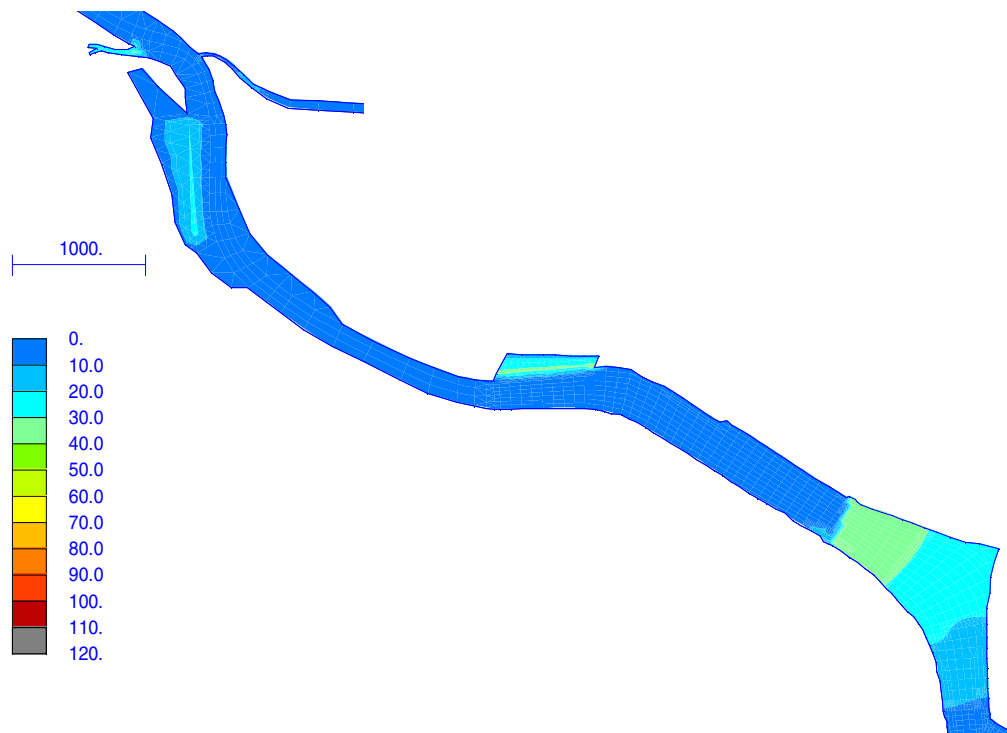


Figure D5: Predicted depths of deposited cohesive sediment (mm) at end of dredging operation for suspension favourable scenario, in South Arm

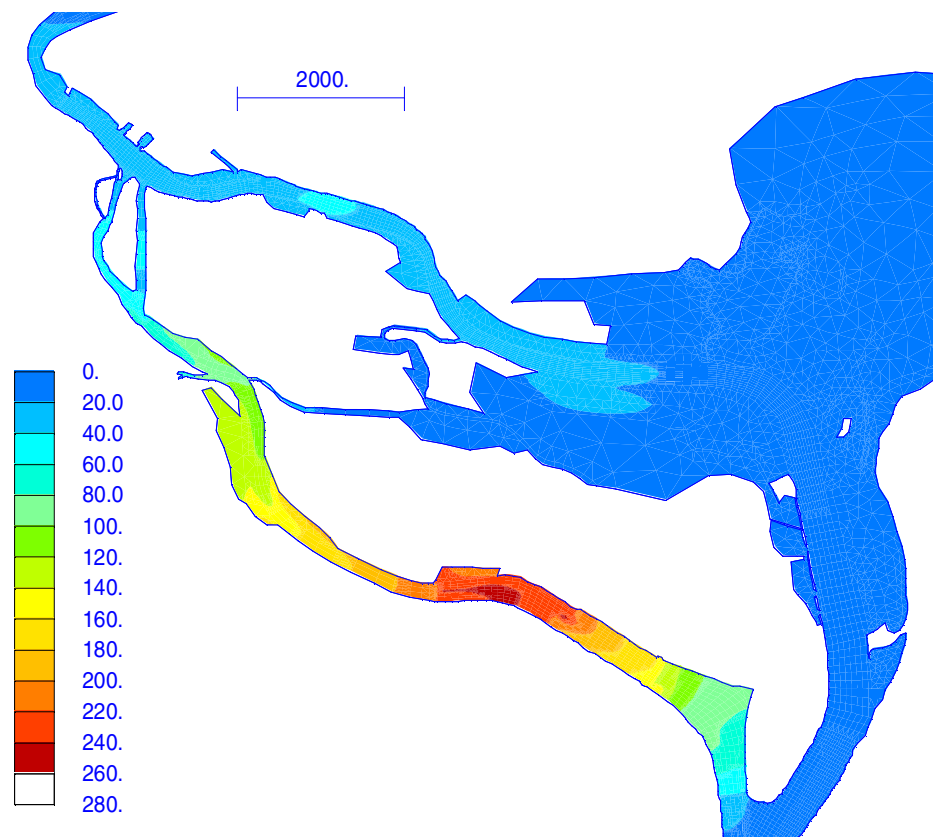


Figure D6: Cohesive suspended sediment concentrations (mg/L) at end of 29 day tidal simulation for suspension favourable scenario

As previously, in this simulation, a total of 4350 tonnes of sediment was introduced into the model over the 29 days. At the completion of the simulation, about 1067 tonnes of sediment (25% of that introduced) had deposited on the bed and 2914 tonnes (67%) of sediment was still in suspension, with the remaining 369 tonnes (8%) having exited out of the model into the ocean.

D3.8.3 Non Cohesive Sediment

For the non-cohesive sediment simulation, the arbitrary extrapolated depths of deposited sediment at the end of the dredging operation are shown in **Figure D7**. Note that deposited depths were less than 10mm outside (and in most areas inside) the region shown in Figure D7.

Arbitrary predicted suspended sediment concentrations as a result of the dredging, at the end of the 29 day tidal simulation, are shown in **Figure D8**. Note that suspended sediment concentrations outside the region shown were negligible (and most areas shown also have concentrations close to zero).

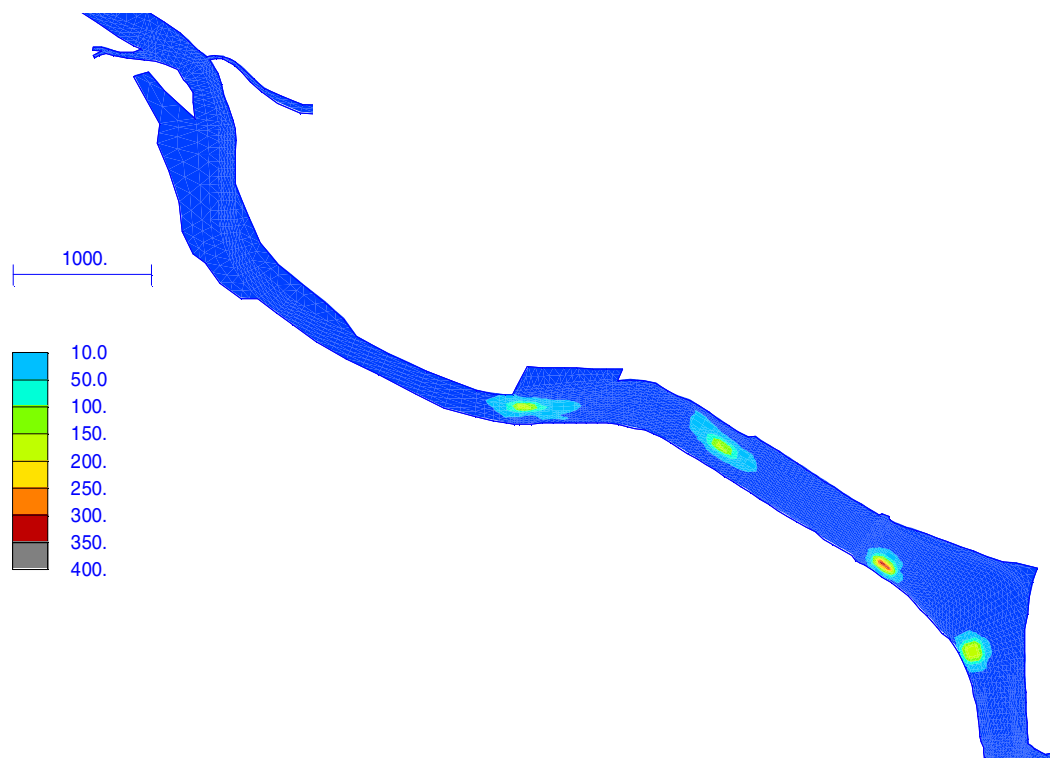


Figure D7: Arbitrary predicted depths of deposited non-cohesive sediment (mm) at end of dredging operation, in South Arm

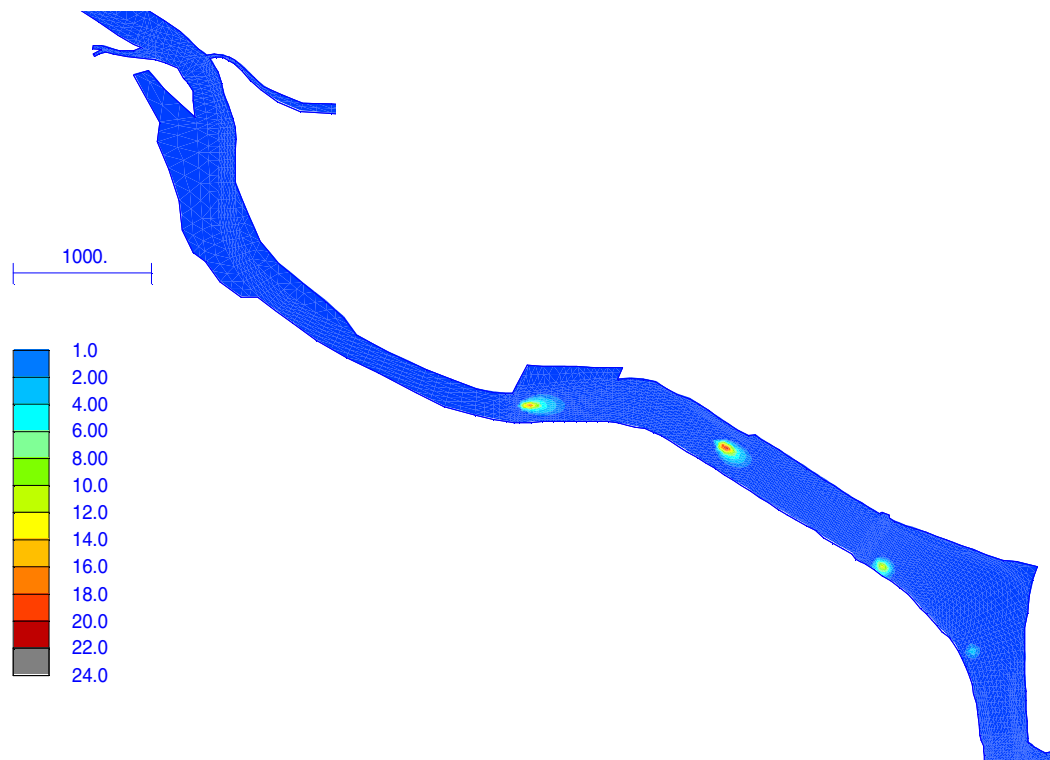


Figure D8: Arbitrary non-cohesive suspended sediment concentrations (mg/L) at end of 29 day tidal simulation

As previously, in this simulation, a total of 4350 tonnes of sediment was introduced into the model over the 29 days. At the completion of the simulation, about 4347 tonnes of sediment (99.9% of that introduced) had deposited on the bed and 2 tonnes (0.05%) of sediment was still in suspension, with the remaining 1 tonne (0.02%) having exited out of the model into the ocean.

D3.8.4 Discussion

It is evident that cohesive and non-cohesive sediment behave very differently. With the non-cohesive sediment settling velocity about 750 times faster than that for cohesive sediment, the sandy material tended to quickly deposit very close to where it was suspended. That is, it would not be expected that sandy material would disperse out of the dredged area itself under tidal conditions. Therefore, there would be no concern regarding deposition of sandy materials on sensitive mangrove areas, and suspended sediment concentrations would be relatively low.

Conversely, due to the slow settling velocity of the cohesive sediment it can disperse over a wider area before depositing on the bed. The sensitivity tests indicated the wide range of potential behaviour of the muddy sediments suspended during dredging.

In the deposition favourable scenario, cohesive sediments deposited from Walsh Point to Ironbark Creek, with up to 30-40mm accreting over the mangrove areas south of Ironbark Creek. Suspended sediment concentrations were typically about 30mg/L near the dredged area.

In the suspension favourable scenario, cohesive sediments again deposited from Walsh Point to Ironbark Creek, but in smaller quantities compared to the deposition favourable scenario (up to

20-30mm accreting over the mangrove areas south of Ironbark Creek). Suspended sediment concentrations were much larger than for the deposition favourable scenario, and spread over a wider area. Concentrations were in the order of 220mg/L near Tourle St Bridge, reducing to around 40mg/L near Walsh Point (downstream) and Hexham Island (upstream).

Given the potential range of sediment behaviour during the dredging operations, it is recommended that monitoring of suspended sediment movement during the dredging operation is undertaken. As noted in the main report, mitigating measures are available to restrict the migration of suspended sediment if necessary.

D3.9 INTERPRETATION OF RESULTS

As noted in the main report, results at the end of the 29-day simulation were extrapolated to take account of the dredging period lasting for a longer period of time. However, there are a number of limitations to this extrapolation.

Firstly, sediment (especially cohesive) is still in suspension at the end of a the 29-day simulation. No account is made of where this material may deposit over a longer period of time, and in comparing scenarios, no account is made of the varying proportions in suspension.

Secondly, sediment is assumed to be stable at a deposited location. However, although some locations tend to steadily build up with sediment, other locations may have cyclic tidal deposition and resuspension. Results can thus be skewed by the point in the tidal cycle that the 29-day simulation ceases. In this study the simulation ended at a neap tide which would conservatively favour deposition.

Sediment accumulation depths will also vary with time due to consolidation. The depths presented in this study were based on a freshly deposited layer which had a somewhat open structure.

Note that wind and wave effects were not included in the modelling. These may alter erosion and deposition patterns especially in exposed nearshore regions.

Suspended sediment concentrations shown were only those caused by the suspension of dredged spoil; there was no consideration of ambient suspended sediment concentrations (that is, the background level was assumed to be zero).

D4 CONCLUSIONS

Salinity simulations carried out to investigate saline intrusion under tidal conditions in the Hunter estuary were based on calibrated and verified tidal hydrodynamic behaviour and measured eddy-diffusivities. They were also shown to match the measured pattern of saline intrusion into the estuary after relatively large freshwater flows.

Parameters used in simulations of sediment transport were based on measured sediment properties (where available) and an extensive literature review. Sensitivity testing was also undertaken to take account of the potentially wide variation in behaviour for cohesive sediments.

It was evident that cohesive and non-cohesive sediment behave very differently, the latter settling much faster. Therefore, sandy material would tend to quickly deposit very close to where it was suspended, and there would be no concerns regarding deposition of sandy materials on sensitive mangrove mangroves. Non-cohesive suspended sediment concentrations would also be relatively low and of no concern.

Due to the slow settling velocity of the cohesive sediment it can disperse over a wider area before depositing on the bed. The sensitivity tests indicated the wide range of potential behaviour of the muddy sediments suspended during dredging. However, it is likely that the reach from Walsh Point to Ironbark Creek would have the most sediment deposition.

Given the potential range of sediment behaviour during the dredging operations, it is recommended that monitoring of suspended sediment movement during the dredging operation is undertaken. This would dictate the need for introduction of any mitigation measures.

D5 REFERENCES

Ackers, P. and W.R White (1973), "Sediment Transport: New Approach and Analysis", *Journal of Hydraulics Division, American Society of Civil Engineers*, Volume 99, No. HY11, November

Ariathurai, Ranjan (1982), "Two and Three Dimensional Models for Sediment Transport", *Resource Management Associates Report RMA 9180*, prepared for U.S. Army Corps of Engineers, Waterways Experiment Station, Vicksburg, Mississippi, July

Department of Public Works NSW [DPW] (1967), "Newcastle Harbour Siltation Investigation", *Report No. 114*, Harbours and Rivers Branch, Manly Hydraulic and Soils Laboratory, in conjunction with the Hydraulic Research Station, Wallingford, period of investigation February 1962 to September 1967

Horton, PR and IP King (1999a), "RMA Modelling of the Disposal of Sediments from Darwin Naval Base", *Water Research Laboratory Technical Report 99/16*, for Gutteridge Haskins and Davey, May

Horton, PR and IP King (1999b), "RMA Modelling of the Disposal of Sediments from the Outer Marina of Cullen Bay, Darwin", *Water Research Laboratory Technical Report 99/17*, for the Northern Territory Department of Lands, Planning and Environment, June

Krone, RB (1962), "Flume Studies on the Transport of Sediment in Estuarine Shoaling Processes", Hydraulic Engineering Laboratory, University of Berkeley, California USA

Lide, David R, Editor-in-Chief (1996). *CRC Handbook of Chemistry and Physics*, 77th Edition, 1996-1997, CRC Press, Boca Raton

McEwan, James (1998), *Calibration and Application of RWQM2 Sediment Transport Model*, Draft Final Report, for the Brisbane River and Moreton Bay Wastewater Management Study, August

Mehta, AJ and E Partheniades (1975), "An Investigation of the Depositional Properties of Flocculated Fine Sediment", *Journal of Hydraulic Research*, Vol. 13, No. 4, pp. 361-381

Nielsen, AF (1999a), "Darwin Harbour Sediment Testing (for Scott Wilson Irwin Johnston)", *Water Research Laboratory Technical Report 99/14*, May, for Dames and Moore

Nielsen, AF (1999b), "Darwin Harbour Sediment Testing (for Gutteridge Haskins and Davey)", *Water Research Laboratory Technical Report 99/15*, May, for Dames and Moore

Otsubo, K and K Muraoko (1988), "Critical Shear Stress of Cohesive Bottom Sediments", *Journal of Hydraulic Engineering, American Society of Civil Engineers*, Volume 114, No. 10, October

Partheniades, E (1963), "Erosion and Deposition of Cohesive Soils", *Journal of Hydraulics Division, American Society of Civil Engineers*, Volume 91, No. HY1, January

Patterson Britton & Partners (1989), *Mobility Study, Dumped Dredge Spoil, Port of Newcastle*, December, for MSB Hunter Ports Authority, J585/R330

Patterson Britton & Partners (2003), *Proposed Extension of Shipping Channels, Port of Newcastle, Sediment Quality Data*, Issue No. 2, March

Sanderson, Dr Brian; Redden, Dr Anna and Matthew Smith (2002), *Salinity Structure in the Hunter River Estuary*, report submitted to Newcastle City Council and Manly Hydraulics Laboratory, Centre for Sustainable Use of Coasts and Catchments, University of Newcastle, January

US Army Corps of Engineers (1997), *Feasibility Report, Upper Newport Bay, Orange County, California, Final Model and GUI Development and Implementation Report*, October

van Rijn, Leo C (1982), "Equivalent Roughness of Alluvial Bed", *Journal of Hydraulics Division, American Society of Civil Engineers*, Volume 108, No. HY10, October

van Rijn, Leo C (1989), "Handbook, Sediment Transport by Currents and Waves", *Delft Hydraulics Report H 461*, June